THE UNIVERSITY
of LIVERPOOL

Novel sites of CCK2R expression: Characterisation and functional significance of gastrin receptor expression in gastrointestinal myofibroblasts and human melanoma cancer cells

Thesis submitted in accordance with the requirements of the University of Liverpool and University of Szeged for the dual degree of Doctor in Philosophy by

Dr. Akos Janos Varga

2019

Disclaimer

I hereby declare that this dissertation is my own original work and has not been submitted before to any institution for assessment purposes. All sources used have been cited in the reference section. The research was performed in the Department of Physiology, Institute of Translational Medicine, University of Liverpool and Department of Dermatology, University of Szeged.

Acknowledgments

First and foremost, I would like to express my deep and sincere gratitude to my supervisors Professor Andrea Varro, Professor Graham J. Dockray and Professor Lajos Kemeny for their continuous support, motivation and guidance throughout my whole research project. Without their vast knowledge and experience in the field of physiology, gastroenterology and dermatology this work would have not been possible. I do consider myself lucky to have had the chance to work with them together and to learn scientific thinking, reasoning and problem solving directly from prominent, very well recognised professionals.

Special thanks to Dr. Dinesh Kumar who introduced me to the new research environment and helped me to get familiar with a number of new techniques I did not use before. In particular, I would like to thank Dr. Istvan Nemeth for providing the histological samples and Dr. Tunde Buknicz for helping with the organisation of serum sample collection. I would also like to thank Dr. Steven Dodd for providing qPCR and gastric RIA data and everyone else in Green Block for the supportive work atmosphere.

Finally, I would like to thank my whole family for their personal and financial sacrifice, especially my mother for her continuous encouragement and for providing a loving environment and my father who has been a great influential figure for me and the main reason I chose medicine and surgery in the first place.

List of publications

Thesis is based on the following publications:

Varga A, Kumar JD, Simpson AWM, Dodd S, Hegyi P, Dockray GJ, Varro A. Cell cycle dependent expression of the CCK2 receptor by gastrointestinal myofibroblasts: putative role in determining cell migration. Physiol Rep. 2017 Oct;5(19). pii: e13394.
Doi: 10.14814/phy2.13394; SJR **IF 0.948**

Shawe-Taylor M, Kumar JD, Holden W, Dodd S, **Varga A**, Giger O, Varro A, Dockray GJ. Glucagon-like petide-2 acts on colon cancer myofibroblasts to stimulate proliferation, migration and invasion of both myofibroblasts and cancer cells via the IGF pathway. Peptides. 2017 May;91:49-57.
Doi:10.1016/j.peptides.2017.03.008; **IF 2.851**

Other papers related to the subject of the dissertation:

Garalla HM, Lertkowit N, Tiszlavicz L, Reisz Z, Holmberg C, Beynon R, Simpson D, **Varga A**, Kumar JD, Dodd S, Pritchard DM, Moore AR, Rosztóczy AI, Wittman T, Simpson A, Dockray GJ, Varro A. Matrix metalloproteinase (MMP)-7 in Barrett's esophagus and esophageal adenocarcinoma: expression, metabolism, and functional significance. Physiol Rep. 2018 May;6(10):e13683.
Doi: 10.14814/phy2.13683; SJR **IF 0.963**

Impact factor of full papers related to the dissertation: 3.799

Cumulative impact factor related to the subject: 4.762

Contents

List of figures

List of tables

List of abbreviations

Abbreviation	Meanings
AAD CPG	American Academy of Dermatology Clinical Practice Guidelines
AC	Adenocarcinoma
ADAM	A desintegrin and metalloprotease
AJCC	American Joint Committee on Cancer
AKT	Protein kinase B
ALCAM	Activated leukocyte cell adhesion molecule
ALM	Acral lentiginous melanoma
ALP	Alcalic-phosphatase
AlpA/B	Adherence lipoprotein A and B
AMPK	5’ adenosine monophosphate-activated protein kinase
AP2	Activating protein 2
APC	Adenomatous polyposis coli
ARID2	AT-rich interaction domain 2
ASI	Acid secretion inhibitor
ATM	Adjacent tissue myofibroblast
ATP	Adenosine-5'-triphosphate
BabA	Blood group antigen binding adhesion
BCC	Basal cell cancer
BCH	Basal cell hyperplasia
BD	Boyden insert
BMP	Bone morphogenetic protein
BRAF	B-Raf proto-oncogene
BSA	Bovine serum albumin
CAF	Cancer-associated fibroblasts
CagA	Cytotoxin associated gene A
CAM	Cancer-associated myofibroblasts

cAMP	Cyclic adenosine monophosphate
CCK	Cholecystokinin
CCK2R/CCKB	Cholecystokinin-2 / -B / gastrin receptor
CCK2Ri4sv	CCK2 receptor intron 4-containing splice variant
CCK-8 / CeCo	Cell counting Kit-8
CCK8	Cholecystokinin-8
CCL17 (22, 24)	Chemokin (C-C motif) ligand 17 (22, 24)
Cdc42	Cell division control protein 42
CDK	Cyclin-dependent kinase
CDKI2A	cyclin-dependent kinase inhibitor
CDKN2A	Cyclin-dependent kinase inhibitor 2A
CgA	Chromogranin A
CM	Conditioned media
CMLR1	Chemokine like-receptor 1
CNS	Central nervous system
COX	Cyclooxygenase
CPE	Carboxypeptidase E
CRE	cAMP response element
CREB	cAMP response element binging protein
Ct	Cycle threshold
CTFP	C-terminal flanking peptide
CTLA-4	Cytotoxic T lymphocyte-associated antigen
CuSO4	Copper sulphate
CXCL12	C-X-C motif chemokine ligand 12
CXCR	Chemokine receptor
CXCR3	C-X-C Motif Chemokine Receptor 3
DAB	3,3-diaminobenzidine
DAG	Diacylglycerol
DAPI	4′,6-diamidino-2-phenylindole
DFS	Disease free survival
DMEM	Dulbecco’s Modified Eagle’s Medium
DNA	Deoxyribonucleic acid
ECL	Enterochromaffin-like cell
ECM	Extracellular matrix
EDTA	Ethylenediaminetetraacetic acid

EdU	5-Ethynyl-2´-deoxyuridine
EGF	Epidermal growth factor
EGFR	Epidermal growth factor receptor
Egr-1	Early growth response protein 1
EGTA	Ethylene glycol-bis(2-aminoethylether)-N,N,N′,N′-tetraaceti acid
EIU	Enzyme immune unit
ELISA	Enzyme-linked immunoassay
EMT	Epithelial mesenchymal transition
EndMT	Endothelial-to-mesenchymal transition
EP4	Prostaglandin E2 receptor 4
ER	Endoplasmic reticulum
ERK1/2	Extracellular signal-regulated kinase 1/2
F. Ch	Fold change
FACS	Fluorescence-activated cell sorting
FAK	Focal adhesion kinases
FAMMM	Familial atypical multiple mole-melanoma syndrome
FBS	Fetal bovine serum
FDA	U.S Food and Drug Administartion
FDR	False Discovery Rate
FGF	Fibroblast growth factor
FISH	Fluorescent in situ hybridization
FITC	Fluorescein isothiocyanate
FM	Full medium
FOX	Forkhead box
FSC	Forward scattering
GAP	GTPase-activating proteins
GAPDH	Glyceraldehyde 3-phosphate dehydrogenase
GDPR	General Data Protection Regulation
GI	Gastrointestinal tract
GIM	Gastrointestinal metaplasia
GIST	Gastrointestinal stromal tumour
GLP	Glucagon-like peptide
GLP-1	Glucagon-like peptide-1
GLP-2	Glucagon-like peptide-2

GORD / GERD	Gastroesophageal reflux disease
GPCR	G-protein-coupled receptors
GPR19	G Protein-Coupled Receptor 19
GRP	Gastrin releasing peptide
GTE	Genotype tissue expression
GTP	Guanosine-triphosphate
H&E	Haematoxylin-eosin
H. pylori / *Hp*	Helicobacter pylori
H2RB / H2RA	Histamine type 2 receptor antagonist
HB-EGF	Heparine-binding EGF-like growth factor
HDC	Histidine decarboxylase
HDI	High dose interferon
HEPES	Hydroxyethyl piperazineethanesulfonic acid
hG17	Human heptadecapeptide gastrin
HGD	High grade dysplasia
HGF	Hepatocyte growth factor
HKG	House keeping gene
HOX	Homebox gene
HPA	Human protein atlas
HPLC	High-performance liquid chromatography
HRP	Horseradish peroxidase
ICC	Immunocytochemistry
IFN	Interferon
IGF	Insulin-like growth factor
IGFBP	Insulin-like growth factor binding protein
IGF-IR	Insulin-like growth factor-receptor type 1
IHC	Immunohistochemistry
IL	Interleukin
IL-1RA	Interleukin-1 receptor antagonist
INFγ	Interferon γ
INS-GAS	Insulin-gastrin transgenic mice
IP3	Inositol 1,4,5-triphosphate
JAK	Janus kinase
JNK	c-JUN N-terminal kinase
KGF	Keratinocyte growth factor

LBIH	Liverpool Bio-Innovation Hub
LC-MS	Liquid chromatography–mass spectrometry
LGD	Low grade dysplasia
LGR5	Leucine-rich repeat-containing G-protein coupled receptor 5
LMM	Lentigo maligna melanoma
M	Molar
MAFFT	Multiple Sequence Alignment using Fast Fourier Transform
MAG	Multifocal atrophic gastritis
MAPK	Mitogen-activate protein kinase
MAS	Melanoma-astrocytoma syndrome
MC1R	Melanocortin 1 receptor
MCAM	Melanoma cell adhesion molecule (CD146)
MDSC	Myeloid cell-derived suppressor cell
MEK / MAPKK	Mitogen-activated protein kinase kinase
MEN-1	Multiple endocrine neoplasia type-1
MLC	Myosin light chain
MM	Malignant melanoma
MMP	Matrix metalloprotease
MS	Mass spectrometry
MSC	Mesenchymal stem/stromal cell
MSCBM	Mesenchymal Stem Cell Basal Medium
MT1-MMP	Membrane type-Matrix metalloprotease
MSCGM	Mesenchymal Stem Cell Growth Medium
MSH	Melanocyte stimulating hormone
MSLT-1	Multicentre Selective Lymphadenectomy Trial-1
NCCN	National Comprehensive Cancer Network
NET	Neuroendocrine tumor
NF1	Neurofibromin 1
NF-κB	Nuclear Factor kappa-light-chain-enhancer of activated B cells
NMM	Nodular melanoma
NRAS	Neuroblastoma RAS viral oncogene homolog
NSCLC	Non-small cell lung cancer
NTM	Normal tissue myofibroblast

OipA	Outer inflammatory protein A
OIS	Oncogene-induced senescence
OR	Odds ratio
OS	Overall patient survival
PA	Pernicious anaemia
PAGE	Polyacrylamide gel electrophoresis
PAI	Plasminogen activator inhibitor
PAM	Peptidyl-alpha-amidating mono-oxygenase
PANTHER	Protein ANalysis THrough Evolutionary Relationships
PAR1	Proteinase activated receptor 1
PBS	Phosphate buffered saline
PD-1L	Programmed cell death 1 receptor ligand
PD-1R	Programmed cell death 1 receptor
PDGF	Platelet derived growth factor
PDGFR	Platelet derived growth factor receptor
PegIFN	PEGylated interferon
PFA	Paraformalydehyde
PGE2	Prostaglandin E2
PI	Phosphatidylinositol
PI3K	Phosphatidylinositol-3-kinase
PIP_2	Phosphatidylinositol 4,5-bisphosphate
PK	Protein kinase
PKC	Protein kinase C
PLC	Phospholipase C
PO	Peroxidase
PPI	Proton pump inhibitor
PTEN	Phosphatase and tensin homolog
qPCR	Quantitative polymerase chain reaction
Rac1	Ras-related C3 botulinum toxin substarte 1
REG	Regenerating protein family
RGP	Radial growth phase
rh	Recombinant human
RIA	Radioimmunoassay
RNA	Ribonucleic acid

RPMI	Roswell Park Memorial Institute medium
RSV	Rous sarcoma virus
RT	Room temperature
RTK	Receptor tyrosine kinases
SabA	Sialic acid binding adhesion
SCLC	Small cell lung cancer
SDF-1	Stromal cell-derived factor 1
SDS	Sodium dodecyl sulfate
SEM	Standard error of the mean
SF	Serum free
SIDLS	Stable Isotope Dynamic Labeling of Secretomes
SILAC	Stable Isotope Labelling by Amino-acid in Culture
siRNA	Small interference RNA
SLNB	Sentinel lymph node biopsy
SMA	Smooth muscle actin
Sp1	Specificity protein 1
SPC2,3	Subtilisin-like prohormone convertases 2,3
SRE	Serum response element
SSC	Side scattering
SSM	Superficial spreading melanoma
STAT	Signal transducers and activators of transcription
STR	Short tandem repeat
T4SS	Type IV secretion system
TAMs	Tumour-associated macrophages
TBS	Tris buffered saline
TCFs	Ternary complex factors
TERT	Telomerase reverse transcriptase
TFA	Trifluoroacetic
TGF	Transforming growth factor
TIMP	Tissue inhibitors of matrix metalloproteases
TME	Tumour microenvironment
TNF	Tumour necrosis factor
TP53	Tumour protein p53
tPA	Tissue-type plasminogen activator
UICC	Union for International Cancer Control

uPA	Urokinase-type plasminogen activator
uPAR	Urokinase-type plasminogen activator receptor
UV	Ultraviolet
VacA	Vacuolating cytotoxin A
VAMT2	Vesicular monoamine transporter 2
VEGF	Vascular endothelial growth factor
VGP	Vertical growth phase
WB	Western blot
ZE	Zollinger Elison syndrome

Abstract

The well-known action of the gastric hormone gastrin in stimulating gastric acid secretion is mediated by activation of cholecystokinin-2 receptors (CCK2R). The latter are expressed by a variety of cell types suggesting that gastrin is implicated in multiple functions. During wound healing in the stomach CCK2R may be expressed by myofibroblasts. We have now characterized CCK2R expression in cultured myofibroblasts. Immunocytochemistry showed that a relatively small proportion (1–6%) of gastrointestinal myofibroblasts expressed the receptor regardless of the region of the gut from which they were derived, or whether from cancer or control tissue. Activation of CCK2R by human heptadecapeptide gastrin (hG17) increased intracellular calcium concentrations in a small subset of myofibroblasts indicating the presence of a functional receptor. Unexpectedly, we found over 80% of cells expressing CCK2R were also labelled with 5-ethynyl-20-deoxyuridine (EdU) which is incorporated into DNA during S-phase of the cell cycle. hG17 did not stimulate EdU incorporation but increased migration of both EdU-labeled and unlabelled myofibroblasts; the migratory response was inhibited by a CCK2R antagonist and by an inhibitor of IGF receptor tyrosine kinase; hG17 also increased IGF-2 transcript abundance. The data suggest myofibroblasts express CCK2R in a restricted period of the cell cycle during S-phase, and that gastrin accelerates migration of these cells; it also stimulates migration of adjacent cells probably

through paracrine release of IGF. Together with previous findings, the results raise the prospect that gastrin controls the position of dividing myofibroblasts which may be relevant in wound healing and cancer progression in the gastrointestinal tract.

In addition to gastrointestinal stromal cells, dermal fibroblasts and melanoma cancer cells were also identified as novel sites of CCK2R expression. An initial cross-sectional study of patients with various stages of melanoma revealed a close correlation between advanced disease stage and elevated fasting serum gastrin concentration. Hypergastrinaemia was associated with *H.pylori* infection and long term acid secretion inhibitor consumption, as might be expected. Experiments with primary melanoma cultures revealed no effect of gastrin on cancer cell proliferation, however chemotactic assays with Boyden chambers showed increased invasion and migration of melanoma cells. Since dermal cells of fibroblastic linage also express CCK2R we designed 3d organotypic and spheroid models to mimic the complexity in human skin. Stromal cells (cancer associated myofibroblasts, mesenchymal stem cells, dermal fibroblasts) were found to stimulate melanoma growth independently of gastrin emphasizing paracrine signalling. Nonetheless gastrin further increased the invasion of tumour cells in presence of stromal components. Proteomic analysis of melanoma secretomes revealed upregulation of MMP-2 and downregulation of TIMP-3 following gastrin treatment suggesting a protease-mediated, gastrin-driven, ECM degradation via CCK2R as a possible mechanism behind the increased invading capacity of melanoma cells exposed to gastrin. Furthermore, inhibition of MMP-2 with siRNA or

substitution of TIMP-3 reverted these changes. Serum MMP-2 and TIMP-3 concentration showed no correlation with disease progression.

In conclusion the metastasising capacity of *in situ* melanomas may be significantly influenced by gastrin, and suggesting the need for closer surveillance in those patients with hypergastrinaemia. Moreover, CCK2R may provide a putative therapeutic target. Future research could usefully focus on these issues.

Chapter 1

Introduction

1.1 Overview of cancer

Understanding cancer has undergone major revision over the centuries. There have been numerous theories that try to incorporate progressively acquired knowledge over the years. Historically, interesting concepts include the *lymph theory* by Hoffman and Stahl, where fermentation of lymph was considered to replace “black bile” leading to malignant tumour formation (Kardinal et al. 1979, Javier et al. 2008). With the ability to investigate cellular structures due to the development of microscopy focus was switched from lymph to cells. Müller, Virchow and Rokitansky transformed views of cancer by proposing that tumour is a solid lesion composed of budding particles dispersed within normal tissue introducing the *blastema theory* (Diamandopoulos 1996). Despite identifying malignantly transformed cells as the core elements of cancer from which a tumour originates, there was still speculation regarding the aetiology and factors that contribute to cancer development. Virchow suggested chronic irritation, while Ribbert identified trauma as a main cause responsible for tumour formation.

Due to lack of experimental data the significance of infections in the origin of cancer was dismissed for almost half of a century. With the development of microbiology, the concept of tumour viruses and viral oncogenes were introduced in the early 20th century. Peyton Rous was amongst the first one to discover that avian sarcoma could be transmitted into healthy animals by a virus (later named Rous sarcoma virus (RSV)) generated from tumour extracts (Rous 1911). RSV was recognised later as the first identified tumour virus capable of inducing cancer. Intense research in this field led to the

identification of Epstein-Bar virus associated with Burkitt's lymphoma, hepatitis B virus linked to human hepatocellular carcinoma or human papilloma virus responsible for cervical cancer to name a few (Epstein et al. 1965, Blumberg et al. 1967, zur Hausen 1996). Furthermore apart from viruses, bacteria are also able to exploit the host cell niche and stimulate growth related genes thereby promoting cancer formation, for example increased risk of gastric adenocarcinoma in *H.pylori* positive patients or colon carcinoma in Salmonella infection (Van Elsland et al. 2018). This led to the revolutionary concept that cancer arises from disturbances of different factors regulating normal cell growth.

Essentially, cancer can be defined as an accumulation of consecutive somatic mutations affecting multiple cells which then undergo a selection process eventually leading to a mutation-driven clonal evolution of tumour cells (Nowell 1976, Vogelstein et al. 1993). There are now multiple environmental and genetic factors known to be associated with this process. The target genes on which these effects take place are characterised as oncogenes and tumour suppressors. Tumours arise as a result of loss of function of tumour suppressors and/or gain of function of oncogenes. A common link between oncogenes is that their activation results in disruption of proper cell growth regulation and can, but not necessarily does, initiate neoplastic transformation of cells. The latter depends on the number of pathways affected and whether the cell is capable of maintaining sufficient control through tumour suppressor genes (e.g. retinoblastoma gene, Wilms' tumour gene, neurofibromatosis type 1 gene, the p53 gene, familial adenomatous polyposis coli gene) acting as negative regulators (Stanbridge 1990).

Rapid local growth through expansion of proliferating cancer cells is an important determinant of malignant behaviour. The concept of systemic dissemination leading to distant metastases was first introduced by Paget in 1889 referred to as the “seed and soil” theory that seeks to explain why certain tumours are likely to metastasize to specific organs (Paget 1989). By definition, metastasis is formation of cancer at a different location from the primary lesion with similar histological parameters and genetic alterations (Mathot et al. 2012). Most cancer related deaths are the result of therapy-resistant metastases in vital organs (Ribatti et al. 2006). Intravasation of cancer cells is the initial step followed by colonisation of secondary sites. This complex process is regulated by different endogenous and exogenous factors of which proteolytic activity and extracellular matrix degradation are key elements (Chambers et al. 2002). It should, however, be noted that tumour cells are recognised to undergo many changes through their migration (Waghorne et al. 1988). Whether this is due to a clonal selection process or whether cells destined for metastasis are already formed within the original tumour is still under debate. Nonetheless, this realisation highlighted the importance of multimodal combined therapies targeting primary and distant sites differently introducing modern oncotherapeutical approaches.

In recent years the importance of the tumour microenvironment consisting of stromal, inflammatory and immune cells in or close to tumour cells and responsible for the production of several hormonal and growth factors, cytokines and extracellular matrix has gained attention. Tumours are no longer considered as an isolated self-sustaining tissue mass, rather as a constantly

evolving group of genetically diverse malignantly transformed cells interacting continuously with their surroundings (Joyce et al. 2009). The microenvironment also plays an important role in the process of metastasis. Tumour stroma contains a number of different cells i.e. pericytes, fibroblasts, macrophages, neutrophils, mast cells, myeloid cell-derived suppressor cells (MDSCs) and mesenchymal stem cells (MSCs) (Tlsty et al. 2006). These cells are modified by the tumour to support growth and invasion. It is important to note that while tumour cells contain mutations, as previously described, the stromal cells do not, instead their behaviour seems to have been modified by surrounding tumour cells. Macrophages are able to alter their polarisation state and adopt a cancer associated phenotype by producing cytokines and chemokines (i.e. IL-10, the IL-1 decoy receptor, IL-1RA, CCL17, CCL22 and CCL24) that are generally known to have a pro-tumorigenic effect (Biswas et al. 2010, Quail et al. 2013). Furthermore, tumour cells are able to undergo an epithelial to mesenchymal transition (EMT) and generate a subpopulation of cells (cancer associated fibroblasts (CAFs), myofibroblasts(CAMs)) which are capable of producing growth factors to promote angiogenesis and intravasation by increasing vascular permeably through CXCL12 and NF-kB signalling pathways (Zeisberg et al. 2007, Semenza 2013).

Overall tumour formation is a complex process involving multiple mechanisms many of which are still not fully understood. It involves a constant interaction between cancer cells and surrounding stroma, which eventually transforms the microenvironment into a supportive cancer promoting site from which selected tumour cells with increased migration and invasion can disseminate to distant

secondary sites. Whether there are receptors with well described physiological roles that acquire a different set of functions in the tumour environment, including novel uncharacterised sites of expression, is an interesting topic. The present thesis asks whether receptors for the gastric acid-stimulating hormone, gastrin, are a case in point. These receptors are now known as cholecystokinin-2 receptors, CCK2R, but earlier literature also referred to them as CCK-B or gastrin/CCK-B receptors. Although cholecystokinin has also affinity towards the CCK2 receptor the antral hormone gastrin is the dominant physiological agonist.

1.2 Gastrin

1.2.1 Discovery and characterisation of the peptide hormone

Gastrin was first described by Edkins in 1905. He showed that extracts of the pyloric antral mucous membrane stimulated an increase in gastric acid secretion (Edkins 1906). Later, histamine was found to be a gastric acid secretagogue and there was some confusion as to whether gastrin and histamine might not be the same substance (Popielski 1919). Gregory and Tracy subsequently showed that gastrin and histamine were, in fact, distinct substances and identified the gastrins in hog antral mucosa as a pair of heptadecapeptide (G17) amides differing in the presence or absence of a sulphated tyrosine residue located six amino acids from the carboxyl terminus. (Gregory et al. 1964). Later, NH_2 extended versions of G17 were identified, namely G34 which is now recognized as a biosynthetic intermediate. The relationship between gastrin and histamine eventually became clear with the development of H2 receptor antagonists that inhibit acid secretion stimulated by both histamine and gastrin (and also food consumption) (Black et al. 1972). The cellular origins of gastrin were subsequently elucidated by immunochemistry which identified scattered endocrine cells (G-cells) in the epithelium of the antral mucosa. Since the local concentration of former is 15-20 fold higher than the other, stimulatory effect of gastrin is mainly mediated through the amidated version containing 17 amino acid residues (Dockray et al. 1996). It should be noted however, that precursor forms have also been shown to have a proliferative effect on GI mucosa mainly observed with colonic cancers (Nemeth et al. 1993).

1.2.2 Synthesis of gastrin: from gene to biologically active products

The *gastrin* gene is located at chromosome 07q21 and consists of three exons separated by two introns; it is around 4.0-kilobase-pair long (Ito et al. 1984). The main source of gastrin expressing G-cells is the antrum but there are also G-cells present to a lesser extent in duodenum, in humans. The initial product of mRNA translation, preprogastrin, consisting of 101 amino acids, is rapidly cleaved between residues 21-22 or 26-27 to yield progastrin which is then transferred from the endoplasmic reticulum to the *trans*-Golgi network and then to secretory vesicles. A number of vesicular enzymes are implicated in the conversion of progastrin to its biological active forms prior to secretion. Posttranslational modification through subtilisin-like prohormone convertases acting at pairs of basic residues, and then of carboxypeptidase E acting at the exposed COOH-terminal basic residues results in Gly-extended gastrins; G34-Gly is converted into G17-Gly by proteolytic cleavage at a pair of lysine residues. The final forms of both G17 and G34 are produced by COOH-terminal amidation mediated by peptidyl-alpha-amidating mono-oxygenase acting at the COOH-terminal glycine residue (Varro et al. 1994, Dockray et al. 2001). The G-cell secretory vesicles that contain gastrin are part of the regulated secretory pathway and release is mediated by calcium-dependent exocytosis. It is worth noting that there are also intermediary forms of gastrin including longer versions containing 71 residues or smaller fragmented ones with 6 or 14 amino acids, but these have not yet been proven to be functionally significant. The two main circulating forms are G17 and G34 (Figure 1.1).

As previously stated, the main site of expression under physiological circumstances is endocrine G-cells located in the antrum of the stomach. However gastrin mRNA has also been successfully detected in duodenal mucosa, colon, pituitary gland, pancreas and spermatozoa (Dockray 2004). On the other hand, there are a number of malignant conditions recognised to be associated with continuous *gastrin* gene expression. In the case of gastrin-secreting tumours of the Zollinger-Ellison syndrome, the pattern of biosynthetic processing may resemble that in antral G-cells or may be truncated leading to the production of biosynthetic intermediates (Dockray et al. 1975, Dockray et al. 1975, Rehfeld et al. 1992, Rehfeld et al. 1994). The latter, mostly progastrin and Gly extended variants, appear to predominate in other types of cancer including colorectal and lung adenocarcinomas, although perhaps amidated forms occur in pancreatic adenocarcinomas (Nemeth et al. 1993, Goetze et al. 2000, Koh et al. 2004).

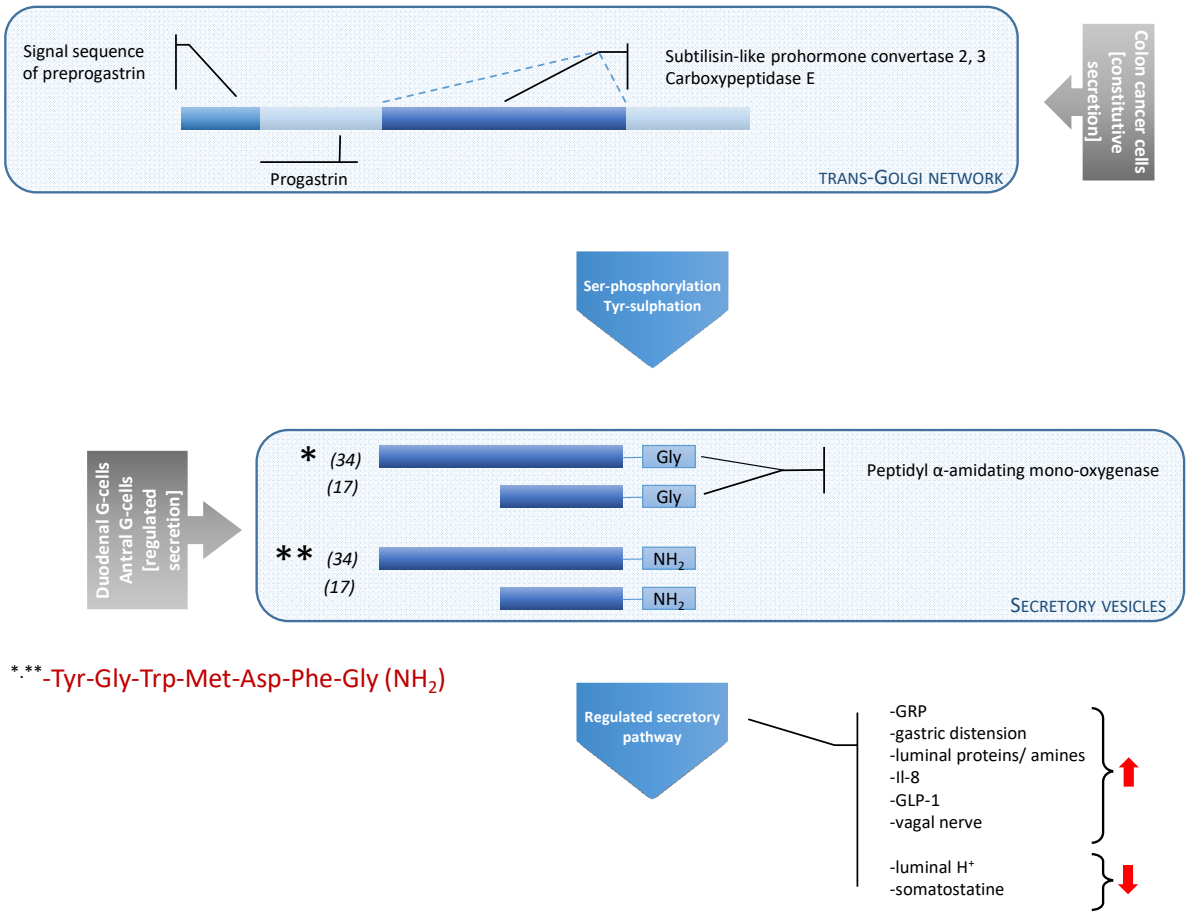

Figure 1.1. Schematic representation of gastrin synthesis.
Preprogastrin is cleaved and converted to progastrin by SPC2,3 and CPE. After phosphorylation and sulphation, Gly extended gastrines (G34Gly, G17Gly) are terminally amidated via PAM and undergo regulated secretion.

1.2.3 Effects of gastrin and regulation of secretion

1.2.3.1 Regulation of secretion and gene expression

Gastrin is released from antral G cells in response to luminal aromatic amino acids (tryptophan and tyrosine), dietary amines and luminal calcium. Beside food stimuli, mechanical stress due to distension of stomach, cephalic vagal stimuli and intrinsic neural factors i.e. gastrin releasing peptide (GRP) liberated from the mucosal innervation are responsible for gastrin release (Schubert 2017). GRP secreted from neuronal fibres of the myenteric plexus and enteric ganglia seem to be regulated independently from vagal reflex arches and involve non-cholinerg mechanisms including β adrenerg stimulation (Wolfe et al. 1987, Weigert et al. 1997). This is also supported by the observation that vagal blockade does not inhibit GRP mediated gastrin release (Greenberg et al. 1985). Different stimulatory signals converge and collectively result in the elevation of cytosolic cyclic adenosine monophosphate (cAMP), intracellular calcium and stimulate pathways leading to the activation of protein kinase C (Campos et al. 1990).

Fasting gastrin concentration is reported to be in the range of 15-30 pM among healthy individuals (Blair et al. 1975). Variations in concentration can be attributed to different fasting conditions and methodology of detection or type of immunoassay applied. Age of individuals is also reported to be a factor that influences basal gastrin concentration. Although gastrin response is dependent on G cell mass and feeding dose, hence the applied test meal in related research, interestingly majority of studies report a similar peak gastrin

concentration (100-150 pM) independent form composition and caloric content of consumed meal in healthy volunteers (Blair et al. 1975, Woussen-Colle et al. 1977). This however does not necessary resemble gastric acid output. A more sophisticated meal related gastrin response can be calculated by deducting preceding fasting values from integrated gastrin responses (measured as area under curve taking temporal course into consideration). Comparison of latter showed gastrin concentrations higher in the group receiving protein and calorie enriched meals (Blair et al. 1975).

Gastrin both directly and indirectly (through ECL cell, see below) simulates gastric acid secretion, which in turn serves as a negative regulator. The pH threshold for complete inhibition of gastrin secretion by gastric acid in normal tissue is around pH 2.5 (Walsh et al. 1975). This is achieved via inhibition of gastrin release through somatostatin and simultaneous liberation of intestinal enterogastrone secretin (Johnson et al. 1971). Somatostatin release form D cells located in the oxyntic mucosa is the main paracrine inhibitor acting on G, parietal and ECL cells (Schubert 2017). Furthermore, glucagon-like peptide-1 (GLP-1) secreted by intestinal L cells also contributes to decreased gastric acid production through stimulating D cells (Schubert 2016).

1.2.3.2 Physiological effects of gastrin

It is well established that gastrin plays an important role in the regulation of gastric acid secretion. Postprandial elevation in serum gastrin concentration results in the liberation of histamine from enterochromaffin-like (ECL) cells in the corpus mucosa, which then acts in a paracrine manner on acid-secreting parietal cells to cause gastric acid secretion (Figure 1.2). Immunophenotyping of the gastrin receptor in stomach revealed CCK2R expression by both ECL cells and also parietal cells of the gastric mucosa. Experimental data from mice that are null for the *gastrin* gene or *CCK2R* gene, suggest, however, that CCK2Rs are more likely to be involved in the maturation of parietal cells rather than providing a direct route for acid stimuli (Koh et al. 1997, Wang et al. 1999). Moreover, gastrin is also capable of regulating production and storage of histamine in ECL cells via stimulating histidine decarboxylase and vesicular monoamine transporter type 2 involved in the synthesis and transportation of histamine into secretory vesicles (Dimaline et al. 1996, Hocker 2004).

Gastrin plays an important role in the organisation of gastric epithelium. Thus, it regulates the numbers of both parietal and ECL cells. The effect on ECL cells is particularly evident in hypergastrinaemic conditions for example due to long term PPI therapy, gastrin secreting tumours or chronic inflammation leading to loss of parietal cells (Jensen 2002). Moreover, the trophic effect of gastrin can result in ECL hyperplasia. If inflammation (due to i.e. pernicious anaemia) or mutation of the *menin* gene (responsible for MEN-1, see below) is simultaneously present this can lead to dysplasia or the development of

neuroendocrine tumours (NETs, previously known as carcinoids).The latter are reported to develop in 30% of patients with gastrinomas as part of the autosomal dominant hereditary multiple endocrine neoplasia type-1 (MEN-1) syndrome and in 5% of patients with pernicious anaemia (Bordi et al. 1995, Gibril et al. 2004).

Gastrin stimulates maturation and proliferation of progenitors cells found in the isthmus part of gastric glands. Since this niche of gastric epithelial precursor cells are not recognised to express CCK2R the mitogenic effect of gastrin is likely to be mediated indirectly through other growth factors e.g. members of EGF (HB-EGF, TGFα) and REG family (Figure 1.2) (Miyazaki et al. 1999, Dockray et al. 2001).

Precursor gastrins have recently been identified to exert their own biological effects. The importance of this in normal gastric physiology is still under debate, however it looks that there might be a synergistic relation with amidated gastrins in regulating acid secretion (Dockray et al. 2001). In colonic epithelium they are reported to induce hyperproliferation and increase risk of colorectal cancer. The receptor on which they act is thought to differ from CCK2R, although in transgenic mice overexpressing progastrin deletion of CCK2R resulted in an abolished proliferative effect suggesting the presence of a CCK2R dependent pathway beside the previously identified P42/44 MAP kinase and Src tyrosine kinase signalling (Hollande et al. 2001, Jin et al. 2009). More data is available on the pro-tumorigenic and co-carcinogenic effect of progastrin and glycine extended precursor forms. The former is also reported to have a pro-angiogenic effect by inducing vascularisation and endothelial

permeability in colorectal cancer (Najib et al. 2015). Expression of precursor gastrins in transgenic mice was shown to increase the numbers of colonic goblet cells (Koh et al. 1999), furthermore similar results were achieved after ionising radiation where progastrin stimulated mitosis of murine colonic epithelium compared to wild type or gastrin overexpressing mice (Ottewell et al. 2003). Overall it looks like non amidated gastrines mainly target colonic mucosa and have a proliferative effect (Singh et al. 2012).

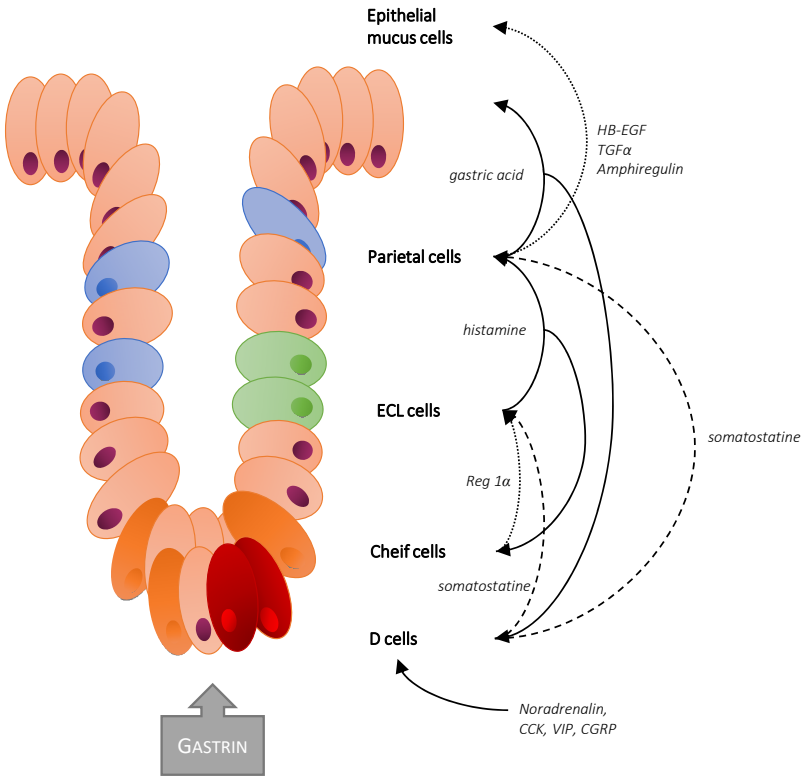

Figure 1.2. Effects of gastrin on different cell types of the gastric epithelium. Continuous arrows represent stimulatory while dashed arrows indicate inhibitory feedback loops. Dotted arrows show factors liberated as a result of chronic hypergastrinaemia.

1.2.4 The gastrin receptor

The gastrin family consists of two members: cholecystokinin (CCK) and gastrin itself. Both of them act at G-protein coupled receptors, CCK1R and CCK2R, albeit with different affinity. Gastrin is the predominant agonist for the CCK2 receptor in the periphery (in the brain there is abundant CCK2R and CCK is the main ligand), while CCK has similarly affinity towards both receptors (Dockray et al. 2012). Although there is a 50% homology in amino acid sequence between the two receptors structural studies found a five amino acid segment located in the second extracellular helix of CCK2R to be responsible for a 100-fold selectivity towards gastrin (Silvente-Poirot et al. 1996). The postprandial circulating concentration of gastrin is almost 10 fold higher than that of CCK thus competitive agonism favours former.

There are multiple splice variants of CCK2R. Among the first characterized was an intron 4-containing splice variant: CCK2Ri4sv mRNA expression was later found to be present in the majority of insulinomas, gastrointestinal stromal tumours (GIST) and small cell lung cancer (SCLC) examined (Körner et al. 2010). Retained intron 4 was related to constitutive gene activity increasing proliferation thus promoting tumour growth. Ryberg et al. identified other variants with deletions in intron 4 and exon 5 resulting in truncated proteins (Ryberg et al. 2011). A single nucleotide polymorphism at positon 32 in intron 4 was related to increased risk and poor survival of pancreatic adenocarcinoma patients (Smith et al. 2012). Somatic mutations in the coding regions of *CCK2R* have also been linked to angiogenesis and increased

migration of cancer cells through stimulation of VEGF, MMP-2 and IL-8 expression in colorectal and gastric cancers (Willard et al. 2012).

The Gαq/11 subunit of heterotrimeric G-proteins couples to 7 transmembrane domain receptors and is responsible for conveying the effect downstream of CCK2R activation. Classical pathways include activation of phospholipase C, which by inducing a rapid hydrolysis of phosphatidylinositol bisphosphate cleaves inositol trisphosphate from the lipid membrane and simultaneous activates protein kinase C via diacylglycerol contributing to the liberation of Ca^{2+} from internal stores (Dufresne et al. 2006, Dockray et al. 2012). Additional pathways have also been reported to be affected by gastrin. Mitogen-activated kinase cascades consist of a heterogeneous group of serine/threonine kinases of which extracellular signal-regulated kinase 1/2 (ERK1/2) has been shown to be regulated by CCK receptors (Mao et al. 2014). This particular protein cascade is involved in cell migration and proliferation through transcriptional regulation of targeted genes. Gastrin is also capable of inducing autophagy through upregulation of AMPK proteins thereby stimulating RAS/Raf/MEK pathways and assembly of autophagosomes (Kun et al. 2017). By promoting the release of HB-EGF and inducing direct phosphorylation of EGF receptors, transactivation by gastrin is also part of the broad spectrum of diverse signalling pathways which have recently been proven to modulate the angiogenic potential of endothelial cells (Clarke et al. 2006). The effect of gastrin on cell proliferation is also conveyed through JNK and p38-MAPK cascades via CCK2R activation (Dehez et al. 2002). Tyrosine phosphorylation of focal adhesion kinases (i.e. p125-FAK, p130Cas, paxillin), which are

responsible for cell morphology and stress fibre formation have also been described as a downstream effect of CCK2R activation (Li et al. 2008). Janus kinases (JAKs) are known to be associated with the binding and phosphorylation of a distinct group of “signal transducers and activators of transcription (STATs)” family of transcriptional factors. Gastrin was shown to stimulate JAK2/STAT3 pathway through the $G_{\alpha/q}$ subunit and NPXXY segment of the seventh TM domain of CCK2R (Ferrand et al. 2005). Receptor activation on the other hand can be limited by RGS2 desensitisation. Internalisation of CCK2R via β-arrestin 1 or 2 binding is another way to restrict signalling mechanisms (Magnan et al. 2011).

CCK2 receptors can be found on a number of gut cells i.e. ECL cells, parietal cells or smooth muscle cells. Despite being recognised mainly for their role in regulating acid secretion, there have been reports showing upregulated CCK2 expression in response to tissue damage suggesting a putative role of the receptor in orchestrating epithelial regeneration by affecting proliferation. This however is still not yet fully understood (Schmassmann et al. 2000, Ashurst et al. 2008).

Non classical gastrin receptors

Progastrin, Gly-extended forms and even the C-terminal flanking peptide (CTFP) of progastrin have been all linked to biological effects mainly involving stimulation of proliferation and inhibition of apoptosis via PI3-kinase dependent pathways (Patel et al. 2010). These effects, however, are not mediated

through CCKR2 and are often exhibited only by cancer cells. There has been research focusing on putative targets for these alternatively processed proteins. Annexin A2 was suggested as a potential non-classical gastrin receptor. Sarkar et al. reported a clathrin-mediated internalisation of progastrin and a subsequent activation of p38MAPK/ERKs pathways (Sarkar et al. 2012). Others found the F1 subunit of ATPase to be involved in mediating the effect of precursor gastrins (Kowalski-Chauvel et al. 2010).

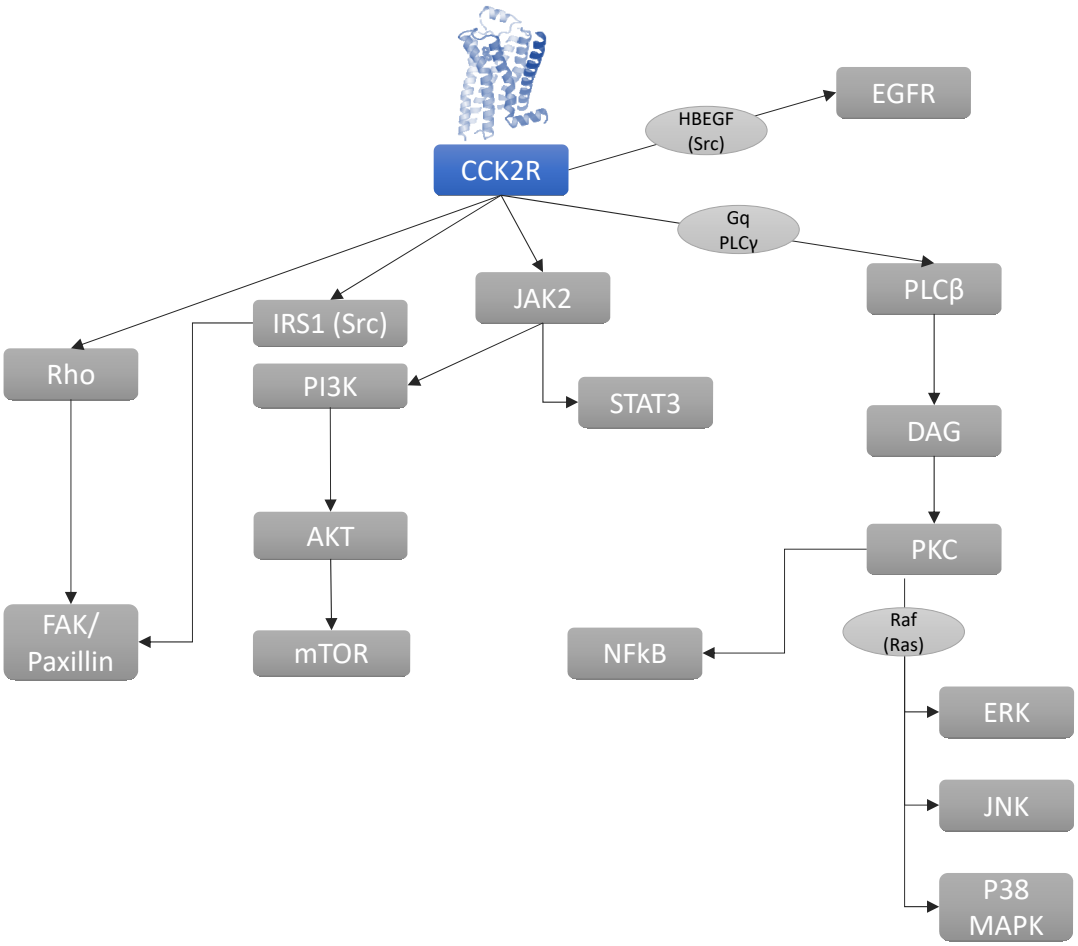

Figure 1.3. Schematic representation of pathways activated by the CCK2 receptor.

1.2.5 Role of CCK2R and gastrin in cancer

A substantial body of evidence from transgenic rodent models, cell line experiments and clinical studies support the fact that gastrin and CCK2R are expressed by a number of malignancies and can promote cancer development by increasing invasiveness and proliferation of tumour cells (Ferrand et al. 2006). This can be both direct through CCK2R, indirect through paracrine liberation of growth factors and by autocrine signalling resulting in a continuously active self-simulating niche of cancer cells. Merchant et al. provided evidence that the *gastrin* gene itself is a potential target of oncogenic pathways (Merchant et al. 1991). Mutation in the *Apc* gene was reported to result in reduced gastrin expression, while Wnt signalling via β-catenin resulted in overexpression of the *gastrin* gene (Lei et al. 2004). Interestingly, the reverse is true for gastrin, which can induce nuclear translocation of catenins and stimulate expression of cyclin D1 (see section X.X). This crosstalk is also present between Wnt, TGF- β and Ras pathways proving the *gastrin* gene to be target of multiple cancer signalling routs.

Apart from its well-known physiological effects, gastrin is a potent growth factor for the gastric mucosa and promotes invasiveness of tumour cells. Epithelial to mesenchymal transition is a phenomenon observed in cancer development and can be characterised by malignant cells acquiring mesenchymal features. Alteration of cellular morphology and intercellular connections are key features of this process, together with increased cell migration and invasion (Noble et al. 2003). Gastrin was reported to decrease intercellular adherent junctions via CCK2R by stimulating Src and ERK pathways leading to internalisation of β

catenins and eventually disrupting adhesions to the extracellular matrix (Bierkamp et al. 2002). Through affecting JAK2 signalling gastrin was found to stimulate cell migration, moreover in cell culture experiments with gastric adenocarcinoma cell lines upregulation of MMP-2 and 9 was observed (Wroblewski et al. 2002).

Gastric cancer is one of the leading causes of death worldwide with an incidence of 3-10% of all cancer related deaths (Dicken et al. 2005). Out of the multifactorial causes that can lead to gastric cancer formation amidated gastrins gained attention after research in this field revealed a strong relation between *H.pylori* infection, secondary hypergastrinaemia and the combined contribution of these to cancer development. In *H.pylori* positive INS-GAS mice models overexpressing amidated gastrin a significant temporary burst was observable in the number of parietal and ECL cells, which compared to *H.pylori* free controls showed an accelerated progress of endocrine cell loss and pronounced epithelial atrophy, which was followed by dysplasia and finally adenocarcinoma formation (Wang et al. 2000). Gastrin was shown to upregulate HB-EGF, cyclin D1, COX-2 and Reg gene expression, which taken together with the fact that histological examination of these tumours also revealed CCK2R expression suggests a strong endocrine effect on cancer growth.

The pancreatic adenocarcinoma cell line AR42J and transgenic ElasCCK2 mice also showed signs of both CCK2R expression and *gastrin* gene upregulation. Receptor expression contributed to tumour growth in both cases (Mathieu et al. 2005). In humans compared to rodents there is conflicting data

on CCK1R and -2R expression in pancreatic tissue, however it looks like CCK2R is mainly expressed by islet cells and rarely in acini or ducts in healthy individuals. Interestingly in chronic pancreatitis some acinar cells were found to exhibit CCK2R expression, however that majority of pancreatic adenocarcinomas were negative for CCK2R expression (Reubi et al. 2003). It is of note, that the majority of gastrins expressed by pancreatic adenocarcinomas consist of non-amidated forms.

Barrett's metaplasia often arises in patients with gastroesophageal reflux disease (GORD), where constant exposure of the oesophageal lining to irritating gastric acid results in metaplastic changes resembling intestinal-like columnar epithelium with goblet cells. Histological analysis of endoscopic biopsies from metaplastic sites found CCK2R expression (Haigh et al. 2003). Cell culture experiments confirmed stimulation of Erk and PI3 pathways leading to increased proliferation following gastrin administration (Moore et al. 2004). Since PPIs are used as the first line of treatment for GORD, and lead to hypergastrinaemia, there is a fear that they might therefore contribute to cancer development: long term administration of acid inhibitors should be avoided therefore where there is a potentially increased risk of malignant changes.

Neuroendocrine tumours including vipomas, insulinomas, NETs of the bronchial structures and small intestine are frequent sites of CCK2R expression (Reubi et al. 2003). Moreover, gastrin receptors were also found to be present in tumours of organs outside the gastrointestinal tract i.e.

astrocytomas, stromal ovarian cancer, Wilms' tumor, leiomyosarcomas, small cell lung cancer and medullary thyroid carcinomas (Reubi et al. 1997). A pentagastrin stimulation test is widely used in the latter case as a diagnostic tool based on stimulation of calcitonin release via activation of CCK2R expressing tumorous parafollicular C cells (Wells et al. 1978).

Based on the fact that CCK2Rs are expressed by a broad variety of cancers and therefore possess the ability to promote cancer progression through increasing proliferation and invasion of tumour cells they also provided a putative target for diagnostic and therapeutic approaches i.e. receptor scintigraphy or radionuclide therapy which is currently under intense research given its great potential (Kaloudi et al. 2015).

1.2.6 Relation of *Helicobacter pylori* and gastric cancer

Helicobacter pylori is a Gram negative microaerophilic bacterium first described by Marshall and Warren in 1982 (Warren et al. 1983). It is capable of colonising gastric epithelium by producing urease, which neutralises gastric acid via hydrolysis of urea into ammonia and carbonic acid (Hu et al. 1992). Through adhesins such as adherence lipoprotein A and B (AlpA/B), blood group antigen binding adhesion (BabA), outer inflammatory protein A (OipA) and sialic acid binding adhesion (SabA) proteins bacteria is capable of binding to the gastric mucosa (Logan 1996). *H.pylori* infection remains mainly extracellular and inflammation is achieved by multiple factors. Ammonia produced by the bacterium is a chemical irritant towards the gastric mucosa, proteases like vacuolating cytotoxin A (VacA) and cytotoxin associated gene A (CagA) contribute to direct cellular damage, furthermore depending on bacterial localisation regulation of acid secretion might also be disrupted resulting in hypo- or hyperchlorhydria (Dixon et al. 1996, Liu et al. 2012).

The prevalence of *H.pylori* infection in still high worldwide and is estimated to be over 50% in east European countries. The majority of infections remain asymptomatic and therefore often undiagnosed providing a large reservoir of carriers (Cave 1996). Interpersonal transmission and contaminated water supplies are recognised to be the main source of infection especially among people with low socioeconomic circumstances (Axon 1995, Schwarz et al. 2008, Eusebi et al. 2014). Genetic polymorphisms in CagA and VacA expression are related to different risks of malignant transformation. Cag-

positive and VacA s1/m1 *H.pylori* strains are associated with high risk of developing gastric cancer (Correa et al. 2012).

H.pylori infection results in the inhibition of H^+,K^+-adenosine triphosphatase expressed by gastric parietal cells. Binding of virulence factors of the type IV secretion system (T4SS) to epithelial membrane bound integrin $\alpha_5\beta_1$ lead to internalisation of this complex and stimulates ADAM17 dependent liberation of HB-EGF. Subsequent EGFR activation results in the repression of H^+,K^+-ATPase expression through ERK1/2 kinase cascade by binding of NF-κB homodimer to the promoter segment of the *H^+,K^+ ATPase* gene (Smolka et al. 2012).

H.pylori mediated acute gastritis is mainly associated with hypochlorhydria and infiltration of the lamina propria with polymorphonuclear neutrophils (Morris et al. 1987, Correa et al. 2012). This is mostly dominated by a T-helper 1 type pro-inflammatory response involving interleukin 1β (IL-1 β), tumour necrosis factor α (TNFα) and interferon γ (IFNγ) (Blanchard et al. 1998). Over time this can evolve into chronic active gastritis characterized by mononuclear cell invasion (Correa et al. 2012). Depending on the localisation, types of antrum- or corpus-predominant and pangastritis can be distinguished (Dixon et al. 1996). The former is associated with hypergastrinaemia and increased acid secretion due to simulation of G-cells. Prolonged inflammatory processes, however, may result in glandular atrophy and subsequent hypo- or achlorhydria (Sipponen et al. 2002, Vaananen et al. 2003). These changes are mainly characteristic for corpus-predominant type gastritis.

The consequences of untreated *H.pylori* infection include peptic and duodenal ulceration, MALT lymphoma and gastric cancer (Polk et al. 2010). The latter is the second leading cause of cancer-related death worldwide. The steps of malignant transformation include non-atrophic chronic gastritis, which can advance to multifocal atrophic gastritis (MAG), followed by complete and incomplete intestinal metaplasia (GIM), then low and high grade dysplasia (Correa et al. 2012). The latter is considered as *in situ* carcinoma and can progress into invasive gastric cancer if left untreated. Several studies report *H.pylori* eradication to reduce the overall risk of gastric cancer, however it does not seem to affect metachronous cancer development (Maehata et al. 2012). Eradication of the bacteria is likely to alter the cellular phenotype of the gastric mucosa though (Watari et al. 2008). Chan et al reported a reverse in the methylation status of the *E-cadherin* gene after eradication therapy in patients with chronic gastritis (Chan et al. 2006).

Overall *H.pylori* is an aggressive pathogen for the gastric mucosa, which depending on the bacterial strain and host genotype can potentiate gastric carcinogenesis by initiating inflammatory responses and altering normal gastric epithelial physiology. On the other hand, it also provides potential biomarkers i.e. CagA oncoprotein to identify patients at higher risk of developing gastric tumours.

1.2.6.1 Effects of long term acid suppressive treatments

Proton pump inhibitors (PPIs) first introduced in the 1980s were developed as an effective and safe drug for the treatment of hyperacidity related gastric disorders including gastroesophageal reflux diseases (GERD), peptic ulcer or dyspepsia.

Overutilization of PPIs is becoming an increasing problem since unjustified prescription only exposes patients to a health risk (Heidelbaugh et al. 2012). Acid secretion inhibitor overuse in ambulatory practice is confirmed by a number of large scale studies. In almost half of the cases prescription of PPI or histamine receptor antagonist are clinically unsubstantiated (Jacobson et al. 2003, Heidelbaugh et al. 2010). In a retrospective study carried out on the General Practitioner Research Database for the former West Midlands region including 612,700 patients found that in a 5 year long period prescription of PPIs rose 10-fold with repeat prescribing rising to 77% of total in the UK. Unlicensed indications i.e. non-ulcer dyspepsia and non-specific abdominal pain also showed increase (Bashford et al. 1998).

A systemic review of 16 studies with a total of 1920 patients investigating the effect of long-term PPI usage revealed that moderate hypergastrinaemia and increased prevalence of NET occur most commonly (Lundell et al. 2015). Another important discovery was that patients with pre-existing *H.pylori* infection are more prone to corpus-predominant gastritis, where PPI usage is responsible for the alteration of antrum to corpus predominant localisation, which is known to have a higher risk of developing gastric cancer (Uemura et

al. 2000). Moreover, Uemura et al. report that even temporary use of PPIs can aggravate corpus predominant gastritis of *H.pylori* positive patients (Uemura et al. 2000).

Use of acid secretion inhibitors therefore requires caution since it might worsen symptoms and disease progression especially in patients with *H.pylori* positive gastritis.

1.2.7 Gastrin regulated genes

As mentioned, gastrin stimulates ECL cells to release histamine and therefore gastric acid secretion. Three genes are involved in the biosynthesis and storage of histamine that are known to be regulated by gastrin, namely: histidine decarboxylase (HDC), vesicular monoamine transporter 2 (VAMT2) and chromogranin A (CgA). There is a common pathway involving activation of Raf/MEK/ERK1/2 cascade which is independent of Ras, however diversity occurs at the level of *cis*- and *trans*-activating regulatory factors and enhancer elements (Dockray et al. 2005. HDC, which is a pyroxidal dependent enzyme responsible for the decarboxylation of histidine to histamine is regulated by two as yet uncharacterised gastrin responsive element binding proteins (1 and 2) acting on the promoter segment of HDC gene {Hocker, 2004 #337). CgA is a neuroendocrine secretory protein that plays a role in the generation of secretory granules and contributes to vesicle stability. Binding of Sp1, CREB and Egr-1 transcriptional factors are recognised to mediate the effect of gastrin on the CgA gene (Dufresne et al. 2006). The *VMAT2* gene, which encodes an integral membrane protein responsible for the transport of histamine into secretory vesicles contains two overlapping promoter elements i.e. AP2/Sp1 site and CRE consensus element, which are regulated by an uncharacterized nuclear protein and CREB respectively (Dimaline et al. 1996, Dufresne et al. 2006).

Gastrin is capable of regulating cell growth by stimulating proliferation. This effect is mediated by upregulation of growth related genes including *c*-f*os, c*-j*un* and *c*-m*yc*. Gastrin-induced expression of the latter proto-oncogenes is not

yet fully elucidated but multiple pathways have been identified to be involved in c-Fos activation. The classical trophic effects of gastrin are mediated through MAPK pathways which requires a PKC dependent binding of ternary complex factors (TCFs) to the serum response element (SRE) to achieve promoter activation of *c-fos* (Stepan et al. 1999). Gastrin regulation of the cell cycle via cyclins D1, D3 and E has been reported (Zhukova et al. 2001). Gastrin seems to increase cyclin D1 expression through binding of CREB and β-catenin to CRE and TCF sites of the cyclin D1 promoter in gastric adenocarcinoma cell line AGSE (Pradeep et al. 2004).

A number of studies confirmed the upregulation of Reg proteins in response to tissue damage in various organs e.g. after partial pancreatectomy, nerve injury, Alzheimer's disease. In the stomach, it is thought to promote mucosal growth. Gastrin stimulates expression of Reg proteins through transcriptional activation of Reg-1 gene by SP1 and SP2 via activation of PKC and RhoA in gastric ECL cells (Ashcroft et al. 2004).

Plasminogen activator inhibitor-2 expression (PAI-2), which exhibits low levels in normal gastric epithelium was found to be increased in hypergastrinaemic conditions and gastric cancer. Direct activation of CCK2Rs result in PKC mediated binding of CREB and c-jun to CRE and AP-1 sites respectively (Varro et al. 2002).

Moreover, studies with colonic and gastric cell lines report upregulation of COX-2 gene expression through ERK1/2 and PI3 cascades (Colucci et al. 2005). COX pathways have been well researched in the last few years regarding their role in colon cancer formation. The observation that mortality

of colorectal adenocarcinomas significantly decreased in patients on anti-inflammatory drugs was attributed to the inhibition of COX enzymes and thus reduced turnover of arachnoid acid into prostanoids (Dubois et al. 1998). Similar results were obtained with intestinal epithelial cells where gastrin simulated expression of COX-2 and thereby the production of PGE2 and downstream recruitment of EP4 receptors through MAPK signal pathways involving ERK5 kinase and EGFR transactivation. Binding of activating transcription factor-2, activator protein-1 and myocyte enhancer factor-2 to COX-2 promoter was responsible for induction by gastrin (Guo et al. 2002).

Finally, the ability of gastrin to influence gastric epithelial organisation and remodelling by proteolytic degradation of extracellular components was found to be mediated in part by upregulation of matrix metalloproteinase-9 (MMP-9) and MMP-7 in gastric cancer cells and stomach biopsies of patients with chronic hypergastrinaemia (Wroblewski et al. 2002). Moreover, MMP-7 was found to induce epithelial-mesenchymal transition and proliferation of myofibroblasts (Varro et al. 2007). Induction of PKC/Raf/Ras/MEK pathways were identified to mediate stimulatory effect of gastrin resulting in increased invasion of cancer cells (Wroblewski et al. 2002).

Overall gastrin seems to affect the cellular composition and architecture of the gastric mucosa through regulating a number of genes. Long term effects especially in upregulation of growth related genes can therefore contribute to progression of tumours of the alimentary tract.

1.3 Myofibroblasts

In recent years, myofibroblasts have emerged as important determinants of mucosal organisation in health and disease (Ohlund et al. 2014). The role of these cells in wound healing in many different tissues is well known (Powell et al. 1999). In addition, however, a sheath of myofibroblasts lies just under the basement membrane in the gastrointestinal tract and is responsible for the secretion of a number of proteins involved in extracellular matrix formation and turnover, as well as a range of growth factors including insulin-like growth factors (IGF)-1 and -2 (Hemers et al. 2005, Powell et al. 2005). In cancer, it is now clear that modified myofibroblasts (cancer-associated myofibroblasts, CAMs) play a role in defining the cancer niche and in influencing cancer progression (De Wever et al. 2008). These cells may originate by epithelial-mesenchymal transition (McCracken et al. 2014), from inward migration of bone-marrow derived mesenchymal stem cells (Quante et al. 2011), or from tissue-resident cells including fibroblasts and pericytes (Hosaka et al. 2016). Recent studies confirmed, that CCK2R is expressed in the gastric mucosa and submucosa of cryoinjured rats; these cells were later identified as myofibroblasts based on coexpression of vimentin and smooth muscle α actin (α-SMA) (Ashurst et al. 2008). This raises the possibility of a novel yet uncharacterized niche of stromal cells expressing the gastrin receptor, which might add a new dimension to the known effects conveyed by the enteral hormone. The regulation of myofibroblast function and the role of CCK2R in this aspect remains incompletely understood and needs further research.

1.4 Cutaneous melanoma

1.4.1 Epidemiology, diagnosis and clinical types of melanoma

Melanoma is a tumorous malformation of melanocytes located in the *stratum basale* of the epidermis primary responsible for melanin synthetisation. It mainly affects skin, but can also occur on mucosal surfaces, meninges or choroid (Kanitakis 2002). The reported incidence of melanoma is increasing annually affecting hundreds of thousands of people worldwide. This increase is fast compared to other solid tumours and currently melanoma is thought to be the 15th most common cancer worldwide (Ferlay et al. 2015). It affects mostly the middle aged population with a female predominance, however gender distribution changes over the years with males being overall 1.5 fold more prone to develop melanoma throughout their lives (Markovic et al. 2007). Among the risk factors, chronic or intermittent sun exposure is the most important one. This is best represented by the fact that the highest melanoma incidence accounting for 4-6 cases/10,000 inhabitants can be found in Australia where the combination of a predominantly fair skinned population and strong sun light is particularly striking (MacKie et al. 2009). Interestingly, in Europe there is a gradient from north to south with a decreasing incidence (MacKie et al. 2009). This is most likely due to the difference in UV protection practices and sun exposure between these countries. Mortality-to-incidence ratios were reported to be between 0.09-0.44 in Europe as a whole and specifically 0.23 for Hungary - meaning one death for an estimated four new cases yearly (Forsea et al. 2014).

In addition to environmental factors (mainly sun exposure), genetic susceptibility also provides a risk for melanoma formation. Compared to chronic exposure, which is more often associated with non-melanotic skin cancer, intermittent sun exposure especially with multiple cases of previous sunburns provides an increased risk for melanoma (Elwood et al. 1997). Beside the UV-B spectrum of sun light (315-400 nm), which is responsible for direct DNA damage, UV-A (280-315 nm) exposure from tanning bed or radiation photochemotherapy used for the treatment of psoriasis have also been reported to increase melanoma risk (Stern 2001, 2007). Host risk factors include the presence of multiple congenital and acquired melanocytic nevi, genetic susceptibility and hereditary syndromes. Bevona et all. reported that 25% of melanomas arise on pre-existing nevus (Bevona et al. 2003). A meta-analysis assessing the risk factors for cutaneous melanomas found that patients who have over 100 nevi are 7-fold more prone to develop melanoma (Gandini et al. 2005). Similar discoveries were made in relation to size, irregular border and inhomogeneous pigmentation characteristic for atypical or dysplastic nevi, which possess a high risk of malignant transformation (Tucker et al. 1997). Melanocortin 1 receptor (MC1R) polymorphism responsible for different skin pigmentation among various ethnical groups also plays a role in UV vulnerability of skin. The white population has a 10-fold risk of developing melanoma compared to people with darker skin tone (Lasithiotakis et al. 2006, Dessinioti et al. 2011). Hereditary cases are generally considered to be rare. The familial atypical multiple mole-melanoma syndrome (FAMMM syndrome), the melanoma-astrocytoma syndrome (MAS) with cyclin-dependent kinase inhibitor 2A or 4 mutations, *xeroderma pigmentosum*, familial retinoblastoma,

Lynch syndrome type II and Li-Fraumeni cancer syndrome are amongst the ones reported as inheritable conditions with increased risk of melanoma (Goldstein et al. 2001, Soura et al. 2016).

Early diagnosis is crucial, since a favourable prognosis exponentially decreases with the depth of invasion. Definitive diagnosis is based on histology and immunohistochemistry, however there are clinical signs which are suggestive of malignancy. The ABCDE criteria referring to asymmetry, irregular boarders, inhomogeneous pigmentation (colour), large size (diameter > 6 mm), evolving phenotype are widely used among clinicians to identify lesions suspect for melanoma (Rigel et al. 1993, Robinson et al. 2006). Other less commonly used guidelines e.g. the Glasgow checklist, are also available (MacKie 1990). The latter contains 3 major (size, shape, colour) and 4 minor (inflammation, crusting or bleeding, paraesthesia, diameter) criteria, the presence and, or, change of which determine the score. Dermoscopical features of melanoma include an atypical pigment network usually with reticular pattern, irregular dots and streaks (pseudopods), inhomogeneous pigmentation, regression structures (as a combination of fibrosis and melanosis), blue-whitish veil and hairpin vessels (Neila et al. 2011).

There are four major subtypes of invasive cutaneous melanoma: superficial spreading (SSM), nodular melanoma (NMM), *lentigo maligna* melanoma (LMM), and acral lentiginous melanoma (ALM) (Markovic et al. 2007, Paek et al. 2008). SSM accounts for the majority of cases (above 70%). It is usually associated with a pre-existing nevus and presents as a thin plaque rarely affecting deeper structures. NMM is mainly located on the trunk and limbs.

Ulceration is a frequent feature. Aggressive behaviour is best represented by the rapid vertical growth phase and metastasis formation (Duncan 2009). LMM occurs on skin areas exposed to long term sunlight i.e. head and neck. It usually affects the elderly population and occurs in form of a gradually enlarging lesion arising from a precursor *lentigo maligna*. ALM is the least frequent form localized plantar, palmar and subungual surfaces. It is most often found among dark-skinned ethnicities (Duncan 2009).

Rare forms include desmoplastic melanoma, which usually presents as a amelanotic, flash-coloured papule, rhabdoid melanoma, myxoid melanoma, osteogenic melanoma and spitzoid melanoma, the latter morphologically resembling Spitz tumours (Markovic et al. 2007). Because of the low occurrence rate and atypical features histological differentiation of these lesion can be challenging, often requiring additional molecular tests.

1.4.2 Biology of melanoma

Under physiological circumstances, UV radiation stimulates keratinocytes to produce melanocyte stimulating hormone (MSH), which in turn binds to MCR1 on melanocytes resulting in melanin production. This provides a protective layer and protects against UV-mediated DNA damage of cells (Lin et al. 2007).

Melanoma is considered as one of the most aggressive form of cancer due to its metastasising capability. Disrupting the peritumoural stroma through upregulated expression of matrix metalloproteinases is a key component of melanoma invasiveness. For alterations present in the tumour microenvironment see section 1.4.3.

It is now recognised that there is no single evolutionary trajectory for melanoma development. Different subtypes can evolve from different precursor lesions with different combinations of gene mutations involved (Table 1.1). However three driver mutations have been identified: B-Raf proto-oncogene (BRAF), neurofibromin 1 (NF1) and neuroblastoma RAS viral oncogene homolog (NRAS)) which are present in majority of melanomas (Leonardi et al. 2018). Even so, these mutations do not necessarily mean there is malignant transformation from a pre-existing nevus into a cutaneous melanoma (Shain et al. 2016). Interestingly, mutation of the BRAF gene can be found in 80% of benign nevi which rarely progress further and remain indolent due to immune cell mediated attrition (Speeckaert et al. 2011). Usually, secondary and tertiary mutations targeting genes regulating growth and metabolism (i.e. phosphatase and tensin homolog (PTEN) and KIT proto-oncogene receptor tyrosine kinase), cell identity (i.e. AT-rich interaction domain 2 (ARID2)),

resistance to apoptosis (i.e. tumour protein p53 (TP53)), cell cycle control (i.e. cyclin-dependent kinase inhibitor 2A (CDKN2A)) or pre-existing mutations of genes controlling replicative lifespan (i.e. telomerase reverse transcriptase (TERT)) are needed for progression towards invasive melanoma (Shain et al. 2016, Leonardi et al. 2018).

The major driver somatic mutations (BRAF, NRAS, NF1, KIT) affecting crucial cellular process play a central role in the high proliferative capacity of melanoma cells. RAS/RAF/MEK/ERK and PI3K/AKT are the two main pathways responsible for conveying the effect (Chappell et al. 2011).

Up to 50% of melanomas are reported to carry a missense mutation of the BRAF gene, namely a glutamic acid substitution at valine 600 (V600E), less frequently lysine, aspartic acid or arginine (V600K, V600D, V600R respectively) (Davies et al. 2002). BRAF is a serine/threonine protein kinase responsible for the phosphorylation of the mitogen activated protein kinase family. Substitution of valine to glutamic acid results in an altered conformation of the catalytic domain leading to a constantly active BRAF protein (Wan et al. 2004). The NRAS proto-oncogene, which is a member of the Ras gene family responsible for regulating cell growth was found to be mutated in 15% of melanomas (Hodis et al. 2012). A point mutation at codon 12,13 (exon 1) or 61 (exon 2) results in prolonged NRAS signalling causing constitutive activation of MAPK and PI3K pathways (Jakob et al. 2012). This is one of the mechanisms responsible for therapeutic resistance against BRAF inhibitors i.e. vemurafenib or dabrafenib (Fedorenko et al. 2013).

Similar hyperactivation of NRAS mediated pathways occurs in melanomas with mutation of the neurofibromin 1 (NF1) gene. This tumour suppressor gene encodes a GTPase and regulates RAS family by hydrolysing RAS-GTP to inactive RAS-GDP severely impairing negative control of MAPK and PI3K signalling (Maertens et al. 2013).

The NF1 mutation was first described as part of the familial cancer syndrome, neurofibromatosis type 1, but recent studies indicate the presence of a dysfunctional protein in glioblastoma and lung cancer also (Ding et al. 2008, McGillicuddy et al. 2009). Mutation of NF1 in melanoma genesis prevents BRAF mediated oncogene-induced senescence (OIS) (which is a protective response to restrict progression), subsequently leading to increased tumour cell proliferation and accelerated melanoma progression (McGillicuddy et al. 2009). Additional genetic alterations include mutation of the receptor tyrosine kinase KIT found in 8% of acral and mucosal melanomas. Mutations in the extracellular domain (i.e. exon 11) of the receptor are reported to be responsible for constitutive KIT activation and therefore provide a potential target for KIT kinase inhibitors (Handolias et al. 2010).

Although driver mutations might be initially present in a high percent of benign nevi, accumulation of secondary and tertiary mutations are needed to initiate melanoma genesis. These typically include TERT promoter mutation, CDKN2A alteration and PTEN dysregulation (Leonardi et al. 2018). Telomerase reverse transcriptase (TERT) encoding the catalytic subunit of the enzyme responsible for telomere maintenance is reported to be mutated in 70% of melanomas. Promoter mutation results in a new binding motif for ETS

and TCF transcription factors with a two- to four-fold increase in transcription (Horn et al. 2013, Huang et al. 2013). Homozygous deletion or mutations (i.e. missense, nonsense, frameshift) of cyclin-dependent kinase inhibitor 2A (CDKN2A) results in the lack of inhibition of CDK4 and -6 via p16, which enables melanoma tumour cells to progress unrestrained from G1 to S phase (Castellano et al. 1997, Read et al. 2016). Last but not least, the *PTEN* gene was found mutated in a majority of melanomas (10-30%) (Wu et al. 2003). As a negative regulator of the Akt/PKB signalling pathway it plays a central role in controlling cell growth, survival and migration. It is still controversial whether somatic mutations or epigenetic alterations of PTEN expression resulting in loss of function happen at an early or later stage in melanoma tumourgenesis, but it likely occurs in melanoma subtypes harbouring a mutated BRAF gene (Wu et al. 2003, Hodis et al. 2012).

Understanding the genetic evolution of melanomas throughout their progression from precursor lesions into invasive metastatic forms provides a deeper insight into the complex network of different histological subtypes and various genetic alterations that can be matched to them. This is crucial in finding new therapeutic approaches for cases of non-responder and secondary resistant melanomas.

Gene	*Mutation*	*Pathway*	*Effect*
*B-Raf proto-oncogene (**BRAF**)*	V600E V600K, V600D, V600R	MAPK	Gain of function
*Neuroblastoma RAS viral oncogene homolog (**NRAS**)*	point mutation at codon 12,13, 61	MAPK	Gain of function
*Neurofibromin 1 (**NF1**)*	deletions	MAPK	Loss of function
*Phosphatase and tensin homolog (**PTEN**)*	epigenetic alterations	PI3K	CpG island hypermethylation
***KIT** proto-oncogene receptor tyrosine kinase*	mutations at. exon 11	MAPK, PI3K, JAK/STAT and PLC	Gain of function
*AT-rich interaction domain 2 (**ARID2**)*	disabling mutations	Chromatin remodelling*	Loss of function
*Tumour protein p53 (**TP53**)*	disabling mutations	p53	Gain of function
*Cyclin-dependent kinase inhibitor 2A (**CDKN2A**)*	missense, nonsense, frameshift mutations	RB	Loss of function
*Telomerase reverse transcriptase (**TERT**)*	promoter mutation	Telomerase	Gain of function

Table 1.1. Common mutations in melanoma pathogenesis.

1.4.3 Microenvironment

The tumour microenvironment (TME) is an important determinant of cancer behaviour (Quail et al. 2013). A number of lines of evidence indicate continuous information exchange between tumour cells and different cell types of the TME. Tumour associated macrophages have been described to be capable of altering their polarisation state and acquiring a M2 phenotype known to be associated with pro-tumourigenic behaviour (Biswas et al. 2010). Endothelial-derived cancer associated fibroblasts (CAF) located in the tumour milieu in mouse melanomas were reported to produce a number of growth factors (i.e. VEGF) and activate NFκB signalling pathways promoting intravasation and dissemination of tumour cells (Zeisberg et al. 2007). Besides the classical signalling mechanisms including paracrine acting cytokines, extracellular proteins and chemokines, and tumour derived exosomes have all recently been described in melanomas as a novel way of communication within the TME (Peinado et al. 2012, Quail et al. 2013). Moreover circulating exosomes in stage IV melanoma patients were found to be able to reprogram bone marrow derived cells via MET upregulation towards a vasculogenic phenotype thereby contributing to the development of pre-metastatic niches in target organs (Boccaccio et al. 2006, Peinado et al. 2012). The family of RAB genes were identified as key elements in the regulation of exosome production. Inhibition of Rab27a expression significantly decreased exosome secretion and liberation of other proangiogenic factors such as osteopontin or platelet derived growth factor severely impairing metastasizing capability of melanoma cells (Ostrowski et al. 2010).

Independently from melanoma types metastasis formation involves common steps. Benign melanocytic nevi located in the epidermis that adopt dysplastic changes thereby initiate an accelerated proliferation of malignant cells parallel with the basement membrane (horizontal or radial growth phase(RGP)) (Gaggioli et al. 2007). Melanoma cells at this stage are still embedded in an environment composed mainly of keratinocytes and some dendritic (i.e. Langerhans) cells. Further progression requires genomic and proteomic changes, since by penetrating the basement membrane (vertical growth phase (VGP)) melanoma cells need to adapt to a new microenvironment (Gaggioli et al. 2007). Because cancer cells remain in a cluster with only a few cells detaching that can penetrate smaller ECM gaps, melanoma cells need to alter their cytoskeletal organisation and remodel the surrounding ECM to be able to invade lymphovascular structures. As detailed in section 1.4.2 a number of genetic changes take place during melanoma progression, with the frequency of these significantly increasing when changing from radial to vertical growth (Leonardi et al. 2018). There is still controversy in assigning mutations (driver, secondary or tertiary) to selected time points of progression, nonetheless there are some proteins identified which can clearly be related to vertical spreading. Decrease in E-cadherin expression and upregulation of N-cadherin to form novel connections with stromal components (Smalley et al. 2005), overexpression of MCAM adhesion molecule and increased production of VEGF-A, -C responsible for the recruitment of endothelial cells are crucial for melanoma invasion and metastatic dissemination (Carmeliet et al. 2000, Bogenrieder et al. 2002).

Melanoma migration requires formation of extending protrusions and adhesions followed by contraction and simultaneous detachment to avoid intracellular tension. Continuous remodelling of the surrounding ECM is necessary to allow stromal penetration of tumour cells (Gaggioli et al. 2007). A number of studies report modification of the actin cytoskeleton via activation of TGFα, HGF and SDF-1 receptors, which stimulate the small GTPases Rac1 and Cdc42 leading to polymerization of actin filaments (Kurisu et al. 2005, Ridley 2006). Through integrins, such as αvβ3 characteristic for melanoma and CD44 non-integrin receptors novel focal contacts and adhesions are formed (Hibino et al. 2004, Dang et al. 2006). RhoC was identified as a key regulator of actomyosin-mediated contractility by binding to Rho associated kinases and inhibiting myosin phosphates thus modulating MLC phosphorylation (Clark et al. 2000, Fukata et al. 2001). Proteolysis of ECM elements through upregulated expression of specific matrix metalloproteases (MMPs), serine/cysteine/disintegrin and metalloproteases (ADAMs) are essential for metastasis formation (Hofmann et al. 2000). These enzymes are regulated at a transcriptional (promoter) level by several growth factors, moreover epigenetic and posttranslational mechanism also contribute to their complex regulation (Clark et al. 2008).

The family of metalloendopeptidases consisting of MMPs (matrix metalloproteinase), ADAMs are key players in cancer progression. Expression of collagenases MMP1 and 13 were found to be increased in the vertical growth phase of melanoma by peritumoural stromal cells, mostly fibroblasts (Airola et al. 1999). MMP1 indirectly through PAR1 is capable of promoting

endothelial cell activation thereby enhancing tumour progression, while MMP13 induces vascularisation via release of VEGF from ECM (Goerge et al. 2006, Lederle et al. 2010). Serum MMP8 concentrations showed a close correlation with vascular invasion of primary tumours and might therefore be used as a prognostic biomarker of haematogenous spreading (Vihinen et al. 2008). Gelatinases MMP-2 and 9 are mainly expressed at the tumour periphery (Kurschat et al. 2002). The former is reported to be involved in the proteolytic cleavage of fibronectin regulating migration and invasion of tumour cells via stimulating adhesion (Jiao et al. 2012). Rotte et al found that expression of MMP-2 was significantly increased in metastatic and primary melanomas compared to controls and showed association with p-Akt status and patient survival. Similar to MMP8, MMP-2 could therefore also serve as a prognostic marker (Rotte et al. 2012). Membrane type MMPs i.e. MMP14 and 16 were mainly localised to the tumour edge and perivascular space. These are reported to be involved in angiogenesis, endothelial cell migration and intravasation of melanoma cells (Kurschat et al. 2002, Devy et al. 2009). Interestingly patients with mutations in the BRAF and N-RAS genes had also increased MMP14 expression (Iida et al. 2004).

On the other hand, there are also metalloproteinases i.e. MMP9 and 12, which can act as tumour suppressors and have an anti-angiogenic effect by converting plasminogen to angiostatin (Ribatti 2009). The diverse function of MMPs is one of the main reasons why broad spectrum inhibitors failed to perform successfully in clinical trials. Novel inhibitors targeting signalling molecules of MMP synthesis are currently the subject of research (Xie et al. 2013).

Beside proteases, ECM remodelling and turnover is regulated by endogenous inhibitors of matrix metalloproteinases (TIMPs). A number of studies report changes in the patterns of TIMP1, 2 and 3 expression in melanoma patients (Airola et al. 1999, Moro et al. 2014). TIMP-3 is generally considered to be a tumour suppressor that exerts antitumoural (antiangiogenic) properties and has been found to be downregulated in advanced stage melanoma (Das et al. 2016). However, some authors report increased expression of TIMP1 and 3 as a late event correlating with melanoma invasion (Airola et al. 1999, Hofmann et al. 2000). An explanation for these contradictions might be that increased TIMP expression is usually observed at the edges of the tumour and in the surrounding stroma, where it can reflect a host response trying to limit and control invasion of cancer cells, while decreased TIMP expression and loss of inhibition is mainly detected in the central part of the tumours (Hofmann et al. 2000). Nonetheless this requires further clarification based on comprehensive data from large scale studies.

Overall, the tumour microenvironment strongly defines the metastasizing capability of cancer cells. Components of the ECM and regulatory molecules (especially MMP-2 in case of melanoma) provide an unexplored source of prognostic biomarkers. Furthermore, selective inhibitors in future can be used to potentiate the effect of targeted biological adjuvant therapies.

1.4.4 Treatment of melanoma

Management of cutaneous melanomas is a multidisciplinary task combining surgical and oncological approaches. Surgical excision remains the gold standard treatment for *in situ* cutaneous melanoma. However, there has been a debate in recent years about the optimal resection margins. The necessity for radical surgery was revised in the late 1970's, when the prognostic value and importance of tumour depth was described (Balch et al. 1979). Several clinical trials concluded no significant difference in survival of melanoma patients with tumour thickness <2.0 mm undergoing radical surgery with large tumour margins compared to narrow excisions (Veronesi et al. 1988). Similar observations were made with intermediate (1-4.0 mm) and thick (>4.0mm) melanomas (Balch et al. 2001). Although the local regional recurrence was somewhat higher in the non-radical group it did not reach statistical significance in either of the multicentred randomized trials. According to the American Academy of Dermatology Clinical Practice Guidelines 2019 (AAD CPG) recommended surgical margins are the following (Bichakjian et al. 2011, Swetter et al. 2019): 0.5-1 cm for *in situ* melanomas or narrow resection using complete circumferential peripheral and deep margin assessment (Mohs surgery) with frozen section histology, 1 cm margins for melanomas <1.0mm, 1-2 cm for thickness between 1-2 mm and 2 cm resection margins for melanomas with Breslow thickness greater than 2 mm. Fewer studies have focused on dissection depth, however all concluded that resection should stop at the muscle fascia, since removing that did not increase patient outcome but might provoke nodal dissemination (Olsen 1964).

Melanoma spreads through the lymphatic system, therefore regional lymph node involvement is an important prognostic factor and is essential for disease staging (Morton et al. 1999). Pervious clinical practice consisted of immediate elective lymph node dissection in case of intermediate to thick melanomas. Several studies concluded no actual benefit from automatic radical lymph node *en block* dissection in overall survival, moreover patients had significantly more postoperative complications i.e. seroma collection or lymphedema of the limbs (Sim et al. 1986, Slingluff et al. 1994). This led to the introduction of sentinel lymph node biopsy (SLNB) based on the concept that lymphatic drainage is organised in a chain like network where a single lymph node can be identified for each skin area at the beginning of the chain (Morton et al. 1992). Double labelling with intradermally injected methylene blue dye and radiocolloid detected intraoperatively with a gamma probe enables surgeons to successfully identify this sentinel node (Gershenwald et al. 1998). The Multicentre Selective Lymphadenectomy Trial-1 (MSLT-1) concluded that 5-year melanoma-specific survival was significantly higher in the subgroup of SLNB positive patients, where immediate completion lymphadenectomy was performed (Morton et al. 2006). Current indications for SLNB based on National Comprehensive Cancer Network (NCCN) melanoma guidelines are the following (Coit et al. 2019, Swetter et al. 2019): for *in situ* and melanomas <0.8 mm (T1a based on the eight edition of the AJCC staging system) it is not recommended. There is an absolute indication for SLNB with melanoma thickness >1mm (>T2a). In case of patients with melanoma <0.8 mm with ulceration or 0.8-1.0 mm (T1b) it should be discussed and considered for high risk patients. Completion of lymph node dissection in case of SLNB positivity

should be always a decision of an interdisciplinary team of surgeons, oncologists and dermatologists taking into consideration all other factors.

Due to the aggressive behaviour and early dissemination of melanoma often combinations of adjuvant targeted biological therapy, immunotherapy and chemotherapeutic approaches are needed.

Advanced stage and metastatic melanomas have undergone intense research in the last decade for adjuvant therapies. Following radical surgery risk of recurrence is based on a number of histological parameters. Beside thickness, which is generally considered as the best indicator of prognosis, presence of ulceration, number of mitoses greater than 1 per square millimetre or serum lactate dehydrogenase elevation all suggest an aggressive tumour behaviour with increased risk of recurrence (Keung et al. 2018). Combinational adjuvant therapies have been proven beneficial both in increasing overall patient survival (OS) and disease free survival (DFS).

Currently immunotherapy for melanoma consist of high dose interferon (HDI) or PEGylated interferon (PegIFN) given for 1 and 2 years respectively (Davar et al. 2012). Melanoma can be considered as an immunogenic tumour with systemic immune-responses targeting several differentiation antigens conveying an anti-tumoural effect. Currently indication for HDI or PegINF consist of either SNB positive disease or melanomas with thickness ≥T2b (Coit et al. 2019). A number of studies report (NCCTG, ECOG, EORTC) significantly increased OS and DFS for this subgroup of patients (Kleeberg et al. 2004, Davar et al. 2012).

Unfortunately, immunotherapy alone often is not sufficient. In these cases, especially for patients who lack somatic mutations that could be specifically targeted, chemotherapy might be an alternative. Currently dacarbazine is the only FDA approved alkylating agent for melanoma treatment (Crosby et al. 2000). Temozolomide is widely used for the treatment of glioblastomas, therefore is often considered off label for melanomas with brain metastasis (Bleehen et al. 1995). Carboplatin and taxans (i.e. paclitaxel and docetaxel) have also been investigated in advanced stage melanomas with promising results (Wilson et al. 2016). However, most studies do not report a chemotherapy-only based survival benefit, it still offers an alternative (especially when applied as part of a multimodal therapy) for cases of resistant and aggressive melanomas.

With the identification of driver mutations and immune tolerogenic mechanisms novel family of inhibitors have been developed targeting BRAF/MEK or CTLA-4/PD-1/PD-L1 proteins.

Checkpoint blockade with antibodies against cytotoxic T lymphocyte-associated antigen (CTLA-4) and programmed cell death 1 (PD-1) receptor have undergone intense research in the last decade (Callahan et al. 2016). CTLA-4 expressed by regulatory T cells is responsible for the downregulation of immune responses therefore inhibition of this receptor leads to an enhanced immune surveillance of cancer cells (Thompson et al. 1997). Following a randomized phase III trial conducted by Hode et al (40) ipilimumab was granted FDA approval (Hodi et al. 2010).

PD-1 via inhibition of kinase pathways also serves as a negative regulator of T cell activity (Freeman et al. 2000). Overexpression of PD-1 receptor and its ligand (PD-L1) have been found in a number of urogenital (i.e. renal cell carcinoma, bladder cancer) and GI derived tumours (i.e. gastric, oesophageal, pancreatic cancer) (Wang et al. 2016). Currently nivolumab and pembrolizumab are available for adjuvant melanoma therapy as PD-1 inhibitors, latter with FDA approval.

With the identification of BRAF mutation novel tyrosine kinase inhibitors like vemurafenib and dabrafenib were developed targeting BRAF positive metastatic melanomas as potent highly effective new alternatives (Hauschild et al. 2012, McArthur et al. 2014). Unfortunately, only a fraction of melanomas express the mutated BRAF gene and even then therapeutic response is often temporary due to de novo or acquired resistance (Wagle et al. 2011). To resolve this issue other inhibitors targeting different parts of the MAPK signalling pathways i.e. activated or resting RAF kinases are under ongoing research.

Though pembrolizumab has the highest overall response rate with 24% when applied solitary (Robert et al. 2014), preclinical data suggest that combination of targeted and immunotherapy is able to augment therapeutic response and allow a better long-lasting disease control compared to treatment with a single agent alone.

1.5 Aims and objectives

The aim of this research was to identify novels sites of CCK2R expression and characterise their functional significance. As previously highlighted by a number of authors despite the broad knowledge we have of gastrin and the CCK2 receptor new aspects of their multiplex role in human physiology and pathophysiology are still emerging. Stromal myofibroblasts form a niche of cells which are important determinants of the tumour microenvironment and tissue regeneration. The recent concept that tumours can also be considered as chronic non healing wounds adds another link to this issue. There is a suggesting in the literature that myofibroblasts of the gut might express the gastrin receptor, however the role of this is far from clear. Hence we decided to screen the complete alimentary tract for myofibroblasts expressing the CCK2 receptor with experiments aimed at understanding the functionality of it.

Elevated plasma concentration of gastrin is a common complication of long term acid secretion inhibitor therapy. Open source protein databases provide evidence that melanoma cancer cells express the gastrin receptor. Taken together with the possibility that dermal stromal cells might also express CCK2R we decided to investigate a possible relation between gastrin and melanoma behaviour both *in vitro* and *in vivo,* including the prospective collection of histology and serum samples from patients with different stage melanomas.

Overview of objectives:

1. To characterise CCK2R expression in myofibroblasts derived from different parts of the GI tract. Investigate receptor functionality and the effect of gastrin on stromal cell growth and motility.
2. To evaluate CCK2R expression in biopsy samples from melanoma patients, to determine serum gastrin concentrations in these patients and examine possible correlating with pTNM stages, *H.pylori* infection and acid secretion inhibitor consumption.
3. To investigate the effect of gastrin and stromal cells on melanoma cell proliferation, adhesion, migration and invasion.
4. To analyse the secretome of gastrin-treated melanoma cells and to identify relevant pathways

More specific objectives are provided in each of the Results chapters.

Chapter 2

Materials and methods

2.1 Materials

2.1.1 Drugs, antibodies

Drugs and antibodies used below in alphabetical order: 4-(2-hydroxyethyl)-1-piperazineethanesulfonic acid (HEPES) was obtained from Sigma-Aldrich (Poole, Dorset, UK); 5'-FAM, 3'-TAMRA double dye probes from Eurogentec (Southampton, UK); AG1024 from Calbiochem (Darmstadt, Germany); Amaxa® Cell Line Nucleofector® Kit V from Lonza (Basel, Switzerland); antibodies for immunochemistry and Western blot (see Table 2.1 and 2.2); BD inserts and BD BioCoat™ Matrigel™ invasion chambers from SLS (Nottingham, UK); bovine serum albumin (BSA) from Jackson Immunoresearch (PA, USA); Cell Counting Kit-8 assay from Dojindo Laboratories (Munich, Germany); Click-iT EdU Imaging kit from Invitrogen (Paisley, UK); donkey serum from Sigma-Aldrich (Poole, Dorset, UK); Dulbecco's modified Eagle's medium (DMEM) from Sigma-Aldrich (Poole, Dorset, UK); ECL substrate (Clarity™) for membrane development from Bio-Rad (Hercules, USA); Ethylene glycol-bis(2-aminoethylether)-N,N,N′,N′-tetraacetic acid (EGTA) from Sigma-Aldrich (Poole, Dorset, UK); fetal bovine serum (FBS) from Lonza (Basel, Switzerland); fibroblast basal medium from Lonza (Basel, Switzerland); Fluo-4 AM from Thermo Fisher Scientific (Waltham, MA, USA); *H.pylori* ELISA detection kit from Biohit Health Care (Helsinki, Finland); Ham's nutrient mixture F12 from Lonza (Basel, Switzerland); human unsulfated heptadecapeptide gastrin (hG17) from Bachem (St Helens, UK); human unsulphated hepadecapeptide gastrin (hG17) with ^{125}I label from Perkin Elmer (NEX176010UC); ionomycin from

Sigma-Aldrich (Poole, Dorset, UK); L740093 was a gift from Dr R. Freidinger (Merck Sharpe and Dohme, Rathway, New Jersey, USA); Matrigel® Basement Membrane Matrix from Corning (Tewksbury, MA, USA); Mesenchymal Stem Cell Growth Medium (MSCGM) from Lonza (Basel, Switzerland); MS grade Trypsin Gold from Promega (Madison, USA); Nitrocellulose Amersham™ Protran® membranes from Biotech (Little Chalfont, UK); NuPAGE™, Novex™ 4-12% bis-tris protein gels and transfer buffer for Western blots form Invitrogen (Parsley, UK); oligo-dT primers from Promega (Madison, USA); OmniKine™ ELISA kit for TIMP-3 detection from AssaybioTech Stratech Scientific (Fermont, USA); PageRulerTM prestained protein ladder from Fermentas (York, UK); Pluronic F-127 from Thermo Fisher Scientific (Waltham, MA, USA); Precision Plus 29 real-time PCR master mix from Primer Design (Southampton, UK); Qiagen quantisect qPCR mastermix from Primer Design (Southampton, UK); Quantikine® ELISA kit for MMP-2 detection from R&D Systems (Abingdon, UK); Quick-Diff from Reagena (Toivala, Finland); RapiGest™ anionic surfactan from Waters (Hertfordshire, UK); Recovery™ cell freezing medium from Invitrogen (Paisley, UK); Roswell Park Memorial Institute medium (RPMI)-1640 from Sigma-Aldrich (Poole, Dorset, UK); saponin as non-ionic surfactant from Sigma-Aldrich (Poole, Dorset, UK); SILAC Protein Quantitation Kit from Thermo Fisher Scientific (Waltham, MA, USA); Silencer® siRNA for MMP-2 from Ambion®, Life Technologies (Warrington, UK); StrataClean resin from Agilent Technologies (Santa Clara, CA, USA); sulfinpyrazone from Sigma-Aldrich (Poole, Dorset, UK); TaqMan primer/probe sets (for human IGF-1, IGF-2 and GAPDH) from Primer Design (Southampton, UK); transforming growth factor - β1 (TGF-β1) recombinant

human protein from Thermo Fisher Scientific (Waltham, MA, USA); Tri-Reagent from Sigma-Aldrich (Poole, Dorset, UK); Tris buffered saline (TBS) from Sigma-Aldrich (Poole, Dorset, UK); Triton™ X-100 from Sigma-Aldrich (Poole, Dorset, UK); TWEEN® 20 from Sigma-Aldrich (Poole, Dorset, UK); Type I collagen from Life Technologies (Warrington, UK); Vectashield with DAPI from Vector laboratories (Peterborough, UK). All routine chemicals including supplements for culture media (i.e. 0.25 % w/v trypsin-EDTA, 1% v/v L-glutamine, 1% v/v non-essential amino acids, 1% v/v antibiotic-antimycotic solution, 1% v/v penicillin-streptomycin solution and phosphate buffered saline (PBS)) were purchased from Sigma-Aldrich (Poole, Dorset, UK) unless otherwise stated.

2.2 Tissue culture

2.2.1 Human myofibroblasts

Unless otherwise stated experiments were performed on human primary gastric CAMs previously generated from patients undergoing surgery for gastric cancer (Holmberg et al. 2012); some studies were also made on CAMs or myofibroblasts from tissue adjacent to cancers (ATMs) from colonic, pancreatic or oesophageal cancer, normal tissue myofibroblasts (NTMs) from healthy stomach and oesophagus, and myofibroblasts from chronic pancreatitis. The patients and the myofibroblasts obtained from them have all been described previously (Czepan et al. 2012, Holmberg et al. 2012, Kumar et al. 2014). The work was approved by the Ethics Committee of the University of Szeged, Szeged, Hungary. Myofibroblasts were cultured in DMEM supplemented with 10% v/v FBS, 1% v/v penicillin-streptomycin, 1% v/v antibiotic-antimycotic solution and 1% v/v non-essential amino acids (referred later as full medium; FM) and were used between passages 3 and 10 (Holmberg et al. 2012).

2.2.2 Human melanoma cells

Human melanoma cell lines G361 and Skmel-2 were provided by Krisztina Buzas (University of Szeged, Department of Oral Biology and Experimental Dental Research) and were previously authenticated by short tandem repeat (STR) analysis (Microsynth AG, Balgach, Switzerland). Cells were cultured in

RPMI-1640 media (Sigma Aldrich) supplemented with 10% fetal bovine serum and 1% antibiotic/antimycotic solution together with 1% L-glutamine (Sigma Aldrich). Cells were used up to passage 30.

2.2.3 Human dermal fibroblasts and myofibroblasts

Human dermal fibroblasts were produced from skin specimens obtained from patients undergoing surgery at the Plastic Surgery Unit, University of Szeged after informed consent and approval of Regional Human Biomedical Research Ethics Committee of University of Szeged. Skin samples were incubated overnight in a dispase solution at 4°C as previously described (Kemeny et al. 2016). Dermis was digested in aliquots of 4 ml low glucose DMEM containing collagenase (10.8 mg), hyaluronidase (5 mg) and deoxyribonuclease (0.4 mg) for two hours at ambient temperature. The cell suspension was than filtered through a 100 μm cell strainer. Fibroblasts were cultured in fibroblast basal medium (Lonza, Basel, Switzerland) supplemented with 1% penicillin/streptomycin and 1% glutamine (Sigma Aldrich). Cells were used up to passage 10. Dermal myofibroblasts were differentiated by incubating fibroblasts in culture medium containing 10 ng/ml TGF-β1 for 72 h as described previously (Midgley et al. 2013). Culture conditions were similar that those used for fibroblasts.

2.2.4 Human mesenchymal stromal cell (MSC)

Human bone marrow derived mesenchymal stem cells (CD105, CD166, CD29, CD44, α-SMA and vimentin positive; CD14, CD34, CD45, cytokeratin and desmin negative) were cultured in T-75 flasks containing 20 ml of special MSCGM basal medium (Lonza) containing mesenchymal cell growth supplement (MCGS), L-glutamine and GA-1000 (SingleQuots™) provided by the manufacturer (Kumar et al. 2014). Cultures were incubated at 37 °C in 5% CO_2. Media was changed every second day. Cells were passaged at 80% confluency. After repeated PBS washes, 2 ml trypsin (0.25% w/v)-EDTA was added for 1 min. The effect of trypsin was suspended by the addition of 8 ml full medium. MSCs passaged up to 10-15 times in an undifferentiated state were used for these experiments.

2.2.5 AGS cells and transfection

Gastric adenocarcinoma cells were cultured in HAMS/F12 medium supplemented with 10% v/v FBS and 1% v/v penicillin-streptomycin. Cells stably transfected with CCK2R or a control vector have previously been described (Watson et al. 2001).

2.2.6 Cryopreservation of cell lines

Sub-confluent cell cultures were trypsinised as detailed above and centrifuged at 800 rpm for 7 min at 4°C. Pellets were resuspended in 1 ml of freezing medium. The cell suspension was transferred to cryovials, which were placed in polistirol containers filled with propane-1, 2,-diol, overnight at -80 °C. Cryovials were moved to liquid nitrogen tanks the following day.

2.2.7 Recovering frozen cell lines

Cryopreserved cells were recovered from liquid nitrogen and placed into a preheated water bath at 37°C for 1-2 minutes. Cell suspensions were then transferred into T-75 flasks containing 20 ml of appropriate culture medium with growth supplements. Flasks were placed into a cell incubator (37°C, 5% CO_2) and media was changed the following day.

2.3 Immunochemistry

2.3.1 Immunocytochemistry

Myofibroblasts were fixed with 4% w/v paraformaldehyde (30 min, ambient temperature) and processed for immunocytochemistry as previously described (Wroblewski et al. 2003, Kumar et al. 2014). Cells were permeabilized with 0.2% Triton X-100 in PBS (30 min) followed by incubation with 5% w/v bovine serum albumin in PBS (30min) and blocking with 10% v/v donkey serum. Myofibroblasts were stained with anti-CCK2R polyclonal IgG antibody (1:200, overnight, 4°C) followed by incubation with FITC conjugated anti-rabbit secondary antibody (1:400, 1h). In some experiments, cells were incubated in SF medium or hG17 (10 nmol/L, 24 h) and stained with an antibody to caspase-3 (New England Biolabs,UK). Slides were mounted in Vectashield with 0,6-diamidino-2-phenylindole dihydrochloride (DAPI) and images were acquired using a Zeiss Axioplan-2 fluorescence microscope (Zeiss Vision, Welwyn Garden City, UK) equipped with a XF22 filter for the detection of FITC signals at 520 nm and XF33 filter for detecting TexasRed signals at 620 nm. Images were recorded at 10x and 43x magnification using AxiosVision software version 4.9.1.

Sub confluent melanoma cultures were trypsined for 4 min in 2 ml 0.25 % w/v trypsin-EDTA. Cells were counted using a haemocytometer and appropriate numbers of cells were plated on chamber slides. After 24 h incubation in culture media, cells were fixed with 4% w/v paraformaldehyde (30 min, ambient temperature) and permeabilised with 0.2% Triton X-100 in PBS 30

min each at ambient temperature. 5% w/v bovine serum albumin and 10% v/v donkey serum was used to block nonspecific binding sites. Melanoma cells were stained with anti-CCK2R polyclonal IgG antibody (1:200, overnight, 4°C) followed by incubation with FITC conjugated anti-rabbit secondary antibody (1:400, 1h) as described before (Wroblewski et al. 2003, Kumar et al. 2014). In selected cases, primary antibody was visualized with peroxidase (DAB) reaction using a cytospin. Slide were prepared by centrifuging 5-10 x 10^4 melanoma cells onto glass slides in a cytocentrifuge Slides were left to dry at ambient temperature overnight. CCK2R expressing cells were indicated by brown (3,3-diaminobenzidine) chromogen product. For complete list of antibodies and dilutions applied see table 2.1 below.

2.3.2 Immunohistochemistry

For immunohistochemistry, 4 µm sections were cut from formalin-fixed and paraffin embedded biopsy blocks from selected patients. Sections were placed on microscope slides, put in a tissue-drying oven for 45 minutes at 60ºC, deparaffinised in xylene for 15 minutes, and rehydrated in decreasing concentrations of alcohol for 9 minutes. Antigen retrieval was performed in 0.01 M sodium citrate buffer, pH 6.0 at 103ºC for 20 minutes. Sections were cooled at ambient temperature for 30 min, then rinsed in 1x TBS for 1 min. Before immunostaining, universal protein block was applied for 20 min. Primary antibodies against CCK2R, Melan-A, MMP-2 or TIMP-3 were applied for 60 min (for dilutions, species and manufacturer see table 2.1). After rinsing in TBS, high affinity polymer (Envision, Dako; Denmark) was applied for 30

min. Single (CCK2R, MMP-2 and TIMP-3 only) and double labelling for Melan-A also were performed. Different enzyme-substrate systems were applied to avoid cross reaction. For visualisation alcalic-phosphatase (ALP) conjugated secondary antibody was used against primary antibodies. Melan-A detection was based on a peroxidase (PO) reaction. ALP produced red (naphtanol AS-TR phosphate), and PO brown (3,3-diaminobenzidine) chromogen products. Finally, slides were dehydrated in increasing concentrations of alcohol for 7 min, washed in xylene for 3 min, counterstained with haematoxylin for 1 min and covered carefully. Receptor expression was quantified by scoring slides into 4 semi quantitative categories (0; 1; 2; 3) according to the intensity of reaction.

2.3.3 Densitometry

Optical densitometry was performed using single labelled sections for CCK2R. Complete slides were scanned and quantified with Image Pro Plus software. After standardisation focal density of cytoplasm of 5 cells/ filed were measured. Data presented in means ± SE.

	Antibody	Species	Dilution	Source
Primary ab	CCK2 (polyclonal)	rabbit	1:200 1:400 (ih)	Atlas AB, Sweden
	Caspase-3 (polyclonal)	rabbit	1:400	New England Biolabs
	Melan-A (monoclonal)	rabbit	1:300 (ih)	Dako, Denmark
	Vimentin (monoclonal)	mouse	1:200	Dako, Denmark
	Desmin (monoclonal)	mouse	1:200	Dako, Denmark
	α-SMA (monoclonal)	mouse	1:200	Dako, Denmark
	CKMNF116 (monoclonal)	mouse	1:200	Dako, Denmark
	MMP-2 (polyclonal)	goat	1:40 (ih)	R&D Systems, UK
	TIMP-3 (monoclonal)	mouse	1:50 (ih)	R&D Systems, UK
Secondary ab	FITC (anti-rabbit)	donkey	1:400	Jackson ImmunoResarch, PA
	Texas Red (anti-rabbit)	donkey	1:400	Jackson ImmunoResarch, PA
	Alexa F546 (anti-mouse)	goat	1:400	ThermoFisher, UK
	Alexa F647 (anti-mouse)	goat	1:500	ThermoFisher, UK

Table 2.1. List of primary and secondary antibodies used for immunostaining of cell cultures.
Dilutions for immunohistochemistry are marked with “ih” otherwise refer to concentrations used for immunocytochemistry.

2.4 Flow cytometry

Cultured myofibroblasts were incubated in SF or FM for 48 h, or were incubated in SF with or without hG17 (10 nmol/L, 24 h). Cells were harvested and fixed in 4% PFA at 37°C for 10 min prior to permeabilization with 90% methanol for 30 min at 4°C. Myofibroblasts were then washed twice with the incubation buffer containing 0.5% BSA dissolved in 1xPBS. Samples were incubated with anti-CCK2R primary antibody (1:200, 1h, ambient temperature and FITC-conjugated secondary antibody (1:400, 30 min, ambient temperature) prior to nuclear staining with DAPI in a final concertation of 1 µg/ml. For cell cycle analysis, cells were fixed in 70% ethanol (30 min) and were stained with DAPI after permeabilisation with saponin (5% in 1xPBS, 5 min). Cells were sorted with a FACSCanto II flow cytometer (BD Biosciences, San Jose, USA). CCK2R-positive cells were separated based on FITC fluorescence excited at 492 nm. Gating for cell cycle was done by detecting DAPI signals excited at 340 nm. Distinct peaks of emission spectra were assigned to cell cycle stages based on chromosomal ploidy. Data was analysed using FACSDiva software version 6.1.3.

For melanoma experiments 10^6 cells were seated in T-75 flasks and were incubated in culture medium for one day. Cells were serum starved for two days followed by treatment with 10 nM G17 or FM (supplemented with 10% fetal bovine serum and amino acids) overnight. Control flasks were either kept in full or SF medium throughout the process. Cultured cells were harvested and fixed in 70% ethanol for 30 min at 4°C. Following repeated washing and blocking steps with 0.5% BSA, cells were permeabilised with 0.5% saponin

(Sigma-Aldrich). 1 µg/ml DAPI dissolved in PBS was used for nuclear staining. Cell sorting was done with FACS Canto II flow cytometer as described above.

2.5 Calcium signal detection

Sub-confluent myofibroblasts were loaded with Fluo-4 AM ester (2 µmol/L, 45 min, 37°C in HEPES saline buffer containing 10 mmol/L glucose, 1 mmol/L calcium, 200 µmol/L sulphinpyrazone to reduce dye leakage and 25% w/v Pluronic F-127 to increase cellular uptake of dye) as previously described (Homolya et al. 1993, Kao 1994). EGTA (1 mmol/L) was added to the solution to reduce spontaneous calcium activity. Myofibroblasts were stimulated with hG17 (10 nmol/L) or ionomycin (1 µmol/L) as a positive control. Fluorescent signals were detected with a Leica SP2 AOBS multiphoton confocal microscope (Leica Microsystems, Wetzlar, Germany) equipped with an argon-ion laser at 488 nm absorbance and 516 nm emission peaks. Data analysis was carried out in LAS X 2.0 software.

Melanoma cells were plated (1-3x10^4) in 6-well plates and incubated in FM for 24 h. Sub-confluent cells were loaded with fluo-4 AM ester as a calcium indicator (2 µmol/L, 45 min, 37°C) in HEPES saline as described above (Homolya et al. 1993, Kao 1994). Melanoma cells were stimulated with hG17 (10 nmol/L). Signals were recorded for 5 min. Controls and filters applied for signal detection were the same as reported above.

2.6 Bioassays

2.6.1 Proliferation assays

2.6.1.1 EdU incorporation

Proliferating cells were detected using 5-ethynyl-2´-deoxyuridine (EdU) as previously described (Holmberg et al. 2012, Kumar et al. 2016). Myofibroblasts were synchronized by incubation in SF medium for 48 h followed by treatment with medium containing 10% fetal bovine serum (FM), or hG17, or fresh SF, and incubation with EdU reagent for up to 24 h. After EdU incorporation, cells were fixed in paraformaldehyde and processed using Click-iT^{TM} reagent (300 μl) mix containing the reaction buffer, CuSO4, alexa 4-azide (10 nM), ascorbic acid and distilled water according manufacturer's instructions. Staining of CCK2R was performed as described above. Images were acquired using a Zeiss Axioplan-2 microscope connected to a JVC-3 charged coupled device camera. Alexa Fluor 488 labelled cells were visualized with an XF22 filter at 519 nm.

In the case of melanoma, cells were trypsinased and plated (3-5x10^3) on cover slips in 24 well plates. Cells were incubated in culture medium for 24 h followed by 48 h serum starvation. Cells were either treated with hG17 (0.1-1-10 nM) for 24 h or were left in SF medium as a control. EdU reagent was added to media for 2h. Cells were fixed in 4% PFA at ambient temperature for 30 min. Cover slips were immersed in a solution containing 3% BSA and 0.5% Triton-X for permeabilisation. Click-iT^{TM} reagent mix was added to each well as described above. Plates were incubated for 30 min at ambient temperature in

the dark. After repeated washing and blocking steps, cover slips were immunostained using protocols described above.

2.6.1.2 Cell Counting Kit-8 (CCK-8; CeCo) assays

Cell Counting Kit-8 assay (Dojindo Laboratories, Munich, Germany) was used to measure cell number according to manufacturer's instruction (Shawe-Taylor et al. 2017). Since the abbreviation CCK8 also stands for cholecystokinin octapeptide, in order to avoid confusion, we decided to use the more distinguishable "CeCo" abbreviation when referring to this assay. Melanoma cancer cells (10^4 per well) were plated in 96 well plates and incubated overnight in FM. Cells were treated with hG17 (0.1-1-10 nM) or CM medium in phenol red free SF medium for 72 h. After treatment with gastrin, 10 µl CeCo reagent was added to each well for 2–4 h as optimised. Absorbance was measured at 450 nm using a GenioPlus plate reader (Tecan, Zurich, Switzerland). Proliferation was calculated based on cell numbers and expressed as fold change.

2.6.2 Invasion and migration assays with Boyden chambers

Transwell migration and invasion assays were performed using BD inserts or BD BioCoat™ Matrigel™ invasion chambers (SLS, Nottingham, UK) as described previously (Varro et al. 2004). Serum free medium containing 10 nM hG17 with or without the CCK2R antagonist L740093 (100 nmol/L) was added to 24 well plates. Boyden inserts or BioCoat™ Matrigel™ invasion chambers with a pore size of 8.0 µm (SLS, Nottingham, UK) were placed in each well prior to incubation in FM for 30 min at 37 °C, 5% CO2.

For myofibroblasts, 1.5 or 2.5 x 10^4 cells were seeded per insert. In some experiments EdU was added to the upper well and cells were incubated overnight. Membranes were then processed following the EdU protocol (see above) or alternatively cells were stained with Quick-Diff (Reagena, Toivala, Finland).

Melanoma cells (2 or 3 x 10^4) were harvested and resuspended in SF medium. Cell suspensions were placed in the upper well of chambers as previously described. After incubation in hG17 for 24h at 37°C, 5% CO2; membranes were stained with Quick-Diff (Reagena, Toivala, Finland) and were cut out and placed on glass slides. Cells were counted in a total of 5 fields per membrane.

2.7 Gene expression arrays

2.7.1 Microarray data

Microarray data on pairs of CAMs and corresponding ATMs from 13 gastric cancer patients have previously been deposited at *http://www.ncbi.nlm.nih.gov/geo/query/acc.cgi?acc=GSE44740.* The TNM classification system (Sobin et al. 2009) had been applied to these tumours which had shown that patients with early stage disease indicated by low lymph node involvement (pN0-1) had significantly longer survival than those with advanced disease indicated by high lymph node involvement (pN2-4) (51 vs. 12 months, respectively, $P < 0.01$) (Holmberg et al. 2012; Balabanova et al. 2014). The present analysis therefore focused on a comparison of CCK2R expression in these two groups. The abundance of CCK2R transcripts was expressed relative to GAPDH.

2.7.2 Quantitative polymerase chain reaction (qPCR)

Myofibroblasts ($0.25 - 1.5 \times 10^6$) were plated in Petri dishes (5 cm). Cells were then either serum starved for 72 h or incubated in full media. RNA from control (SF) and gastrin (10 nmol/L, 24 h) treated myofibroblasts was extracted in Tri-Reagent (1.25 mL; Sigma) according to the manufacturer's instructions. Pellets were resuspended in nuclease free water (50 µL) and RNA (4 µg) reverse transcribed with avian myeloblastosis virus reverse transcriptase and oligo-dT primers (Promega, Madison, USA). Real-time PCR was carried out

using an ABI7500 instrument (Applied Biosystems, Warrington, UK) and TaqMan primer/probe sets for human IGF-1, IGF-2 and GAPDH, together with Precision Plus 29 real-time PCR master mix (Primer Design, Southampton, UK) and 50-FAM, 30-TAMRA double dye probes (Eurogentec, Southampton, UK). Values were standardized to GAPDH and assays included no-template controls and a standard curve as previously described (Kumar et al. 2015). Primers and probes for detection of human IGF-1, IGF-2 and GAPDH, cDNAs were intronspanning and were: IGF-1: 50-TGT ATT GCG CAC CCC TCA A-30 (forward), 50-CT CCC TCT ACT TGC GTT CTT CA-30 (reverse), 50-ACA TGC CCA AGA CCC AGA AGG AAG TAC A-30 (probe); IGF-2, 50-CCG TGC TTC CGG ACA ACT T-30 (forward), 50-GGA CTG CTT CCA GGT GTC ATA TT-30 (reverse), 50-CCC AGA TAC CCC GTG GGC AAG TTC-30 (probe); GAPDH: 50-GCT CCT CCT GTT CGA CAG TCA-30(forward), 50-ACC TTC CCC ATG GTG TCT GA-30 (reverse), 50-CGT CGC CAG CCG AGC CAC A-30 (probe).

Melanoma cells (5 x 10^5) were plated in medium sized Petri dishes (5 cm diameter) and incubated in FM for 72 h. Cells were lysed using TRI reagent (1.25 mL; Sigma). RNA was extracted and converted to cDNA using Promega RT reagents followed by a 1/3 dilution to a final concentration of 22 ng/μL. 2 μL (44ng) of each sample was run in triplicate using GAPDH and CCK2R probes with Qiagen quantisect qPCR mastermix (Primer Design); TAMRA-NFQ and FAM-NFQ probes were employed (Eurogentec, Southampton, UK). The primer sequences were: CCK2R: TGACTCTGGGATGCTCCTAGT (forward), GGTCAGAGGTATGAGATTAGGC (reverse), ACCTCACAGTGACCCTTCCCAATCAGC (probe); GAPDH:

GCTCCTGTTCGACAGTCA (forward), ACCTTCCCCATGGTGTCTGA (reverse); GTCGCCAGCCG AGCCACA (probe). The mean ΔCt for CCK2R and GAPDH for the two sample sets was converted to a fold-change. Real time PCR was carried out using an ABI 7500 platform (Applied Biosystems) and AB software ver2.3 for analysis.

2.8 Radioimmunoassay

Serum gastrin was determined by radioimmunoassay (RIA) using antibody L2 to the C-terminus of G17 which reacts equally with G17 and G34, but not with progastrin or C-terminal variants of G17 as described previously (Dockray et al. 1991)**.** Standards were created using synthetic human unsulphated G17 (Bachem) dissolved in 0.05 M ammonium bicarbonate over the range 0.0.1 - 1 pmol/ml with sodium barbitonate buffer. 100 µl of prediluted samples (1:20) were incubated for two days at 4°C in the presence of ^{125}I labelled synthetic human unsulphated hepadecapeptide gastrin G17 (Perkin Elmer, NEX176010UC) and 100 µL gastrin antibody.100 µl D-4751 dextran coated charcoal suspension was added to the samples to remove unbound radiolabel (0.5g skimmed fat-free milk powder, 0.5 g D-4751 dextran, 1 g active charcoal in 50 ml distilled water). Samples were centrifuged at 3000 rpm for 15 min at 4°C. After centrifugation supernatants were carefully removed into polystyrene tubes and radioactivity was measured in charcoal pellets and supernatant in a Packard Bell RIAstar gamma counter (Packard Instrument Company, Rungis, France) for one minute. Non-specific binding was determined by measuring radioactivity of control samples without gastrin antibody. Ratio of free to antibody bound label was calculated and corrected for non-specific binding. Gastrin concentration of serum samples were calculated by comparing binding of samples with unknown gastrin concertation with those of standards used to create a standard curve.

2.9 *H.pylori* detection

H.pylori antibodies were detected in serum samples of patients using a commercially available ELISA kit (Biohit Health Care, Helsinki, Finland). 100 µl of prediluted (1:200) patient samples together with positive and negative controls were added in duplicate and incubated for 30 min at ambient temperature. Wells were washed three times with wash buffer according the manufacture's instruction. 100 µl of conjugated antibody was added to each well. Plates were sealed and incubated on shaker for 30 min at ambient temperature. Samples were washed again three times And 100 µl of substrate solution provided by the manufacturer was added to each well for 30 min in dark. The reaction was terminated by adding 100 µl of stop solution. Absorbance was measured on a Tecan GENios plate reader at 450 nm. Enzyme immune units (EIU) were calculated from absorbance readings using a calibrator curve generated from standards provided by the manufacturer. Samples with EIU>40 were considered as positive.

2.10 Tissue modelling

2.10.1 Spheroids

Confluent flasks of melanoma cells (Skeml-2 and G361) were trypsinized and counted. Appropriate numbers of cancer cells (3000 /droplet) were resuspended in a mixture of full media (80%) and methylcellulose (20%). 25 µl droplets were placed on Petri dishes and flipped upside down to allow cell aggregation and spheroid formation. Petri dishes with PBS inside to keep the droplets moist were place in incubator for 48 h. Collagen "sandwiches" containing the spheroids were prepared in advance using a mixture of Dulbecco's Modified Eagle's Medium 10x (Sigma Aldrich); type I collagen (Life Technologies) and 0.1 M NaOH in a ratio of 1:8:1. 250 µl of collagen solution was placed in each well of a 24 well plate and incubated for 30 min to allow collagen to solidify. Spheroids were then transferred from the droplets using sterile pipette tips to the top of previously created collagen layers. Each well contained one spheroid. A second layer of collagen solution prepared similarly was positioned on top of the spheroids thereby providing protection from mechanical stress and infection also creating an environment where the cancer spheroids are completely surrounded by collagen. 1 ml of SF media was put in each well to avoid collagen dehydration. To investigate the effect of stromal cells on cancer spheroids 10^4 cells (gastric myofibroblasts or dermal fibroblasts) per well were dispersed in the collagen solution. For gastrin treatment, the hormone in a final concentration of 10 nmol/L was added in the media. Gastrin was added every day, while complete media was changed every second day. Spheroids were followed up to 6 days with images being

recorded each day at 10 x magnification using a Zeiss 25 Axiovert Microscope (Carl Zeiss Microscopy) (Fig. 5.1 A).

Quantification was performed by two methods. 1) Spheroid growth was calculated by measuring difference in surface area compared to day 0 expressed as a fold change. 2) Invasion of individual melanoma cells was also assessed by determining the distance of cancer cells from the spheroid centre at four different angels in each case. Distances were averaged and expressed as means ±SEM. The experiment was done in triplicate (Fig. 5.1 B).

2.10.2 Organotypic cultures

Stromal cells (gastric CAMs or dermal fibroblasts) were trypsinized and counted in a haemocytometer. 5 x 10^5 cells/ well were centrifuged at 800 rpm for 7 min at ambient temperature. Cell were resuspended in DMEM full medium (100 µl/well) and were kept on ice. An organoid base resembling the dermis of skin was prepared by mixing Dulbecco's Modified Eagle's Medium 10x (Sigma Aldrich), Matrigel® Basement Membrane Matrix (Corning, Tewksbury, MA, USA), type I collagen (Life Technologies, Warrington, UK); Millipore, Watford, Hertfordshire, UK), fetal calf serum (Lonza, Basel, Switzerland) and in selected cases stromal cells in a 1:7:7:1:1 ratio, respectively as described previously (Smola et al. 1993, Nystrom et al. 2005). 1 ml of collagen solution with or without stromal cells was placed in wells of a 24 well plate carefully avoiding formation of bubbles. Plates were incubated (37°C, 5% CO_2) for 1 h to allow collagen to solidify. Subsequently organoids were covered with 1 ml of full

medium until further use. The following day sub-confluent melanoma cells (Skmel-2) were trypsinized and counted. Appropriate numbers of cells following previous optimisation ($1x10^6$/ well) were resuspended in RPMI-1640 full medium. 100 µl of melanoma cell suspension was placed on top of each organoid and returned to the incubator for 24 h. On the third day organoids from 24 well plates were transferred to the top of nylon sheets covered with wire mesh and placed in 6 well plates (Figure 5.2). Nylon sheets were previously covered in gel containing collagen, 10x DMEM, fetal bovine serum and 10% DMEM in a ratio of 7:1:1:1, respectively and neutralised with 0.1 M NaOH. Hydrophilic 100 µm pore sized nylon net filters of 25 mm diameter were each covered with 250 µl of gel solution. Organoids were treated with gastrin for two weeks. Gastrin (10 nmol/L) was added daily, while media was changed every second day. After two weeks, culture media from each well was removed and replaced with 4% PFA. Organoids were fixed for one day and then cut into half. Samples were sent to Liverpool Bio-Innovation Hub (LBIH) Biobank (University of Liverpool, UK) for sectioning and haematoxylin eosin staining. Slides were scanned with Aperio AT2 (Leica Biosystems) slide scanner and were analysed with Aperio ImageScope v12.3. Fields were captured at 10x magnification across the whole section. The experiment was done in triplicate and two sections were scored for total of 6 sections from each organoid.

2.11 Western blots

2.11.1 Preparation of protein samples and SDS-PAGE

Condition media was concentrated using StrataClean resin as described previously (Agilent Technologies, Santa Clara, CA, USA) (Holmberg et al. 2012). 15 µl of sample containing LDS sample buffer 4x, reducing agent 10x, deionized water and protein in a ratio of 10:4:1:25 respectively were loaded in wells of 4-12% bis-tris protein gels (NuPAGE™, Novex™, Invitrogen, Parsley, UK) together with 5 µL of PageRuler^{TM}Plus prestained protein to provide standard molecular weight ladder as reported by Kumar et. al. (Kumar et al. 2015). Samples were previously heat treated for 4 min at 100 °C to allow denaturation. Chambers were filled with 1x MOPS SDS running buffer supplemented with 500 µL antioxidant provided by manufacturer. Gel was run for 50 min at 200 V.

2.11.2 Transfer onto nitrocellulose membrane

Protein gels were blotted using transfer buffer containing (20x NuPage® transfer buffer and antioxidant provided by manufacturer, methanol and deionized water in a ratio of 50:1:200:750 respectively) onto nitrocellulose blotting membranes (Amersham™ Protran®, Sigma-Aldrich). Electrophoresis was run for 1 h at 30V. Membranes were then washed 3 times with 1x Tris buffered saline containing 0.1% Tween-20 solution. Blocking was achieved by incubating membranes in 5% W/V Marvel milk powder diluted in TBS-Tween

buffer for 1 hour at RT. Membranes were incubated in 5ml blocking buffer containing primary antibody overnight at 4 °C followed by incubation with secondary antibody for 1 h with repeated washing steps in-between (for antibodies and dilutions see table 2.2). Blotting membranes were developed using two component ECL substrate (Clarity™, Bio-Rad, Hercules, USA) applied for 5 min protected from light.

2.11.3 Densitometry evaluation and exposure of protein bands

Bio-Rad ChemiDoc XRS system (Bio-Rad) was used to detect protein bands via chemiluminescence. Colorimetric reaction was used for reference protein ladder. Membranes were exposed for 20 minutes. Images were captured and densitometry analysis of bands was perfumed using Image Lab software v. 6.0.1.

	Antibody	Species	Dilution	Source
Primary ab	Prosaposin	rabbit	1:200	Atlas AB, Sweden
	MMP-2 (polyclonal)	goat	1:200	R&D Systems, UK
	TIMP-3 (monoclonal)	mouse	1:500	R&D Systems, UK
	TIMP-1 (monoclonal)	goat	1:100	R&D Systems, UK
Sec. ab	Anti-Mouse	goat	1:10000	Sigma, UK
	Anti-Goat	rabbit	1:10000	Sigma, UK
	Anti-Rabbit	goat	1:10000	Sigma, UK

Table 2.2. List of primary and secondary antibodies used for western blot.

2.12 Sandwich - enzyme linked immunosorbent assay (ELISA)

Serum samples obtained from melanoma and basal cell cancer patients as described before in chapter 4 together with conditioned media from gastrin treated melanoma cell cultures (Skmel-2, G361) were analysed for TIMP-3 and MMP-2 using precoated colorimetric ELISA plates. MMP-2 was detected with Quantikine® ELISA kit (R&D Systems, Abingdon, UK). Serum samples diluted with calibrator diluent in 1:5 ratios according to the manufacturer's instructions and undiluted aliquots of cell culture supernatants were added to 96 well microplates previously precoated with antibody specific for total MMP-2. Plates were covered and incubated for 2 h at ambient temperature on a horizontal orbital microplate shaker at 500 rpm. Supernatants were aspired and wells washed three times with wash buffer provided by manufacturer. 200 µl of MMP-2 conjugate was added to each well and plates were incubated for further two h. After repeated washing steps, 200 µl of substrate solution was added to wells to develop the colorimetric reaction. Plates were incubated for 30 min protected from light. Reaction was terminated by adding 50 µl of stop solution to wells.

TIMP-3 was detected using OmniKine™ ELISA kit (AssaybioTech, Stratech Scientific, Fermont, USA). Serum samples were diluted 1:10 (occasionally where final concentration exceeded detection range samples were re-run with 1:100 dilution) with assay diluent provided by the manufacturer. Condition media from cell cultures was used undiluted. 100 µl of samples and standards were added into wells of microplates precoated with TIMP-3 and were

incubated at ambient temperature for 2 h on shaker. Supernatant was removed and wells were washed three times with the wash buffer provided by the manufacturer. Biotinylated-antibody was added at a final concentration of 2 µg/ml for further two h at ambient temperature. After repeated washing steps 100 µl of 1x streptavidin-HRP solution was added to each well for 30 min. Unbound peroxidase was aspired and three consecutive washes were done before tetramethylbenzidine (3,3',5,5') substrate was applied. Once colorimetric reaction ceased to develop further 100 µl of stop solution (2N sulphuric acid) provided by manufacturer was added to wells. Samples were run in duplicate. Absorbance was measured at 450 nm for both systems using a Tecan GENioPlus plate reader. A standard curve was generated by applying a four parametric logistic curve fit (4-PL) to absorbance readings of control and a standard series. GraphPad Prism v.7 was used to plot average optical density values measured in absorbance units against known standard concentrations. Data are presented as original sample concentrations (ng/ml).

2.13 Condition media

Melanoma cells (Skeml-2 and G361) were cultured at a seeding density of 10^6 cells per T75 flask in FM for 24 h. Supernatant was removed and cultures were washed three times with 1x PBS. Cells were resuspended in 10 ml SF medium either with or without 10 nmol/L G17 for treated and control groups respectively. Flasks were incubated for 24 h at 37° C, 5% CO_2. Media were collected ("24 h" samples), centrifuged at 800 rpm for 7 min at 4°C and stored at -80°C until further use. Cultures were washed repeatedly with 1X PBS and media were replaced as described above. After 6 h incubation with or without gastrin media were again collected and stored accordingly ("6 h" samples).

For Western blots and proteomic analysis, media were concentrated using StrataClean resin (Agilent Technologies) as describe previously (Holmberg et al. 2012, Hammond et al. 2018). To avoid protein degradation samples were handled on ice during the whole process. In brief, media were centrifuged (800 rpm, 4 min) to remove any remaining debris. StrataClean beads were added to media (25µl/10 ml sample) and mixed for 1 min using a vortex mixer. StrataClean bound proteins were separated from media by centrifugation at 1780 rpm for 3 min at 4°C. Supernatant was removed and pellets were resuspended in 500 µl of 50 mmol/L ammonium bicarbonate solution (ambic). Samples were centrifuged at 1780 rpm for 3 min at 4°C. Pellets were resuspended and centrifuged again three times in total. Protein concentrates were stored at -80°C until later use.

2.14 Proteomic analysis of the melanoma secretome

2.14.1 Stable Isotope Dynamic Labeling of Secretomes (SIDLS)

Melanoma cells were seeded at a density of 10^6 in T75 flasks and incubated for 24 h. Media were changed the next day to 10 ml RPMI-1640 (Sigma Aldrich) with or without gastrin (10 nmol/L). After 24 h media were removed and cultures were washed 3 times with 1x PBS. For gastrin-treated samples media were changed to RPMI-1640 containing heavy lysine ([$^{13}C_6$]-labelled L-lysine). Media of controls were supplemented with light lysine ([$^{12}C_6$]-labelled L-lysine). Cells were further incubated for 6 h at 37°C at 5% CO_2. Media were collected and processed as described before (Kristensen et al. 2012, Hammond et al. 2018). In brief, supernatants were centrifuged at 800x g for 4 min to remove any remaining cell debris. Protein was concentrated using StrataClean resin (Agilent Technologies) as described in section 6.2.1.

2.14.2 Digestion of StrataClean bound proteins

Samples were resuspended in 25 mM ambic, denatured with 5 µL of 1% (w/v) RapiGest (Waters, Hertfordshire, UK) for 10 min at 80°C. Proteins were reduced by addition of 60 mM DTT at 60°C for 10 min and alkylate iodoacetamide at ambient temperature protected from light for 30 min. Samples were digested with 1 µg trypsin (MS grade Trypsin Gold, Promega) at 37°C overnight followed by acidification with 1 µL of trifluoroacetic acid (TFA) for 45 min at similar temperature.

2.14.3 Liquid chromatography–mass spectrometry (LC-MS)

Samples were further processed by the Centre for Proteome Research (Institute of Integrative Biology, University of Liverpool). Peptide digests were prepared for LC-MS/MS as described previously (Pratt et al. 2006). In brief, samples were loaded on a trap column (Acclaim PepMap 100) at a rate of 5 µl min^{-1} combined with an analytical column (Easy-Spray PepMap® RSLC). After loading, peptides were eluted using HPLC grade acetonitrile buffer and were separated with an Ultimate 3000 nano system (Dionex/Thermo Fisher Scientific). Mass spectrometry was perfumed with a Q-Exactive quadrupole Orbitrap mass spectrometer (Thermo Fisher).

2.14.4 Quantification of secretomes and pathway analysis

Mass spectral data were analysed using MaxQuant 1.1.1.36 and searched against the human UniProt database v3.68. Recommended default settings were applied as described previously (Cox et al. 2008). Oxidation was set as variable while carbomethylation was a fixed modification. The initial precursor, MS/MS tolerance and protein false discovery rates (FDRs) were set to 20 ppm, 0.5 Da and 1-5% respectively. To quantify the rate of heavy isotope label incorporation into secreted proteins and to measure the effect of gastrin on protein secretion, relative isotope abundance was calculated (RIA) and expressed as a ratio of heavy to light labelled peptides. Therefore, H/L > 1 referred to upregulation while H/L < 1 to downregulation of identified proteins as a result of gastrin treatment. FASTA sequences were generated from the

UniProt database using a cut-off 0.001 and uploaded to SignalP v.4.0 . Classically secreted proteins were identified with a Dmax cut off score > 0.45 (Petersen et al. 2011). To identify protein class and biological function proteins with a signal sequence were then submitted to the Panther v 10.0 database (Mi et al. 2013).

2.15 Adhesion assay

Melanoma cells (Skmel-2, G361) were seeded (10^5/well) in 24 well plates and incubated for 24 h at 37°C, 5%CO_2. Cells were treated with 10 nmol/L G17 for 45 min. After repeated washing steps (3x) with PBS to remove debris and media, 0.02% crystal violet was added to each well to stain adherent cells as described previously (Gillies et al. 1986, Kueng et al. 1989). Cells were solubilized with 2 mmol/L Na_2HPO_4-50% ethanol. Absorbance detected by a Tecan GENioPlus plate reader was measured at 550 nm and analysed with XFluor4 software version 4.51. Data are expressed as means ± SEM after standardisation with blind controls.

2.16 Transfection of melanoma cells with siRNA for MMP-2

Transfection was performed using Amaxa® Cell Line Nucleofector® Kit V according to the manufacturer's instructions. Human melanoma cells (Sklem-2) were used at low passage number (<10) up to a confluency of 80%, passaged 5 days in advance. Cells were harvested as described previously and were counted in a haemocytometer. Suspensions containing 10^6 melanoma cells were centrifuged at 800x g for 7 min. Cells were reconstituted in 100 µL Nucleofector® solution provided by the manufacturer. Silencer® siRNA for MMP-2 (Ambion®, Life Technologies, Warrington, UK) resuspended in nuclease-free sterile water was added to cell suspensions at a final concertation of 10 pmol/L. Solutions were transferred into a special cuvette provided by the manufacturer and were inserted into the device. To obtain optimal gene transfer efficiency and cell viability Nucleofector® program T-019 was run. After transfection, 500 µl culture medium was added to cuvettes and samples were transferred into T75 flask and incubated until further use.

2.17 Patient recruitment and database

Whole blood was collected from patients referred to the Department of Dermatology University of Szeged, Szeged, Hungary between February and May 2017 with the initial diagnosis of malignant melanoma or basal cell cancer. Patients where final histology did not confirm clinical diagnosis were excluded from the study. No further exclusion criteria were applied. In all cases informed consent was obtained. Patients were anonymized and medical records were handled according EU GDPR legislation. In selected cases biopsy samples form tissue archives of the Departments of Dermatology and Pathology, University of Szeged were retrieved for immunohistochemically analysis. The study was approved by the Human Biomedical Research Ethics Committee of the University of Szeged (protocol ref.: MCC-INTER–002, approval No.: IF-964-2/2016)

2.17.1 Serum collection and preservation

Whole blood was collected from patients in covered test tubes. Samples were left undisturbed at ambient temperature for 15 min to allow clot formation. Samples were then centrifuged at 1000x g for 10 min at 4° C. Following centrifugation of the supernatants (serum) were transferred into clean polypropylene tubes under sterile circumstances. 1.5 ml aliquots were prepared and stored at –20°C until further use.

2.17.2 Human biopsy and histology samples

Patients underwent excision biopsy or complete excision of melanoma lesions under local anaesthesia following the guidelines on surgical margins on melanoma and non-melanoma skin tumours (1992, Nahhas et al. 2017). From paraffin embedded blocks 4 µm sections were placed on salinized slides, deparaffinised in a Leica BOND Max Autostainer (Leica Biosystems, UK). Melanin deposition was detected using anti-mouse MelanA (clone M7196, Dako). Visualization of the primary antibody was performed by colorimetric polymer-based systems. DAB and Fast Red solutions were used for brown and red colorimetric reactions, respectively. Sections were counterstained by conventional haematoxylin for 30 sec than washed in tap water and cover slipped. The final histological record included tumour dimensions, depth (Breslow and Clark stages) number of mitosis, tumour margins and pTNM stage (1992, Balch et al. 2009, Ingraffea 2013).

CCK2 antibody validation was performed on archived gastric adenocarcinoma samples obtained from the Department of Pathology, University of Szeged.

2.18 Applied TNM classification and grading systems

2.18.1 Gastric adenocarcinoma TNM staging

There are two major classification systems currently used for gastric cancer staging. The Japanese version focuses more on anatomical location and perigastric lymphoglandular stations (Shuppan 1993). The other staging system, which we also applied was developed by the American Joint Committee on Cancer (AJCC) and the Union for International Cancer Control (UICC) and centres attention more on tumour size, number of affected lymph nodes and distant metastasis (Sano et al. 2017). See Table 2.3 for a description of the various pTNM categories.

T category		T criteria
TX		Primary tumor cannot be assessed
T0		No evidence of primary tumor
Tis		Carcinoma *in situ*: Intraepithelial tumor
T1		
	T1a	Tumor invades the lamina propria or muscularis mucosae
	T1b	Tumor invades the submucosa
T2		Tumor invades the muscularis propria
T3		Tumor penetrates the subserosal connective tissue
T4		
	T4a	Tumor invades visceral peritoneum
	T4b	Tumor invades adjacent structures/organs

N category		N criteria
NX		Regional lymph node(s) cannot be assessed
N0		No regional lymph node metastasis
N1		Metastasis in one or two regional lymph nodes
N2		Metastasis in three to six regional lymph nodes
N3		Metastasis in seven or more regional lymph nodes
	N3a	Metastasis in 7 to 15 regional lymph nodes
	N3b	Metastasis in 16 or more regional lymph nodes

Table 2.3. pTNM staging of gastric adenocarcinoma.

2.18.2 Malignant melanoma TNM staging

The pTNM classification defined by the eighth edition of the American Joint Committee on Cancer (AJCC) on cutaneous melanomas was applied for scoring (Table 2.4) (Gershenwald et al. 2017). Although mitotic rate was recoded in all cases staging criteria for primary tumour were based on measured tumour thickness (Breslow thickness). Tumour depth following the Clark scale was also defined (Table 2.4). Patients were scored into two prognostic stage groups based on tumour size (Table 2.5). Stage I consisted of patients with low risk primary melanoma without lymph node involvement or distant metastasis (pT1a-2a), while Stage II included patients at higher risk of recurrent tumour (pT2b-4b).

Clark stage	Tumor depth
I.	Melanoma in situ – the melanoma cells are located in the epidermis
II.	Cancer cells reach the papillary dermis
III.	Melanoma cells invade the papillary dermis
IV.	Melanoma has spread into the reticular or deep dermis
V.	Tumor has grown into the subcutaneous fat

Table 2.4. Clark stages used to describe melanoma invasiveness.

T category	Thickness	Ulceration status
TX: ***Primary tumor thickness cannot be assessed***	Not applicable	Not applicable
T0: ***No evidence of primary tumor***	Not applicable	Not applicable
Tis (*melanoma in situ)*	Not applicable	Not applicable
T1	≤1.0 mm	Unknown or unspecified
T1a	<0.8 mm	Without ulceration
T1b	<0.8 mm	With ulceration
	0.8 to 1 mm	With or without ulceration
T2	>1 to 2 mm	Unknown or unspecified
T2a	>1 to 2 mm	Without ulceration
T2b	>1 to 2 mm	With ulceration
T3	>2 to 4 mm	Unknown or unspecified
T3a	>2 to 4 mm	Without ulceration
T3b	>2 to 4 mm	With ulceration
T4	>4 mm	Unknown or unspecified
T4a	>4 mm	Without ulceration
T4b	>4 mm	With ulceration

Table 2.5. pT classification based on melanoma thickness and ulceration.

2.19 Statistics.

Results were calculated as mean ± standard error of means (SEM). Parametric tests including student t-test, Fisher exact test, Pearson's chi-squared test and ANOVA were performed on the data as appropriate. Where normal distribution failed Mann-Whitney and Kruskal-Wallis tests were applied with significance at $p<0.05$ using Systat Software Inc. v. 12.0 (London, UK) and IBM SPSS Statistics V26.0 (New York, USA) unless otherwise stated.

Chapter 3

Characterisation and functional significance of CCK2R expression in gastrointestinal myofibroblasts

3.1 Introduction

There is growing recognition of the role of gastrin in gastrointestinal cancers including those of the oesophagus, stomach, pancreas and colon (Ferrand et al. 2006). The concept that tumours are wounds that do not heal is well recognised (Dvorak 1986, Desmouliere et al. 2004). In this context it is notable that expression of CCK2R occurs during wound healing in the stomach. Schmassmann and Reubi (2000) used *in situ* hybridization to show increased CCK2R in rat stomach following cryo-ulceration (Schmassmann et al. 2000). Ashurst *et al.* (2008) then showed that after gastric cryo-ulceration in mice, CCK2R expression was co-localised with α-smooth muscle actin (α-SMA) which is a biomarker for myofibroblasts (Ashurst et al. 2008). However these data are derived from rodent models and the specific physiological mechanisms leading to *de novo* receptor expression and cell recruitment in a clinical context remain unknown.

The data therefore raise the possibility that CCK2R is expressed in activated myofibroblasts, but even so the significance of this is poorly understood and there has been no direct study of CCK2R expression in human myofibroblasts. Because myofibroblasts are motile the data also suggest the hypothesis that gastrin regulates migration of these cells via CCK2R.

3.1.1 Objectives

1. To determine whether CCK2R is expressed by myofibroblasts using immunohistochemistry, immunocytochemistry and flow cytometry.
2. To characterise CCK2R expression in myofibroblasts from different parts of the gastrointestinal tract.
3. To investigate receptor functionality based on fluorescence measurement of cytosolic Ca^{2+}.
4. To determine the relationship between CCK2R expression and the cell cycle.
5. To investigate the effect of gastrin on stromal cell growth (proliferation, apoptosis) and motility (migration and invasion).

3.2 Methods

3.2.1 Cell culture

Unless otherwise stated experiments were performed on human primary gastric CAMs or ATMs from colonic, pancreatic or oesophageal cancer, NTMs from healthy stomach and oesophagus, and myofibroblasts from chronic pancreatitis (Czepan et al. 2012, Holmberg et al. 2012, Kumar et al. 2014). Cells were cultured as described previously in sections 2.2.1 and were used between passages 3 and 10.

3.2.2 Immunocytochemistry

Myofibroblasts were fixed and stained with anti-CCK2R polyclonal IgG antibody (1:200, overnight, 4°C) as described in sections 2.3.1. In some experiments, cells were stained for caspase-3 after gastrin treatment. For applied antibodies, filters and wavelength see section 2.3.

3.2.3 Microarray data

Microarray data on pairs of CAMs and corresponding ATMs from 13 gastric cancer patients have previously been deposited at *http://www.ncbi.nlm.nih.gov/geo/query/acc.cgi?acc=GSE44740.* The abundance of CCK2R transcripts was expressed relative to GAPDH.

3.2.4 Intracellular calcium

Subconfluent cells were loaded with the Ca^{2+} fluorophore Fluo-4 AM as previously described (Homolya et al. 1993, Kao 1994). Myofibroblasts were stimulated with hG17 (10 nmol/L) or ionomycin (1 µmol/L) as a positive control (See section 2.5)

3.2.5 EdU incorporation

Myofibroblasts were synchronized in serum-free (SF) medium and treated with full medium (FM), hG17 (10 nmol/L), or fresh SF, followed by incubation with EdU reagent for up to 24 h as previously described in 2.6.1.1. Staining of CCK2R was performed as described above.

3.2.6 Flow cytometry

Cultured myofibroblasts were incubated in SF or FM for 48 h after synchronisation. In some cases cells were treated with 10 nmol/L hG17 overnight. For cell cycle analysis, cells were directly stained with DAPI (1 µg/ml). In experiments aimed at detecting receptor expression, myofibroblasts were incubated with CCK2R primary antibody (1:200, 1 h, ambient temperature) and FITC-conjugated secondary antibody (1:400, 30 min, ambient temperature) prior to nuclear staining. Cells were sorted with FACS Canto II flow cytometer. See detailes in section 2.4.

3.2.7 Migration assays

Transwell migration and invasion assays were performed using BD inserts or BD BioCoat™ Matrigel™ invasion chambers (SLS, Nottingham, UK) as previously described (2.6.2) (Varro et al. 2004). Cells were treated with hG17 (10 nmol/L) with or without L740093 or AG1024. Membranes were processed following the EdU protocol (see above) or alternatively with Quick-Diff (Reagena, Toivala, Finland).

3.2.8 qPCR

Myofibroblasts (0.25 - 1.5 x 10^6) were plated and then either serum starved for 72 h or incubated in full media. RNA was extracted and real-time PCR was carried out using TaqMan primer/probe sets for human IGF-1, IGF-2. Values were standardized to GAPDH. For primers and probes see section 2.7.2.

3.3 Results

3.3.1 Validation of CCK2R immunocytochemistry.

In initial experiments we validated the antibody used for immunocytochemical localisation of CCK2R by comparison of wild type gastric (AGS) and oesophageal adenocarcinoma (OE33) derived cancer cells (which do not express the receptor) with their counterparts that have been stably transfected with cDNA encoding CCK2R i.e. AGS-Gr and OE33-Gr cells (Varro et al. 2002). As expected, the parental cell lines were not stained while transfected cells were strongly positive (Fig. 3.1A and B). Although the receptor is known to be present on the cell surface we added permeabilisation as an extra step in the immunostaining protocol to see whether there were intracellular protein fragments or trafficking vesicles, which could serve as potential epitopes thus enhancing staining quality. Neither in the case of AGS-Gr nor in OE33-Gr cells, was there a significant difference between permeabilised and control cells, confirming that the receptor was mostly localised to the plasma membrane. Almost all cells showed CCK2R positivity in both cases.

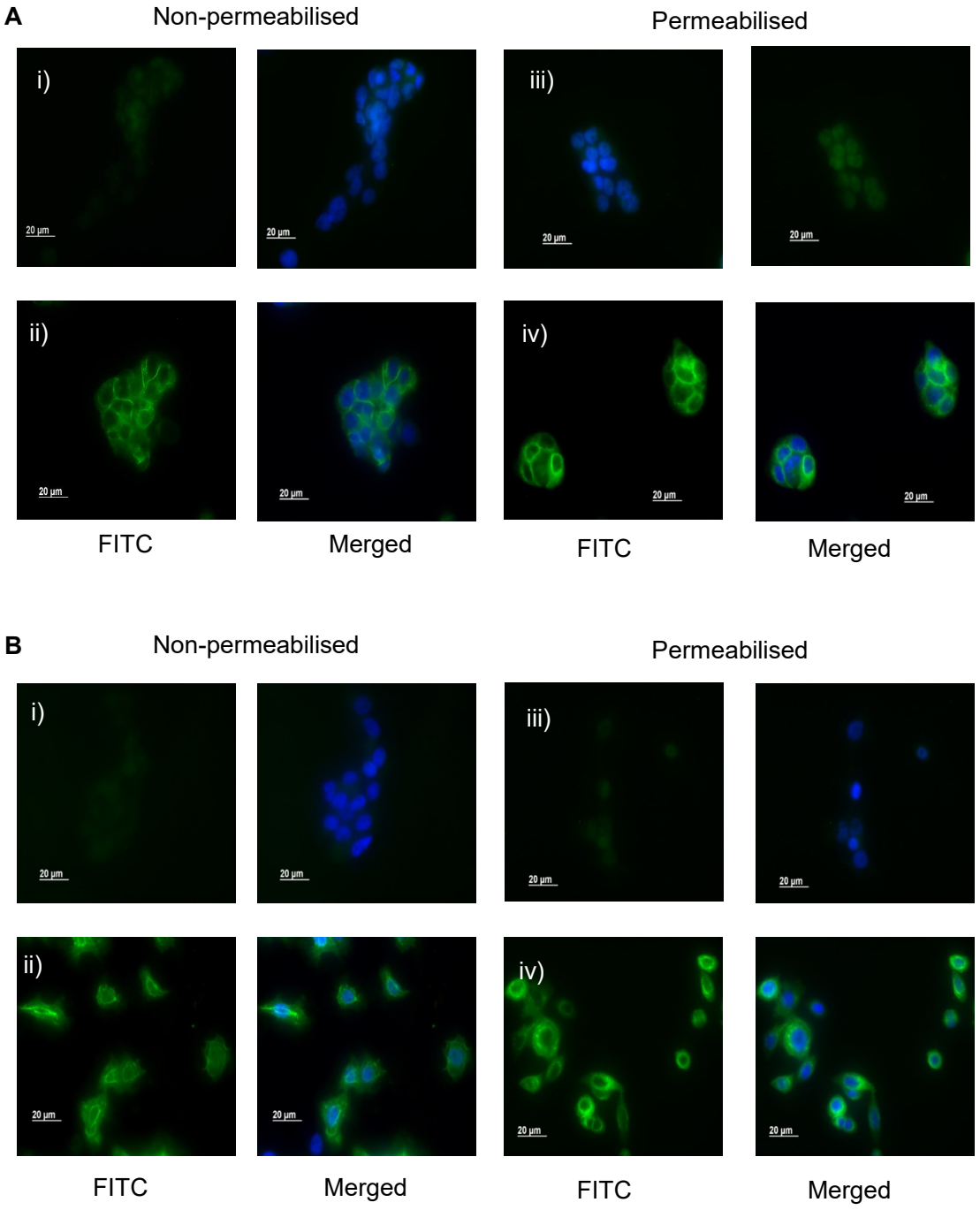

Figure 3.1. Validation of CCK2R antibody specificity.
In wild type gastric AGS cells (A) and oesophageal adenocarcinoma OE33 cells (B), which do not express CCK2R (i, iii), there is no signal compared with a strong CCK2R signal in AGS-Gr and OE33-Gr cells (ii, iv), which have been stably transfected with a receptor-encoding construct (nuclei stained blue with DAPI, CCK2R green with FITC). Permeabilisation did not influence staining intensity.

3.3.2 CCK2R is expressed in a subset of putative myofibroblasts in vivo

Subsequently we performed immunohistochemistry using the same CCK2R antibody on histological samples from patients with gastric and oesophageal adenocarcinoma. The peroxidase reaction showed intense brown staining of the epithelial layer and glandular mucosa with staining of putative parietal and enterochromaffin-like cells as anticipated. In addition, however, some spindle shaped cells in the underlying stroma that were putative myofibroblasts showed strong positivity (Fig 3.2).

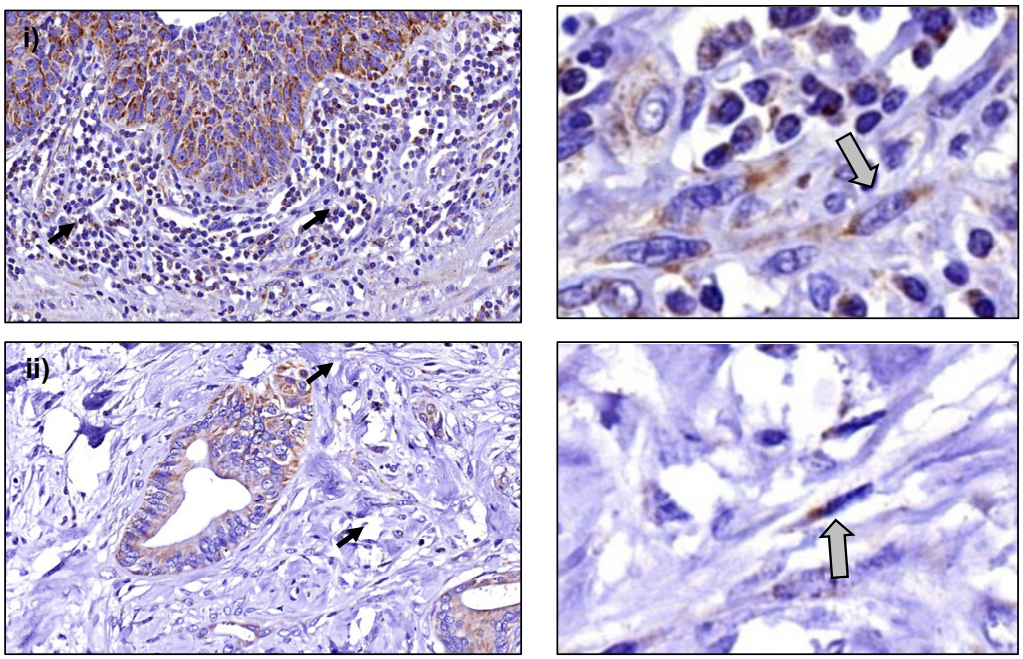

Figure 3.2. DAB immunohistochemistry with HRP for CCK2R detection.
Low (x20, left) and high power (x50, right) images of gastric (i) and oesophageal (ii) adenocarcinoma histology samples. Arrows indicate CCK2R positive stromal cells characteristic for myofibroblasts. Note the strongly positive glandular structure with epithelial cells.

3.3.3 CCK2R is expressed in a subset of cultured myofibroblasts

To further investigate the expression of CCK2R by cells of a fibroblastic lineage we examined myofibroblast cell lines. Using normal cycling cells double labelled with DAPI for nuclear staining and anti-CCK2R primary antibody, immunocytochemistry confirmed receptor expression in a subset of cells.

3.3.3.1 Receptor expression is associated with cell density

CCK2R expression was examined in a variety of conditions and proved to be dependent on cell number and confluency. Under standard culture conditions, subconfluent (6 x 10^4 cells per well) myofibroblast populations exhibited expression in 5.7 ± 1.0% of cells. At high cell densities there was decreased expression, thus we aimed for a confluency between 70 and 80% in later experiments (Fig. 3.3A). Prolonged incubation in culture media did not lead to accumulation or persistent increase of CCK2 positive cells suggesting a fluctuating expression perhaps relates to the cell cycle (Fig. 3.3B).

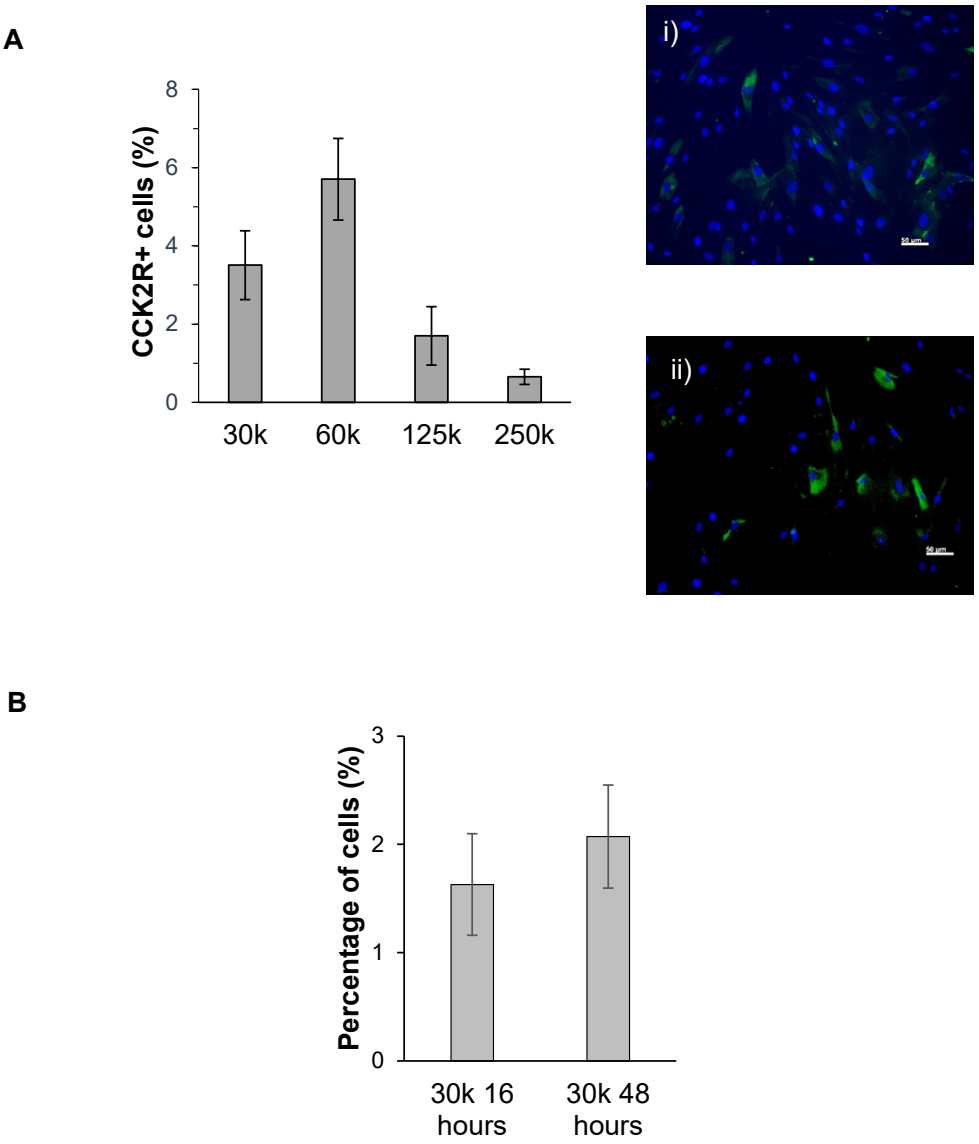

Figure 3.3. CCK2R expression was influenced by cell density (A) but not by length of incubation (B). Lack of cell-cell contact (i) showed similar inhibitory effect on receptor expression as insufficient space for cellular spreading and distorted morphology as a result of over confluent cultures. Under optimised culture conditions CCK2R expression significantly increased. Prolonged incubation in culture media did not have an effect on overall CCK2R expression using asynchronised myofibroblasts (B).

3.3.3.2 Flow cytometry confirmed CCK2 receptor expression

Flow cytometry as an alternative technique also supported the hypothesis that CCK2R is expressed by gut-derived myofibroblasts. Being a homogenous population based on cell size and granularity, forward and side scattering facilitated the identification of viable target cells. Under the aforementioned circumstances gating for FITC channels at 492 nm revealed receptor expression in 3.0 ± 1.8% (n=3) of cells (Fig. 3.4).

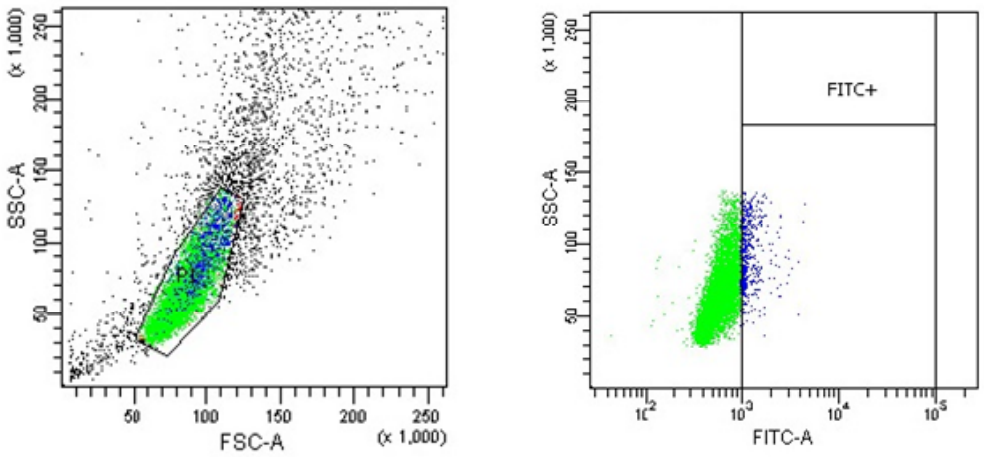

Figure 3.4. Flow cytometry confirmed CCK2R expression in gastric CAMs.
Green dots represent viable cells gated based on morphology and granularity, while blue ones refer to the CCK2R positive fraction excited for FITC signal. Left panel shows viable population of cells outlined based on FSC and SSC parameters referring to size and granularity respectively. Right panel shows gating for FITC signal within the viable myofibroblast population.

3.3.3.3 Systematic screening of GI tract myofibroblasts revealed consistent expression of CCK2 receptors in a subset of cells

We then examined expression of CCK2R in a number of myofibroblast populations recovered from normal tissue, cancer or cancer-adjacent tissue from oesophagus, stomach, omentum, colon and pancreas (Table 3.1). We also examined myofibroblast cell lines derived from patients with GI disorders i.e. chronic pancreatitis, vipoma, GIST or pernicious anaemia (Fig 3.5). With higher magnification and post-acquisition image processing, including deconvolution, a granulated intracellular structure became visible. These smaller particles trafficking towards the plasma membrane are suggestive of vesicles containing the whole receptor or at least peptide fragments of it (Fig. 3.6).

#	ID	Organ	Tumorous origin
1	*Sz45/1*	Stomach	CAM
2	*Sz45/2*	Stomach	ATM
3	*Sz195/1*	Stomach	CAM
4	*Sz195/2*	Stomach	ATM
5	*Sz195/7*	Colon	CAM
6	*Sz195/8*	Colon	ATM
7	*Sz173/1*	Oesophagus (adenocc.)	CAM
8	*Sz419*	Pancreas	CAM
9	*Sz480*	Chronic pancreatitis	
10	*Sz452*	Chronic pancreatitis	
11	*Sz190/1*	Stomach (metastatic)	CAM
12	*Sz190/2*	Stomach	ATM
13	*CCd18*	Colon	NTM
14	*Sz237/1*	Vipoma	CAM
15	*Sz255/1*	GIST	CAM
16	*MSC 7F 3458*	Mesenchymal Stem Cell	
17	*L355/22*	Pernicious Anaemia	
18	*L7641/22*	Pernicious Anaemia	
19	*L7642*	Omentum	
20	*L1212/22*	Pernicious Anaemia	
21	*Sz196/2*	Stomach (Corpus)	NTM
22	*Sz195/22*	Stomach	ATM
23	*Sz241/6*	Oesophagus	NTM
24	*Sz246/22*	Stomach (Antrum)	NTM
25	*Sz193/1*	Oesophagus (Cardia)	CAM
26	*Sz193/2*	Oesophagus (Cardia)	ATM
27	*Sz294/1*	Stomach	CAM
28	*Sz294/2*	Stomach (Antrum)	ATM
29	*Sz294/22*	Oesophagus (Cardia)	ATM

Table 3.1. List of GI derived myofibroblasts with corresponding reference ID, place of origin and myofibroblast type.

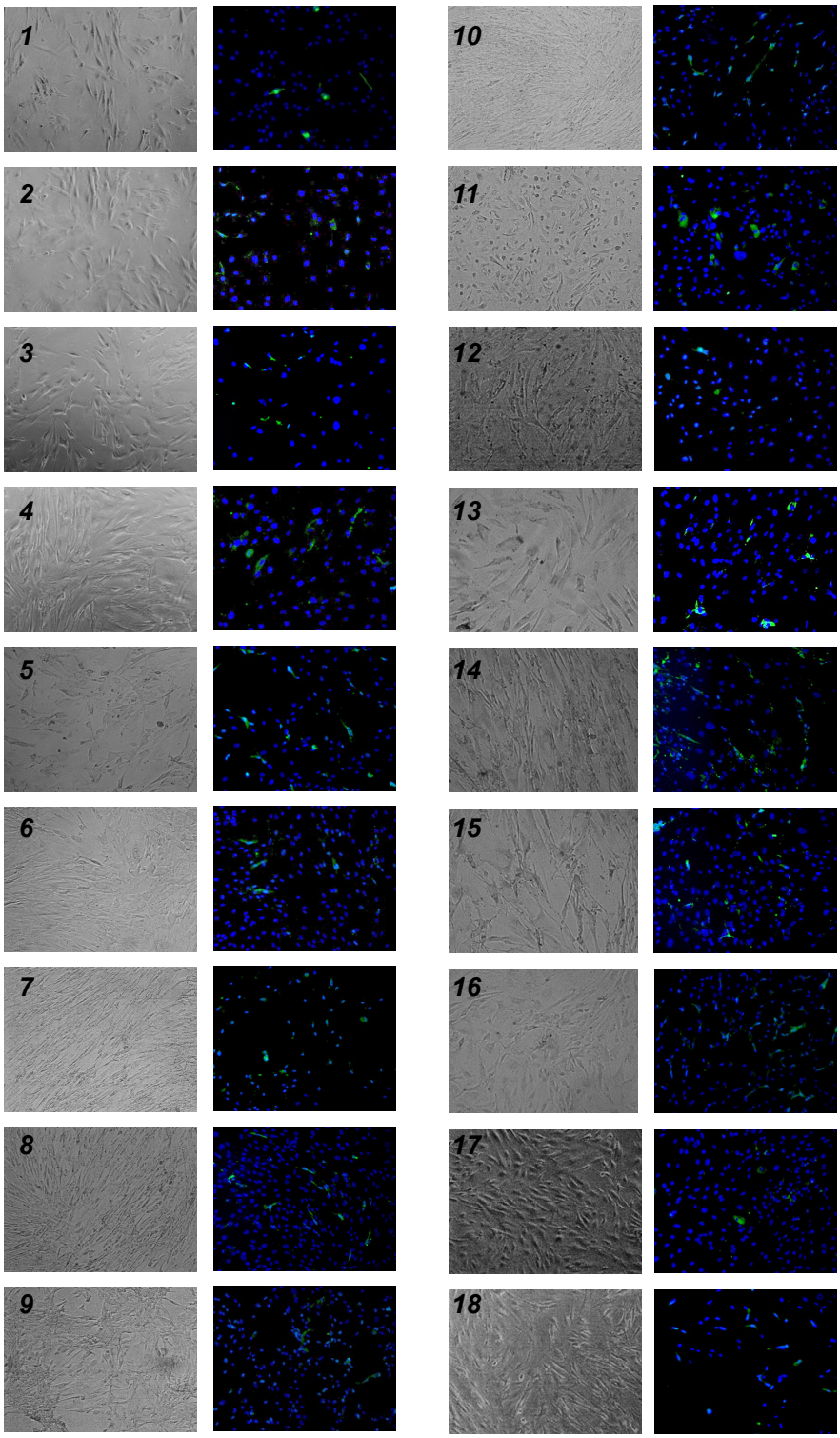
1
2
3
4
5
6
7
8
9
10
11
12
13
14
15
16
17
18

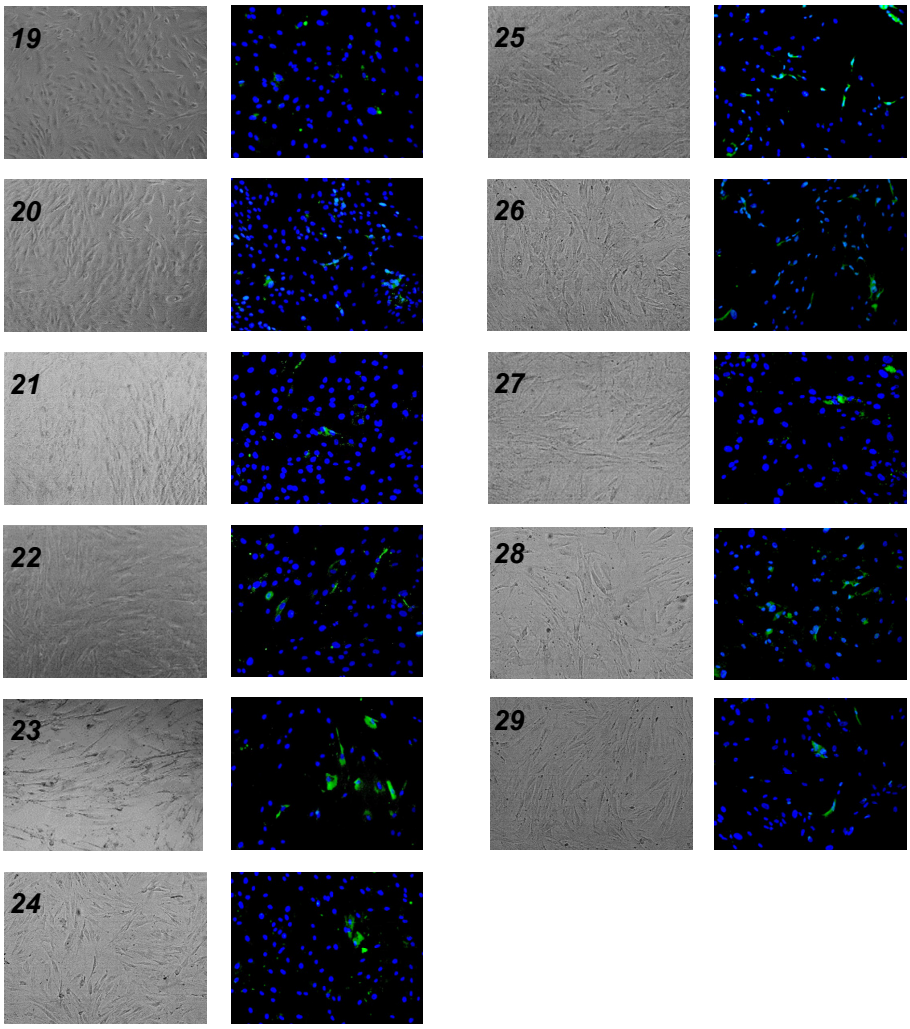

Figure 3.5. Phase contrast and merged channel (DAPI +ve FITC) immunocytochemistry images of myofibroblasts isolated from different parts of the gut (1-29, see Table 3.1 for more details).

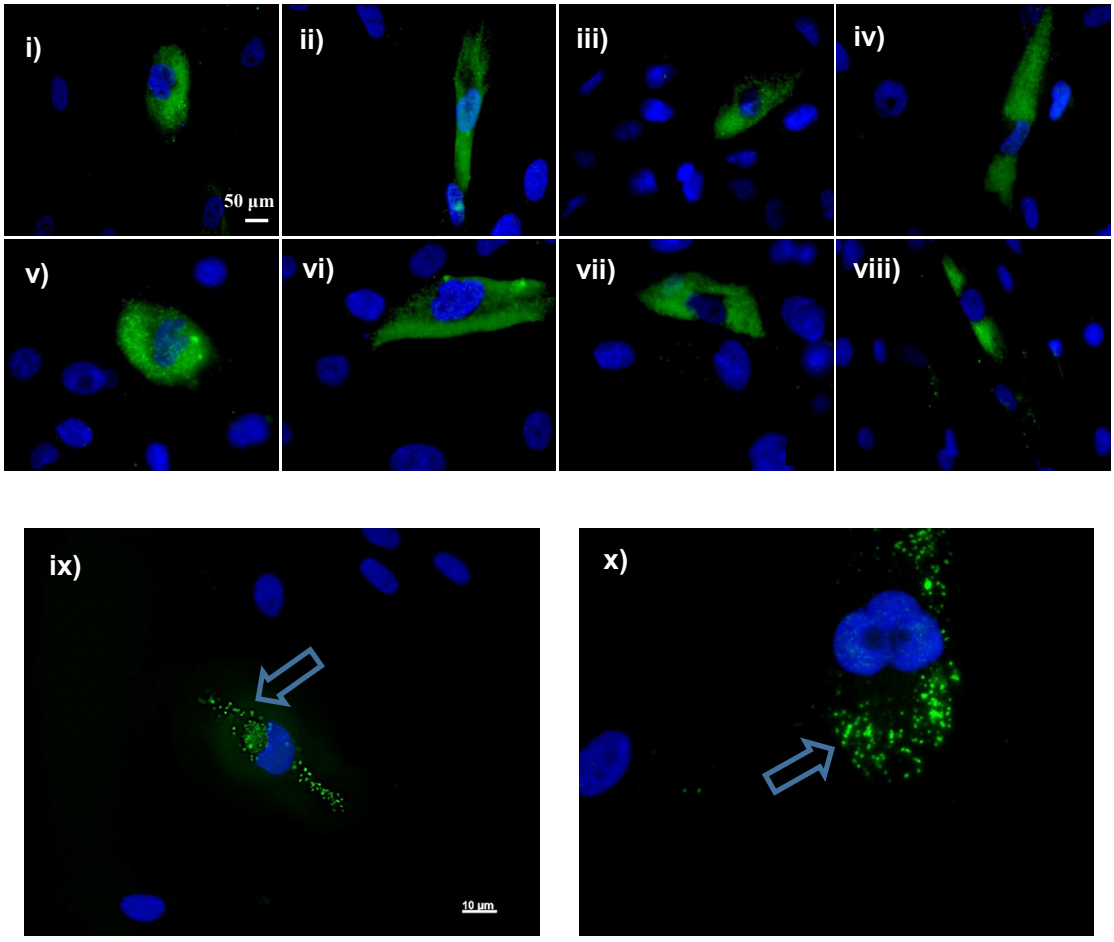

Figure 3.6. Myofibroblasts from several regions of the gastrointestinal tract express CCK2R in a subset of cells. High power immunocytochemistry images (cell nuclei blue with DAPI, CCK2R green with FITC); i) colon derived normal tissue myofibroblasts, ii) gastric myofibroblasts from a pernicious anaemia patient, iii) cancer associated myofibroblasts form pancreas, iv) myofibroblasts from chronic pancreatitis, v) gastric CAMs, vi) gastric NTMs, vii) oesophageal CAMs, viii) oesophageal NTMs. High resolution images of gastric CAMs processed with deconvolution software reveal granulated intracellular structure with receptor carrying vesicles (ix, x). Images represent cells obtained from different patients.

In all cases, only a subpopulation of cells were positive for CCK2R, ranging from 1 to 6% (Fig. 3.7A). Highest expression was seen in colon (5.96 ± 1.41%), followed by oesophagus (5.63 ± 0.81%) and stomach (3.87 ± 0.49%). Myofibroblasts derived from patients with pernicious anaemia, chronic pancreatitis, Vipoma or GIST showed lowest expression. In the case of stomach and oesophagus, there was a significant difference (5.96% vs 0.39% and 5.63% vs 1.75%; $p < 0.05$ respectively) between CAMs and ATMs or NTMs (see below). There was no obvious difference between myofibroblasts from different regions of the gut (Fig. 3.7B).

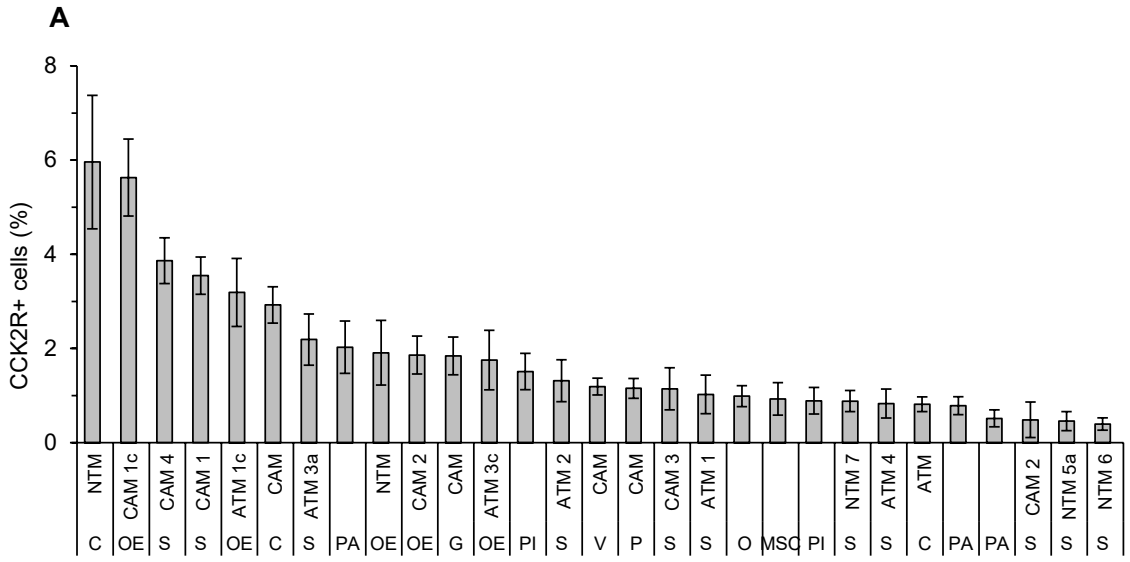

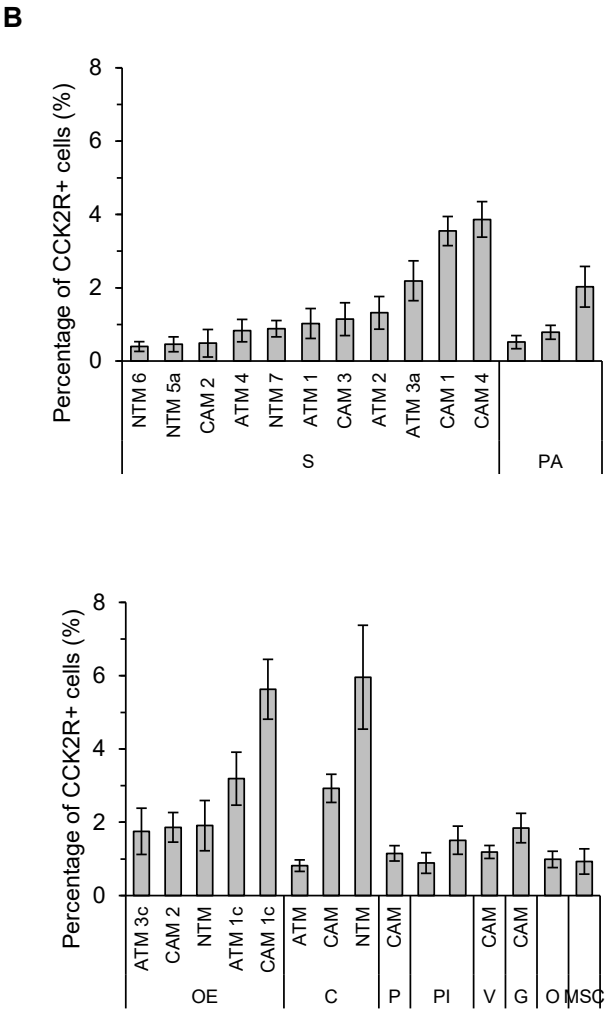

Figure 3.7. CCK2 expression in myofibroblasts from different regions of the gut, and from cancer, adjacent and normal tissue. Results are presented in order by expression levels from highest to lowest (6 to 1%) (A) and based on different organs (B). (C colon, OE oesophagus, P pancreas, PI chronic pancreatitis, V vipoma, G GIST, MSC mesenchymal stem cell, PA pernicious anaemia, O omentum, S stomach, CAM cancer associated myofibroblasts, ATM adjacent tissue myofibroblasts, NTM normal tissue myofibroblasts, Xa antrum, Xc cardia)

3.3.4 CAMs showed increased CCK2R expression compared to their ATM counterparts in patients with advanced lymph node metastasis

Next we examined the expression of CCK2R in a microarray dataset (http://www.ncbi.nlm.nih.gov/geo/query/acc.cgi?acc=GSE44740) of CAMs and ATMs prepared from 13 patients with gastric cancer (Balabanova et al. 2014). Interestingly, in patients with high lymph node involvement (graded pN2-4, see Chapter 2.18.1), which correlates with poor post-operative survival, the expression of CCK2R was higher in 5 of 6 CAMs compared with their matched ATMs, whereas in the subgroup with low lymph node involvement (pN0-1) 6 of 7 CAMs expressed lower CCK2R compared with their matched ATMs (Fig. 3.8A) and the difference was statistically significant ($P < 0.05$, Fisher exact test). A similar pattern could be observed with the immunocytochemistry findings (see above). When grouping patients into ATM and corresponding CAM pairs CCK2R expression was significantly higher in the cancer associated myofibroblast group in the case of patients with multiple lymph node metastasis (SCAM4/ATM4, pN2; S-CAM1/ATM1, pN2) compared to patients with a lower lymph node involvement (S-CAM2/ATM2, pN0; S-CAM3/ATM3, N1) where the converse was true (Fig. 3.8B).

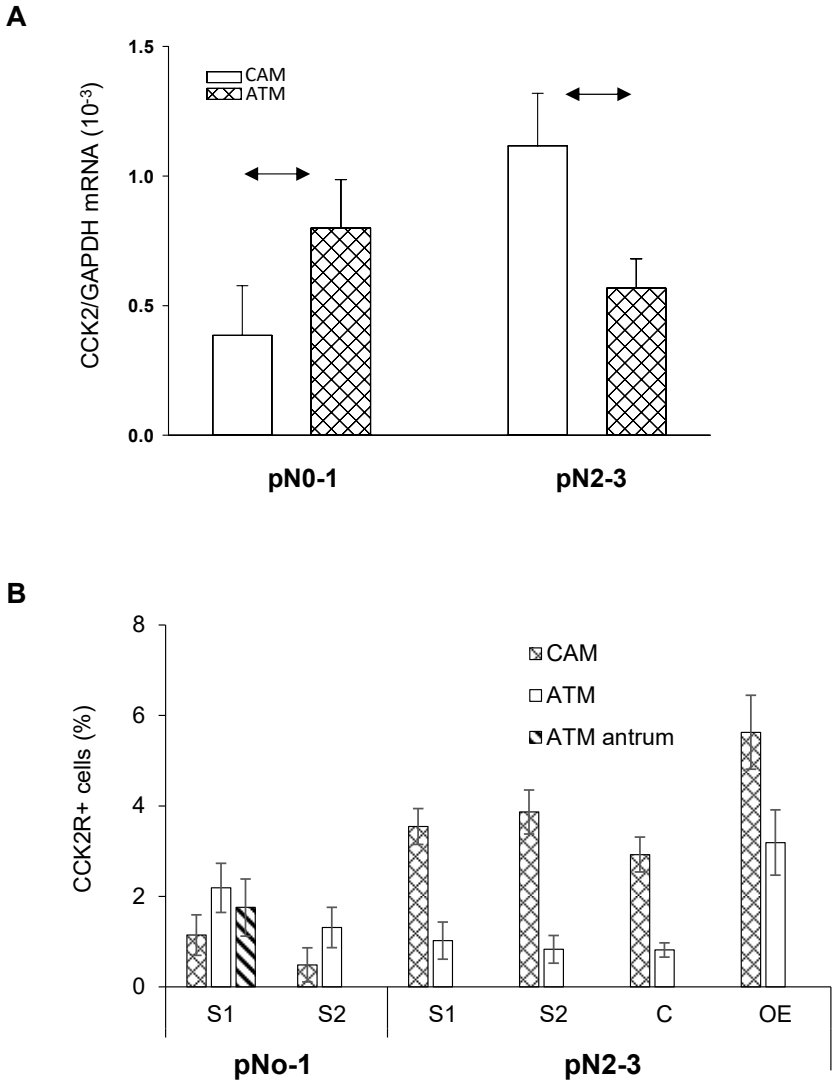

Figure 3.8. Abundance of CCK2R transcripts relative to GAPDH in 13 pairs of CAMs and their corresponding ATMs from gastric cancer patients, derived from microarray data (A). CCK2R expression compared in CAM-ATM pairs from selected patients (B). The patients were divided into two groups depending on lymph node involvement (upper panel (A) pN0-1, n = 7; pN2-4, n = 6; lower panel (B) pN0-1, n = 2; pN2-4, n = 4). There is increased CCK2R expression in CAMs in patients with advanced stage lymph node metastasis (pN≥2-3), whereas the opposite was true in case of patients with metastasis in less than two regional lymph nodes. S indicates stomach, C colon, OE oesophagus. Means ± SE, horizontal arrows significantly different $p < 0.05$ in both cases.

3.3.5 Gastrin increases intracellular calcium in a subset of myofibroblasts.

In order to determine whether myofibroblasts are capable of mounting a functional response to gastrin we then examined changes in cytosolic calcium on administration of hG17. A relatively high proportion of gastric CAMs (5-10%) showed spontaneous activity (Fig. 3.9B). Generally, cells with spontaneous calcium oscillation were more likely to react to gastrin, but the picture was complicated by a persisting refractory period shortly after activation. In order to see the effect of gastrin more clearly, we added EGTA to the solution in advance as a calcium binder. In subsequent experiments we were able to detect a clear gastrin response. In myofibroblasts in SF medium, there was labelling with Fluo-4 referring to a basal calcium level with no or infrequent spontaneous fluctuations in intracellular calcium. Administration of hG17 (10 nmol/L) produced a prompt increase in intracellular calcium in a subset of gastric CAMs (5.3 ± 1.4% of total; 169 cells counted in three fields) (Fig. 3.9A and B). When the calcium ionophore ionomycin was applied as a positive control, there was a sustained increase in intracellular calcium in virtually all cells.

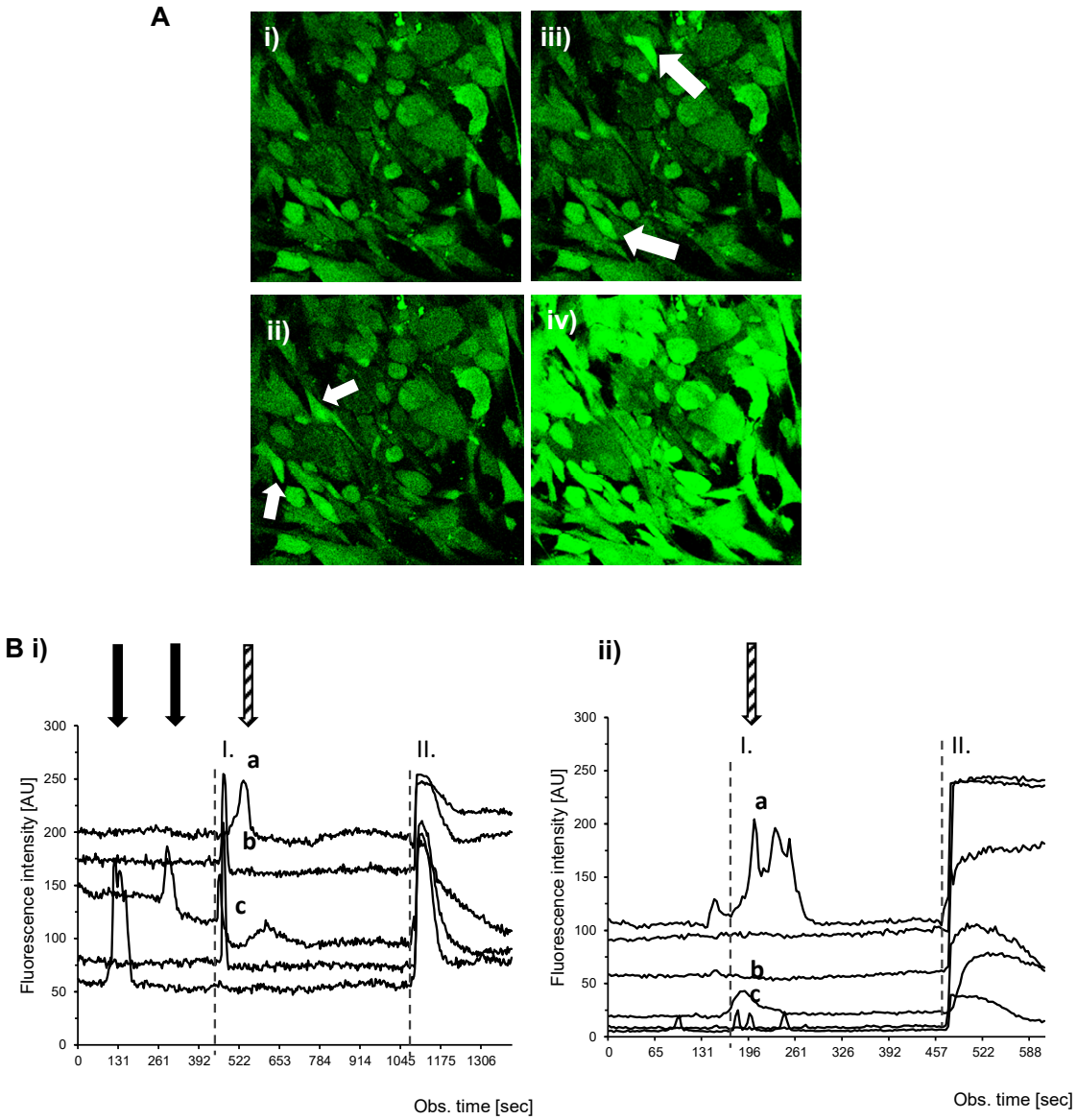

Figure 3.9. Gastrin increases intracellular calcium in a subset of myofibroblasts. (A) Labelling of gastric CAMs with Fluo-4; i), control, ii-iii) stimulation with hG17 (10 nmol/L) (ii spontaneous activity; iii gastrin stimulation), arrows indicate responding cells; iv) effect of ionomycin (1 µmol/L). (B) hG17 (applied at I) stimulated a transient increase in intracellular calcium in a subpopulation of gastric CAMs; ionomycin (applied at II) produced a sustained increase in calcium in the majority of cells. Black arrows indicate spontaneous calcium activity (i), which was diminished after EGTA was applied leaving cells with a basal fluorescence only (ii). Stripped arrows show myofibroblasts responding to gastrin (a,b,c).

3.3.6 CCK2R expression is associated with the cell cycle.

As suggested by the initial data, to further investigate whether CCK2R expression was related to the cell cycle, we incubated gastric CAMs in FM or SF medium and examined expression by flow cytometry. Lack of nutrients and growth factors leading to G0/G1 arrest was verified by nuclear DAPI staining. Cell cycle stages were detected based on nuclear density resembling chromosomal ploidy. After 48 h there was a significant decrease in proliferation following serum starvation with cells accumulated at the G0/G1 checkpoint (77.3 ± 8.4% vs 66.8 ± 1.2% G0/G1 in SF and FM respectively; $p < 0,05$) (Fig 3.10A). Upon receptor staining the subset of cells expressing CCK2R amounted to approximately 2% of total cells in FM, but when cells were cultured in SF medium to depress proliferation, the population of CCK2R-labelled cells was approximately 0.6% total (Fig. 3.10B).

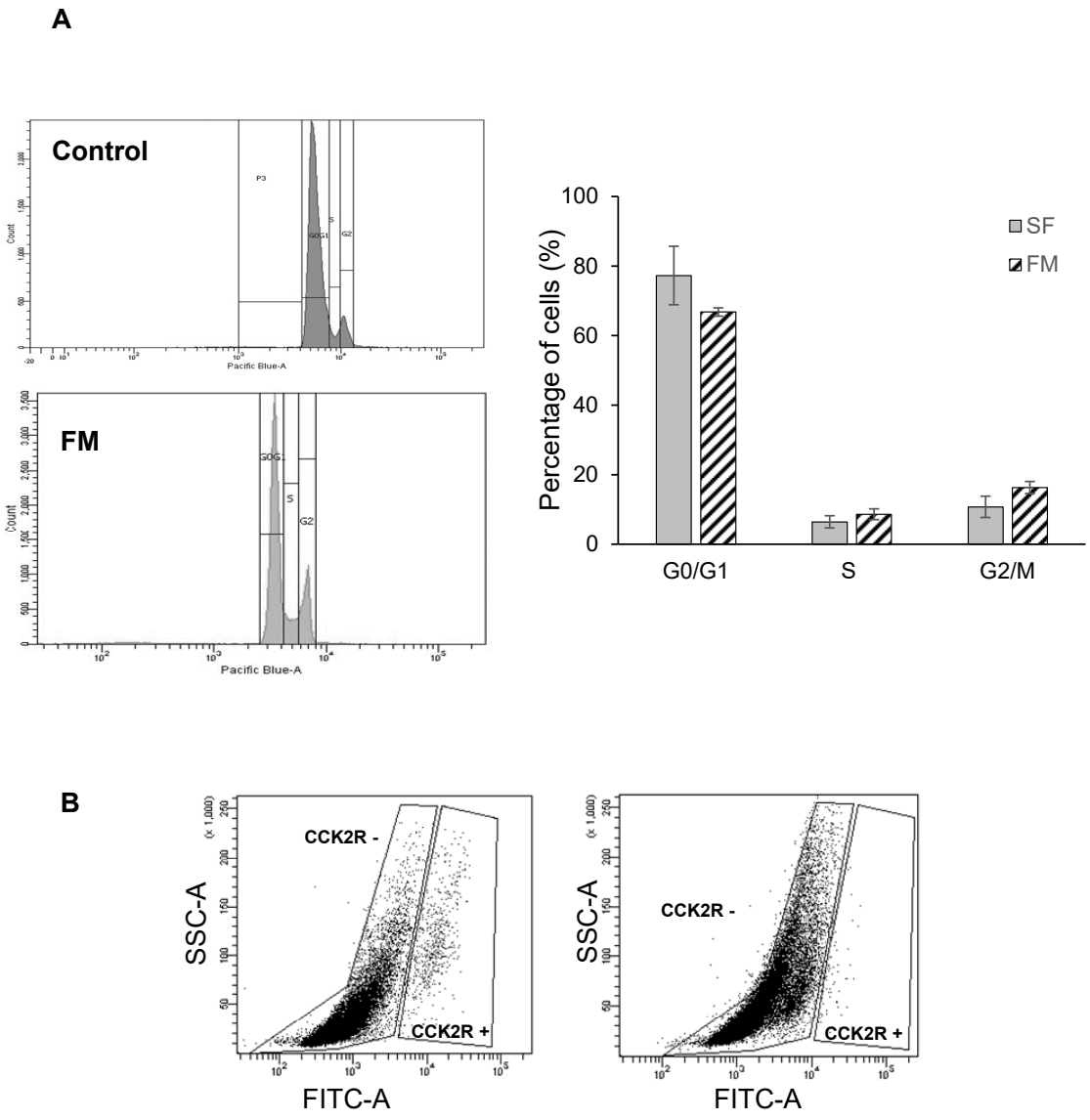

Figure 3.10. Proportion of cells in different stages of the cell cycle before and after serum starvation. Representative histograms show a decrease in proliferation following serum starvation with cells arrested at the G0/G1 checkpoint (A). CCK2R expression is associated with proliferation. (A) Flow cytometry shows a subpopulation of cells cultured in full medium express CCK2R (left) but this population is diminished by incubation of cells in serum free medium (right) with suppressed proliferation (B). Means ± SE, n=3.

We then considered the hypothesis that expression of CCK2R was dependent on the cell cycle. To this end, we used EdU (5-ethynyl-2´-deoxyuridine), which is a nucleoside analogue that is incorporated into DNA during S-phase. After synchronisation, cells were examined for co-localisation of EdU and CCK2R (Fig. 3.11A). Experiments were carried out using two independent primary gastric CAM cell lines derived from separate patients.

In the conditions of the experiment most cells were negative for both EdU and CCK2R (79.5 ± 4.0%). There were substantial numbers of EdU positive cells that were CCK2R negative (15.9 ± 4.0%) (Fig. 3.11B). CCK2R positive cells accounted for 5% of the total population. Interestingly, over 80% of cells expressing CCK2R were found to be labelled with EdU (Fig 3.11).

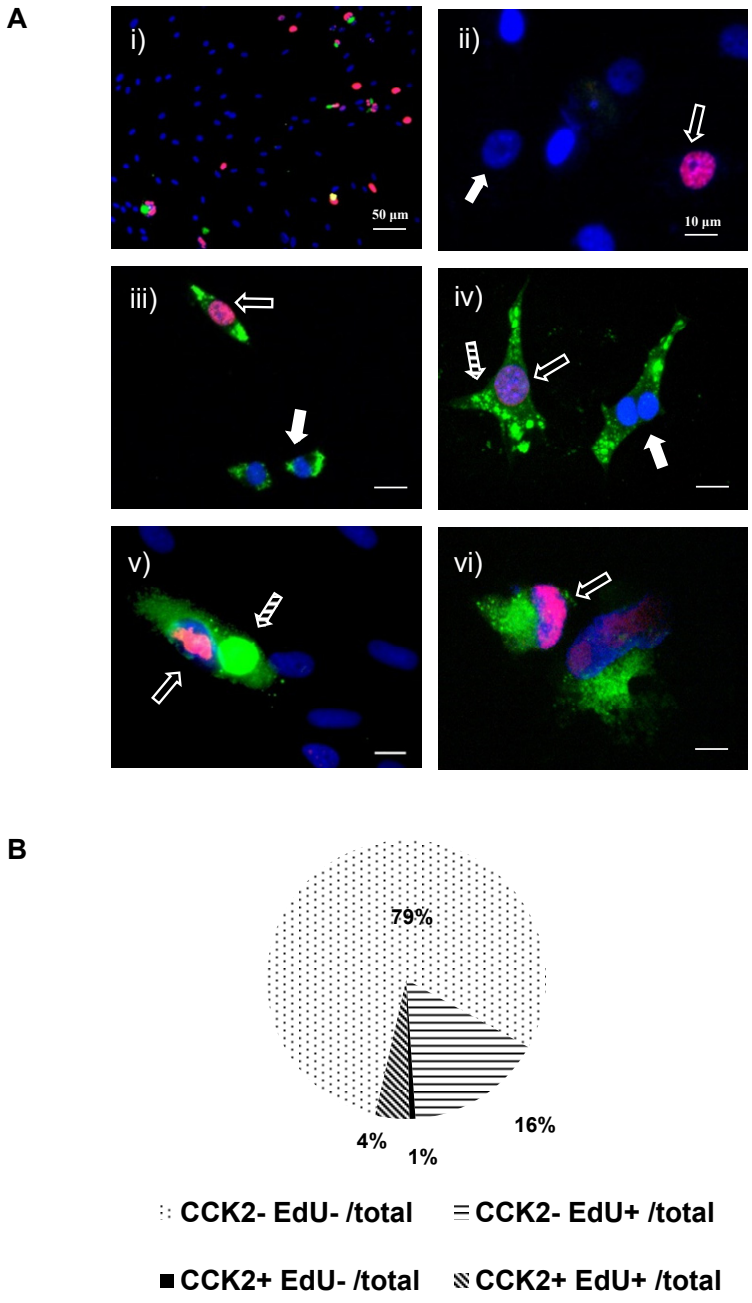

Figure 3.11. Low (i) and high power images (ii) of proliferating cells incorporating nucleoside analogue EdU (A). Distribution of myofibroblast based on immunostaining for EdU and CCK2R (B). In order to assess the relation between proliferation and CCK2 expression, different gastric CAMs were also double labelled for the receptor (CAM1 iii-iv, CAM2 v-vi). Immunostaining for markers above revealed the majority of cells to be negative for both CCK2 and EdU (79%), a bigger proportion of cells incorporated EdU but were missing the receptor (16%). Myofibroblasts positive for both markers accounted for 4% of total. The fourth distinguishable group consisted of gastric CAM exhibiting CCK2 expression but not EdU incorporation with less than 1%. Open arrows EdU – red nuclei, filled arrows - DAPI stained nuclei, stripped arrows – CCK2R.

In order to resolve the possibility of a cell cycle dependent receptor expression we performed kinetic experiments with myofibroblasts in either FM (i.e. normally cycling) or SF (i.e. arrested at the G0/G1 checkpoint) incubated in EdU for periods of 0.5 to 24 h. As expected, cells incubated in FM exhibited significantly higher labelling with EdU compared with cells in SF medium after 4 h (28.7 ± 0.3 vs 5.2 ± 0.6% cells incorporating EdU, respectively, $p < 0.001$) (Fig. 3.12A). However, while the proportion of cells showing EdU incorporation increased with duration of incubation in FM the proportion of CCK2R labelled cells remained relatively constant at 3-10% of total. CCK2R expression was highest in the earlier time points and then declined after about 4h in EdU. Similarly, the subpopulation of CCK2R positive cells that were not labelled with EdU (<1% of total) remained relatively constant (Fig. 3.12B and C). The data are consistent with transient expression of CCK2R by cells in S-phase with a possible loss of expression or inactivation thereafter.

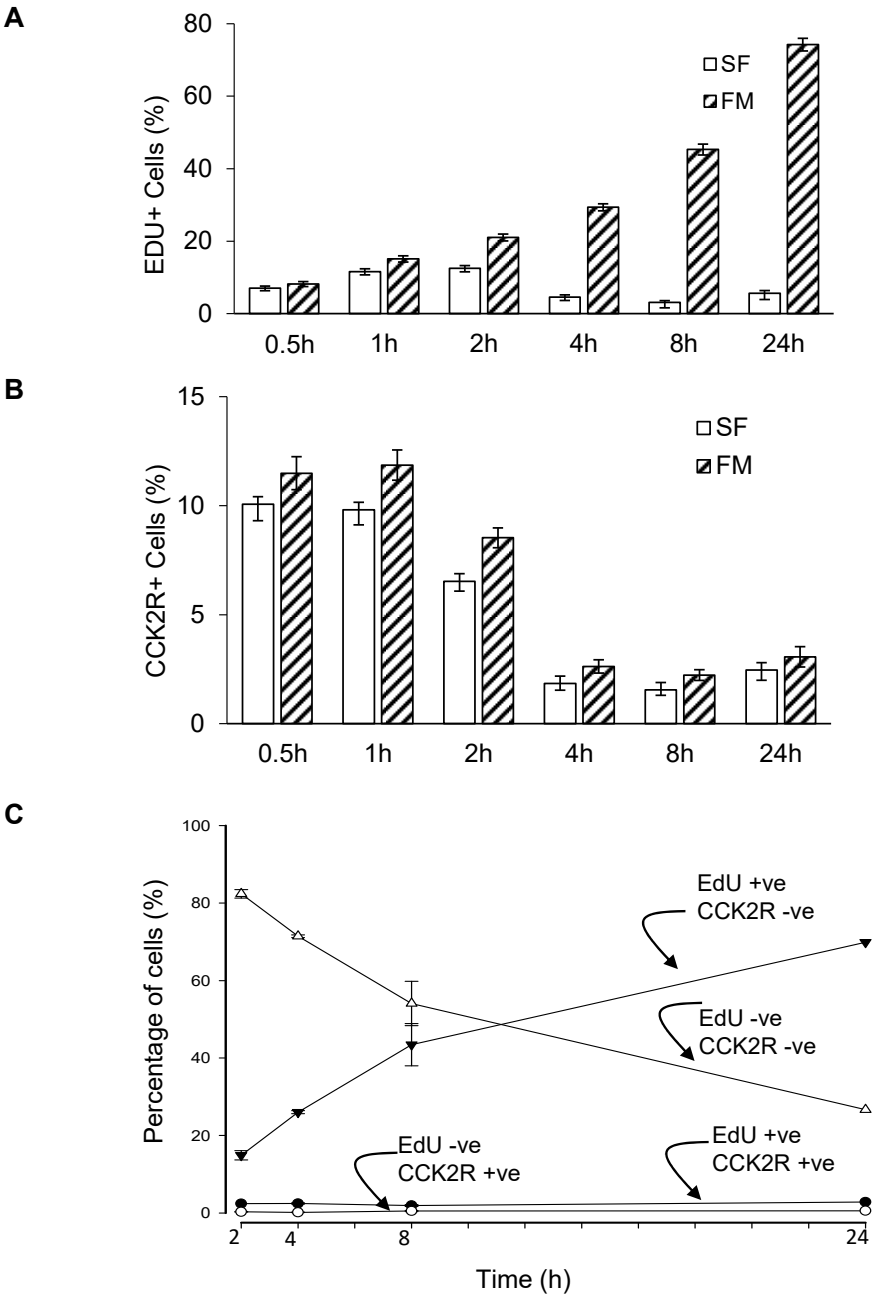

Figure 3.12. Relation of EdU labelling and CCK2R expression with extent of incubation. (A) Progressive increase in total of EdU labelled cells with duration of incubation in full medium, compared with serum free medium. (B) Proportion of all CCK2R expressing cells is relatively high at early time points and then decreases after 4 hours indicating receptor presence in the early S phase. (C) Breakdown of EdU incorporation and receptor expression in different labelled groups. Incorporation of proliferation marker only increases with time (▼), but the proportion of cells expressing CCK2R, that are also labelled with EdU (●) remains relatively constant at 2-3% total. Less than 1% of cells express CCK2R and are not labelled with EdU (○). A decreasing proportion of cells are both EdU and CCK2R negative. Means ± SE (n = 3).

3.3.7 Gastrin does not stimulate proliferation or apoptosis of myofibroblasts

Since CCK2R expression was associated with EdU incorporation we then asked whether gastrin influenced EdU uptake. Myofibroblasts were treated with different concentrations of gastrin (0.1 - 10 nmol/L hG17) overnight. We found no significant difference in EdU incorporation in response to the peptide hormone (Fig 3.13A). Because the receptor is only expressed by a small proportion of cells, we evaluated proliferation in the CCK2R positive subgroup, but there was no measurable effect of gastrin (Fig. 3.13B). Moreover, there was no significant difference in EdU incorporation between control and gastrin-treated groups either in the case of ATMs or the corresponding CAMs (22.9 vs 19.8%; 12.8 vs 12.1%; 10nmol/L hG17 vs SF in CAM and ATM respectively). Gastrin also had no effect on CCK2R expression amongst these pairs (25.1 vs 26.5%, 4.1 vs 5.2%; 10nmol/L hG17 vs SF in CAM and ATM respectively), although a higher number of receptor positive cells could be observed in the CAM group as described before (Fig. 3.13C and D).

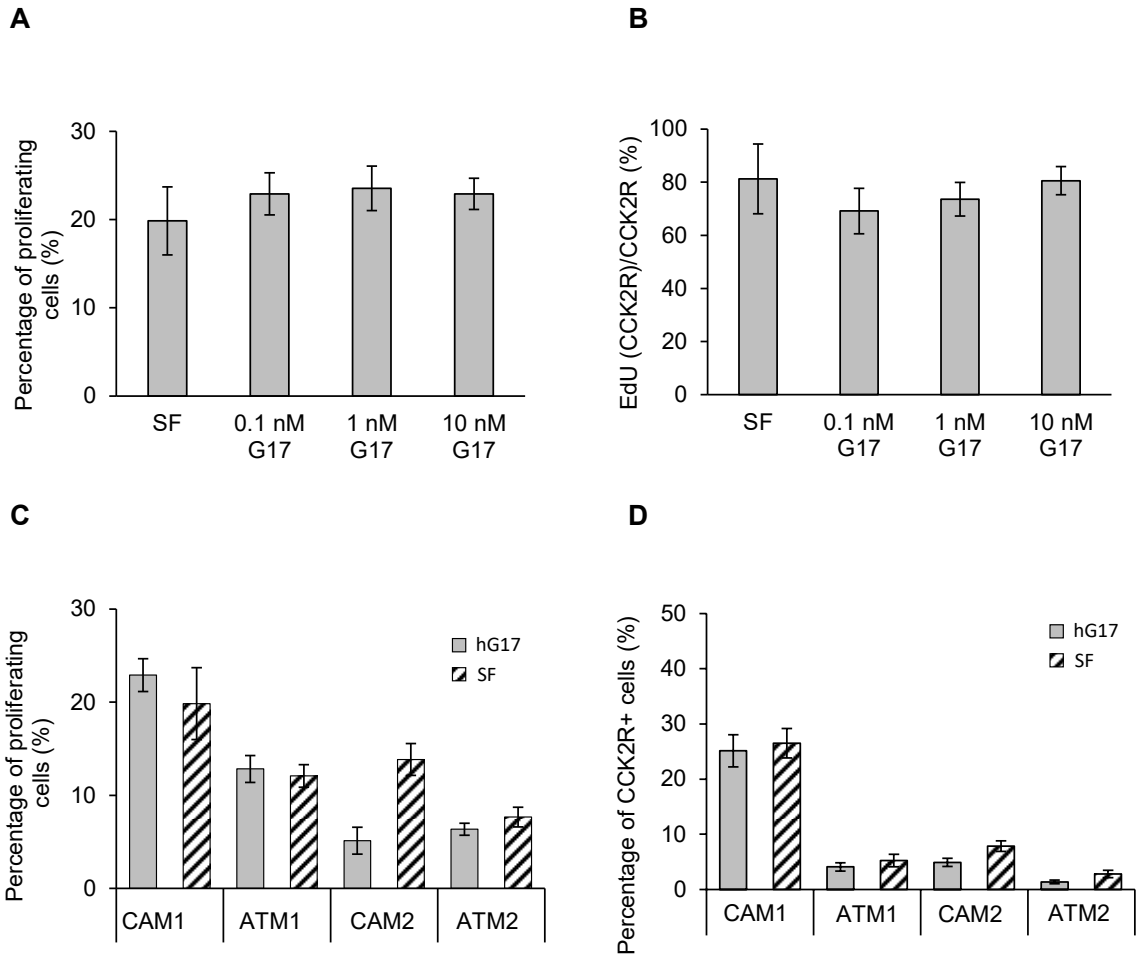

Figure 3.13. Effect of gastrin on selected CAM-ATM pairs. (A) Incubation in hG17 (for 24h) in a 100-fold range to broadly cover physiological concentration had no effect on EdU incorporation. (B) CCK2R positive cells did also not present increased proliferation after gastrin treatment. Similar observations were found in CAM-ATM pairs with gastrin having no significant effect on EdU incorporation (C) or CCK2R expression (D). In both pairs CAMs exhibited higher number of CCK2R positive cells as shown before in figure 5B. Means ± SE (n = 3).

Moreover with flow cytometry, the proportions of cells in G0/G1, S or G2/M phases of the cell cycle were not significantly different after incubation with hG17 (77.3 vs 79.25%, 6.45 vs 6.55%, 10.75 vs 9.45%; SF vs G17 in phases G0/1, S, G2/M respectively) (Fig. 3.14A and B).

Gastrin also had no significant effect on caspase-3 labelling used as a marker of apoptosis which was around 3% of total cells (Fig. 3.14C).

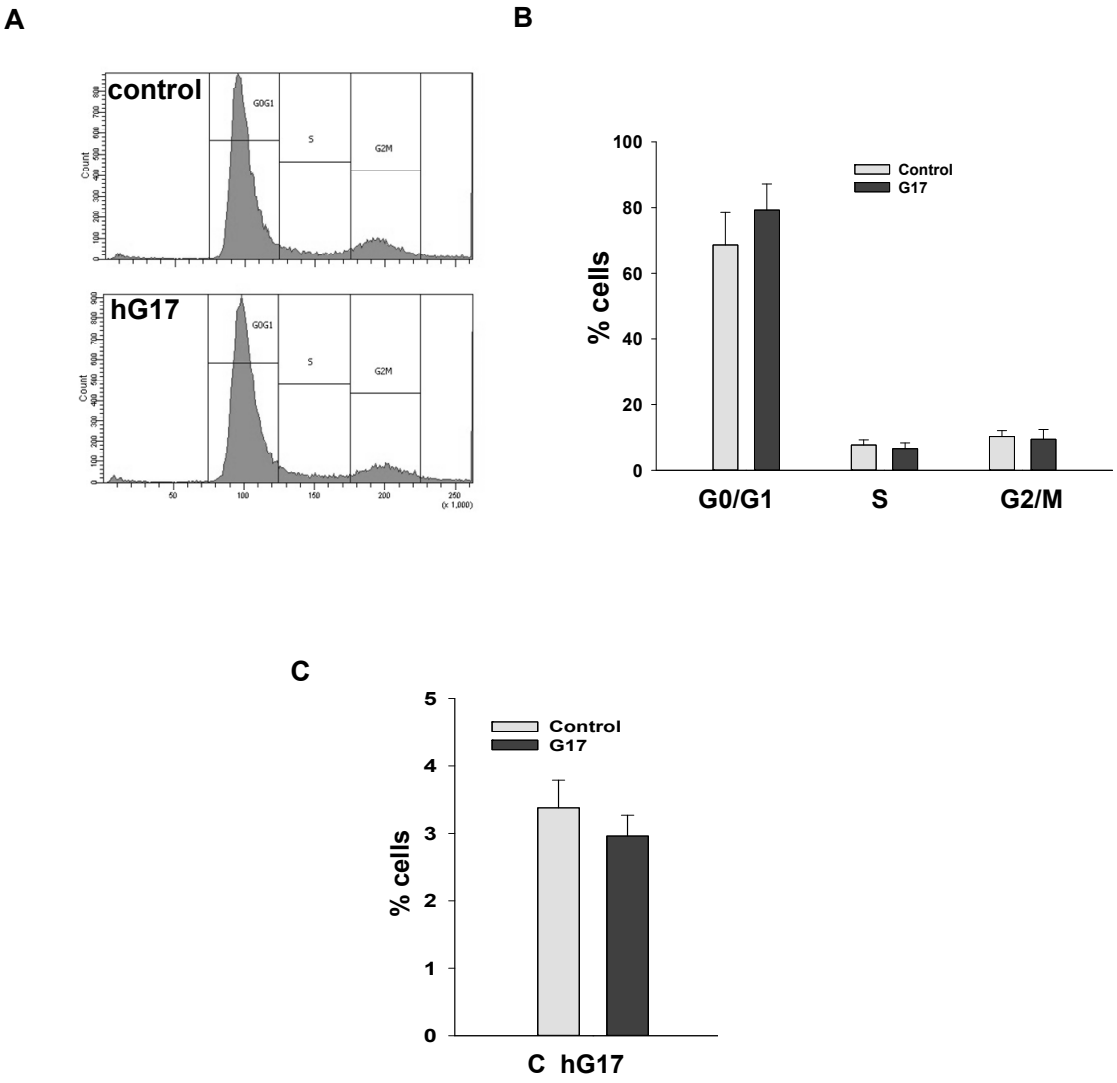

Figure 3.14. Gastrin does not stimulate proliferation or apoptosis in myofibroblasts. (A) Representative flow cytometry profiles show no effect of incubation in hG17 on the proportion of cells in G0/G1, S or G2/M. (B) Quantification of cells in G0/G1, S or G2/M by flow cytometry in three separate experiments. (C) Staining with antibody to caspase-3 shows no effect of hG17 (10 nmol/L, 24 h) on apoptosis. N = 3, means ± SE.

Table 3.2 shows the distribution of myofibroblasts in different subgroups (CCK2R- EdU-; CCK2R- EdU+; CCK2R+ EdU-; CCK2R+ EdU+) after gastrin treatment. The antral hormone did not cause a shift in percentages in the majority of groups, having no effect on proliferation as described before, but it almost doubled the number of those proliferating cells, which happened to express the receptor indicating a possible acceleration of the cell cycle.

	CCK2- EdU- /total	CCK2- EdU+ /total	CCK2+ EdU- /total	CCK2+ EdU+ /total
SF	79.46 ± 3.98	15.89 ± 3.97	0.69 ± 0.52	3.96 ± 1.60
0.1 nM G17	76.41 ± 3.21	13.00 ± 2.89	2.03 ± 0.75	8.55 ± 1.46
1 nM G17	78.00 ± 1.84	1448 ± 2.16	1.25 ± 0.40	6.27 ± 1.22
10 nM G17	77.31 ± 2.12	12.52 ± 1.17	1.37 ± 0.51	8.80 ± 1.20

Table 3.2. Percentage of gastric cancer associated myofibroblasts after treatment with gastrin. Different concentrations (0.1 - 1.0 - 10 nmol/L) of amidated gastrin (hG17) were applied. Cells were double labelled with EdU and anti-CCKBR antibody. N = 4, means ± SE.

Furthermore, a relatively high number of cells were detectable with separating nuclei undergoing mitosis with a distinct variability among the aforementioned subgroups. In order to assess whether gastrin has any influence on this phenomenon, treated myofibroblasts were also evaluated for mitosis. Both in the EdU labelled group and in the CCK2 expressing subgroup gastrin increased the proportion of mitotic cells in a dose depended way (1.9 ± 9.7 vs 40 ± 45%; 37.5 ± 18.3 vs 69.8 ± 7.6%; SF vs hG17 respectively) (Fig 3.15A and B). Cell nuclei with mitotic spindles were observable in almost all cases. A similar effect was seen using CAM-ATM pairs with ATMs having a slightly higher mitotic activity (24.9 ± 5.2 vs 17.4 ± 4.8%, 34.5 ± 5 vs 22.1 ± 4.4%; SF vs hG17 respectively) (Fig 3.15C). This is suggestive of gastrin stimulating progression through G2 via CCK2R expressed in S phase.

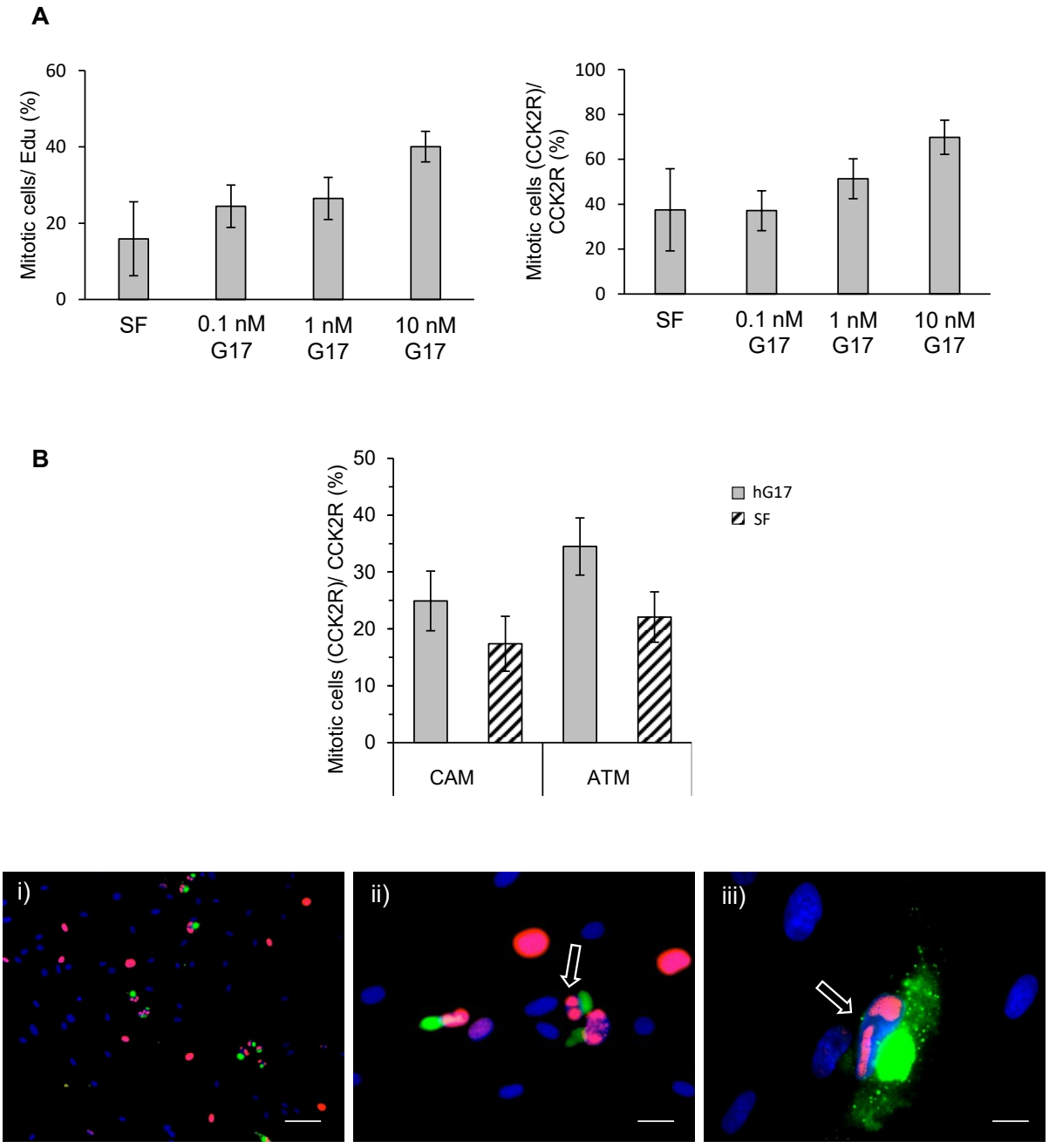

Figure 3.15. Effect of gastrin on cell cycle progression. (A) Gastrin significantly increased the number of cells entering M phase in a dose dependent way suggesting accelerated progression in G2/M of the cell cycle. (B) ATMs exhibited higher mitotic activity when compared to CAMs after treatment with 10 nmol/L hG17. Arrows indicate mitotic nuclei with forming spindle apparatus. N = 4, means ± SE. Scale bar 50μm (i), 20 μm (ii), 10 μm (iii).

3.3.8 Gastrin stimulates migration and invasion of EdU-labelled and unlabelled gastric myofibroblasts

Since other work indicates that stimulation of myofibroblasts is linked to migration and invasion, we then examined the effect of hG17 on these responses using Boyden chambers. There was a clear stimulation of both migration and invasion ($p<0.05$; ANOVA) by 10 nmol/L hG17 that was inhibited by the CCK2R antagonist 100 nmol/L L740093 in gastric myofibroblasts (Fig. 3.16A and B).

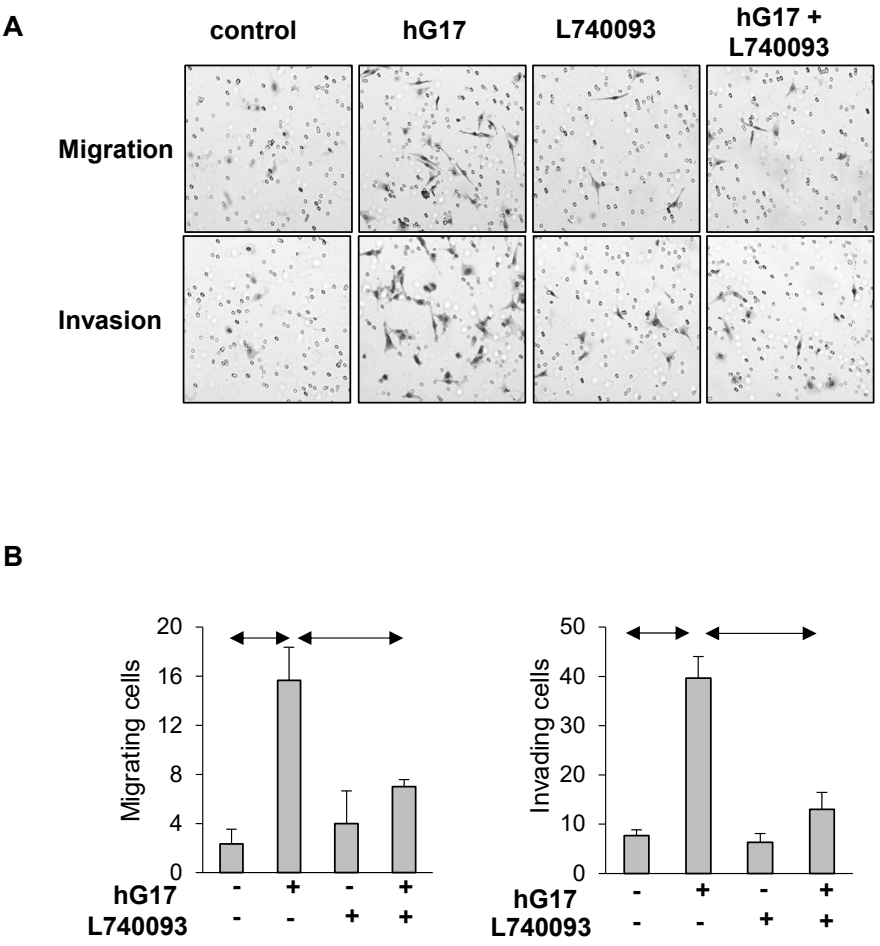

Figure 3.16. Gastrin stimulates myofibroblast migration and invasion. (A) Representative Boyden chamber images showing migration (top) and invasion (bottom) in response to hG17 (10 nmol/L), L740093 (100 nmol/L), and the combination. (B) hG17 stimulates both cell migration (left) and invasion (right) of myofibroblasts in Boyden chambers and the response is inhibited by the CCK2R antagonist, L740093; y-axis mean ± SE number of cells per field. Horizontal arrows, $P < 0.05$, ANOVA.

To further characterize the migrating cells, we examined whether they incorporated EdU. There was indeed hG17-stimulated migration of EdU labelled cells that was inhibited by L740093 ($p < 0.05$; ANOVA) (Fig. 3.17A and B). However, only about 40% of the migrating cells were labelled with EdU suggesting that cells expressing CCK2R were also able to activate other cells via a paracrine pathway. Both the number of EdU labelled and non-labelled cells increased after gastrin treatment and this correlated with concentration of hG17. Nonetheless the proportion of proliferating cells compared with non-EdU labelled ones, expressed as a percentage ($\Delta_{\Sigma\text{-EdU}}\Delta hG17$= -7.57%) showed a modest decrease with higher gastrin concentrations. This most likely puts emphasis on the main, direct route especially at higher gastrin concentrations

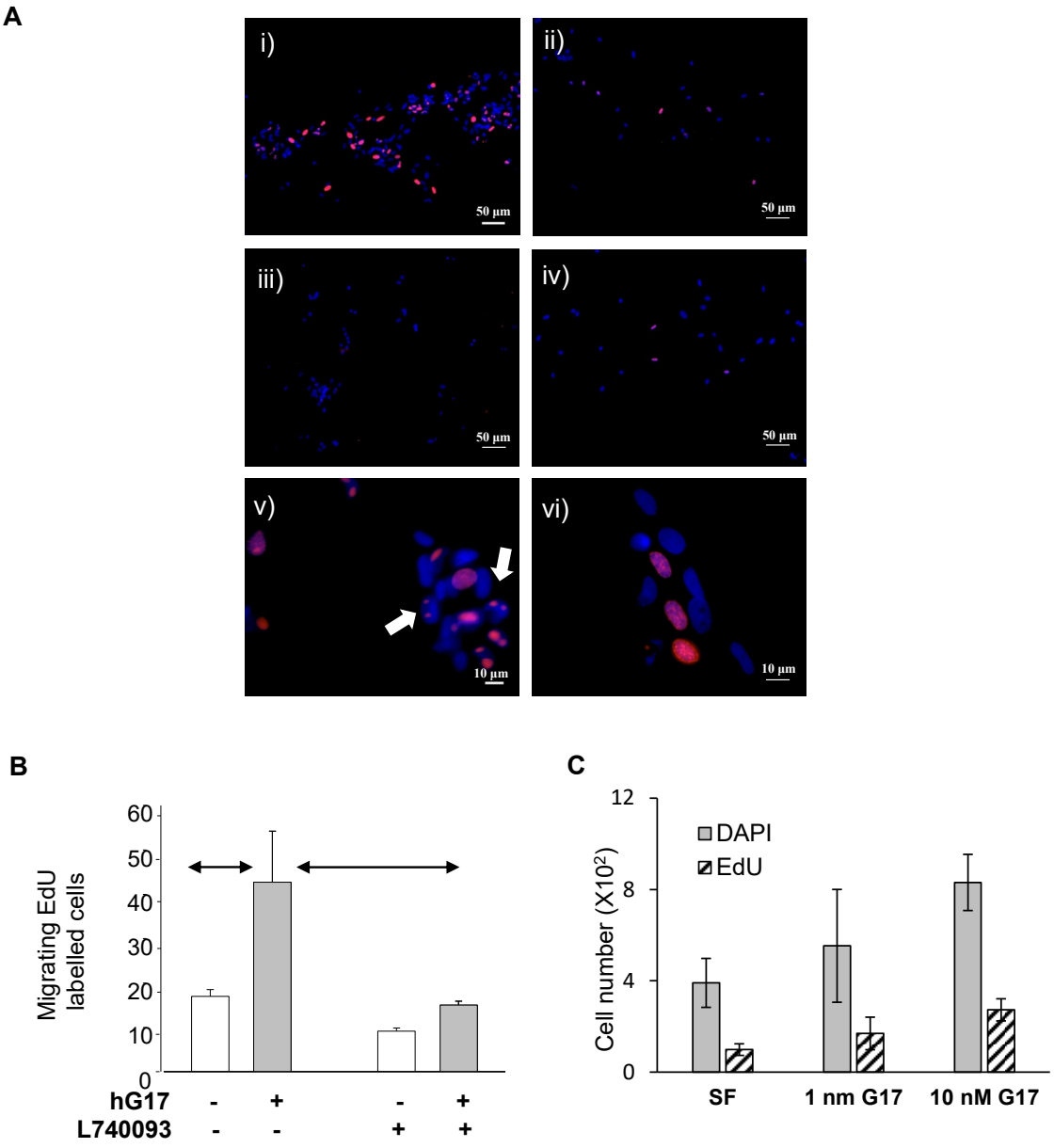

Figure 3.17. Gastrin stimulates migration of myofibroblasts independently of EdU labelling. (A) Representative images after (i) treatment with 10 nM G17, (ii) 10 nM G17 and receptor antagonist (L740093), (iii) control serum free media and (iv) serum free media with L740093. High power images of migrating cells (v, vi). Arrows indicate mitotic cells (blue nuclei Dapi, red nuclei EdU). (B) Gastrin stimulates migration of EdU labelled cells. This effect was inhibited when receptor antagonist L740093 was applied. Y-axis labelled cells per field, horizontal arrows, $P < 0.05$, ANOVA. (C) Gastrin stimulates migration of non-EdU labelled cells showing a decreasing tendency with higher gastrin levels. Y-axis cells per membrane, N = 3, means ± SE.

A role for IGF in mediating autocrine/paracrine signalling in myofibroblasts is well-established (Hemers et al. 2005, McCaig et al. 2006). To determine the role of IGF in mediating the response to gastrin we studied an IGF receptor tyrosine kinase inhibitor AG1024. The latter suppressed hG17-stimulated migration, and to a lesser extent invasion (Fig. 3.18A). Additionally, in the presence of hG17 the relative abundance of IGF-2 transcripts was 2.1 ± 0.1 fold higher than control ($p < 0.05$); IGF-1 transcript abundance was virtually undetectable in these cells. GLP-2 stimulated myofibroblasts were used as positive controls for IGF detection (Fig. 3.18B) (Shawe-Taylor et al. 2017).

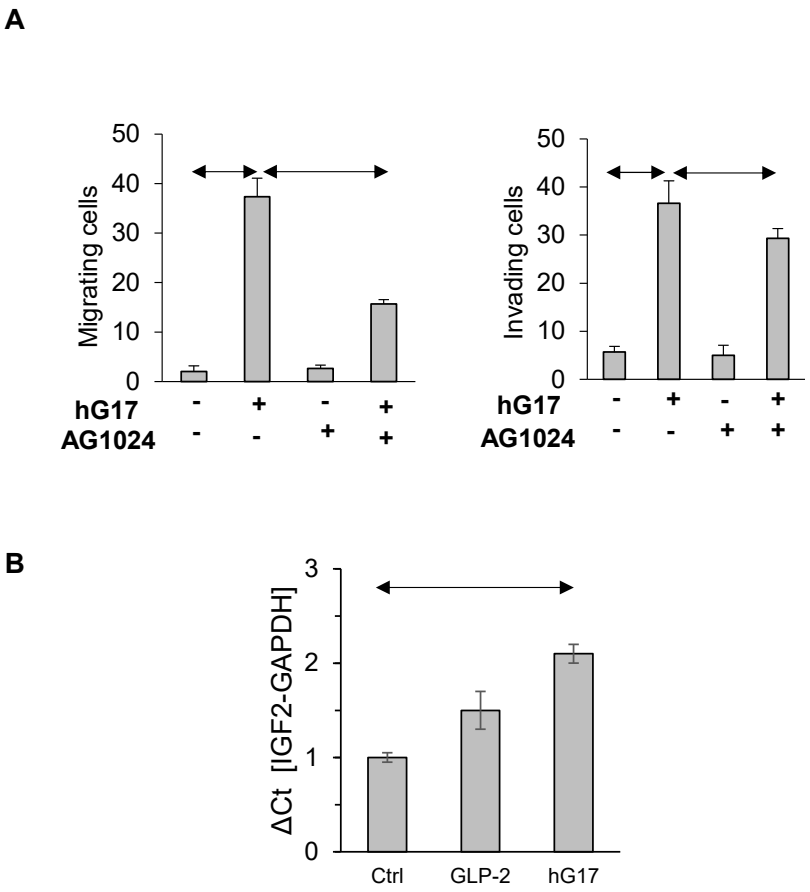

Figure 3.18. Effect of IGF antagonist on gastrin mediated invasion and migration. (A) Migration (left) and invasion (right) in response to hG17 was suppressed by the IGF-1 receptor tyrosine kinase inhibitor (AG1024, 2 μmol/L). Y-axis cells counted per field. IGF-2 transcript abundance was 2 fold higher in the hG17 treated group compared to the control. Y-axis Ct values standardized to GAPDH. Horizontal arrows, $P < 0.05$, ANOVA in both cases.

3.4 Discussion

In the normal gastrointestinal tract, CCK2R expression is localised to parietal cells, ECL cells, LGR5+ antral stem cell populations, smooth muscle and some enteric neurons (Dufresne et al. 2006, Hayakawa et al. 2016). Beside the well known role of gastrin in the control of gastric acid secretion via release of histamine from ECL cells, it also exerts a variety of other actions. For example, it is well known that patients with ZE syndrome have hypertrophic fundic mucosa indicating a trophic effect of gastrin and this is further indicated by the observation that long term hypergastrinaemia in chronic atrophic gastritis or as a result of PPI treatment is associated with hyperplasia of ECL cells and in extreme cases with gastric neuroendocrine tumours (NETs or carcinoids) (Hakanson et al. 1986, Lamberts et al. 2001). In this context, cells of a fibroblastic lineage represent a novel and still poorly described site of CCK2R expression in the gut. The present chapter focuses on CCK2 expression by gastrointestinal myofibroblasts and their role in gastrin mediated cell migration and invasion.

There are well known issues regarding interpretation of immunocytochemical studies with antibodies to G-protein coupled receptors (GPCRs). Recent findings show that only around 50% of all commercially available antibodies, regardless of epitope, are fit for purpose (Berglund et al. 2008, Baker 2015). Therefore it becomes crucial to validate rigorously any antibody used in immunochemistry. The antibody we employed was validated by the finding that wild type AGS cells (which do not express the receptor) were unstained while

there was a strong signal in those cells that were stably transfected with CCK2R. Similar results have also been obtained with an oesophageal cell line (OE33 cells) transfected with the receptor (Haigh et al. 2003). These findings therefore provide direct support for the specificity of the antibody in localizing CCK2R.

The proportion of myofibroblasts expressing CCK2R varied from 1 to 6% and this is probably related to the rate of proliferation of different populations of myofibroblasts since, for example, it is known that CAMs exhibit higher rates of proliferation than myofibroblasts from adjacent macroscopically normal tissue (Holmberg et al. 2012). In relation to CCK2R expression, both immunocytochemistry and data derived from a microarray dataset of gastric cancer patients showed that CAMs exhibit significantly higher receptor expression compared to their ATM counterparts supporting the idea of a relationship between CCK2R expression and cell proliferation. Expression is decreased in serum free medium and in confluent populations of cells which in both cases is attributable to the lower rates of proliferation in these conditions.

Although the proportion of CCK2R-expressing cells appears relatively low, it is similar to the proportion of cells determined to be in S-phase from flow cytometry. We used incorporation of EdU to identify myofibroblasts in S-phase. Because EdU incorporation into DNA is stable, labelled cells correspond to those that were in S-phase at some stage during the labelling period. A high proportion of CCK2R expressing cells incorporated EdU providing direct evidence of cell cycle dependent expression. This was further confirmed by

the observation that while most CCK2R-expressing cells were also labelled with EdU, there were nevertheless populations of EdU labelled cells that were CCK2R negative (i.e. corresponded to cells that had since left S-phase and ceased expressing the receptor). The data indicate, therefore, that CCK2R expression in myofibroblasts is transiently associated with S-phase although in a formal sense we cannot exclude the possibility that there are two distinct populations of cells, one of which expresses CCK2R during S-phase and the other which does not. However, while a relatively small proportion of cells may be expressing CCK2R at any one point in time, expression restricted to S-phase means that all cells in this population do indeed express CCK2R, albeit transiently, at some stage in their life cycle. In this sense looking at the overall frequency of expression at a single time point may be misleading. Kinetic experiments with myofibroblasts incubated in EdU for different periods of time revealed CCK2R expression in the earlier time points which decreased significantly after 4 hours. This is consistent with a transient expression of the receptor.

CCK2Rs are G-protein coupled receptors that following activation result in increased intracellular Ca^{2+} (Simpson 2013). The GPCR agonists that are linked to increases in intracellular calcium are also mitogens for many different cell types where proliferative response frequently reflects release of EGF receptor ligands (Prenzel et al. 1999, Varro et al. 2002). In cells of fibroblastic lineages there is an association between cell shape, cell cycle progression and calcium influx (Harootunian et al. 1991, Pennington et al. 2007)

Ca^{2+} signalling plays an important role in regulating progression through cell cycle. For the most part the focus of previous work in this area has been on progression from the checkpoint to S-phase. In certain conditions where despite the presence of a mitogen activator if the environmental factors are not optimal (i.e. lack of cell-cell contact, or the incapability of spreading) loss of growth factor evoked Ca^{2+} influx was observable and fibroblasts cease to progress through S-phase (Levine et al. 1965, Pennington et al. 2007). Similar observations were made between CCK2R expression and myofibroblast density. Reaching a certain level of confluency with cultured cells inhibited receptor expression. The same was true for low cell densities. The selective expression of GPCRs that serve to increase intracellular calcium only in S-phase suggests mechanisms that are more complex than previously supposed.

Our observations suggest that gastrin does not influence either EdU incorporation during S-phase or caspase-3 labelling as an apoptotic marker. Interestingly a relatively high number of cells showed signs of mitosis. Gastrin increased mitotic activity, therefore it is possible that receptor expression does not affect proliferation directly but it does promote progression through the cell cycle by increasing overall Ca^{2+} influx and maintaining the plateau phase thus accelerating G2 to mitosis. The situation appears to be somewhat similar for some other GPCRs that exhibit cell-cycle dependent regulation of expression. For example, the chemokine receptor CXCR3 is expressed in both S and G2-M phases in human microvascular endothelial cells (Romagnani et al. 2001); moreover, expression of GPR19 in lung cancer cells is triggered by entry into

S-phase and in this case seems to promote progression from G2 to M phase. Furthermore knockdown of the receptor lead to G2-M arrest and diminished cell proliferation (Kastner et al. 2012).

Gastrin plays an important role in tissue organisation with a number of studies reporting it to have a modulatory effect on migration and invasion. In part this is mediated via multiple paracrine pathways (i.e. stimulation of EGF receptors or transactivation of MAP kinases) (Noble et al. 2003). However, there is also evidence that direct activation of CCK2 receptors results in increased MMP1 transcript abundance in most gastric glandular epithelial cells including non-parietal cells (Kumar et al. 2015). Paracrine signalling cascades in epithelial cells include *inter alia* EGF-family members, FGF-2, IL-8, and prostaglandins (Varro et al. 2002, Noble et al. 2003). The capacity of CCK2R/EdU labelled cells to respond to gastrin in chemotaxis assays provides direct evidence that the receptor is linked to a functional response. Interestingly, in these experiments there was also increased migration of unlabelled cells. The present data suggest gastrin may also target the IGF system which is important for mediating paracrine mechanisms initiated by gastrointestinal myofibroblasts (14, 23). Thus, we show here that the IGF receptor tyrosine kinase inhibitor blocked the paracrine effect of gastrin on migration of unlabelled cells, moreover gastrin increased IGF-2 transcript abundance. Whether there are other mediators requires further work.

In experimental studies in rat, CCK2R was shown to be expressed during wound healing in the stomach (Schmassmann et al. 2000); in addition to epithelial cells the evidence indicated that several days after injury CCK2R was expressed in submucosal cells that express the myofibroblast marker, α-SMA (Ashurst et al. 2008). The mechanisms regulating expression have been studied in cultured epithelial cells where it has been shown that serum starvation and gastrin itself increased CCK2R expression (Ashurst et al. 2008). It now seems likely that different mechanisms regulate CCK2R expression in different cell types and at present it would appear that the association between expression and S-phase of the cell cycle is a property of myofibroblasts. Given the importance of myofibroblasts in tissue repair the expression of CCK2R may well underpin the gastrin-stimulated wound healing observed in animal models (Schmassmann et al. 2000). Furthermore, when myofibroblasts were stained for CD105+, which is a mesenchymal stem cell marker, roughly the same proportion of cells showed positivity (7.8 ± 1.4%), which were found to express the CCK2 receptor (not shown). This raises the possibility that those cells which present the receptor might also carry stem cell features.

There has been growing interest in the role of gastrin in promoting cancer progression (Ferrand et al. 2006, Kovac et al. 2008, Boyce et al. 2016). In part, this work has been directed at the non-classical gastrins that are thought not to act at CCK2R. The situation is not clear cut, however, since there may be a role of CCK2R in mediating the effects of progastrin (which is not a classical CCK2R agonist) on colon cancer progression (Jin et al. 2009). To the extent that research in this area has been directed at CCK2R expression it has

generally been focussed on receptor expression by either cancer cells or normal epithelial cells, including stem cells. The idea that CCK2R might also be transiently expressed in myofibroblasts adds a new dimension to this work, which is of particular interesting in view of the emerging consensus that the microenvironment is an important determinant of cancer progression (De Wever et al. 2008, Hanahan et al. 2011, Quail et al. 2013).

3.5 Conclusion

1. CCK2Rs are expressed in a subset of gastrointestinal myofibroblasts ranging from 1 to 6%.
2. CAMs showed increased CCK2R expression compared to their ATM counterparts.
3. Gastrin acting on CCK2Rs increased intracellular Ca^{2+} signalling thereby confirming a functional receptor.
4. Kinetic experiments revealed CCK2R expression to be transient and related to S phase of the cell cycle.
5. Gastrin did not influence cell proliferation or apoptosis through CCK2Rs, however it did increase migration and invasion of myofibroblasts.

Chapter 4

Association between serum gastrin and melanoma progression

4.1 Introduction

CCK2 receptors are expressed by a number of different cell types for example ECL cells, parietal cells, some smooth muscle cells, neurons and, as described in the last chapter, myofibroblasts. They have also been described in certain preneoplastic conditions of the gastrointestinal tract as well as neuroendocrine tumours or epithelial cancers such as Barrett's adenocarcinoma of the oesophagus (Haigh et al. 2003). Although CCK2R expression has been well studied in the CNS, and is well known to occur in medullary carcinoma of the thyroid, nevertheless research in the peripheral expression of CCK2R has mainly focused on cells that constitute the epithelial layer of the alimentary canal.

Melanoma is one of the most dangerous forms of skin cancer with a high metastatic potential (Ingraffea 2013). It arises from malignantly transformed melanocytes, which are melanin producing cells located in the basal layer of the epidermis (Paek et al. 2008). UV exposure is considered to be the most important environmental risk factor while germline mutations in the genes encoding the tumour suppressor cyclin-dependent kinase inhibitor 2A (Jalili et al. 2012), the BRAF gene (Dossett et al. 2015) or melanocortin-1 receptor (Williams et al. 2011) are also known to be associated with increased risk of developing melanoma. In contrast, basal cell carcinomas originating from non-keratinizing cells of the epidermis can be locally aggressive, but compared to melanoma they hardly every give distant metastasis (Karagas et al. 2007).

Data from Human Protein Atlas (HPA), the Cancer Genome Atlas, Genotype-Tissue Expression (GTEx) project and CAGE data from the FANTOM5 project

reveal expression of CCK2R in melanoma (http://www.cbs.dtu.dk/services/SignalP/). These findings raise the interesting question of whether there is a relationship between hypergastrinaemia and the progression of melanoma. Previous research has suggested that gastrin has pleiotropic effects on human melanoma cells in culture (Mathieu et al. 2005). Although the authors were unable to detect CCK2R expression by antibodies or with radioactive binding assays, RT-PCR identified mRNA for CCK2R in three human melanoma cell lines and 6 out of 7 clinical samples of melanoma metastases. It should be noted nonetheless, that these results were obtained with a primer of the noncoding region of the receptor (Mathieu et al. 2005). The initial aim of the present study was to verify expression of CCK2R in melanoma, and then to determine whether there was evidence that melanomas might be influenced by circulating gastrin.

4.1.1 Objectives

1. To evaluate CCK2R expression in histological samples from patients with malignant melanoma (MM) and basal cell carcinoma (BCC) as a control.
2. To characterise cohorts of melanoma and basal cell carcinoma patients recruited for the purpose before and after cross matching for age and sex, together with medical history including acid secretion inhibitor usage, histopathological findings of excised tumourous lesions, and *H.pylori* status established by ELISA.
3. To determine serum gastrin concentrations by radioimmunoassay in both cohorts and to investigate the relationship with pTNM stages, *H.pylori* infection and consumption of acid secretion inhibitors (ASI).

4.2 Methods

4.2.1 Immunohistochemistry

Sections from paraffin embedded blocks were stained in an automatic and standardized manner using Leica BOND Max Autostainer as described in chapter 2 section 2.3.2. Visualization of the CCK2R primary antibody was performed by colorimetric polymer-based systems. Chromoplex Dual Detection Kit was used for double labelling.

4.2.2 Patient recruitment and database

Whole blood was collected from patients referred to the Department of Dermatology, University of Szeged between February and May 2017 with the initial diagnosis of malignant melanoma or basal cell cancer. Paraffin embedded and formalin fixed patient samples for immunohistochemistry were retrieved from tissue archives of the Departments of Dermatology and Pathology, University of Szeged (see section 2.17).

4.2.3 Sample collection

Whole blood was collected, processed and serum stored at –20°C as described in chapter 2 section 2.17.1.

4.2.4 Histology

Paraffin embedded tissue sections were stained as describe earlier in chapter 2 section 2.3.2. Anti-mouse Melan-A was used as a melanocytic differentiation marker to detect melanoma cells (chapter 2 section 2.17.2).

4.2.5 Densitometry

Optical densitometry of MM (n=18) and BCC (n= 10) sections was performed for CCK2R as described in chapter 2 section 2.3.3.

4.2.6 Gastrin radioimmunoassay

Serum gastrin was determined by radioimmunoassay as detailed in chapter 2 section 2.8.

4.2.7 *H.pylori* detection

H.pylori antibodies were detected in serum samples of patients using a commercially available ELISA kit (Biohit Health Care, UK) as described in chapter 2 section 2.9.

4.2.8 pTNM staging of human malignant melanoma

The pTNM classification defined by the eighth edition of the American Joint Committee on Cancer (AJCC) on cutaneous melanomas was applied for scoring (see Chapter 2 section 2.18.1) (Gershenwald et al. 2017).

4.2.9 Statistics

Results are expressed as sum, percentage or means ± standard error. Delta percentage (Δ%) is used to express difference between groups where group values are defined by percentage to indicate distribution changes within the specific group.

Statistical analysis was done with $\chi 2$-test for receptor topography and Mann-Whitney U-test for densitometry with a significance level of $p < 0.05$ using SPSS16.0, SigmaPlot 12.0 software. For gastrin RIA and *H.pylori* ELISA data Fisher exact test and paired t-test were applied.

4.3 Results

4.3.1 Application of immunohistochemistry for the detection of CCK2R in primary tissue

The CCK2R antibody had previously been validated for cell lines (see Chapter 3, section 3.3.1) but the applicability for primary human tissue had not yet been tested. To address this question, paraffin embedded human gastric corpus biopsies (n=6) were sectioned and stained for CCK2R following the same protocol used for processing melanomas in order to provide a positive control. Gastric mucosa exhibited strong positivity while the stroma remained unstained showing that the polyclonal primary antibody revealed a pattern of distribution of CCK2R in epithelial cells compatible with that expected from the literature (Dockray 1999, Goetze et al. 2013) (Fig. 4.1). Skin specimens from basal cell cancer were later found to be negative in nearly all cases (8 out of 10) for the receptor and served therefore as a negative control group. Furthermore, in other studies a tissue array containing normal human samples from uterus, gall bladder, colon, kidney and testis was screened for CCK2R expression. For results see supplement (Figure S10).

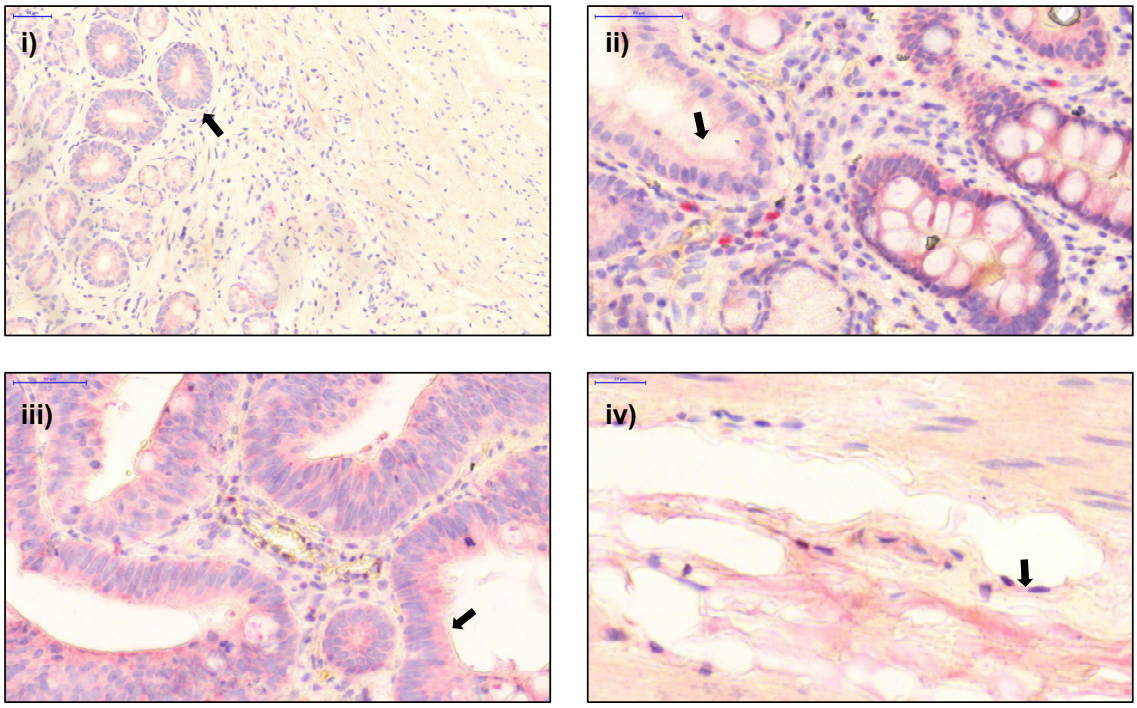

Figure 4.1. Low and high power images of dysplastic stomach and human gastric adenocarcinoma samples show excessive CCK2R expression of gastric glandular epithelium (black arrows). Scale bar 50 μm for i-iii), 20 μm for iv).

4.3.2 CCK2R is expressed in a subset of human melanoma cells

As a first step toward verification of the Human Protein Atlas data (1), immunohistochemistry was performed on skin samples from patients with malignant melanoma. Healthy skin areas from the same patient served for comparison. In an initial pilot study peroxidase staining revealed receptor expression in a subset of melanoma cells in all of three patients examined (Fig. 4.2A). The CCK2R expression was non-uniform and exhibited variability from diffuse strong to focal weak staining. In order to better distinguish between melanophages with dense melanin pigmentation, heathy melanocytes and malignantly transformed melanoma cancer cells, in a second series we then double labelled sections from seven patients with CCK2R and Melan-A, which is a well-known melanoma marker (Fig. 4.2C). Interestingly, a low proportion (2-3%) of healthy melanocytes located in the *stratum basale* of the epidermis exhibited trace CCK2R expression. There were also cases where aggressive tumour cells after dedifferentiation lacked Melan-A positivity, but retained CCK2R expression. Double labelling confirmed that melanoma cells expressed the receptor in all seven patients examined. In order to examine expression more quantitatively, densitometry was used. This revealed higher densities in early stage compared with later stage melanomas (0.18 ± 0.03 *vs* 0.11 ± 0.02 OD units in <pT2a, n = 5, and >pT2b, n = 2 melanomas, respectively; t-test p=0.166). A similar pattern emerged from a comparison of melanocytes with melanoma cells from the same patients (pT3b; n = 2) (0.19 ± 0.02 vs 0.11 ± 0.02 OD units in melanocytes and melanoma cells, respectively; t-test p=0.139).

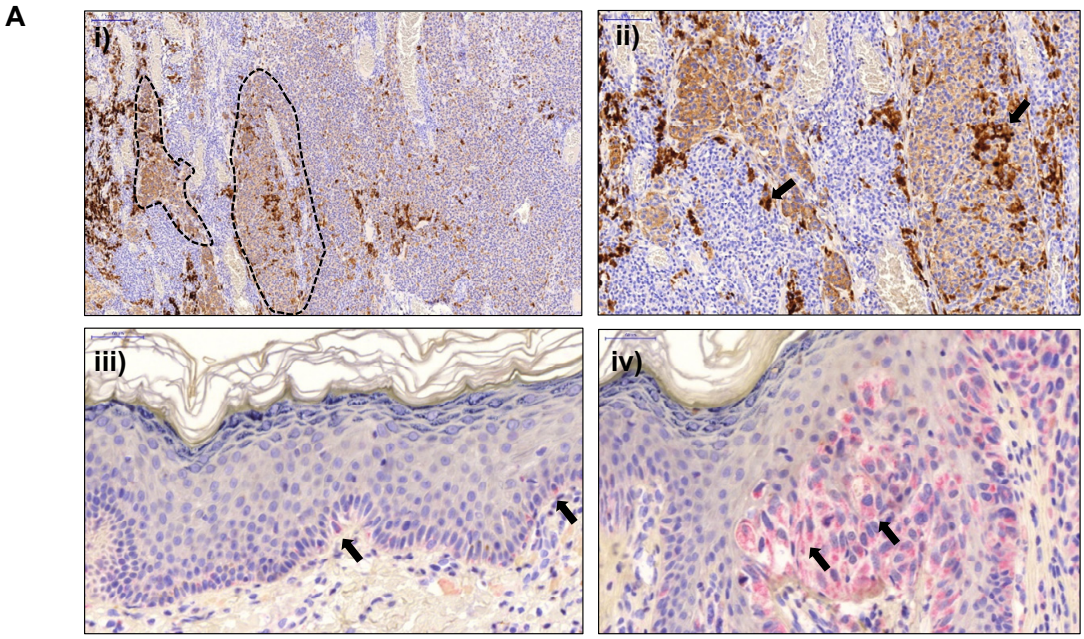
A
i)
ii)
iii)
iv)

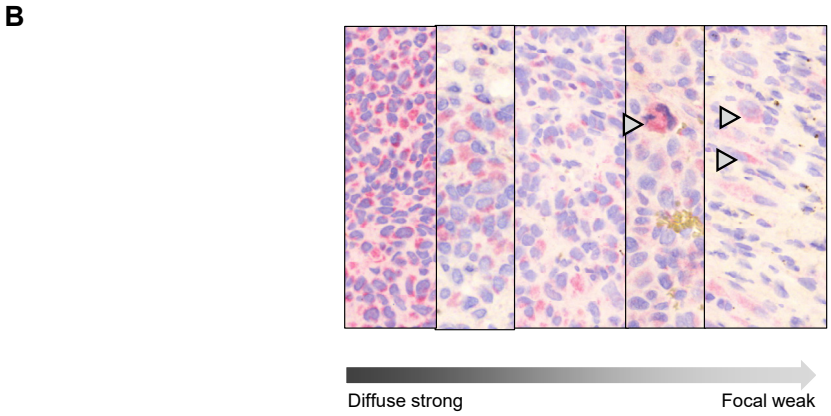
B
Diffuse strong
Focal weak

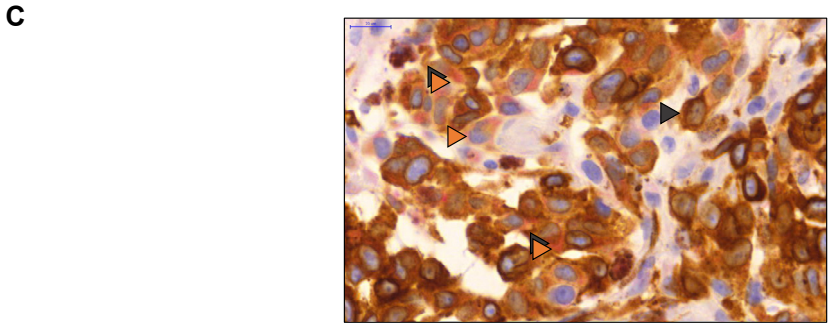
C

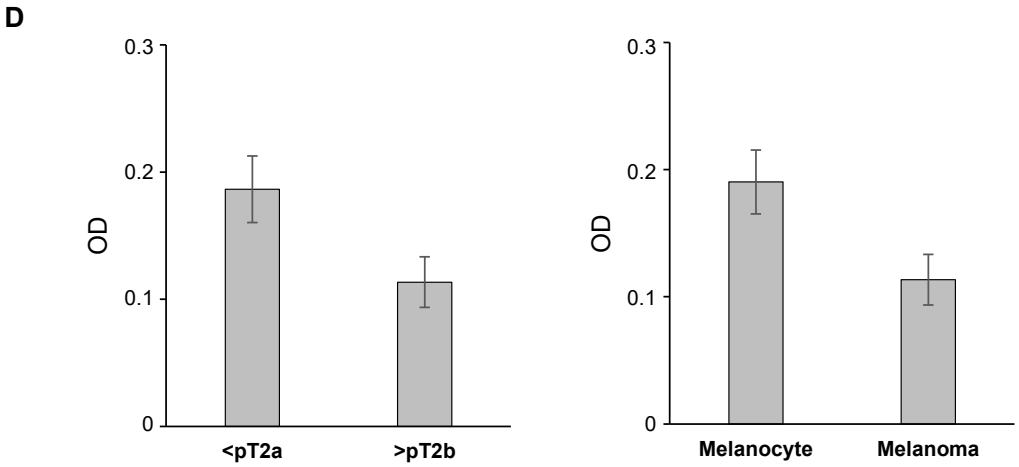

Figure 4.2. CCK2R expression in melanoma.
(A) Peroxidase staining of skin biopsies from a patient with malignant melanoma reveals inhomogeneous CCK2R expression. Brown staining indicates positive melanoma cells (dashed lines). Arrows show scattered highly dense melanophages with melanin pigmentation (Ai-ii). Melanocytes in the deep epidermal layers exhibited also CCK2R positivity in traces (Aiii; black arrow) (scale bar Ai 200 µm, Aii 100 µm, Aiii-iv 50 µm). (B) Alkaline phosphatase based detection with naphthol phosphate chromogen product reveals multiple CCK2R expressing tumourous foci (Aiv) with various staining intensities (scale bar 50 µm). (C) Double-labelling immunohistochemistry with melan-A confirms CCK2R positive cells to be of a melanoma origin, however in some cases dedifferentiated tumour cells lose Melan-A positivity (C; red Δ indicate CCK2R, black Δ Melan-A) (scale bar 20 µm). (D) Densitometry analysis of cytoplasm of CCK2R positive melanoma cells and melanocytes. Comparison of early vs. advanced stage melanomas (left; Means ± SE; n = 7) and melanocytes vs. melanoma cancer cells from the same two patients (right; Means ± SE; n = 2). Melanocytes and early stage melanoma cells show a tendency of increased optical density.

In order to provide context and a point of comparison for the melanoma data, we then examined expression of CCK2R in basal cell cancer (n = 3). There was a clear difference between the latter which showed no detectable CCK2R expression compared with melanoma described above (Fig. 4.3A). Since basal cell cancer also arises from the basal layer of the epidermis where keratinocytes are surrounded by melanocytes, this raises the idea that melanin producing cells, especially in case of a pigmented BSC, alter their CCK2 receptor status. Double labelling revealed that although there were abundant Melan-A positive melanocytes encapsulated inside the basal cell tumours, CCK2R expression did not change (Fig. 4.3B). Independently from tumour type, there were cells of fibroblastic origin (i.e. dermal fibroblasts, myofibroblasts) in the stroma, which showed CCK2R positivity (Fig. 4.3C). This is in accordance with our previous finding (see in Chapter 3 and Chapter 5) that myofibroblasts provide a novel pool of cells expressing CCK2R.

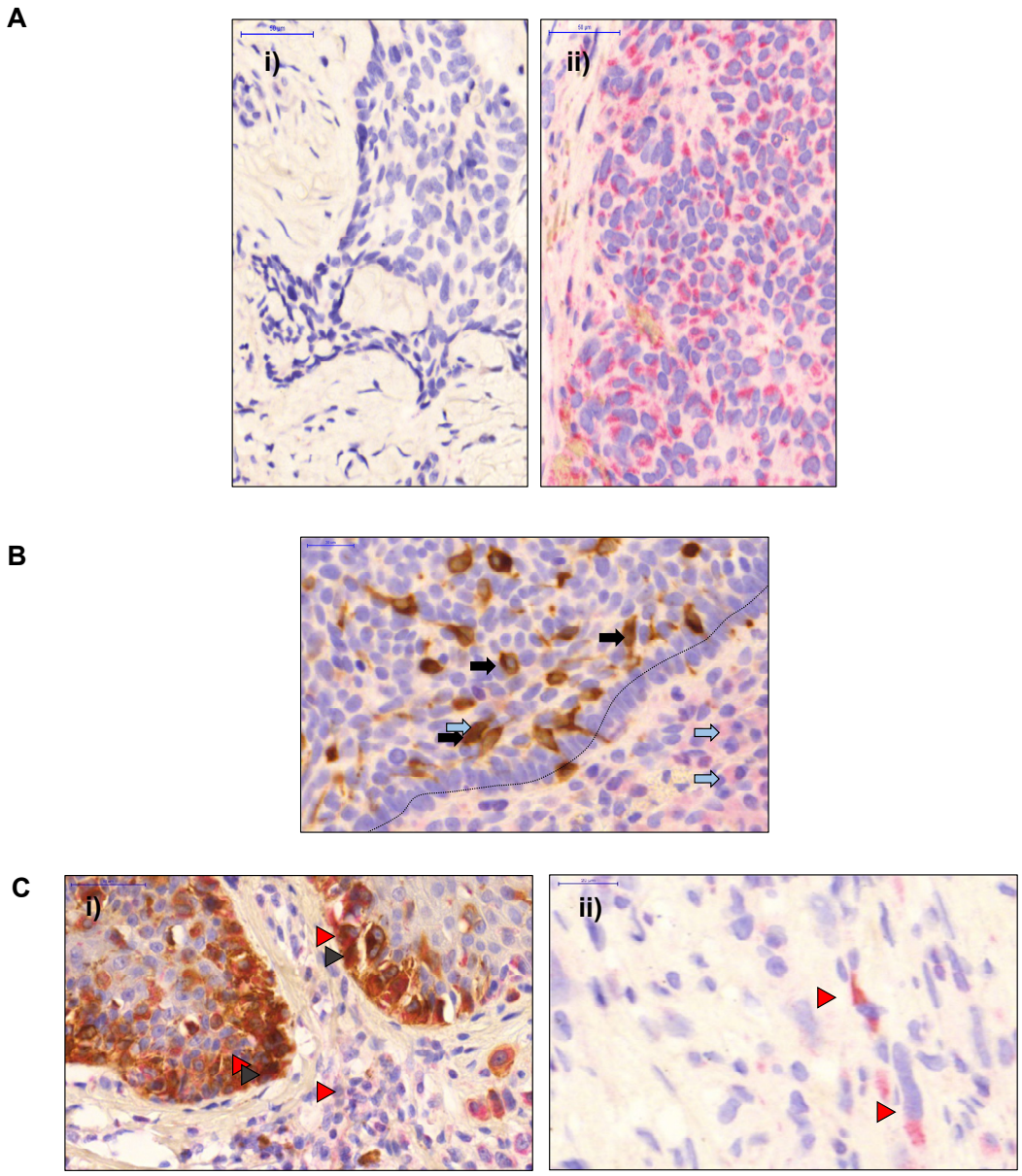

Figure 4.3. Basal cell tumours do not express CCK2R.
(A) Comparison of BCC (Ai) with MM (Aii) immunohistochemistry reveals absence of CCK2R expression in the former surrounded by myxoid tumour stroma (note the characteristic elongated hyperchromatic nuclei) while diffuse positivity (red) can be observed within the melanoma foci (scale bar 50 μm). (B) Double labelling of BCC with melan-A shows melanocytes and melanophages encapsulated inside the lesion (black arrows) with scattered CCK2R expressing cells (blue arrows) in the peritumoural fibrous stroma (scale bar 20 μm). (C) Similar CCK2R positive cells with a probable fibroblastic origin can be observed in the MM stroma also (red Δ; Ci-ii).

The data presented above suggest clear cut qualitative differences in CCK2R expression between melanoma and basal cell tumours. In order to provide a more quantitative basis for the comparison, the presence of receptor expressing cancer cells was then assessed by allocating samples to categories of 0%, 1-25% (designed 1+), 26-50% (designed 2+) or 51-100% (designed 3+) positive cells counted per field at 20x magnification (Fig. 4.4B). Receptor expressing cells were significantly more abundant in patients with malignant melanoma compared to the control basal cell carcinoma group (χ2-test, $p < 0.05$). CCK2R was detectable in 15 out of 18 melanoma patients, whereas it was only present in 2 out of 10 cases in patients with basal cell carcinoma (BCC) (Fig. 4.4B). The proportion of melanoma cells expressing CCK2R was 15 - 20% in the majority (56%) of malignant melanoma (MM) patients. In the remaining cases there was wide variation between complete absence of the receptor (17%) to a homogenous strong positivity (27% of MM patients). Optical densitometry after standardisation revealed that focal density (cytoplasm of 5 cells/ field) representing staining intensity was higher in melanoma cells than in basal cancer cells (Mann-Whitney U-test, $p < 0.05$) (Fig. 4.4A). Similar to the topographic pattern, optical density showed higher variance in the MM group.

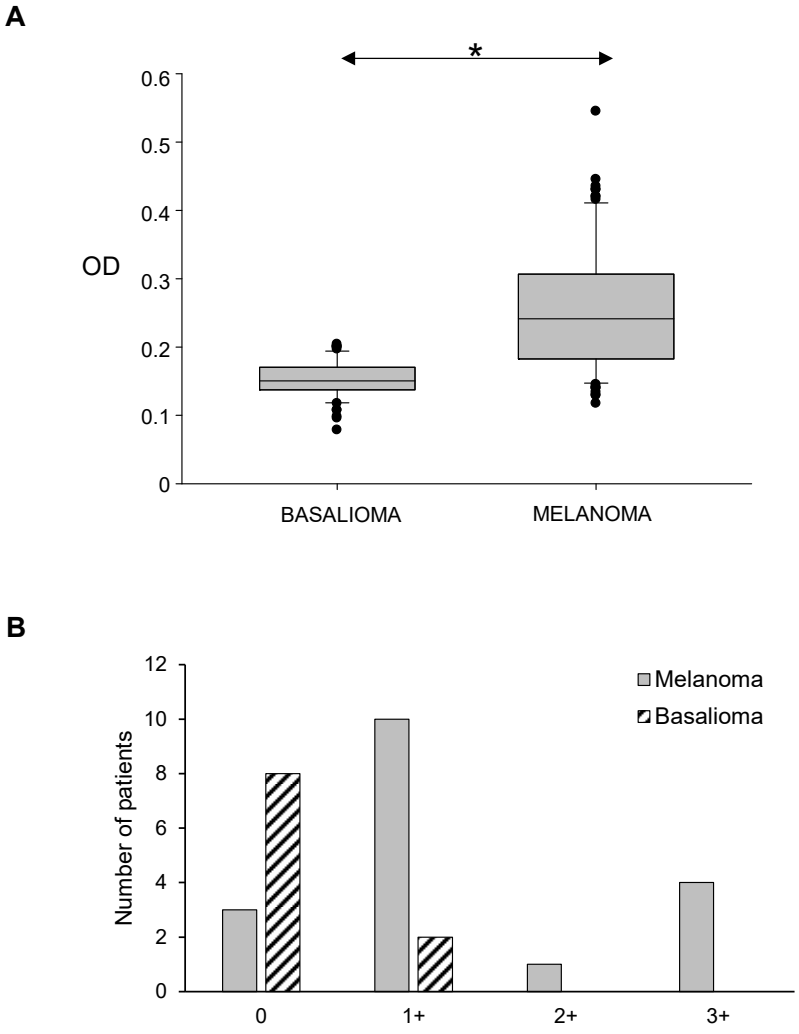

Figure 4.4. Comparison of optical density of CCK2R staining in BCC and MM tissue sections. The data are based on densitometry of the cytoplasm of 5 cells per field averaged; n=10 and 18 in basal cell cancer and melanoma respectively). (A) Significantly higher densities were measurable in the MM group (χ2-test, $p < 0.05$). (B) Semi quantitative evaluation of CCK2R expressing cells revealed 15-20% of melanoma cells to exhibit receptor expression compared with <1% in basal cell cancers.

4.3.3 Characteristics of melanoma and basal cell cancer patients recruited for serum gastrin studies

Following the confirmation of CCK2R expression in melanoma cancer cells described above, it was considered appropriate and necessary to determine serum gastrin concentrations in patients with melanoma (and basal cell cancer for comparison) in order to understand the possible functional relevance of receptor expression. To this end, melanoma and basal cell cancer patients were recruited for a cross-sectional study involving histopathology of the tumour, assay of fasting serum gastrin, determination of *H.pylori* status and medical history including antisecretory therapy (ASI). The melanoma group consisted of 89 patients (n = 39 male; mean age 60 ± 1.6 years; for a fuller demographic description see table 4.1); the BCC control cohort included 26 patients (n = 16 male; mean age 76 ± 2.2 years).

	Melanoma	Basal cell cancer
Total	89	26
Male/Female	39/50	16/10
Mean age [year]	60.6±1.6	76.0±2.2
Min/Max. age [year]	25/89	54/93
Acid inhibitor usage [year]	3.9±0.8	4.22±0.45
PPI/H2RA	16/5	13/2
Hp +ve/-ve	37/51	16/10

Table 4.1. Demographics of melanoma and basal cell cancer patient cohorts including sex, age, *H.pylori* status, type and duration of ASI usage in years. Latter refers to the subset of patients on acid secretion inhibitors.

There was a significant difference between the two cohorts in term of fasting gastrin concentrations. While the majority of MM patients (76%) had fasting serum gastrin concentrations within the reference range used for many years for this assay (<30 pM), almost half in the BCC group (46%) exhibited fasting serum gastrin concentrations above the reference range (Fisher exact test = 0.0012; $p < 0.05$; mean fasting serum gastrin 67 and 32 pM in BCC and MM respectively) (Fig 4.5A). Because, in both groups, there were sizeable sub-sets with serum gastrin concentrations above the reference range, for further analysis the groups were divided into low (<30pM) and high (>30pM) serum gastrin sub-sets. The difference in mean fasting serum gastrin concentrations in the two patient groups was somewhat exaggerated for the high gastrin sub-set (79.1 ± 12 *vs* 116.2 ± 19 pM; MM *vs*. BCC respectively); while, not surprisingly, there was no difference in low gastrin sub-sets (17.1 ± 0.8 *vs* 16.9 ± 2.1 pM; MM *vs*. BCC respectively) (Fig 4.6A). Just over half of the BCC patients were taking some form of acid secretion inhibitor (either PPI or H2RB), while most of the MM patients (76%) did not use acid secretion inhibitors and the different proportions were significant (Fisher exact test = 0.0016; $p < 0.05$) (Fig 4.5A). The mean duration of acid inhibitor usage was around 4 years in both cases. (3.9 ± 0.8 *vs* 4.2 ± 0.5 years, MM *vs* BCC respectively). Not unexpectedly, there was moderate hypergastrinaemia in the sub-sets of both patient groups who were taking acid-secretion inhibitors (46.6 ± 9.2 *vs* 91.4 ± 20.6 in MM and BCC respectively, t-test $p = 0.028$) (Fig 4.6A). Melanoma patients on acid inhibitors were likely to exhibit hypergastrinaemia with an odds ratio of 6.7 ($p < 0.001$; Fisher exact test $p < 0.0011$) (Fig 4.6A).

H.pylori status was determined by serology. No substantial difference was observed between the two groups: thus, a total of 42% and 61% of patients were found to be *H.pylori* positive in MM and BCC groups respectively (Fisher exact test = 0.1165; p = 0.05) (Fig. 4.5A). There were moderately raised fasting serum gastrin concentrations associated with *H.pylori* sero-positive melanoma patients (OR 5.36, p <0.0023; Fisher exact test p <0.002), but *H.pylori* sero-positive basal cell cancer patients actually exhibited reduced serum gastrin concentrations compared with seronegative patients (Fig. 4.6A) (Supplement Fig. S1-4).

To further understand the differences between the two cohorts (taking note particularly of the fact that basal cell cancer patients tended to be older, and serum gastrin tends to increase with age), we then age and sex matched the two groups before repeating the comparisons. As shown in Fig. 4.5B and Fig. 4.6B, there was no significant difference after matching the two groups in either mean serum gastrin concentration or in overall patient distribution

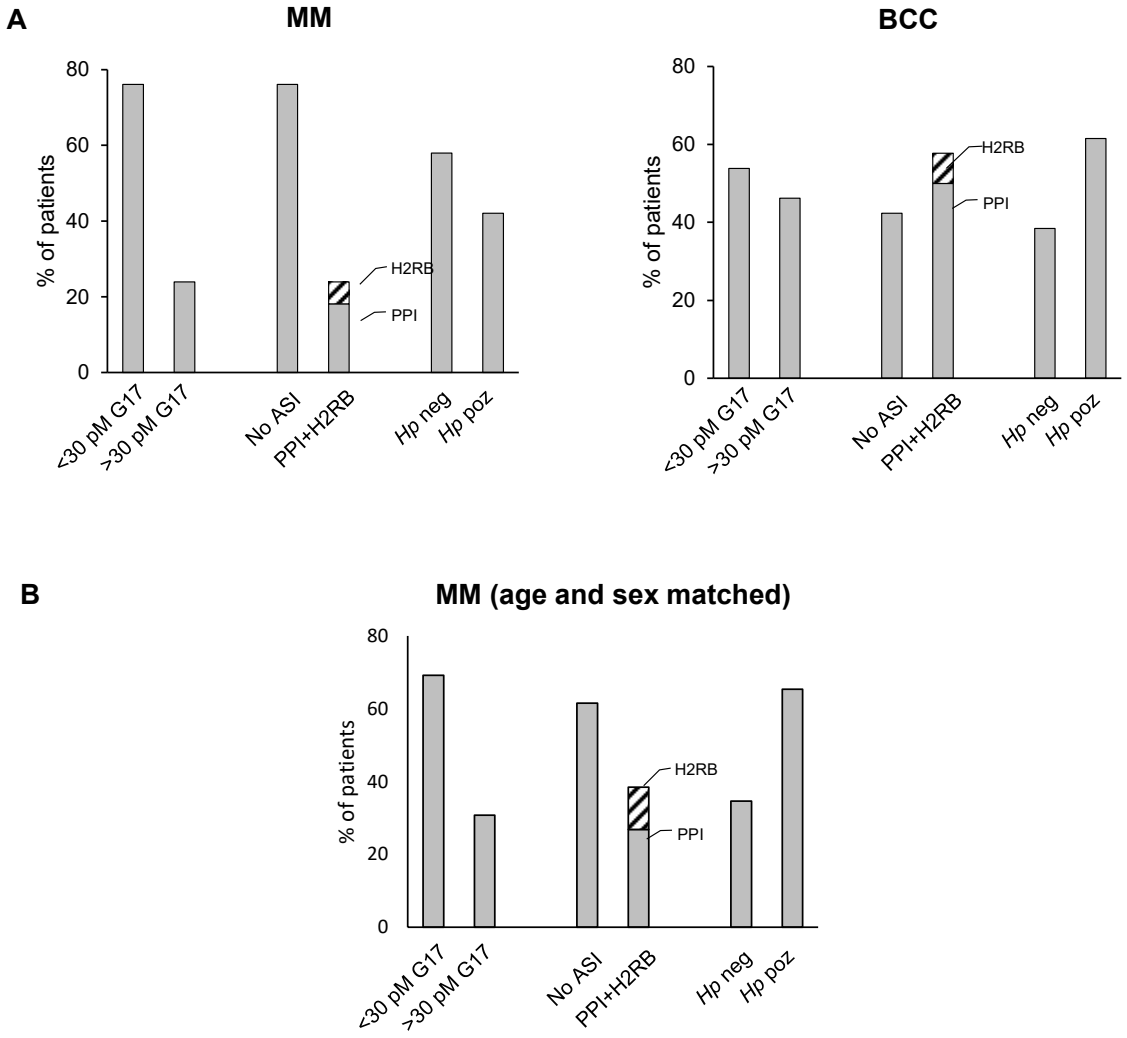

Figure 4.5. Distribution of patients within the MM and BCC cohorts based on serum gastrin concertation, ASI consumption and *HP* status. (A) Majority of patients had circulating gastrin levels below the reference range, did not take acid inhibitors and were seronegative for *Hp* in the MM group, while more BCC patients took ASIs and were found *Hp+ve* than not. (B) Cross matching melanoma patients resulted in a shift regarding *H.pylori* status from seronegative to positive similar to what was be observed within the BBC group. Y axis refers to percentage within the certain group.

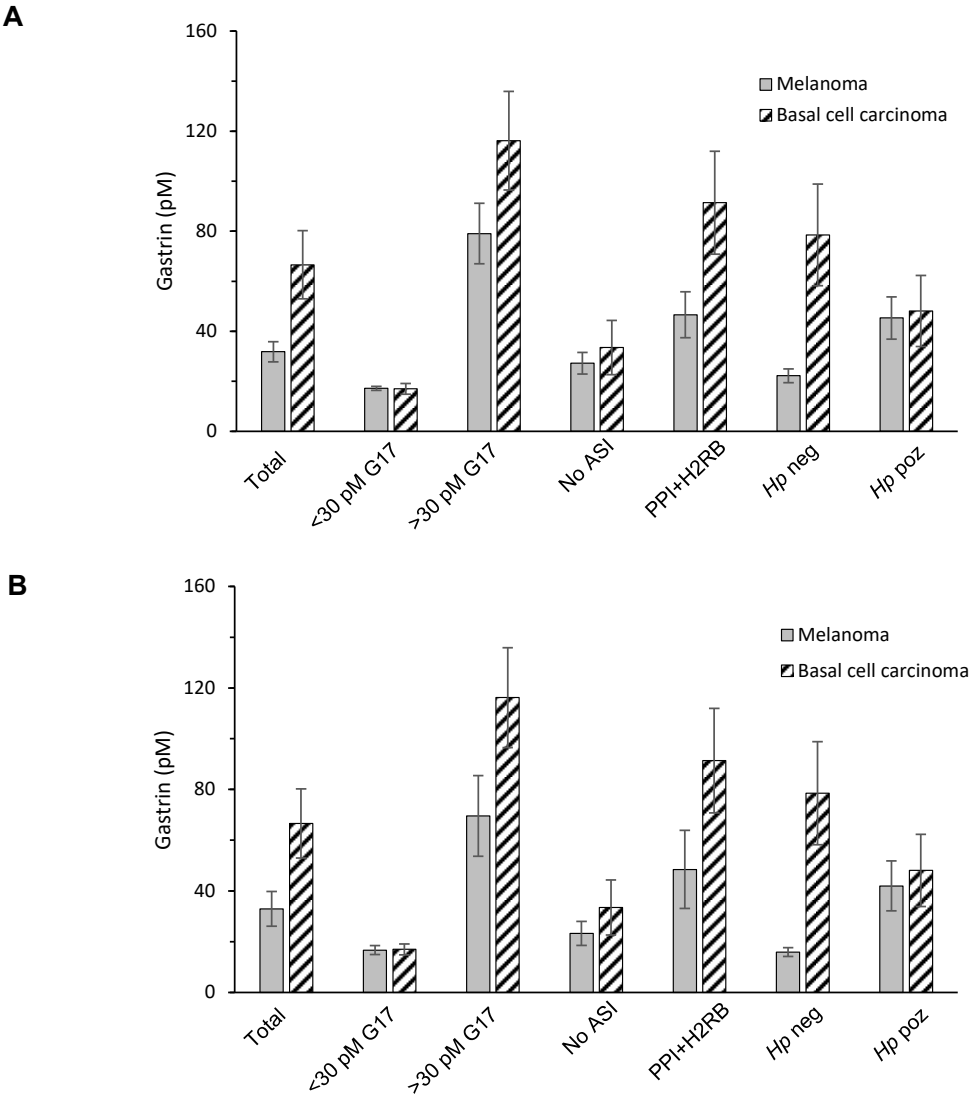

Figure 4.6. Comparison of serum gastrin concentrations (pM) between the MM and BCC cohorts within specific subgroups (i.e. <30pM hG17; >30pM hG17, w/o ASI, w/ ASI, *Hp* –ve, *Hp* +ve) before (n=89) (A) and after (n=26) (B) cross-matching for age and sex. Latter did not significantly alter mean serum gastrin in any of the investigated groups. Means ± SE.

4.3.4 Tumour depth and thickness following Breslow and Clark scale in melanoma patients correlated to pT stages

Based on clinical appearance most patients had nodular (41%) and superficial spreading (40%) melanoma. Acrolentiginous (6%), nevoid (3%) and spitzoid (2%) melanoma also occurred at lower rates; tumour propagation remained *in situ* in 5% of cases (Fig. 4.7A). Mean tumour thickness was 2.9 ± 0.3 mm (min. 0.2 mm; max. 12 mm). Tumour thickness (i.e. Breslow depth) was correlated with pT stages, which also includes the presence or absence of ulceration. Data were plotted on a heat map with a scale of patient number corresponding to each square. The heat map revealed two distinct peaks with most patients predominantly at one or other corner of the map (Fig 4.7B). This distribution is compatible with the fact that tumour thickness is one of the most important prognostic factors of overall survival (Balch et al. 2009); thus, in most cases advanced stages corresponded to greater tumour thickness, while low invasion levels are related to early stages. The distribution of patients in each stage can be seen in Fig. 4.7C. Clark's level which is used together with Breslow depth in routine clinical practice refers to anatomical layers of the skin penetrated by the tumour and revealed most of the patients to have a Clark stage of III meaning cancer cells almost reached the reticular dermis (Fig. 4.7D).

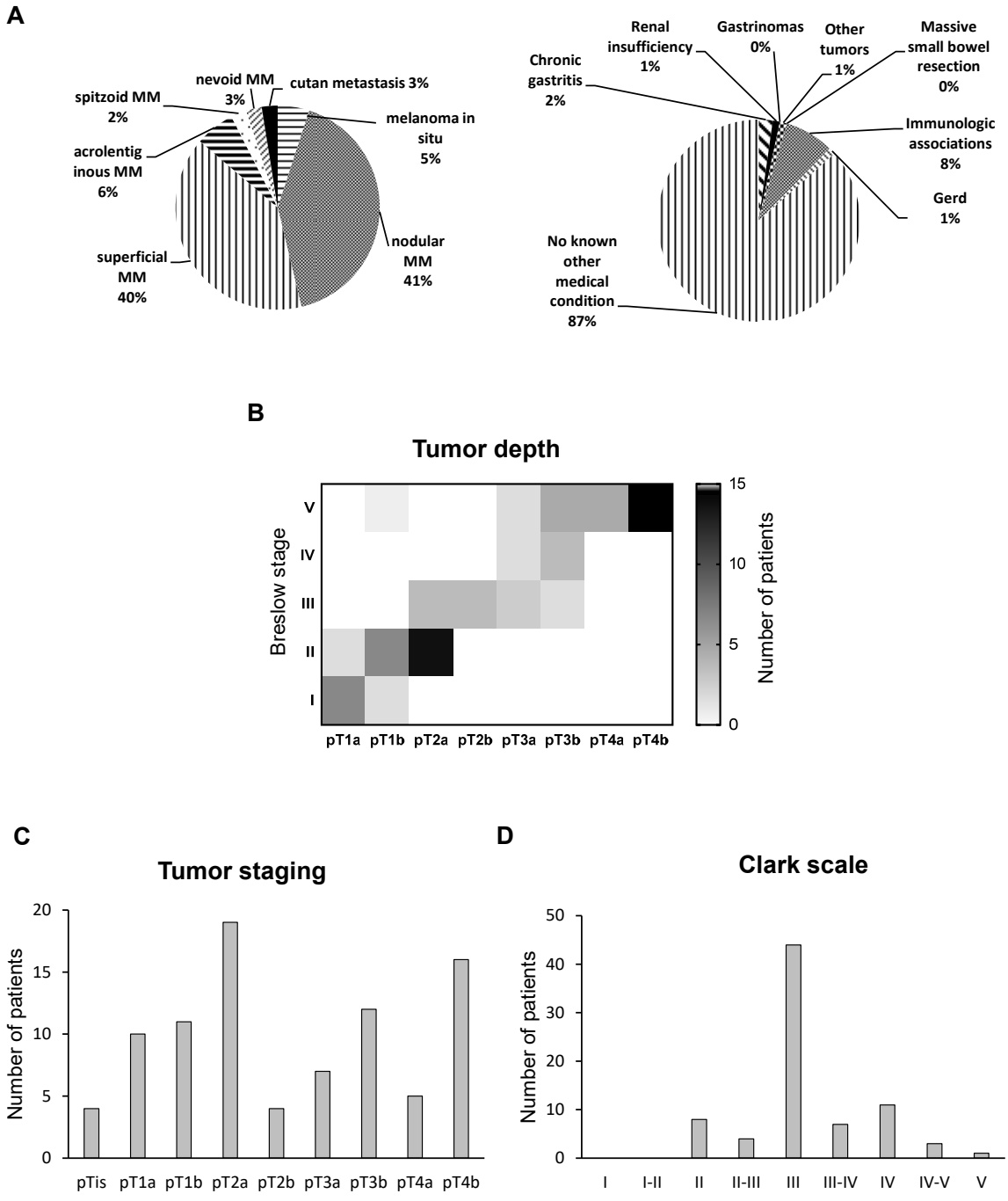

Figure 4.7. Characterisation of the melanoma patients recruited for this study. (Ai) Frequency of different clinical types of melanoma within the cohort reveal superficial and nodular MM to be the most common form, which are known to account for the vast majority of melanomas. (A ii). Percentage of patients with known additional medical conditions that can be related to hypergastrinaemia. (B) Histopathological staging showed a strong correlation with tumour depth with most of the patients being at one or other end of the spectrum. (C) the distribution of patients among different pT stages and (D) Clark stages in the melanoma cohort.

4.3.5 Serum gastrin concentration associated with the progression of melanoma

In order to examine the relationship between serum gastrin and melanoma stage, patients were first divided into groups based on their pT stages derived from histopathology. There was a clear indication that patients with advanced pT stage had higher gastrin concentrations compared with patients in early stages of the disease (Fig 4.8). To facilitate analysis, patients were divided into stage I and II groups defined by pT<2a and pT>2b respectively. This division follows the staging system defined by the 8th edition of American Joint Committee on Cancer used for distinguishing between melanoma patients from a prognostic aspect; stage I refers to patients with low-risk primary melanomas (pT1a, pT1b and pT2a), while stage II includes patients with primary tumours that are at higher risk of recurrence (T2b, T3a, T3b, T4a, and T4b) but without regional lymph node involvement or distant metastasis (Gershenwald et al. 2017). The percentage of patients with low serum gastrin was significantly higher in Stage I (Δ%=43.1 of total cohort). This difference was reduced having almost equal number of patients with low and high gastrin concentrations in Stage II (Δ%=6.8). The data indicated that MM patients in the stage II group had significantly higher gastrin concentrations (OR 8.5, p <0.0005; Fisher exact test p <0.0003), than in stage I (40 ± 6.8 pM *vs* 24 ± 4.4 pM in Stages II and I, respectively).

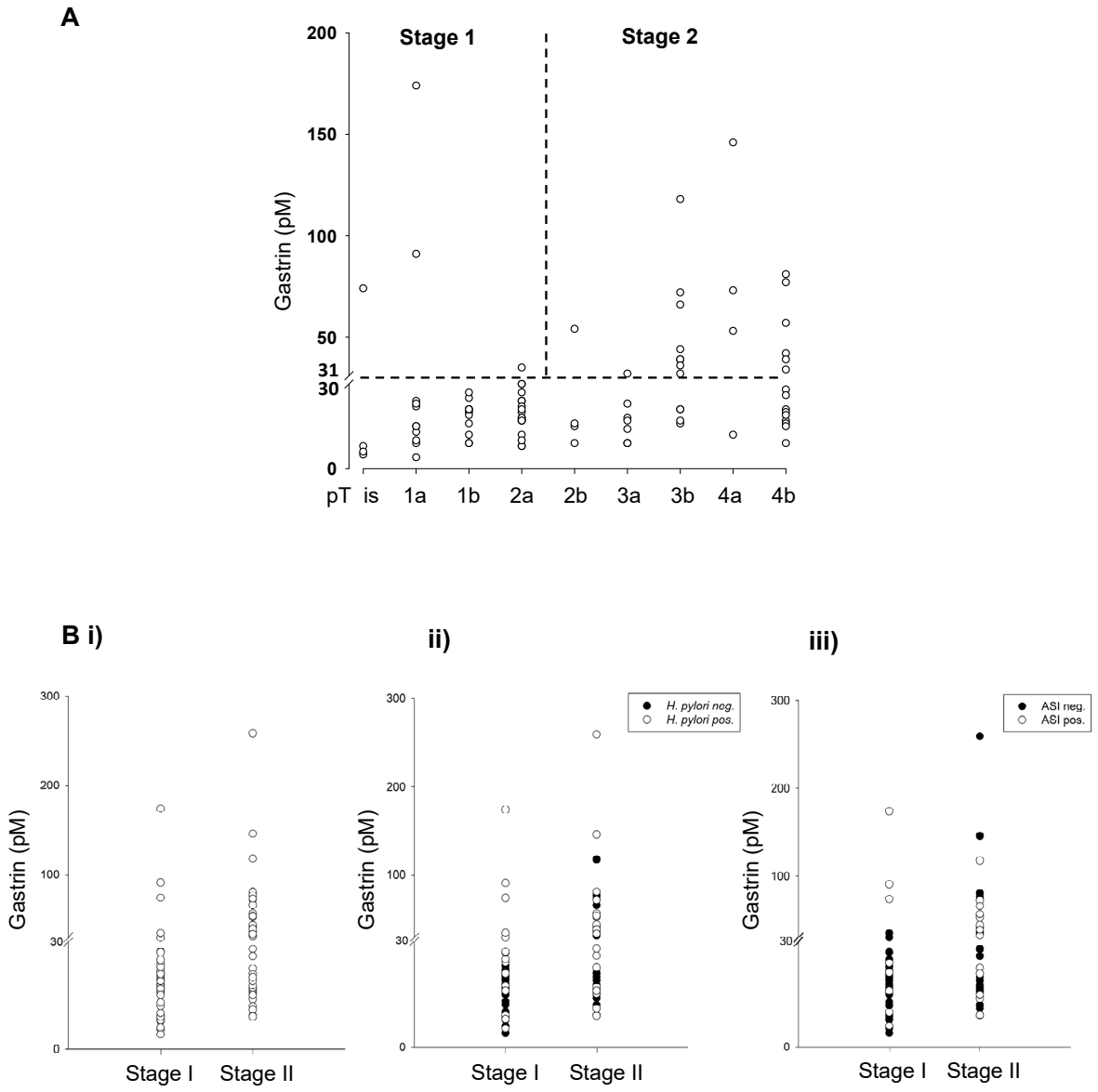

Figure 4.8. Scatter plot of serum gastrin concentrations in different pT stages.
(A) The data reveal that patients in advanced stages exhibit higher serum gastrin. Y-axis hG17 concentration in pM. (Bi) When patients were divided into Stage I with pT<2a and Stage II groups with pT>2b following AJCC guidelines, latter had significantly higher gastrin concentrations (OR 8.5, p <0.0005; Fisher exact test p <0.0003). (Bii) Similar tendency was seen with *Hp* infection and (Biii) ASI usage.

4.3.6 Comparison of *H.pylori* status and ASI usage in Stage I and II of the MM cohort.

The observation that patients with stage II disease were more likely to exhibit elevated fasting serum gastrin concentrations compared with those with stage I disease raises the question of whether known factors influencing serum gastrin, notably acid-inhibitory therapies and *H.pylori* infection, might also be associated with melanoma stage. It is interesting, therefore, that the proportion of stage II patients taking some form acid inhibitor therapy was similar to that in Stage I patients (1:7 to 1:5). Moreover, the proportion of patients that were *H.pylori* sero-positive was also similar in the two groups (Fig 4.9A and B). Thus whether the data were analysed for *H,pylori* status (OR ns; Fisher exact test p <0.663) or acid inhibitor therapy (OR ns; Fisher exact test p <0.619) there was no association with prognostic stage. Moreover, in neither Stage I nor Stage II was there an association between acid inhibitory therapy and *H.pylori* status (Fig 4.9).

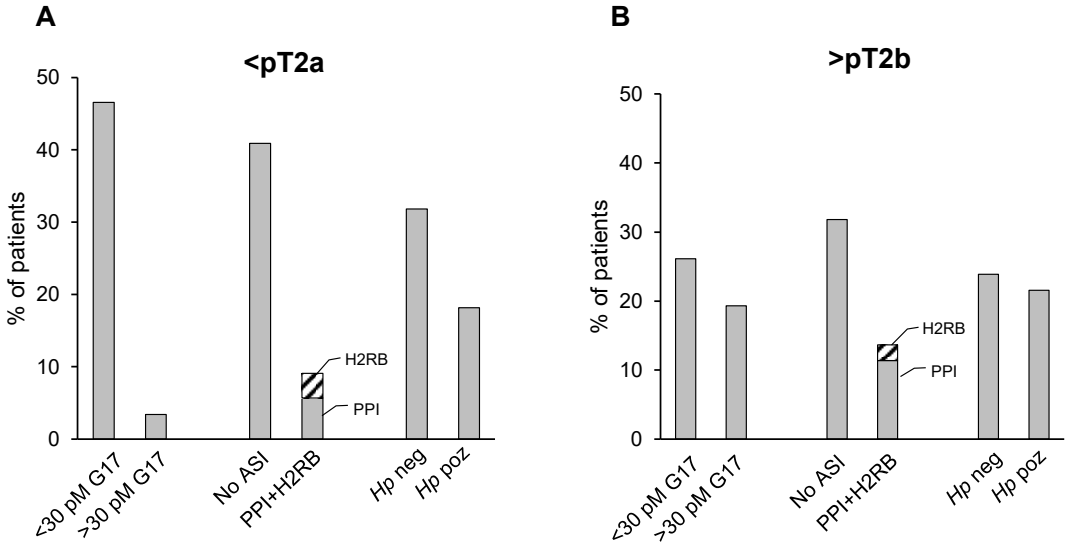

Figure 4.9. Distribution of melanoma patients in Stage I (A) and Stage II (B) prognostic groups based on serum gastrin concentration, ASI usage and *Hp* status. Y-axis refers to percentage of patients within the complete MM cohort.

4.4 Discussion

The expression of CCK2R in the brain and gut is well known; arguably the best understood function of these receptors is in regulating gastric acid secretion (Dockray 1999). However, there is growing interest in the role CCK2R plays in tissue regeneration and wound healing where expression in myofibroblasts may be relevant (Ashurst et al. 2008, Varga et al. 2017). There is also growing interest in the role of CCK2R in preneoplastic conditions and in cancer. Most previous work in this area has focused on gastrointestinal tumours where the capacity of CCK2R expressing cells to respond to gastrin in chemotaxis assays supports the possibility that this receptor might also play role in determining tissue microenvironment and thus cancer progression (Hanahan et al. 2011, Quail et al. 2013). The main finding of this chapter is that CCK2R is expressed in melanoma, and that there is an association between melanoma stage and circulating gastrin. The data raise the prospect that in a subset of patients with elevated serum gastrin the latter may drive progression of their disease.

Melanoma is one of the most common forms of skin cancer. Surveillance data indicate the incidence has increased 60% within the last 30 years in the Caucasian population, making it the fifth and seventh leading type of newly diagnosed tumour among men and women, respectively (Jemal et al. 2001, Ingraffea 2013). Exposure to UV radiation in sunlight is widely recognised as a risk factor. The present data suggest that other risk factors associated with CCK2R expression in skin tumours should be considered too.

As an initial step we immunostained skin samples of melanoma patients for CCK2R. Antibody previously validated on human gastric corpus biopsies (as positive controls) and healthy skin areas (as negative controls) revealed inhomogeneous CCK2R expression localised mainly to melanoma cancer cells. Due to technical considerations, namely stored tissue samples were only available in fixed, paraffin embedded form and access to native material was limited to prospective cases, we decided to use immunohistochemistry as the primary method of CCK2R detection, however alternative techniques i.e. fluorescent in situ hybridization (FISH), real-time quantitative PCR for CCK2 gene expression analysis or western blot for receptor protein detection might also be applied in future studies (Goetze et al. 2013).

Interestingly there were cases were aggressive cancer cells appeared to have lost their melanin pigmentation but retained CCK2R expression. This may be consistent with our previous finding (see chapter 3), that cancer associated myofibroblasts exhibit higher CCK2R expression in gastric cancer patients with poor survival and advanced lymph node metastases. Overall it seems that beside colonic adenocarcinomas, where gastrin is known to promote cancer progression (albeit only confirmed for non-classical agonists mainly through progastrin derived peptides) skin melanomas and gastric tumours behave similarly (Ferrand et al. 2006, Kovac et al. 2008).

The CCK2 receptor is expressed in a wide variety of other tumours including medullary thyroid cancer, pancreatic cancer and non-small cell lung cancer; it is also present in certain types of gastric and colon carcinomas (Dockray et al.

2005, Dockray et al. 2012). It is important to mention that multiple splice variants of CCK2R exist with different functions and sensitivity to non-classical gastrins (Hellmich et al. 2000, Schmitz et al. 2001). An intron 4-containing splice variant (CCK2R i4sv) was one the first to be characterised and was later found in a majority of insulinomas, gastrointestinal stromal tumours and in small cell lung cancers (Hellmich et al. 2000). This splice variant was associated with increased cell proliferation and tumour growth (Körner et al. 2010). There are also somatic mutations in coding regions described in lung and colorectal cancers, which are linked to increased cell migration and angiogenesis (Willard et al. 2012). There is still controversy and uncertainty about the importance of these CCK2R isoforms especially since the relative abundance of some splice variants is very low. Nonetheless in an era of patient-specific personalised medicine with multi-modal and combined therapeutically approaches the clinical importance of knowing all the potential targets, markers which can be pharmacologically addressed is most important. Immunohistochemistry using commercially available antibodies for wild type CCK2R did not allow a detailed investigation of this question in the present study; thus the presence of intron 4 retaining or other possible variants of CCK2R in melanoma cancer cells remains to be investigated further in future.

The CCK2 receptor subtype is the predominant CCK receptor within the CNS and is localised to neocortical and limbic structures with cholecystokinin being its main endogenous ligand (Hill et al. 1987, Nishimura et al. 2015). Melanocytes are recognised to have a neural origin. They derive from the neural crest by delamination from the dorsal part of the neural tube. SOX10-

positive melanoblast/glial bipotent cells are the main progenitor type of melanocytes and originate from specific neural crest cells, which are known to have a high migratory potential (Mort et al. 2015). We found that differentiated melanin producing melanocytes exhibited CCK2R expression, however this was significantly lower compared to the expression observed in melanoma cancer cells. This raises the possibility that there is another niche of cells with a neural origin that encodes the *CCK2R* gene, which at some point during embryogenesis becomes blocked and is reactivated upon tumour dedifferentiation and melanoma cancer cell transformation.

Adjacent to the epithelial layer of the skin, there were also cells in the stroma which exhibited CCK2R expression. This observation has clear links to the previous finding that myofibroblasts of the gut presented a cell cycle dependent expression of CCK2R (Chapter 3). Epithelial-mesenchymal interactions play a key role in tissue organisation and are necessary for adequate responses to certain external stress factors throughout the whole gastrointestinal tract. They are required for proper gut morphogenesis by regulating enterocyte differentiation. A wide range of transcription factors (FoxL1, HOX family, FGFs, TGF-β, Bmps, and Wnts) which are known to be expressed by mesenchymal cells have been identified as morphogens regulating gut development (Fritsch et al. 2002, Grotendorst et al. 2004). To investigate the effect of myofibroblasts on melanoma cells we set up co-cultures treated with gastrin (for details see Chapter 5).

To have a better insight into whether CCK2R expression on melanoma cells has any clinical impact, we collected serum samples of melanoma and basal

cell cancer patients for gastrin measurement and *H.pylori* detection. Circulating gastrin concentration was measured with radioimmunoassay (RIA), using antibody L2 which binds amidated gastrins (G17 and G34) equally, but does not react with progastrin or C-terminal variants (Dockray et al. 1991, Varro et al. 1997). Since plasma gastrin consist of a mixture of biologically active peptides, it is not desirable to use an antibody which is mono-specific towards one active form. Although there is growing body of evidence that precursor forms also have a biological impact (i.e. stimulate cell proliferation in colorectal cancer) only COOH-terminal amidated gastrins are able to bind to the CCK2 receptor (Jin et al. 2009), thus we applied an antibody which however is not selective for sulphated and unsulphated forms of G17 or G34 but discriminates between amidated gastrins and progastrin and Gly-gastrin thereby mimicking the specificity of the CCK2 receptor (Walsh 1975, Varro et al. 2003).

Based on clinical appearance most patients had nodular (41%) and superficial spreading (40%) melanoma, which is in accordance with the literature (Paek et al. 2008). Acrolentiginous (6%), nevoid (3%) and spitzoid (2%) melanoma also occurred at lower rates. An important discovery of this study was that tumour thickness and pT staging available form histology results closely correlated with serum gastrin concentration. Patients with higher serum gastrin were likely to have advanced stage melanomas. Interestingly, however, when patients were divided into two groups (Stage I and II) based on disease progression, even though there was a tendency visible there was no statistically significant correlation found between *H.pylori* infection or ASI

consumption and advanced pTNM stages. This is most likely due to the relatively low power of this study which is an issue that could be addressed in a future study.

Despite the known causes of hypergastrinaemia (i.e. type A and B atrophic gastritis, small bowl resection, renal insufficiency, gastrinomas, etc.) (Dacha et al. 2015) the majority of patients in both the present cohorts had no known medical condition that could be related to hypergastrinaemia other than ASI consumption. As would be expected melanoma patients on acid inhibitors were likely to have moderate hypergastrinaemia (OR of 6.7).

Helicobacter pylori infection is known to be associated with elevated plasma gastrin concentrations and can lead to chronic gastritis which, if undetected, has the potential to give rise to precancerous lesions and therefore posing a risk of gastric cancer development (Watari et al. 2014). The prevalence of *H.pylori* infection has changed over the last few years with a visible decrease in related gastropathies (Eusebi et al. 2014). Estimates among dyspeptic patients in East-Europe indicate a disease prevalence of 40% (Krashias et al. 2013). Since the majority of patients are usually asymptomatic the actual number of infected individuals is likely to be higher (Cave 1996). The proportion of *H.pylori* sero-positive patients in the present melanoma cohort was similar to that reported above. Melanoma patients with *H.pylori* infection had significantly higher gastrin levels, thus beside acid secretion inhibitor consumption (esomeprazole, omeprazole and pantoprazole most commonly)

H.pylori was identified as the other main causes responsible for elevated circulating plasma gastrin.

Basal cell cancer patients were age and sex matched to the melanoma group to exclude any distorting effect arising from demographic differences. In both cases the aforementioned two reasons (namely PPI use and *H.pylori* infection) were accountable for hypergastrinaemia with no significant difference between the two cohorts.

Gastrin release is influenced by stomach pH. Low gastric pH inhibits gastrin secretion and food in the presence of high gastric pH provides a strong stimulus for antral G-cells. Postprandial increases in serum gastrin concentration are therefore a physiological response. In all patients recruited for this study fasting serum gastrin was measured. Presumably, the gastrin concentration that melanoma cells are exposed to throughout the day would include higher concentrations in the post-prandial period. The picture is further more complicated by the fact that PPI use in the long run not only increases fasting serum concentration but also provokes a stronger meal-stimulated increase in circulating gastrin (Helgadottir et al. 2014). Data on postprandial serum gastrin in presence of *H.pylori* infection is controversial, but in adults it also seems to be higher compared to healthy volunteers (Karnes et al. 1991, Hurlimann et al. 1998, Kamada et al. 1999, Kato et al. 2004). Measuring gastrin concentration after a standardised meal would allow a better understanding of the kinetics and peak values that melanoma cells encounter and is therefore worth considering for future studies.

The upper limit of the physiological range of fasting serum gastrin concentration is generally considered to be between 30-50 pM and is increased up to 100-150 pM after food consumption in healthy individuals (Dockray 2004). In certain condition i.e. pernicious anaemia it can reach up to 2000 pM or even higher (McGuigan et al. 1970, Lewin et al. 1976). Patients with gastrinomas have been reported to have gastrin concentrations above 10 000 pM (Maton 1994). Circulating fasting serum gastrin of melanoma patients was in the range of 10-260 pM exceeding the physiological range needed for a biological effect.

The present was a cross-sectional study representing a preselected patient group at a specific time. There was a clear indication that high serum gastrin concentration can be associated with advanced melanoma stages, however whether this observation remains true through the progression of individual patients cannot be answered based on this study. Nevertheless, patients involved in this study are being continuously followed-up which could address the issue. Moreover, a prospective trial of patients on PPIs or placebo would provide a stronger body of evidence, which opposed to a longitudinal cohort study could also measure the clinical impact of long term acid inhibitor usage on melanoma patients.

In conclusion melanoma patients with hypergastrinaemia due to utilization of PPIs or asymptomatic *H.pylori* infection represent a group of patients that are at a higher risk of developing invasive cancer. This adds a new dimension to the known disadvantages of long term PPI therapy, therefore caution should

be advised when prescribing acid secretion inhibitors for melanoma patients keeping the possibility of a potentially increased heath risk in mind. The same is likely to be true for melanoma patients with *H.pylori* infection, therefore routine screening for *H.pylori* antigen in this patient group is worth considering.

In order to have a better understanding how gastrin might effect melanoma cell behaviour we next performed bioassays with G361 and Skmel-2 melanoma cancer cell lines (Chapters 5 and 6).

4.5 Conclusions

1. Immunohistochemistry revealed CCK2R expression in histological samples of patients with melanoma, but failed to show receptor presence in most basal cell cancer patients.
2. Moderate hypergastrinaemia was associated with *H.pylori* infection and ASI consumption in both groups.
3. Melanoma patients with advanced stage (>pT2b) tend to exhibit higher circulating gastrin concentrations, however a statistically significant relation was not observed with *H.pylori* infection and ASI usage.

Chapter 5

CCK2R expression and functional significance in human melanoma cell lines

5.1 Introduction

Myofibroblasts represent a newly discovered pool of cells with a functional gastrin receptor (Chapter 3). Research in this area, however, has been mainly focused towards gastrointestinal myofibroblasts. (Ashurst et al. 2008, Varga et al. 2017). We have recently demonstrated that these cells are capable of increased migration and invasion when treated with gastrin (Varga et al. 2017). Furthermore this effect was not only seen with myofibroblasts expressing the CCK2R, but also in a larger pool of cells that did not express the receptor suggesting a simultaneous paracrine activation; the latter is well described in epithelial cells and is thought to be mediated through a number of paracrine mediators including members of EGF, FGF-2, IL-8 and IGF families (Varro et al. 2002, Noble et al. 2003). In this context it is worth noting that epithelial-mesenchymal interactions play an important role in pathological conditions by defining tumour microenvironment (Hanahan et al. 2000).

Melanoma cells have been shown to express transcripts for CCKRs (Mathieu et al. 2005). Immunohistochemistry also revealed receptor expression in adjacent cancer stroma and importantly a cross-sectional study on 89 melanoma patients found a correlation between serum gastrin concentration and melanoma pT stages with higher serum concentrations being associated with advanced stages (Chapter 4).

Previous studies suggested that gastrin might have pleiotropic effects on melanoma cells, but the relevant pathways and receptors are far from fully described and the available data are inconclusive (Mathieu et al. 2005). It is

well known that melanoma growth from the radial to vertical phases (tumour thickness) is characterized by increased expression on β3 integrins (Sturm et al. 2002). However exactly the opposite was found by Mathieu et al after gastrin treatment, furthermore they reported a decrease of MMP-14, which is known to be associated with the aggressive behaviour of melanomas (Hess et al. 2003).

On the basis of evidence presented in Chapter 3 it seems reasonable to hypothesize that gastrin promotes melanoma progression. The issue is important since patients with hypergastrinaemia due to decreased acid production as a consequence of long-term PPI therapy, *H.pylori* infection or atrophic corpus gastritis might therefore have a higher risk of developing distant metastasis of coincidental melanoma, compared to patients with normal circulating gastrin (Heidelbaugh et al. 2012, Smolka et al. 2012, Watari et al. 2014, Dacha et al. 2015, Haastrup et al. 2018).

The aim of work described in this chapter was to investigate the effect of gastrin on melanoma cell cultures with an emphasis on migratory behaviour and invasion. The picture is somewhat complicated by the fact that cancer associated stromal cells (namely dermal fibroblast and myofibroblasts) also express CCK2R. In order to have a fuller view of the possible underlying mechanism including direct and paracrine signalling pathways mediated by gastrin we therefore designed organoid and spheroid models that contained both melanoma cells and stromal cells.

5.1.1 Objectives

1. To confirm CCK2R expression in melanoma cells using immunocytochemistry and verify by qPCR.
2. To investigate receptor function by intracellular calcium measurements after gastrin treatment.
3. To investigate the effect of gastrin on cancer cell proliferation using EdU incorporation, cell proliferation assays and flow cytometry.
4. To compare the effect of gastrin in the presence and absence of stromal cells on the growth of cancer cell spheroids.
5. To investigate the effect of gastrin on cell migration and invasion using Boyden chambers.
6. To study the adjuvant effect of gastrin and stromal cells on melanoma cell invasion in an organotypic model.
7. To characterise cultured dermal fibroblasts and myofibroblasts and to determine CCK2R expression by immunocytochemistry and flow cytometry.
8. To compare the effect of gastrin in the presence and absence of dermal fibroblasts on melanoma spheroid growth.
9. To investigate the effect of gastrin and dermal fibroblasts on melanoma invasion in organotypic models.

5.2 Methods

5.2.1 Cell culture

Human melanoma cell lines G361 and SK-MEL-2, dermal fibroblasts, myofibroblasts and human mesenchymal stromal cells were cultured as described previously in section 2.2. Cells were used up to passage 15 unless otherwise stated.

5.2.2 Immunocytochemistry

Melanoma cultures were fixed and permeabilised as detailed in section 2.3.1. Cells were stained for CCK2R using polyclonal IgG antibody visualized with FITC conjugated anti-rabbit secondary antibody or peroxidase (DAB) reaction as described before (Wroblewski et al. 2003, Kumar et al. 2014).

5.2.3 qPCR

Melanoma cells (5 x 10^5 / Petri dish of 5 cm) were incubated in full media for 72h. Cells were lysed prior to RNA extraction as described in section 2.7.2. Samples were probed for GAPDH and CCK2R expression using primer and probe sequences described in chapter 2.

5.2.4 Calcium signalling

Melanoma cells (1-3 x 10^4 / well in 6-well plates) were loaded with calcium indicator, Fluo-4, as previously described (Homolya et al. 1993, Kao 1994). Cells were stimulated with hG17 (10 nmol/L) and ionomycin (1 µmol/L) as a positive control (see section 2.5).

5.2.5 EdU proliferation assay

Melanoma cells (seeding density: 3-5 x 10^3 / cover slip in 24 well plates) were treated with hG17 (0.1 – 1.0 – 10.0 nmol/L) for 24 h. Proliferating cells were identified using a Click-iT™ EdU imaging kit (Invitrogen, Paisley, UK) as described in section 2.6.1.1.

5.2.6 CeCo proliferation assay

Cell Counting Kit-8 assay (Dojindo Laboratories, Munich, Germany) was used to detect proliferative activity of melanoma cells as describe in section 2.6.1.2.

5.2.7 Flow cytometry

Melanoma cells (10^6 seeded in T75 flasks) were treated with 10nM G17 or FM overnight. Cells were sorted using FACS Canto II flow cytometer as described in section 2.4.

5.2.8 Spheroids

Skmel-2 cells (3,000 per spheroid droplet) were seeded and incubated up to six days with or without myofibroblasts (10,000 per well in 24 well plates) as described in section 2.10.1 (Fig. 5.1.A). Growth was calculated based on surface area expressed as fold-increase and invasion was determined by measuring the distance of individual cells from the spheroid centre (Fig. 5.1B).

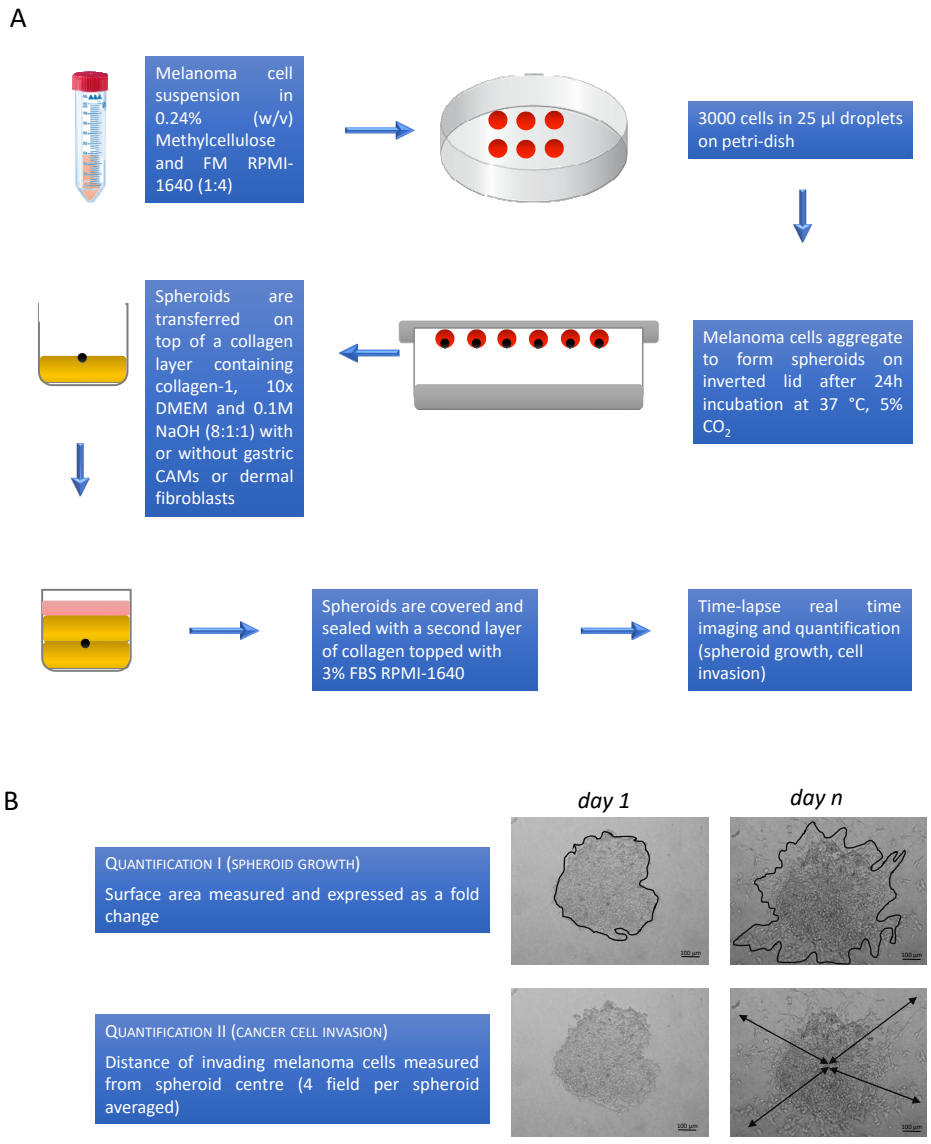

Figure 5.1. Spheroid melanoma model.
(A) Workflow chart of bioassay. (B) Quantification of spheroid growth and cancer cell invasion.

5.2.9 Invasion and migration assays with Boyden chambers

Melanoma cells (2-3 x 10^4) were seeded in Boyden chambers with or without Matrigel™ coating as previously described (Varro et al. 2004). Cells were then incubated in medium containing 10nM hG17 with or without L740093 for 24h prior to staining membranes with Quick-Diff (Reagena, Toivala, Finland) as reported in section 2.6.2.

5.2.10 Organotypic cultures

Organotypic cultures were grown as described in section 2.10.2 (Smola et al. 1993). In brief, Skmel-2 cells (1x 10^6) were seeded on top of a 1:1 Matrigel (Corning, NY, USA):collagen-I (Millipore, MA, USA) layer with or without myofibroblasts (0.5 x 10^6) (Fig. 5.2). After 14 days, cultures were fixed and haematoxylin-eosin (H&E) stained. Invasion of cancer cells was measured to a reference line adjusted to the contact region of the melanoma cell layer with Matrigel.

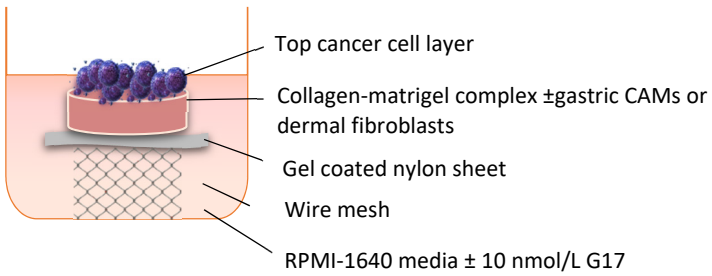

Figure 5.2. Structure of skin organoid used to investigate the effect of gastrin on melanoma invasion.

5.2.11 Statistics

Statistical analysis was done by t-test and one-way ANOVA for proliferation assays with a significance level of $p < 0.05$ using SPSS16.0, SigmaPlot 12.0 software. For migration and invasion assays, including spheroid and organoid models, one-way ANOVA, and in cases where normality test (Shapiro-Wilk) failed Kruskall-Wallis, was applied.

5.3 Results

5.3.1 Expression of CCK2R in human derived melanoma cell lines

In contrast to previous research in this area (Mathieu et al. 2005) we were able to detect CCK2R expression using immunocytochemistry in two melanoma cell lines selected for the purpose (Skmel-2; G361). Both stained positive for CCK2R using two different techniques. First, immunocytochemical staining after cytospin using DAB peroxidase reaction showed intense perinuclear brown staining. Second, conventional immunofluorescence also revealed punctate cytoplasmic staining of the receptor. Peroxidase staining of cultured cells revealed CCK2R expression in 21 ± 5% of cells (Fig. 5.3A and B).

Transcripts of CCK2R were then detected by qPCR in both cell lines. Cycle threshold values for Skmel-2 and G361 were 35.5 ± 0.3 and 33.8 ± 0.4 respectively. Some issues have been raised recently concerning the reliability of GAPDH as a house keeping gene in qPCR, since its expression may vary depending on factors such as tissue type, disease, organism (Fink et al. 2008, Kozera et al. 2013). However, we did not observe any changes in GAPDH expression among different conditions in the cell lines, including myofibroblasts, studied here. Thus using GAPDH as reference, ΔCt values for Skmel-2 and G361 were 15.9 ± 0.2 and 15.2 ± 0.2 respectively (Fig. 5.3C).

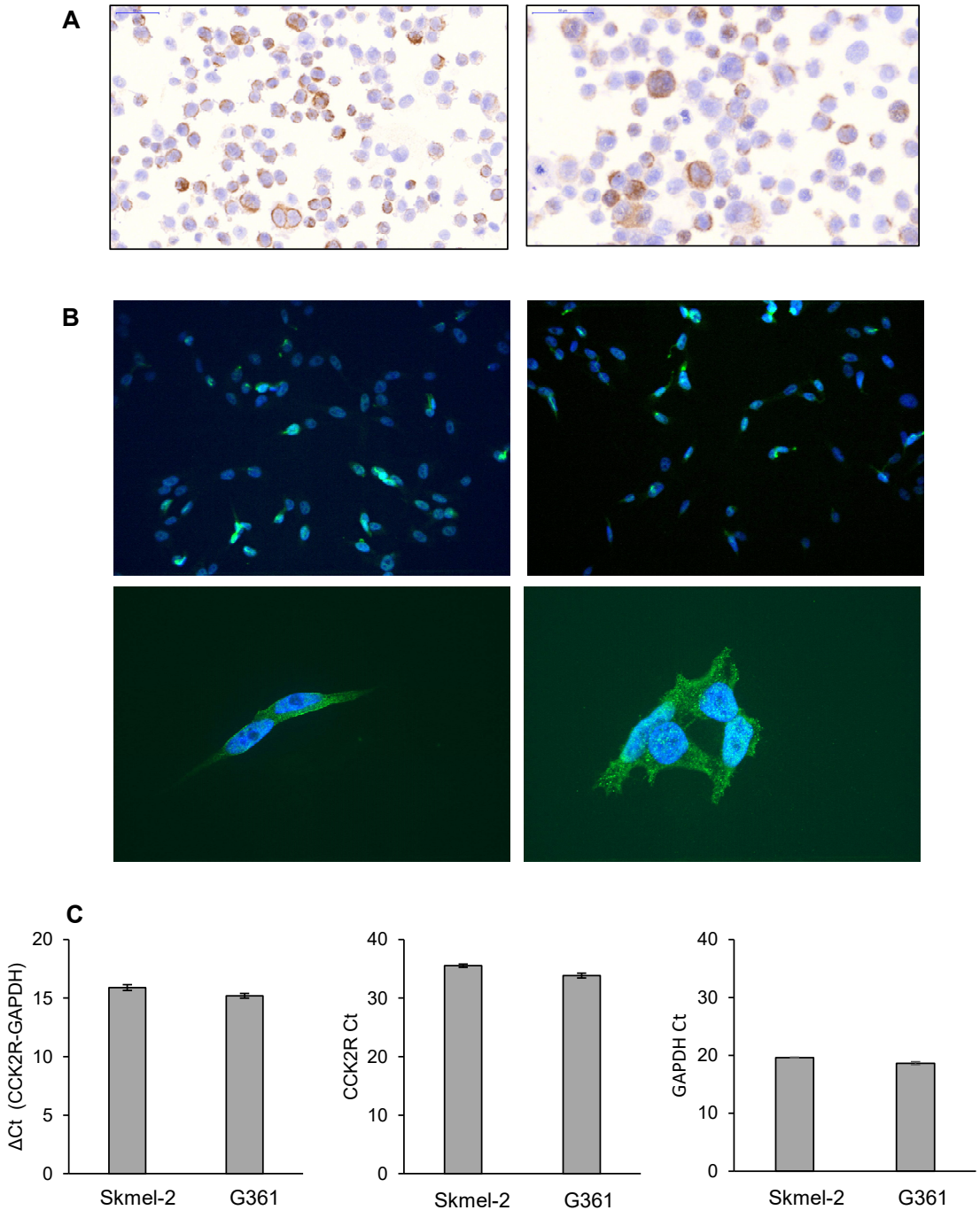

Figure 5.3. CCK2R expression in melanoma cell lines.
(A) Peroxidase reaction with brown discolouring indicates CCK2R positive melanoma cells. Left Skmel-2, right G361 (scale bar 50 μm). (B) Low (10x) and high (40x) power immunofluorescence images of Skmel-2 (left) and G361 (right) melanoma cells. Cells expressing the CCK2R were visualised with FITC (green) conjugated antibody. (C) qPCR data of CCK2R transcripts in both cell lines (Y-axis indicates Ct values for the receptor and reference genes).

5.3.2 Intracellular calcium signals reveal functional CCK2 receptors

Changes in cytosolic calcium concentrations provide a way to monitor CCK2R activation, since the receptor is known to be coupled to activation of $G\alpha_{q/11}$ (Dufresne et al. 2006, Dockray et al. 2012). No spontaneous changes in cytosolic calcium concentrations were observable in either cell line. However, gastrin treatment significantly increased cytosolic calcium in a subpopulation of melanoma cells (6.6 ± 1.1 and 7.9 ± 1.8 % of G361 (n=246) and Skmel-2 (n=204) cells, respectively; data from three independent experiments). Upon treatment with the calcium ionophore ionomycin (Morgan et al. 1994, Muller et al. 2013), there was a sustained increase of cytosolic calcium in almost all cells (>90%)(Fig. 5.4A and B). The refractory period for responses to gastrin was shorter than the total observation time (10 min), since we were able to provoke a secondary response from previously stimulated cells. However, in one case with G361 there were cells which showed increased fluorescence with a delay after hG17 treatment. Whether these late responder cells only regained their excitation potential at that specific time point or rather were activated by adjacent cells in form of a spreading wave like calcium influx similar what can be seen with glial cells (Charles et al. 1991) remains a question that needs further investigation.

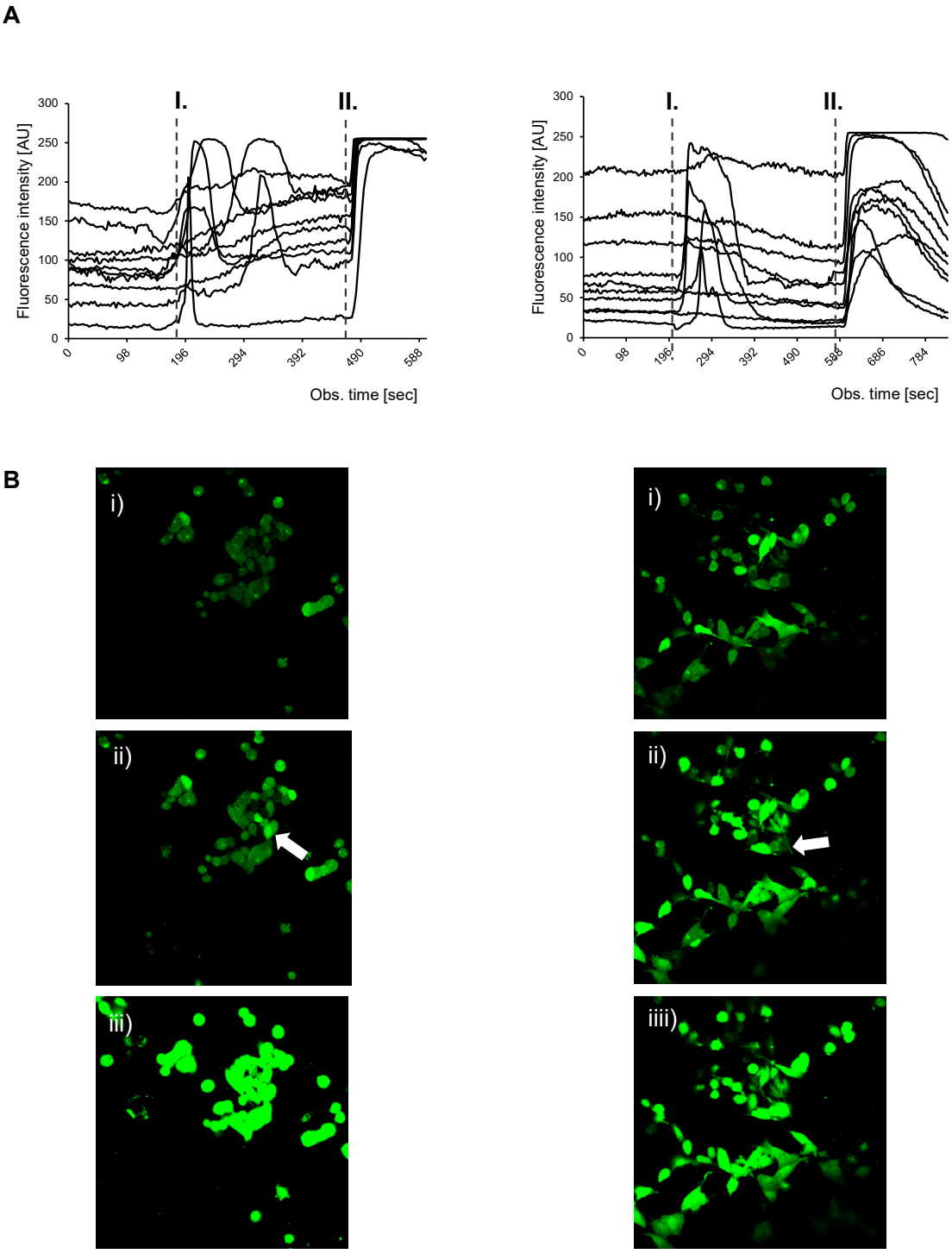

Figure 5.4. Gastrin increases intracellular calcium in a subset of melanoma cells. (A) Fluo-4 labelled melanoma cells (Skmel-2 left, G361 right) simulated with gastrin (10 nmol/L applied at I.) showed a transient increase in fluorescence representing elevated cytosolic calcium as a result of CCK2R activation in a subpopulation of cells. Ionomycin (1 µmol/L applied at II.) served as positive control. (B) Representative images of selected time points show basal fluorescence (i), gastrin treatment (ii, arrows indicate responder cells) and ionomycin provoked calcium influx in majority of cells (iii) (Skmel-2 left, G361 right).

5.3.3 Gastrin does not stimulate EdU incorporation in melanoma cells

In order to assess the effect of gastrin on melanoma cell proliferation we used EdU assays, to mark cells in S-phase. The basal number of G361 cells incorporating EdU was higher compared to Skmel-2 suggesting the former to be a more aggressive cancer cell type (7.0 ± 1.8% vs 9.5 ±4.1% in Skmel-2 and G361 cultured in SF media, respectively). There was no significant increase in the proportion of cells incorporating EdU after gastrin treatment (Skmel-2: 5.2 ± 3.2%; G361: 9.0 ±3.4% after 24h treatment with 10nM G17) (Fig. 5.5A).

The EdU data imply that gastrin has no effect on melanoma cell proliferation. To determine directly whether this was the case we then used a method that estimates the change in cellular biomass (CeCo assays). Absorbance readings expressed as a fold change confirmed little effect of gastrin on cell number (0.1 fold change after 10 nM hG17 for 24hr with both Skme-2 and G361). Considering the fact, that when cells were kept in full medium proliferation rose to 2 and 1.5 fold in G361 and Skmel-2 respectively, minor fold changes as the one described above can be considered negligible (Fig. 5.5B).

To have further insight into whether gastrin shifts the proportion of cells between different stages of cell cycle we also performed flow cytometry analysis. Serum starvation did not markedly change the proportion of cells in S-phase (ΔS%: 2.74 *vs* 6.53 in Skmel-2 and G361 respectively) illustrating the aggressive behaviour and capability of these cancer cells to survive under inhospitable circumstances. Overnight treatment with FM or hG17 did not

significantly alter the proportion of cells in S-phase compared to controls in either cell line (ΔS%: 1.95 *vs* -0.3 after 10 nM hG17 treatment in Skmel-2 and G361 respectively). Minor recruitment of cells from G1 to G2 was observable in case of Skmel-2 (ΔG1%: -5.8; ΔG2%: 4) when treated with hG17, otherwise unchanged (Fig. 5.6).

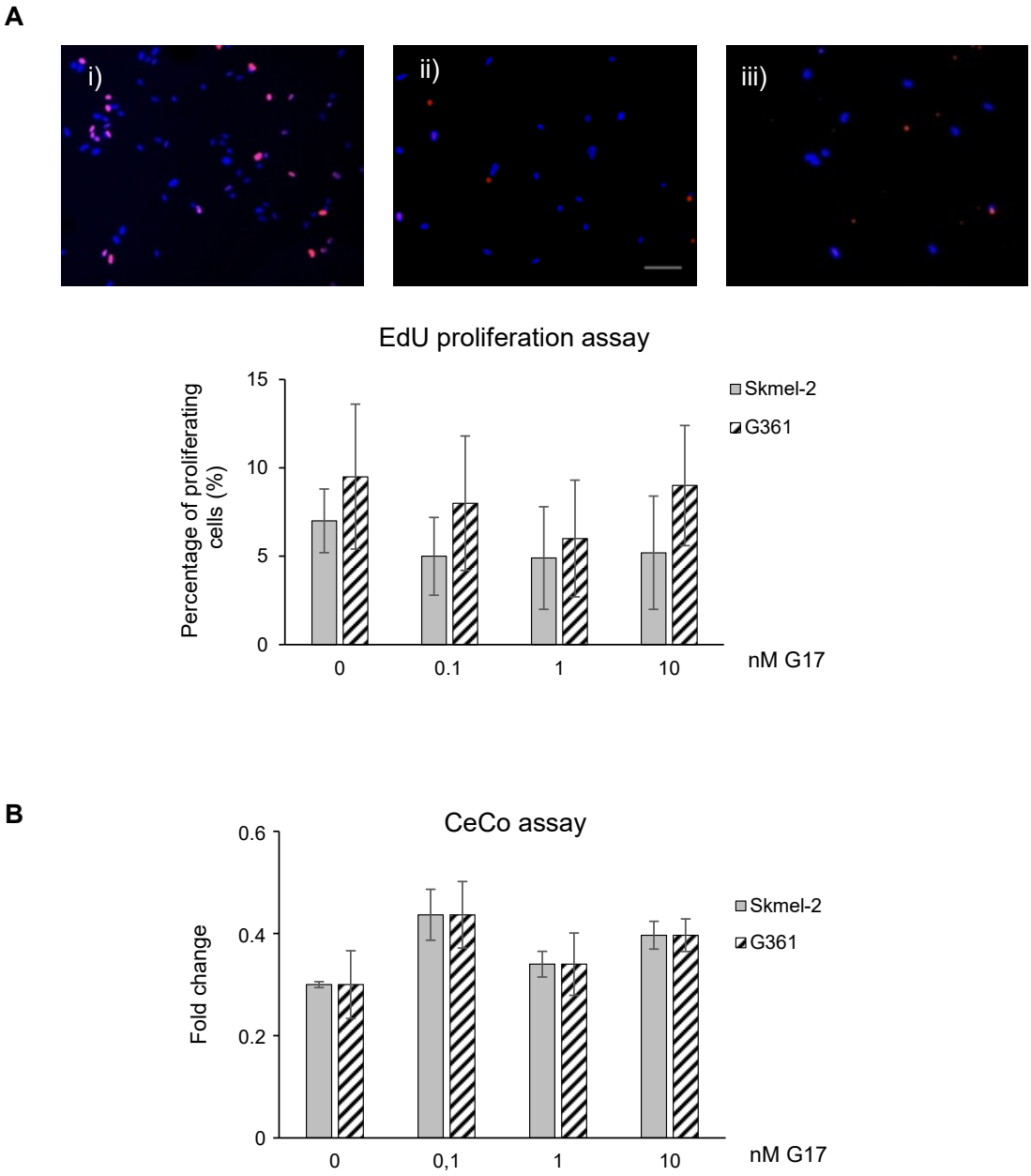

Figure 5.5. Gastrin has no effect on melanoma cell proliferation.
(A) Representative images of melanoma cells incorporating EdU (red nuclei) under normal culture circumstances (i) when treated with gastrin (II) or serum free medium as control (iii) (Scale bar 20 µm). Gastrin treatment covering a 100-fold range had no significant effect on the percentage of EdU labelled cells in either of the melanoma lines investigated. (B) Gastrin had also no effect on total cell number (Y-axis absorbance expressed as fold change) with CeCo assay.

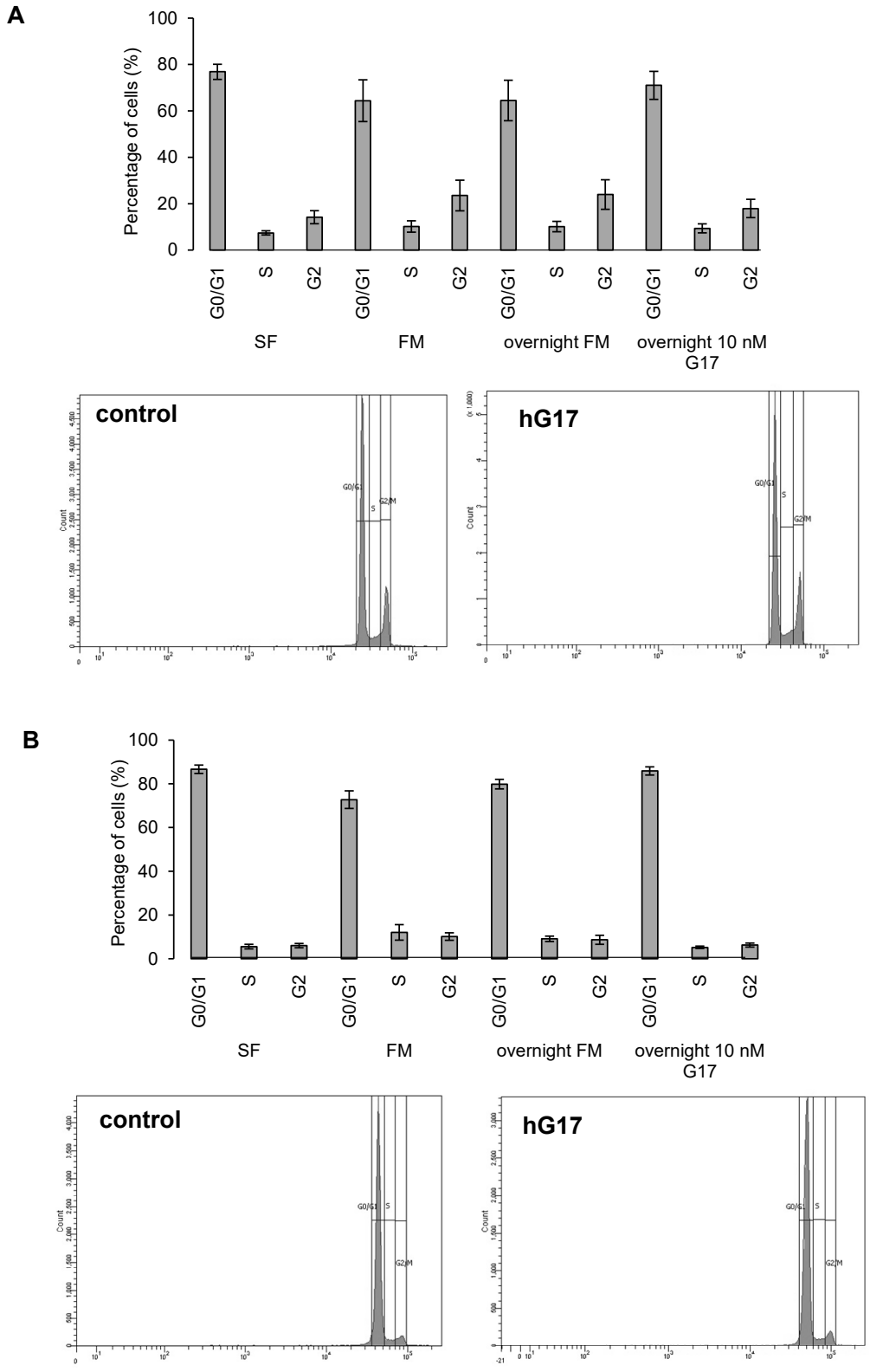

Figure 5.6. Gastrin has no effect on cell cycle of melanoma cells.
(Upper panels) Flow cytometry revealed no changes in the proportion of cells in different stages of the cell cycle when treated with gastrin. (Lower panels). Representative histograms of selected gastrin treated and control samples. (Y-axis indicates percentage of cells in different conditions). Skmel-2 (A), G361 (B).

5.3.4 Gastrin does not affect spheroid growth

In a spheroid model of melanoma cells, we then investigated the effect of gastrin and tumour stroma on the growth of the two melanoma cell lines. Spheroid diameter varied between 100-200 μm and treatments were followed up to 6 days, when there generally developed necrotic changes in the tumour cells located at the core of the spheroid. Consistent with the findings described above, there was no significant difference in size between control and gastrin treated spheroids in either melanoma cell line (Skmel-2, Δ_{6days} Fold change (F.Ch): 0.9 ± 0.3 *vs* 1.0 ± 0.3; G361, and Δ_{6days} F.Ch: 1.2 ± 0.1 *vs* 1.4 ± 0.1, 10nM gastrin *vs* control, respectively) (Fig. 5.7A and B). To investigate the effect of tumour stroma on melanoma growth, we then co-cultured spheroids with gastric CAMs and mesenchymal stem cells in the matrix. Melanoma spheroids embedded in a Matrigel matrix containing stromal cells showed a rapid increase in size compared to controls in both cells lines (Skmel-2, Δ_{6days} F.Ch: 2.5 ± 0.1 *vs* 2.3 ± 0.2 *vs* 1.2 ± 0.3; G361, Δ_{6days} F.Ch: 1.9 ± 0.2 *vs* 1.7 ± 0.2 *vs* 1.1 ± 0.1, melanoma spheroids cultured together with gastric CAMs, MSCs and acellular matrix respectively) (One-way ANOVA p = 0.006 and 0.04 in G361 with CAMs and MSCs respectively; p = 0.019 and 0.036 in Skmel-2 with CAMS and MSCs respectively) (Fig. 5.8A and B). The growth stimulation was almost the same with gastric CAMs and MSCs with the former having a slightly stronger effect in both cell lines. While Skmel-2 cells reached a plateau in size increase at day 4, G361 cells showed a slower response. Gastrin did not influence spheroid growth in the presence of either CAMs or MSCs (CAMs, Δ_{6days} F.Ch: 2.5 ± 0.1 *vs* 2.4 ± 0.1; MSCs, Δ_{6days} F.Ch: 2.3 ± 0.2 *vs* 2.0 ± 0.3,

10nM gastrin *vs* control respectively) (Fig. 5.8C). Although gastrin had no effect on overall spheroid growth, when distances of individually migrated melanoma cells from spheroid core were assessed there was a clear stimulatory effect of gastrin facilitating cancer cell migration indirectly through gastric CAMs (One-way ANOVA, $p = 0.034$). Similar trends were seen with MSCs (One-way ANOVA, $p = 0.315$) (Fig. 5.9).

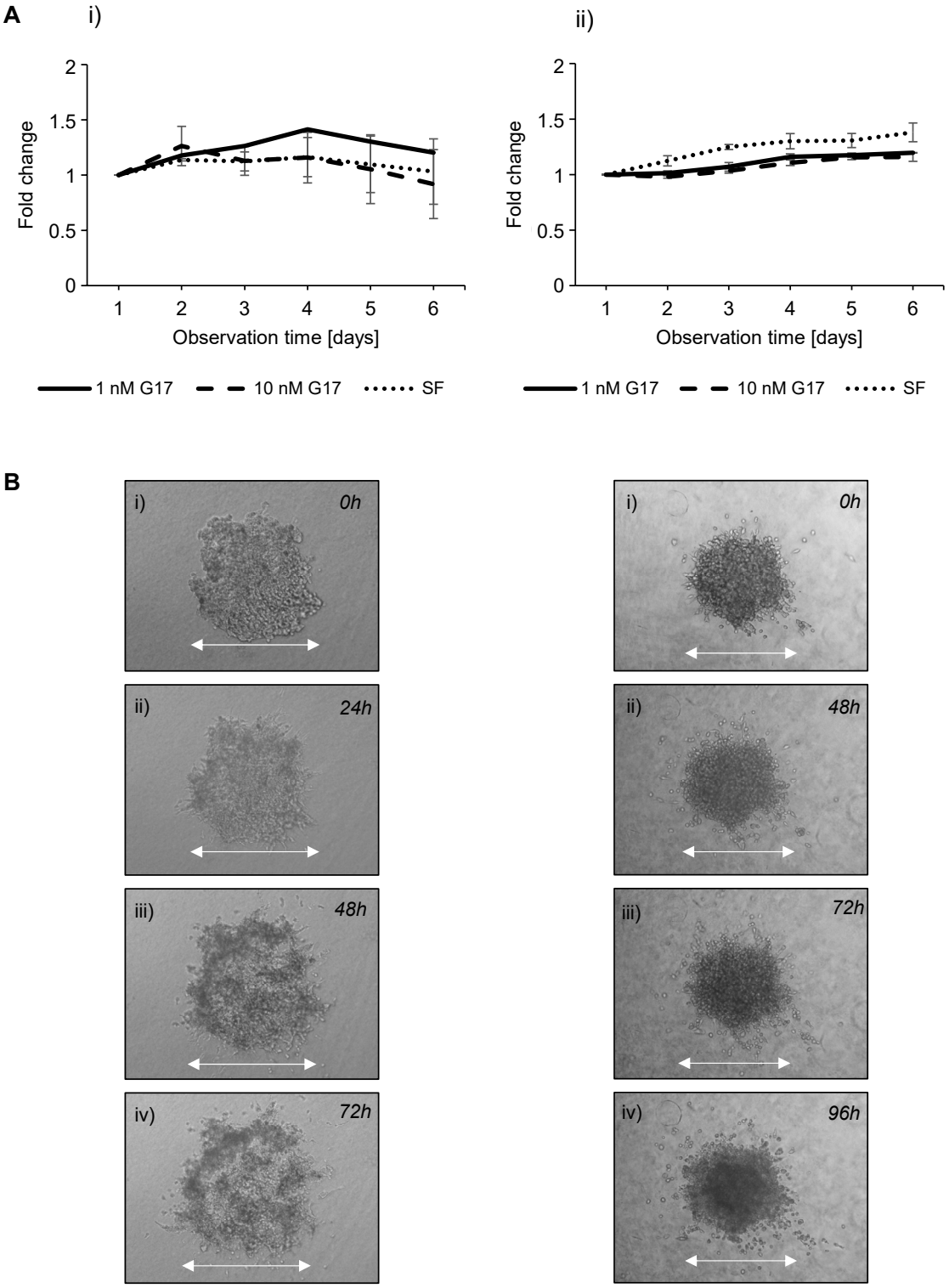

Figure 5.7. Gastrin does not affect melanoma spheroid growth.
(A) Treatment with gastrin for a period of 6 days did not increase cancer spheroid circumference compared to controls in either melanoma cell line (Skmel-2 left, G361 right). (B) Images of a representative spheroid taken at different time points from both cell lines (Skmel-2 left, G361 right). Arrows indicate average spheroid diameter.

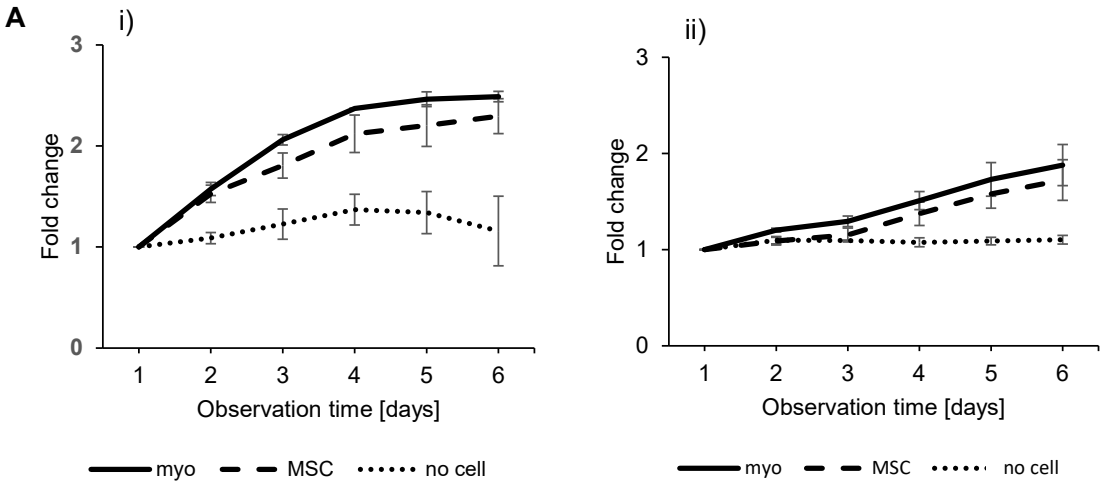
A
i)
Fold change
Observation time [days]
myo
MSC
no cell
ii)
Fold change
Observation time [days]
myo
MSC
no cell

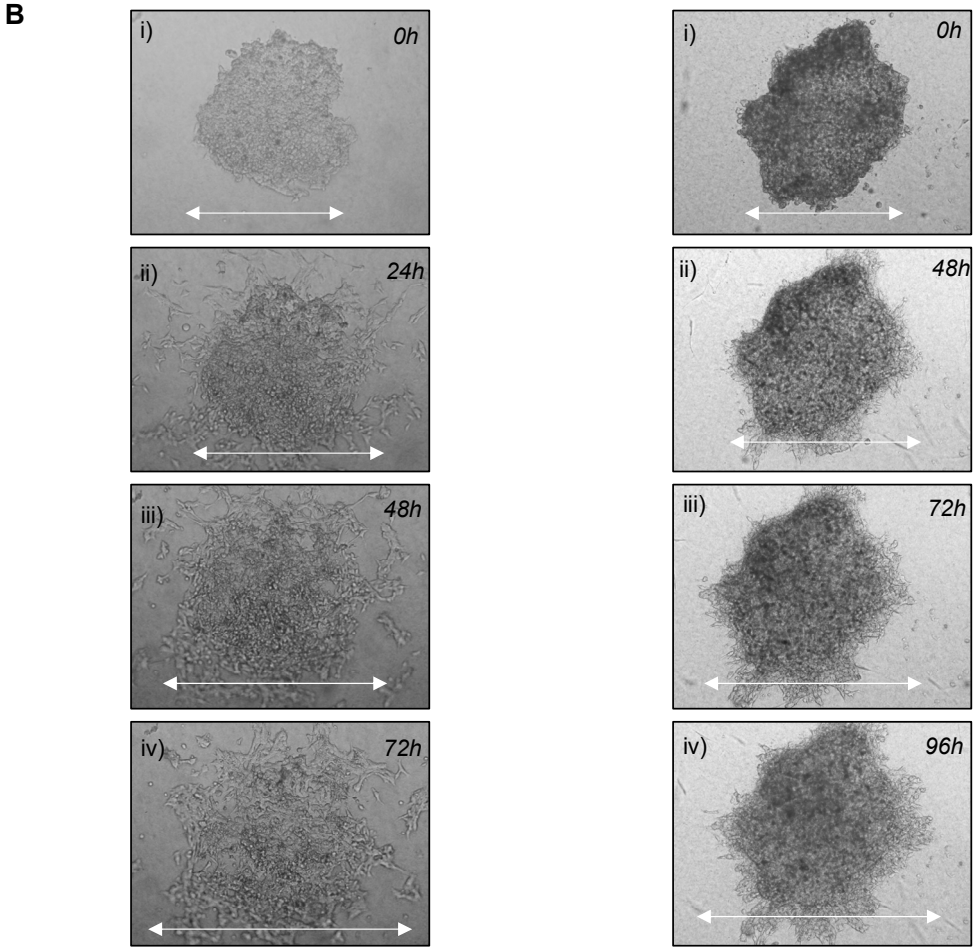
B
i) 0h
ii) 24h
iii) 48h
iv) 72h
i) 0h
ii) 48h
iii) 72h
iv) 96h

C

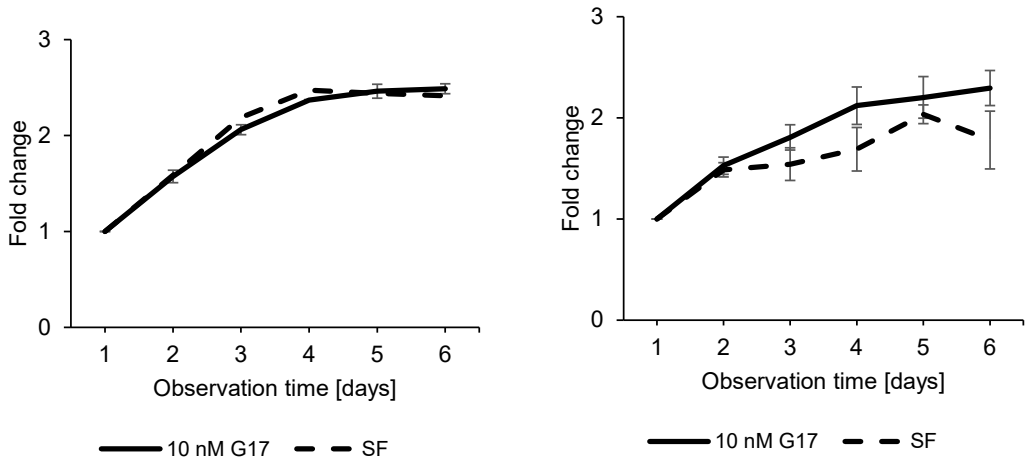

Figure 5.8. Stromal cells stimulate melanoma spheroid growth.
(A) Cancer spheroids surrounded by stromal cells (CAMs or MSCs) increased significantly in size compared to controls (Skmel-2 left, G361 right). (B) Images of representative spheroids taken at different time points from both cell lines (Skmel-2 left, G361 right) embedded in a transparent matrix containing gastric myofibroblasts. Arrows indicate average spheroid diameter. C) Gastrin had no effect on spheroid growth (Skmel-2) either in the presence of gastric myofibroblasts (left) or MSCs (right).

A i)

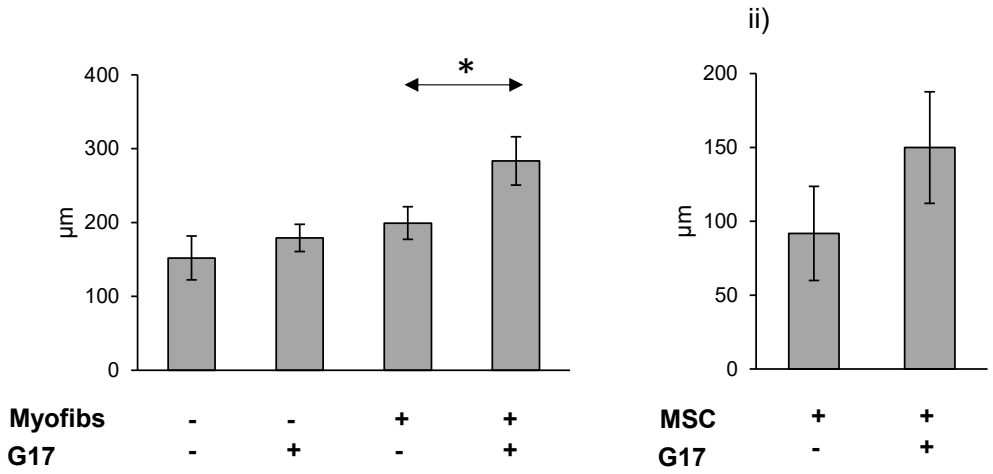

Figure 5.9. Gastrin stimulates invasion of single melanoma cells away from the cancer spheroid. (A) Gastrin treatment significantly increased the distance of individual cancer cells from melanoma spheroid centre (Skmel-2) in the presence of myofibroblasts. A similar tendency was seen with MSCs (Y-axis indicates distance in µm from spheroid centre).

5.3.5 Gastrin stimulates migration and invasion of melanoma cells

The data described at the end of the last section imply that gastrin has an effect on melanoma cancer cell migration and invasion. To examine this question more directly we then used Boyden chamber transwell chemotaxis assays. Gastrin significantly increased migration of both cell lines in these assays (One-way ANOVA, $p < 0.01$). This effect was inhibited by the CCK2 receptor antagonist L740093 at 100 nmol/L which has previously shown to be an effective concentration *in vitro* (One-way ANOVA, $p < 0.01$) (Fig. 5.10A and C). Similarly, gastrin stimulated invasion of Skmel-2 and G261 melanoma cells and the response was reduced by L740093 (One-way ANOVA, $p < 0.01$) (Fig. 5.10B and D).

In view of the strong indication that gastrin stimulated melanoma cell invasion we then turned to a different model of invasion in which Skmel-2 cells were seeded on the top of a layer of a mixture of type I collagen and Matrigel. The incorporation of dispersed gastric CAMs stimulates melanoma cell invasion from the cancer layer into the deeper structures. When organoids were treated with gastrin (10 nM hG17), the depth of invasion was significantly increased (One-way ANOVA; SF vs. Myo: $p < 0.001$ and Myo vs. Myo + hG17: $p = 0.008$). This effect was not seen when organoids were kept in SF media untreated (Fig. 5.11).

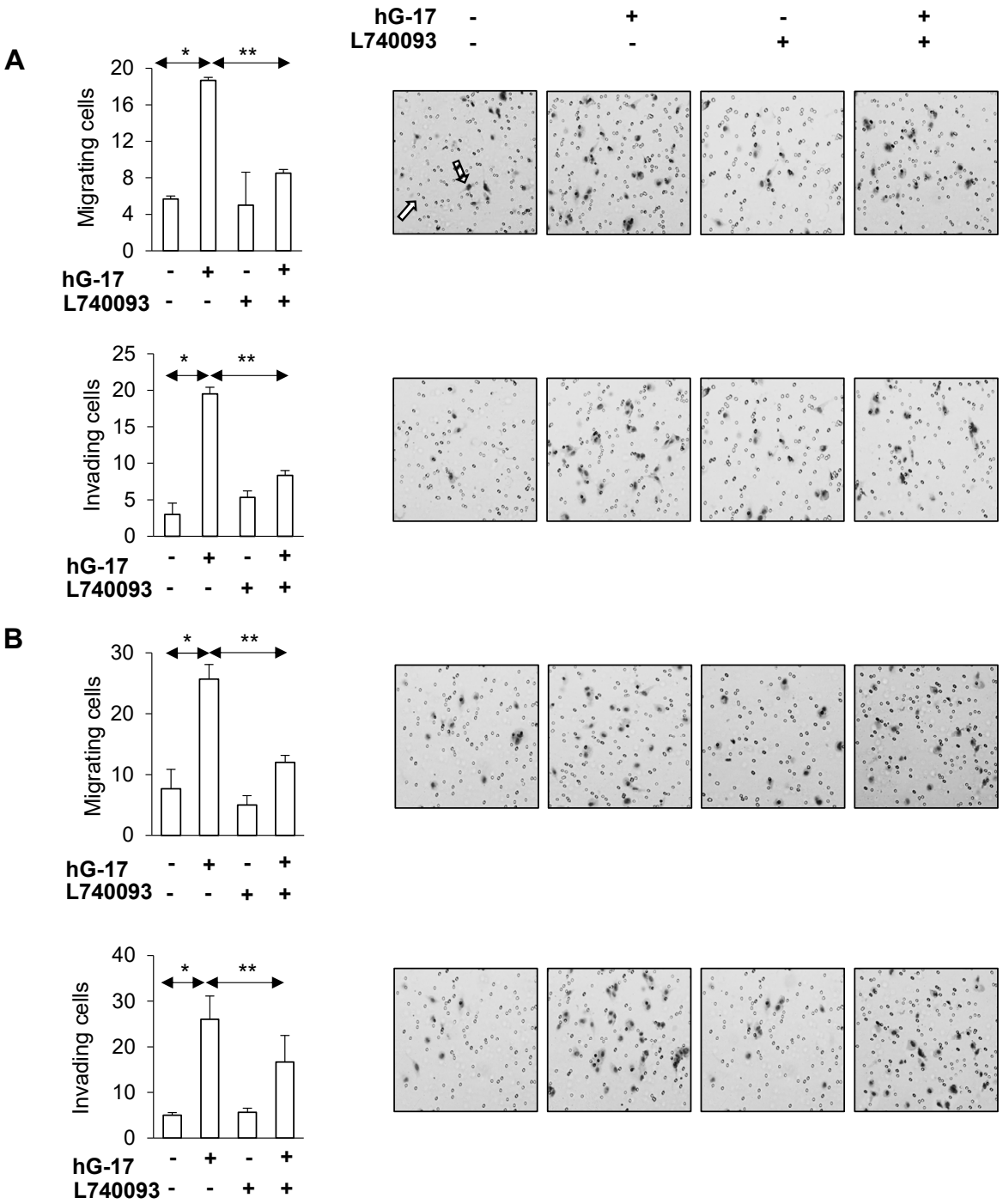

Figure 5.10. Gastrin stimulates migration and invasion of melanoma cells.
(A) Skmel-2, (B) G361; upper panel migration, lower panel invasion in both cases. Gastrin treatment significantly increased the number of migrated and invaded cancer cells in chemotactic assays. This effect was terminated when CCK2 antagonist was introduced. Y-axis represents average number of cells counted in 5 fields. Representative images of cut out membranes from Boyden inserts and Matrigel Biocoat chambers. Hollow arrow shows membrane pores; striped arrow indicates methylene blue stained cells.

A

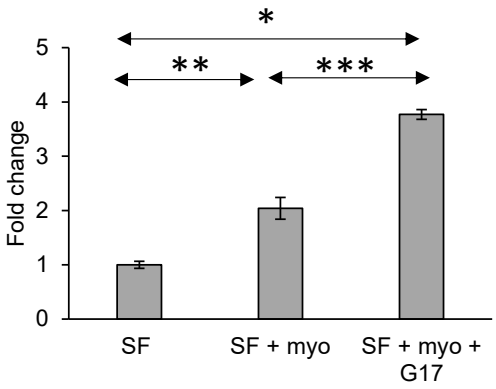

B

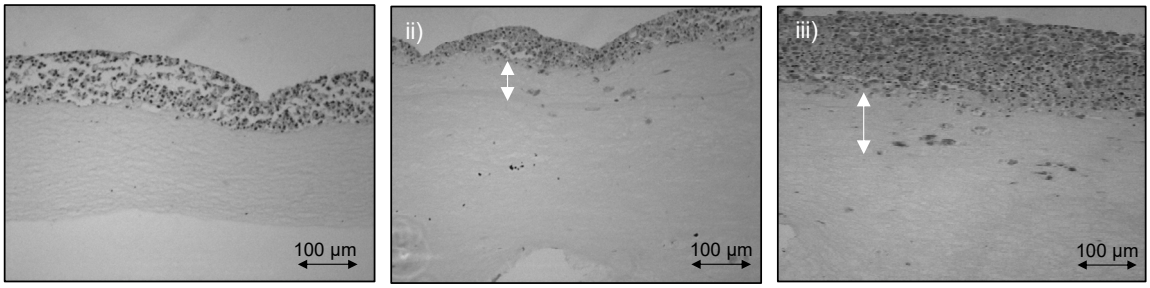

Figure 5.11. Gastrin increases invasion of melanoma cells in organotypic skin model. (A) Cancer cells invaded deeper structures when organoids with gastric myofibroblasts dispersed in the collagen were treated with gastrin. (B) Representative images of stromal cell free control (i), untreated (ii) and gastrin treated (iii) gastric CAM containing Skmel-2 melanoma organoids. See section 5.3.8 for information on the effect of gastrin alone in this model.

5.3.6 Subsets of dermal fibroblasts and myofibroblasts express CCK2R

The results using gastric CAMs described above were obtained at time when dermal fibroblasts and myofibroblasts were not available to us. However, in view of the strong effects obtained it became clear that a more relevant model would be to employ dermal fibroblasts and myofibroblasts. The latter are typically produced by treatment of dermal fibroblasts with TGF-β. Initially, we sought therefore to characterize these two cell types with respect to CCK2R expression. Dermal fibroblasts were strongly positive for vimentin (50.6 ± 5.4%, n=5 fields, 153 cells counted) but were generally negative for the myofibroblast cell marker, SMA (3.0 ± 0.5%, n=5 fields, 1695 cells counted). Dermal myofibroblasts on the other hand exhibited expression of both SMA (40.1 ± 5.1%, n = 5 fields, 369 cells counted) and vimentin (23.4 ± 3.2%, n = 5 fields, 455 cells counted) in significant sub-sets of cells. Neither cell type stained for desmin (data not showed). Flow cytometry revealed the proportion of SMA positive fibroblasts somewhat higher (10%; 11308 viable cells counted), which in combination with the previous finding supports the fact that these patient-derived primary fibroblasts constitute an inhomogeneous cell population that may include partially differentiated myofibroblasts.

The expression of CCK2R somewhat resembled that seen with GI-derived myofibroblasts (Chapter 3) in that only a subset of cells expressed the receptor (dermal fibroblasts: 12.7 ± 2.1%: myofibroblasts: 11.1 ± 2.3%) with no difference between dermal fibroblasts and myofibroblasts (Fig. 5.12A and B).

Flow cytometry was then used to identify the overlapping population of SMA and CCK2R positive cells. In order to have a relatively homogenous population of cells, analysis was only carried out on untreated fibroblasts at low passage. The majority of fibroblasts (78%) were negative for both markers. However, most cells which expressed CCK2R were also positive for SMA (4.9%), while a small proportion (2.3%) were SMA negative but retained CCK2R (7.2 ± 0.6% CCK2 positive cells; n=11262 viable cells in total) (Fig. 5.13A and B).

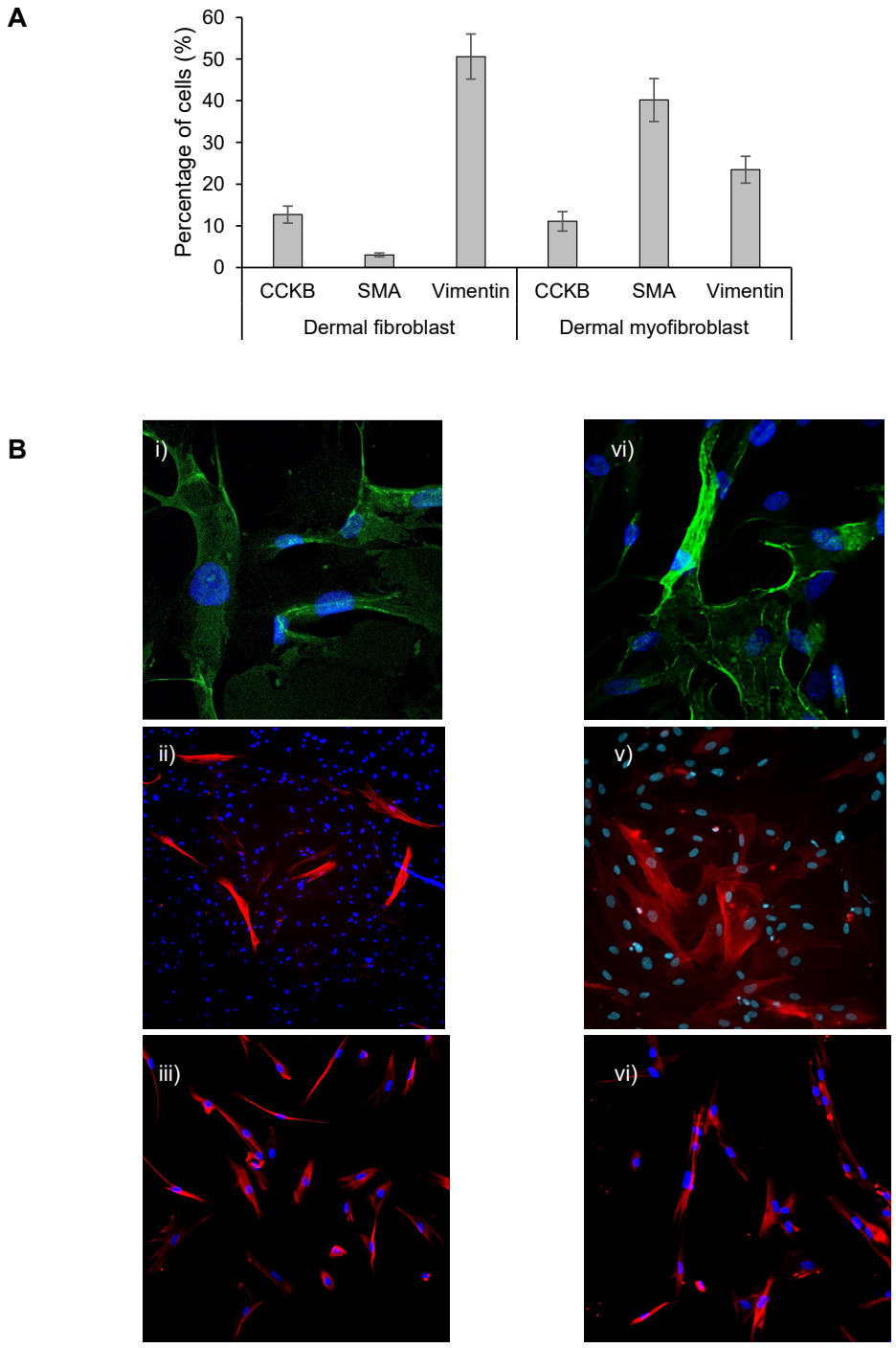

Figure 5.12. Subpopulation of dermal myofibroblasts and fibroblasts express the CCK2R. (A) Immunophenotype of dermal fibroblasts and myofibroblasts. Y-axis represents percentage of positive cells, n = 5; means ±SEM. (B) Representative images of CCK2R positive (i) (alexa-F 546, green), SMA positive (ii) (alexa-F 647, red) and vimentin positive cells (iii) (alexa-F 647, red). Dermal fibroblast left, myofibroblast right panel. Cell nuclei blue (DAPI) in all cases. Magnification 40x (i), 10x (ii, iii).

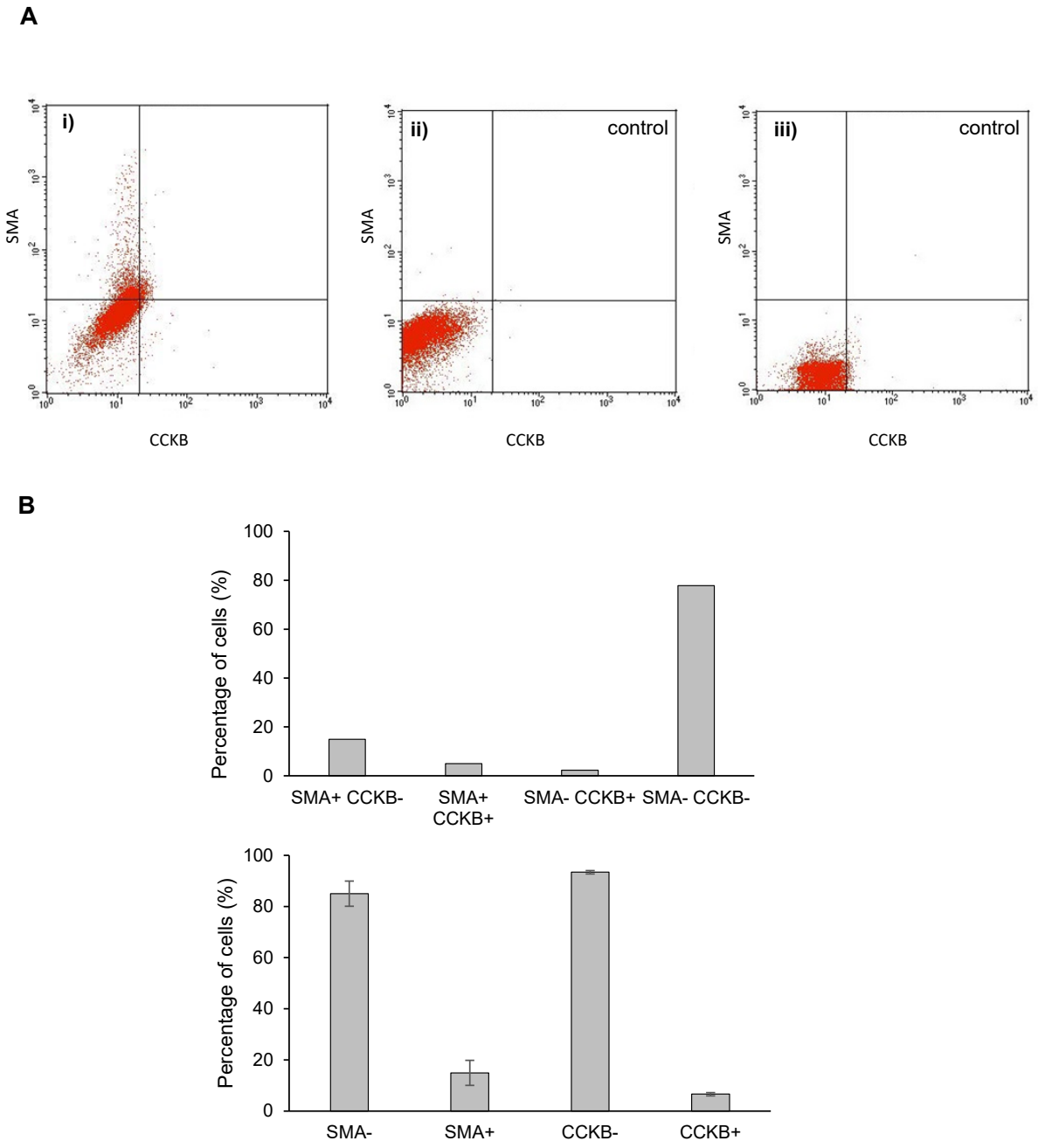

Figure 5.13. CCK2R is partially expressed by SMA positive fibroblasts.
(A) Flow cytometry scatter plots of double labelled (CCK2R, SMA) dermal fibroblasts (i) reveal an overlapping population of cells co-expressing both markers. Isotype control for gastrin receptor (ii) and SMA (iii). Distribution of fibroblasts in main and cross categorise of immunostaining. Y-axis shows percentage of positive cells.

5.3.7 Dermal fibroblasts stimulate melanoma growth in cancer spheroid models

Following the initial characterisation of dermal fibroblasts isolated from healthy patients we then examined the effects of these cells on melanoma spheroids using an approach similar to that described in section 4.3.4 above. Similar to the findings with gastric CAMs, incubation of melanoma cell spheroids in a Matrigel-collagen bed containing dermal stromal cells resulted in a rapid growth reaching a 1.3 ± 0.1-fold change of mean surface area over a 6-day period compared to controls (Kruskal-Wallis test; fib. vs. no fib.: p=0.01). When spheroids were treated with 10nM G17 for the duration of the incubation, there were no effects on spheroid growth either with fibroblasts (Δ_{6days}F.Ch: 1.3 ± 0.1 *vs* 1.3 ± 0.2; treated and controls respectively) or without (Δ_{6days}F.Ch: 1.1 ± 0.1 *vs* 1.0 ± 0.1). The effect of dermal fibroblasts on melanoma growth was seen independently of gastrin treatment (Kruskal-Wallis test; fibs. + hG17 vs. fibs. + no G17 p = 1.0) (Fig. 5.14A and B).

Data from spheroids were also assessed for single cell migration from the spheroid core as reported before in section 5.3.4. Although overall growth of cancer foci was not affected by gastrin, individual cells most likely expressing the receptor were able to migrate furthest when melanoma spheroids surrounded by dermal fibroblasts were treated with gastrin. This burst however in the number of migrating cells was not observed when spheroids were treated with gastrin in the absence of fibroblasts (One-way ANOVA, gastrin vs.

gastrin + fibs: $p < 0.001$), also there was no effect of fibroblasts on cancer cell migration without gastrin (One-way ANOVA, fibs vs gastrin + fibs.: $p < 0.001$) (Fig. 5.15C).

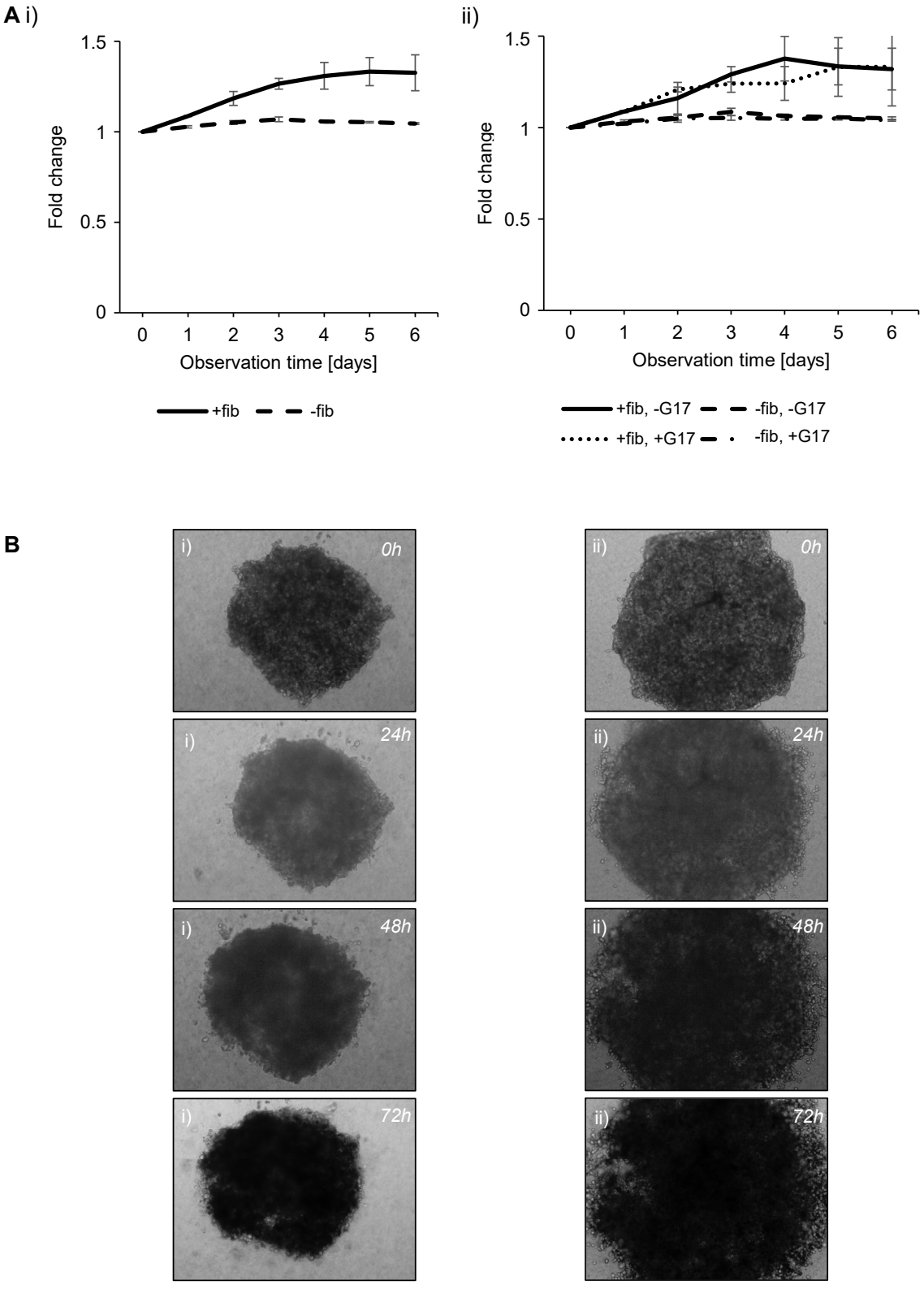

Figure 5.14. Dermal fibroblasts stimulate melanoma spheroid growth independently of gastrin treatment. (A) Stromal cells increased cancer spheroid (Skmel-2) growth compared to fibroblast free controls (i). This effect was not influenced by the presence or absence of gastrin (ii). (B) Representative images of a melanoma spheroid embedded in acellular collagen (left) vs in collagen with fibroblasts dispersed inside (right).

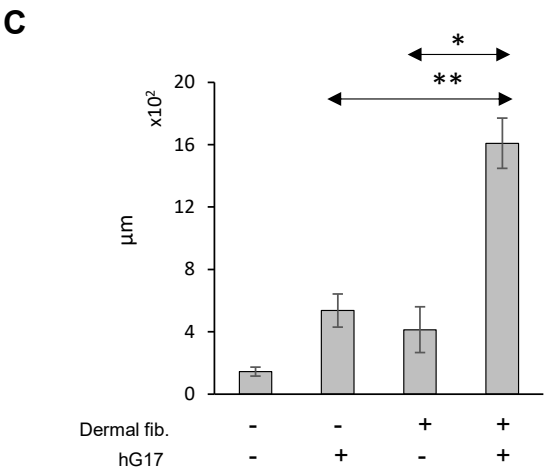

Figure 5.15. Gastrin stimulates melanoma invasion in the presence of fibroblasts. Gastrin markedly increased the distance of individual melanoma cells from spheroid centre if surrounded by stromal cells. Y-axis indicates distance of invaded tumour cells in µm from spheroid core.

5.3.8 Gastrin increases invasion of melanoma cancer cells in the presence of dermal fibroblasts and myofibroblasts

In view of the previous positive results using melanoma cell organoids (see Section 5.3.5) a similar approach was then taken using melanoma cells layered on a gel containing dermal fibroblasts or myofibroblasts. A cancer-stromal border resembling the epidermal-dermal junction remained intact in control samples during the whole observation period (2 weeks) despite the lack of an artificial basement membrane. When melanoma cells were layered on type I collagen matrix with fibroblasts dispersed in it, groups of cancer cells in the form of pedicles or detached nodules (Fig. 5.16A and B) started to penetrate deeper structures (One-way ANOVA, fibs. vs. acellular collagen matrix: $p < 0.001$). Invasion of tumour cells was further increased when organoids with fibroblasts (One-way ANOVA, fibroblasts + G17 *vs* acellular collagen matrix: $p < 0.001$; fibroblasts vs. fibroblasts + G17, $p = 0.002$) were treated with gastrin. This stimulatory effect of gastrin was, however, not seen in the absence of stromal cells in the collagen matrix (Fig. 5.16A).

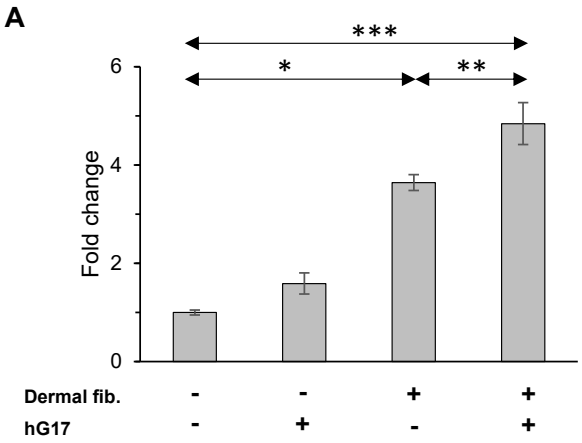

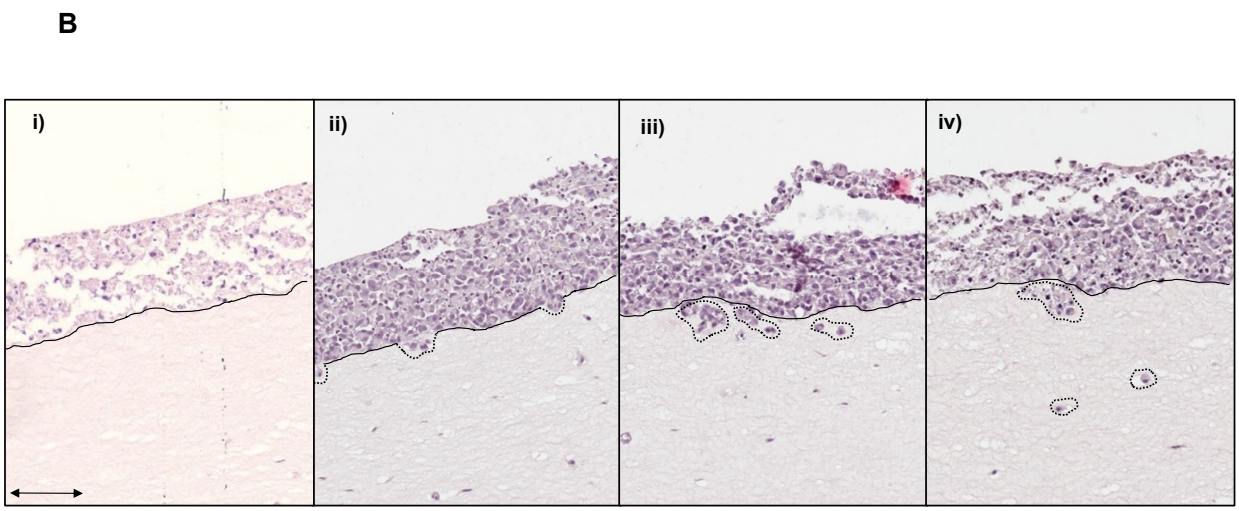

Figure 5.16. Gastrin stimulates invasion of melanoma tumour cells.
(A) Stromal cells increase melanoma cancer cell invasion, which is further enhanced by gastrin. Y axis indicates average distance of melanoma cells from cancer-collagen transition zone expressed as a fold change. (B) Representative images of control (fibroblast free untreated) organoids (i) and gastrin treated ones with stromal cells present in the collagen showing the process of cancer cell detachment and increasing depth of invasion (ii, iii, iv) (Scale bar 90 μm).

5.4 Discussion

There is now growing recognition of the role of gastrin in different tumours. A distinction should, however, be made between tumours expressing the *gastrin* and *CCK2R* genes since although there might be an overlap they do not necessarily occur in the same tumour. Thus, both the receptor and gastrin gene have been reported to be expressed in pancreatic adenocarcinoma, however this is not the case for colorectal cancer where precursor gastrins (progastrin, Gly-gastrin) convey a proliferative effect, with the same being true for lung adenocarcinomas (Nemeth et al. 1993, Ciccotosto et al. 1995, Goetze et al. 2000, Koh et al. 2004). Medullary thyroid cancer is an abundant source of CCK2R, which also led to attempts to visualize thyroid tumours with radiolabelled pharmacons binding to CCK2R (Reubi et al. 1996, Behr et al. 2002, Gotthardt et al. 2006, Roy et al. 2016). To a lesser extent, CCK2R is also expressed by astrocytomas and stromal ovarian cancers (Reubi et al. 1997). Although there is some transcriptome data available on CCK2R expression in human skin and melanoma , it has not fully been confirmed on a protein level and little is known of how gastrin might influence these cancers and thus overall disease outcome.

In this study, two melanoma cells lines (Skmel-2 and G361) were stained with a commercially available anti-CCK2R antibody validated on normal and neoplastic human gastric biopsy samples (see Chapters 3 and 4). Both melanoma lines showed strong immunoreactivity with the antibody, which was further confirmed by quantitative PCR data. Previous studies failed to show a CCK2R mediated gastrin response with melanoma cells (Mathieu et al. 2005),

which raises the question whether these receptors are membrane bound and functionally active.

Both techniques applied for CCK2R detection involved either permeabilisation or tryptic digestion of fixed cells, therefore to answer the former question we employed Ca^{2+} signal detection based on downstream signalling of G-protein coupled receptors to monitor gastrin response of melanoma cells in real-time. CCK2 activation resulted in a measurable increase in cytosolic Ca^{2+} concentration proving a functional receptor.

Gastrin has a wide variety of effects conveyed through CCK2R (Dockray 1999). In hypergastrinaemic conditions, especially in cases where hypochlorhydria and *H. pylori* infection is simultaneously present, there is an increased risk of neoplastic transformation as a result of the trophic effects of gastrin leading to a sequence of hyperplasia, low and high grade dysplasia with the development of gastric adenocarcinomas or Barrett's metaplasia at the end (Bordi et al. 1998, Watson et al. 2006, Dacha et al. 2015). This effect of gastrin on cancer progression have been well studied in the last decade. Gastrin seems to influence a number of signalling pathways which are known to be associated with proliferation, adhesion and apoptosis. It is linked to the activation of Ras/Raf/MEK/ERK, JNK and p38-MAPK cascades amongst others (Daulhac et al. 1997, Dehez et al. 2001). Downstream signalling of the PI3K pathway as a result of receptor activation might in part play role in the loss of adherent junctions and cause cell dissociation in gastrointestinal tumours (Bierkamp et al. 2002, Ferrand et al. 2004).

Malignant transformation of cells while simultaneously acquiring mesenchymal features is a phenomenon generally seen in different tumours. Part of this epithelial mesenchymal transition is the capability of cells to invade lymphovascular structures. CCK2R activation was shown to disrupt intercellular junctions through internalising β-catenins by shifting them to the cytoplasm. Pathways involved in cell detachment and loss of adhesion were later identified as Src, ERK, and PI3K (Bierkamp et al. 2002). Similar changes in expression levels of adhesion molecules can be seen in different stages of melanoma. β_3 integrin subunit of the $\alpha_v\beta_3$ vitronectin receptor has been shown to closely correlate with melanoma cell survival (Hsu et al. 1998). Increase in β_3 integrin levels were related to changes in growth of melanoma form horizontal to vertical phase (Sturm et al. 2002). This raises the question whether gastrin can potentiate disease progression through similar mechanism.

Gastrin is a potent growth factor for many cell types of the gastrointestinal tract (i.e. ECL cells, pancreatic cells), however there is a certain niche of CCK2R expressing cells, which are resistant towards the proliferative effects of gastrin (Dacha et al. 2015), furthermore epithelial progenitor cells which respond to gastrin do not express the receptor. A strong body of evidence suggest that, many of the mitogenic and growth stimulatory effects of gastrin are more likely to be mediated indirectly in a paracrine way through factors such as Reg and heparin-binding epidermal growth factor (Dockray et al. 2001, Varro et al. 2002, Dockray 2004). Melanoma cells grown in cultures did not respond to the proliferative effect of gastrin: thus, EdU incorporation and basal proliferation rates remained unchanged. Cell cycle analysis did not reveal any major

recruitment of cells after gastrin treatment in any stage of the cell cycle compared to controls. Thus in spite of the direct or indirect trophic effects of gastrin in other cases, it seems unlike that gastrin drives the growth of melanomas.

Spheroid and 3-D organoids are becoming favoured models to study diseases in an environment partially mimicking *in vivo* circumstances (Clevers 2016, Fatehullah et al. 2016, Akkerman et al. 2017, Lee et al. 2018). Both models consist of aggregates of cells, with the latter being a more complex structure with layers of cells resembling a tissue-like structure. These models provide an excellent opportunity to study cell-cell and cell-matrix interaction, and tumour behaviour, and have widely been used for example in replicating intestinal crypts, mammary glands or liver sinusoids (Sato et al. 2009, Lancaster et al. 2014).

Similar to the lack of direct proliferative effect, gastrin did not increase overall melanoma spheroid growth. Stromal cells on the other hand provoked a strong response resulting in a rapid tumour expansion highlighting the importance of the tumour microenvironment. Apart from altered immune responses and aberrant homeostasis, the cancer milieu plays a crucial role in sustaining cancer growth (Joyce et al. 2009). Different cell types of the tumour microenvironment have been investigated in recent years, and so far tumour-associated macrophages (TAMs) and cancer-associated fibroblasts (CAFs) have emerged as key players (Qian et al. 2010). Both are able to alter their phenotype and acquire a polarization state responsible for producing a cytokine storm with anti-inflammatory and pro-tumorigenic effects (Biswas et

al. 2010). CAFs are reported to originate from epithelial-to-mesenchymal transition (EMT) or endothelial-to-mesenchymal transition (EndMT) depending on tumor type (Kalluri et al. 2006). Lineage tracing in melanoma revealed CAFs of endothelial origin (Zeisberg et al. 2007). Cells of fibroblastic lineage, namely gastric CAMs and dermal fibroblasts when cultured together with melanoma spheroids caused a rapid increase in tumour mass, which suggest a paracrine activation by factors (FGF, TGF-β, proteases) liberated from tumour stroma.

Despite the fact that gastrin seemed not to affect melanoma proliferation, when the distance of individual cancer cells was measured from the centre of the tumour cell mass, there was a clear stimulatory effect of gastrin on melanoma cancer cell migration and invasion. Similar results were obtained with chemotactic assays using Matrigel coated Boyden chambers. The effect of gastrin on melanoma cells causing Matrigel degradation *in vitro* raises the possibility that the antral hormone might affect secretion of different proteases, through which cancer cells can more rapidly invade lymphovascular structures by digesting ECM. This adds a new dimension to the known pathways gastrin might influence cancer progression. To identify proteins involved we collected conditioned media for analysis of proteins secreted into the extracellular space (secretome) (see chapter 6).

In vitro organoid models provide a novel set of tools to study biological processes, tissue responses to drugs or damage (Fatehullah et al. 2016). They are mostly used in gastroenterological research, but 3D skin models have also been reported to successfully imitate melanoma invasion (Hill et al. 2015). Thus, Melan-A positive melanoma cells were shown to be present in the

dermis after disruption of the basement membrane components and loss of type VII collagen (Hill et al. 2015). In our melanoma organoid model, gastrin significantly increased the invasion of cancer cells in the presence of stromal components (namely gastric CAMs and dermal fibroblasts). A possible explanation for this might be that gastrin liberates certain factors from stromal cells (i.e. IGF or other cytokines as discussed in chapter 3), which than stimulate melanoma invasion and migration. Since tumour cells also express a functional CCK2R (as shown by Boyden chemotactic assays) it might also be possible that although gastrin directly stimulates melanoma cells other cofactors supplied by stromal cells are required for tumour invasion (i.e. heparin binding EGF as seen with CCK2 transfected gastric cancer cells) (Varro et al. 2002). Whichever the underlying mechanism is remains to be investigated further, however most likely it is a combination of the two.

Altogether it appears that gastrin exerts both direct and indirect effects on melanoma cells increasing their migration and invasion capabilities possibly through altering the balance between secreted proteases and protease inhibitors. These effects are mediated through CCK2 receptors expressed by both dermal fibroblasts/myofibroblasts and cancer cells. Additional liberation of growth factors (IGFI-II) and other cytokines (i.e. HB-EGF) from tumour stroma further contributes to cancer growth (Varro et al. 2002, Varga et al. 2017). Overall the data raise the possibility that the metastasising capacity of in situ melanomas is influenced by gastrin.

5.5 Conclusions

1. Melanoma cells express functional CCK2Rs.
2. Dermal fibroblasts and myofibroblasts, like to gastrointestinal ones, belong to the population of cells known to express CCK2R.
3. Gastrin does not affect melanoma proliferation, but increases cancer cell invasion and migration.
4. Stromal cells (gastric CAMs, MSCs, dermal fibroblasts) stimulate cancer growth independently of gastrin.
5. Gastrin in the presence of stromal cells further increases cancer cell invasion.

Chapter 6

The effects of gastrin on the secretome of melanoma cells

6.1 Introduction

Gastrin is known to influence cancer progression through pathways that are associated with cell proliferation, apoptosis and adhesion (Daulhac et al. 1997, Dehez et al. 2001). These effects, which can accelerate neoplastic gastro-intestinal tissue formation, are mediated through CCK2R (Dockray et al. 2012). We reported previously that gastrin is capable of influencing tissue architecture and tumour microenvironment, mainly by defining localisation of GI derived cancer associated myofibroblasts acting as a chemoattractant regulating cell migration and invasion (Varga et al. 2017).

Gastrin does not seem to have any direct proliferative effect on melanoma cancer cells, however it can promote cancer progression *in vitro* through stimulating matrix degradation and promoting invasion in a similar pattern that was seen with myofibroblasts (see Chapter 5).

Proteases are known to play an important role in tumorigenesis (Hua et al. 2011). A number of studies report a correlation between expression of matrix metalloproteases (e.g. MMP-2 and 9) and the clinicopathological course or parameters of cutaneous melanoma, namely tumour thickness and lymph node metastasis (Candrea et al. 2014, Kamyab-Hesari et al. 2014).

Serum gastrin concentration measured in a heterogeneous group of patients with different stages of MM showed a strong association with disease progression (see Chapter 4). Given the fact that melanoma cells express a functional CCK2 receptor (Mathieu et al. 2005), and that *in vitro* studies revealed increased invasion and migration of melanoma cells as a response to gastrin stimuli (see Chapter 5), we collected conditioned media for a

proteomic analysis to identify proteins potentially involved in mediating gastrin regulated cancer progression. We applied a method based on Stable Isotope Dynamic Labelling of Secretomes (SIDLS) as described previously by Hammond et al. to specifically profile secretome proteins by taking advantage of the kinetic differences between classically secreted proteins and intracellular ones (Kristensen et al. 2012, Hammond et al. 2018).

6.1.1 Objectives

1. To analyse the secretome of gastrin-treated melanoma cells and validate by western blot.
2. To identify by gene ontology methods the pathways related to classically secreted proteins.
3. To measure MMP-2 and TIMP-3 secretion of gastrin-treated melanoma cells by ELISA.
4. To investigate the effect of MMP-2 knockdown and addition of TIMP-3 on melanoma migration and invasion using Boyden chambers.
5. To measure serum MMP-2 and TIMP-3 levels of melanoma and basal cell cancer patients by ELISA.

6.2 Methods

6.2.1 Condition media

Culture media of melanoma cells treated with gastrin for 24 and 6 hours were collected and concentrated using StrataClean resin as describe previously in section 2.13 (Holmberg et al. 2012, Hammond et al. 2018).

6.2.2 Proteomic analysis of conditioned media

Putative gastrin targets in Skmel-2 and G361 melanoma secretomes were identified using Stable Isotope Dynamic Labelling of Secretomes (SIDLS) technique previously described in section 2.14 (Kristensen et al. 2012, Hammond et al. 2018). Briefly, cells were incubated with hG17 (10 nmol/L) for 24 h, the last 6h containing either $^{12}C_6$ lysine (light label), or $^{13}C_6$ lysine (heavy label) to mark secreted proteins. Data were searched using MaxQuant 1.1.1.36 against the human IPI database v3.68 (Cox et al. 2008).

6.2.3 Secreted protein search and GeneOntology analysis

Filtered data as detailed in section 2.14.4 were uploaded to Uniprot database to generate fasta sequence files. SignalP v.4.0, SecretomeP v.2.0a (data not shown) and Phobious (data not presented) were used to identify classical (D cut off >0.45) and non-classical (NN score cut-off >0.6) secreted proteins.

Secreted proteins exhibiting signal peptides were run in Panther v.10. to characterise protein classes and biological function (Fig. 6.1) (Mi et al. 2017).

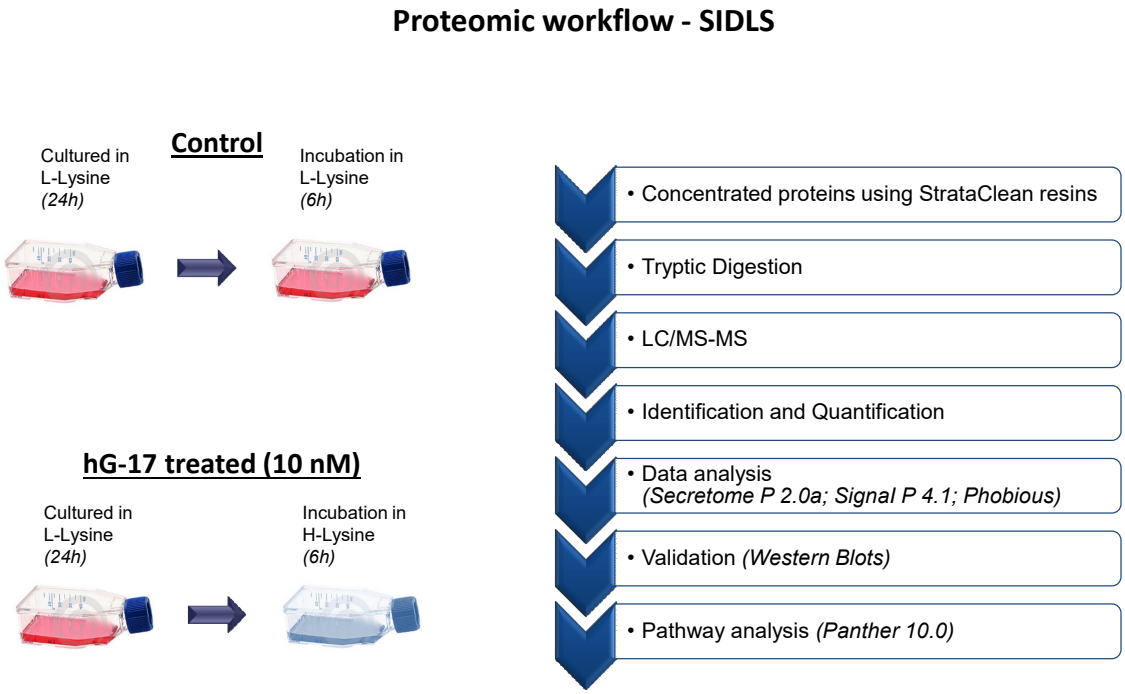

Figure 6.1. Workflow chart of secretome analysis using Stable Isotope Dynamic Labelling technique (SIDLS)

6.2.4 Western blots

Media samples were concentrated with StrataClean resins (Agilent Technologies Ltd) and processed for Western blotting as previously described in section 2.11 (Hemers et al. 2005) using antibodies to MMP-2, TIMP-3 (R&D Systems), TIMP-1, TIMP-2, and prosaposin (R&D Systems).

6.2.5 Adhesion assay

Absorbance of adherent melanoma cells after gastrin treatment for 45 min (10 nmol/L) was detected by a Tecan GENioPlus plate reader at 550 nm as detailed in section 2.15 (Gillies et al. 1986, Kueng et al. 1989).

6.2.6 ELISA

Media and serum samples obtained from melanoma and basal cell cancer patients were analysed for TIMP-3 and MMP-2 using precoated colorimetric ELISA plates (see section 2.12.).

6.2.7 Migration and invasion assays

BD inserts or BD BioCoat™ Matrigel™ chambers (SLS, Nottingham, UK) were used for migration and invasion chemotactic assays respectively as described previously in section 2.6.2 (Varro et al. 2004). Gastrin treatment was applied for 24 h at 10 nmol/L.

6.2.8 Transfection of melanoma cells with siRNA for MMP-2

Cells were transiently transfected using Amaxa™ Cell line Nucleofector™ kits V using the program T-19 for high transfection efficiency (Amaxa, Köln, Germany) according to the manufacturer's instructions. Melanoma cells were treated with scrambled and validated siRNA (3μM) (Sigma) for MMP-2 (Invitrogen, Paisley, UK) (Kumar et al. 2014). The efficiency of knockdown for MMP-2 was verified by western blotting as detailed in section 2.16.

6.2.9 Immunohistochemistry

Samples from MM, BCC patients and controls from gastric and bladder cancer patients were stained for CCK2R, MMP-2, TIMP-3 and Melan-A in an automatic and standardized manner with Leica BOND Max Autostainer. For antibodies and dilutions see section 2.3.2. BOND Refine Red Detection Kit was used for immunohistochemistries unless otherwise stated.

6.2.10 Statistics

Statistical analysis was performed with SPSS software v. 19.0. Shapiro-Wilk was used as normality test for distribution. For intergroup comparisons independent sample t-test, One-way ANOVA were used when applicable. Results were considered significant at p value less than 0.05.

6.3 Results

6.3.1 Secretome and associated pathway analysis of gastrin treated-melanoma cell cultures reveals TIMP-3 inhibition and increased secretion of MMP-2

Cultured melanoma cells were treated with gastrin and secretomes were analysed using methods designed to identify classically secreted proteins that were up or downregulated as a result of gastrin treatment. Proteins were identified based on at least one unique tryptic peptide (Table 6.1). Around 10% of total hits (134 and 187 out of total 1266 and 1507 hits in Skmel-2 and G361 respectively) incorporated Lys in a ratio of H to L isotopes ranging from 0.0012-2.193 in Skmel-2 and 0.0011-1.785 in G361 cells, out of which approximately 50% (65 and 93 in Skmel-2 and G361 respectively) were identified as classical secreted ones based on a ubiquitous protein sorting signal sequence with a threshold of SignalP D-score > 0.45 as suggested by Petersen et al (Petersen et al. 2011) (Table 6.2 and 6.3). Previously we showed (see section 5.3.5) that gastrin increases migration and invasion of cultured melanoma cells by enhancing digestion of Matrigel membranes. Incorporation of heavy lysine (treated samples) expressed as a ratio to light lysine (control samples) revealed increased MMP-2 secretion in Skmel-2 melanoma cells (H to L ratio 1.5). Interestingly the converse was true for G361 melanoma cells, where MMP-2 expression was not influenced, however there was a significant decrease in metalloproteinase inhibitor secretion, namely of TIMP-3 and to a lesser extent TIMP-1 and 2 (0.125; 0.87; 0.7 respectively) (Table 6.4). Since MMP-2 and the TIMPs are complementary to each other in determining ECM

remodelling, this highlights a possible mechanism by which melanoma cells gain increased invading capacity as a result of CCK2R activation. For a detailed list of target proteins with corresponding labelling ratios see supplement (Table S1).

	Skmel-2	G361
Protein hits	1266	1507
Proteins with H/L label	134	187
Classically secreted (Cut-off Dmax >0.45)	65	93
Non-classically secreted	69	94

Table 6.1. Comparison of results of proteomic analysis from melanoma secretome after gastrin stimulations

No.:	Description	Accession	Prot.	Unique Pep.	Pep.	Heavy /Light	AAs	MW [kDa]
1	*CD166 antigen (CD166)*	Q13740	1	1	1	2,193	583	65,1
2	*Prosaposin (SAP)*	P07602	1	4	4	1,907	524	58,1
3	*72 kDa type IV collagenase (MMP-2)*	P08253	1	7	7	1,495	660	73,8
4	*Glia-derived nexin (GDN)*	P07093	1	10	11	0,941	398	44
5	*Sushi repeat-containing protein SRPX (SRPX)*	P78539	1	8	9	0,939	464	51,5
6	*Calsyntenin-1 (CSTN1)*	O94985	2	15	16	0,939	981	109,7
7	*Dystroglycan (DAG1)*	Q14118	1	9	9	0,863	895	97,4
8	*Fibronectin (FINC)*	P02751	1	59	63	0,863	2386	262,5
9	*Neurosecretory protein VGF (VGF)*	O15240	1	14	15	0,795	615	67,2
10	*Cystatin-C (CYTC)*	P01034	2	4	5	0,782	146	15,8
11	*Protein NOV homolog (NOV)*	P48745	1	10	13	0,777	357	39,1
12	*Metalloproteinase inhibitor 2 (TIMP2)*	P16035	1	10	12	0,705	220	24,4
13	*Insulin-like growth factor-binding protein 7 (IBP7)*	Q16270	2	14	15	0,676	282	29,1
14	*Insulin-like growth factor-binding protein 2 (IBP2)*	P18065	1	9	10	0,674	325	34,8
15	*Cadherin-2 (CADH2)*	P19022	1	2	2	0,655	906	99,7
16	*SPARC (SPRC)*	P09486	1	3	4	0,648	303	34,6
17	*Tumor necrosis factor-inducible gene 6 protein (TSG6)*	P98066	1	2	2	0,628	277	31,2
18	*Sulfhydryl oxidase 1 (QSOX1)*	O00391	1	7	7	0,626	747	82,5
19	*Thrombospondin-1 (TSP1)*	P07996	1	22	23	0,613	1170	129,3
20	*Tissue-type plasminogen activator (TPA)*	P00750	1	7	8	0,612	562	62,9
21	*Melanoma-derived growth regulatory protein (MIA)*	Q16674	1	3	3	0,594	131	14,5
22	*Nidogen-1 (NID1)*	P14543	2	13	14	0,559	1247	136,3
23	*Complement factor I (CFAI)*	P05156	1	1	1	0,555	583	65,7
24	*Lactadherin (MFGM)*	Q08431	1	1	1	0,549	387	43,1
25	*Neuroblastoma suppressor of tumorigenicity 1 (NBL1)*	P41271	1	1	1	0,527	181	19,4
26	*Insulin-like growth factor-binding protein 3 (IBP3)*	P17936	1	4	4	0,501	291	31,7
27	*Follistatin-related protein 1 (FSTL1)*	Q12841	1	4	6	0,496	308	35
28	*Tenascin (TENA)*	P24821	2	51	57	0,462	2201	240,7
29	*Lysyl oxidase homolog 2 (LOXL2)*	Q9Y4K0	1	7	7	0,461	774	86,7
30	*Granulocyte-macrophage colony-stimulating factor receptor subunit alpha (CSF2R)*	P15509	1	2	2	0,454	400	46,2
31	*Disintegrin and metalloproteinase domain-containing protein 9 (ADAM9)*	Q13443	1	3	3	0,452	819	90,5
32	*Tumor necrosis factor receptor superfamily member 12A (TNR12)*	Q9NP84	1	1	1	0,381	129	13,9
33	*Peptidyl-glycine alpha-amidating monooxygenase (AMD)*	P19021	1	3	3	0,376	973	108,3
34	*Galectin-3-binding protein (LG3BP)*	Q08380	1	9	10	0,366	585	65,3
35	*Laminin subunit alpha-4 (LAMA4)*	Q16363	1	21	25	0,361	1823	202,4
36	*Protein disulfide-isomerase A4 (PDIA4)*	P13667	5	14	16	0,337	645	72,9
37	*Collagen alpha-1(XII) chain (COCA1)*	Q99715	1	34	34	0,324	3063	332,9
38	*Matrilin-2 (MATN2)*	O00339	1	10	14	0,318	956	106,8
39	*Extracellular matrix protein 1 (ECM1)*	Q16610	1	7	7	0,273	540	60,6
40	*Cathepsin L1 (CATL1)*	P07711	1	3	3	0,271	333	37,5
41	*Apolipoprotein D (APOD)*	P05090	1	3	3	0,245	189	21,3
42	*Serine protease 23 (PRS23)*	O95084	1	2	3	0,221	383	43
43	*Beta-2-microglobulin (B2MG)*	P61769	1	2	3	0,218	119	13,7
44	*Laminin subunit gamma-1 (LAMC1)*	P11047	1	30	34	0,198	1609	177,5
45	*Matrix metalloproteinase-14 (MMP14)*	P50281	1	1	1	0,191	582	65,9
46	*Protein disulfide-isomerase A3 (PDIA3)*	P30101	1	20	20	0,19	505	56,7
47	*Protein disulfide-isomerase (PDIA1)*	P07237	1	6	7	0,175	508	57,1
48	*Disintegrin and metalloproteinase domain-containing protein 10 (ADA10)*	O14672	1	4	4	0,173	748	84,1
49	*Laminin subunit beta-1 (LAMB1)*	P07942	1	19	19	0,15	1786	197,9
50	*Cathepsin D (CATD)*	P07339	1	2	2	0,15	412	44,5
51	*Vascular endothelial growth factor receptor 1 (VGFR1)*	P17948	1	5	5	0,142	1338	150,7
52	*Trans-Golgi network integral membrane protein 2 (TGON2)*	O43493	1	5	5	0,115	480	51,1
53	*LDLR chaperone MESD (MESD)*	Q14696	1	4	5	0,112	234	26,1
54	*Connective tissue growth factor (CTGF)*	P29279	1	26	26	0,112	349	38,1

55	*Multiple inositol polyphosphate phosphatase 1 (MINP1)*	Q9UNW1	1	1	1	0,084	487	55
56	*Collagen triple helix repeat-containing protein 1 (CTHR1)*	Q96CG8	1	5	6	0,079	243	26,2
57	*Nucleobindin-1 (NUCB1)*	Q02818	2	12	15	0,054	461	53,8
58	*Granulins (GRN)*	P28799	1	5	8	0,054	593	63,5
59	*Calumenin (CALU)*	O43852	1	4	4	0,053	315	37,1
60	*Growth-regulated alpha protein (GROA)*	P09341	17	3	6	0,044	107	11,3
61	*45 kDa calcium-binding protein (CAB45)*	Q9BRK5	1	10	10	0,037	362	41,8
62	*Calreticulin (CALR)*	P27797	1	1	1	0,029	417	48,1
63	*Cell surface glycoprotein MUC18 (MUC18)*	P43121	5	12	13	0,029	646	71,6
64	*Glucosidase 2 subunit beta (GLU2B)*	P14314	1	12	13	0,014	528	59,4
65	*Interleukin-8 (IL8)*	P10145	1	4	5	0,012	99	11,1

Table 6.2. List of classically secreted isotope labelled proteins with signal peptide sequence showing alteration after gastrin treatment characterised from Skmel-2 secretome.

No.:	Description	Accession	Prot.	Unique Pep.	Pep.	Heavy/ Light	AAs	MW [kDa]
1	*Prosaposin (SAP)*	P07602	1	7	8	1,785	524	58,1
2	*Neurosecretory protein VGF (VGF)*	O15240	1	34	34	0,933	615	67,2
3	*Glia-derived nexin (GDN)*	P07093	1	4	4	0,917	398	44
4	*72 kDa type IV collagenase (MMP-2)*	P08253	1	17	17	0,9	660	73,8
5	*Metalloproteinase inhibitor 1 (TIMP1)*	P01033	1	5	5	0,87	207	23,2
6	*Granulins (GRN)*	P28799	1	15	16	0,839	593	63,5
7	*Dystroglycan (DAG1)*	Q14118	1	12	12	0,811	895	97,4
8	*Sushi repeat-containing protein SRPX (SRPX)*	P78539	1	9	9	0,791	464	51,5
9	*Calsyntenin-1 (CSTN1)*	O94985	2	17	18	0,771	981	109,7
10	*Insulin-like growth factor-binding protein 2 (IBP2)*	P18065	1	15	16	0,761	325	34,8
11	*Stanniocalcin-1 (STC1)*	P52823	1	2	2	0,734	247	27,6
12	*Metalloproteinase inhibitor 2 (TIMP2)*	P16035	1	14	16	0,7	220	24,4
13	*Insulin-like growth factor-binding protein 3 (IBP3)*	P17936	20	13	13	0,695	291	31,7
14	*Fibronectin (FINC)*	P02751	3	78	78	0,683	2386	262,5
15	*Cadherin-2 (CADH2)*	P19022	1	1	1	0,675	906	99,7
16	*Sulfhydryl oxidase 1 (QSOX1)*	O00391	1	5	5	0,661	747	82,5
17	*ADM (ADML)*	P35318	1	5	6	0,647	185	20,4
18	*Cathepsin L2 (CATL2)*	O60911	2	1	3	0,638	334	37,3
19	*Cadherin-1 (CADH1)*	P12830	1	1	1	0,628	882	97,4
20	*Protein NOV homolog (NOV)*	P48745	1	12	13	0,619	357	39,1
21	*Cystatin-C (CYTC)*	P01034	2	6	6	0,608	146	15,8
22	*Melanoma-derived growth regulatory protein (MIA)*	Q16674	1	5	5	0,606	131	14,5
23	*Testican-1 (TICN1)*	Q08629	2	8	9	0,599	439	49,1
24	*Follistatin-related protein 5 (FSTL5)*	Q8N475	2	3	3	0,585	847	95,7
25	*SPARC (SPRC)*	P09486	1	5	6	0,572	303	34,6
26	*Cell migration-inducing and hyaluronan-binding protein (CEMIP)*	Q8WUJ3	1	7	9	0,553	1361	152,9
27	*Tenascin (TENA)*	P24821	2	24	27	0,544	2201	240,7
28	*Amyloid beta A4 protein (A4)*	P05067	2	11	12	0,534	770	86,9
29	*Insulin-like growth factor-binding protein 7 (IBP7)*	Q16270	1	12	12	0,532	282	29,1
30	*Peptidyl-glycine alpha-amidating monooxygenase (AMD)*	P19021	1	10	11	0,528	973	108,3
31	*Tissue-type plasminogen activator (TPA)*	P00750	1	10	11	0,514	562	62,9
32	*Inter-alpha-trypsin inhibitor heavy chain H5 (ITIH5)*	Q86UX2	1	9	10	0,502	942	104,5
33	*Neuroblastoma suppressor of tumorigenicity 1 (NBL1)*	P41271	1	3	3	0,499	181	19,4
34	*Collagen alpha-3(V) chain (CO5A3)*	P25940	1	2	3	0,489	1745	172
35	*Laminin subunit alpha-1 (LAMA1)*	P25391	2	48	51	0,487	3075	336,9
36	*Amyloid-like protein 2 (APLP2)*	Q06481	1	2	3	0,477	763	86,9
37	*Follistatin-related protein 1 (FSTL1)*	Q12841	1	8	9	0,468	308	35
38	*Serine protease 23 (PRS23)*	O95084	1	3	4	0,467	383	43
39	*EMILIN-2 (EMIL2)*	Q9BXX0	1	6	8	0,445	1053	115,6
40	*Transmembrane glycoprotein NMB (GPNMB)*	Q14956	1	3	4	0,426	572	63,9
41	*Serine protease HTRA1 (HTRA1)*	Q92743	1	12	13	0,425	480	51,3
42	*Tartrate-resistant acid phosphatase type 5 (PPA5)*	P13686	1	2	2	0,391	325	36,6
43	*Apolipoprotein D (APOD)*	P05090	1	4	5	0,39	189	21,3
44	*Lactadherin (MFGM)*	Q08431	1	1	1	0,37	387	43,1
45	*Vitamin K-dependent protein S (PROS)*	P07225	1	5	5	0,353	676	75,1
46	*Extracellular matrix protein 1 (ECM1)*	Q16610	1	16	16	0,351	540	60,6
47	*Laminin subunit gamma-1 (LAMC1)*	P11047	1	43	46	0,343	1609	177,5
48	*Angiopoietin-related protein 2 (ANGL2)*	Q9UKU9	2	5	5	0,341	493	57,1
49	*Matrix metalloproteinase-14 (MMP14)*	P50281	1	6	6	0,341	582	65,9
50	*Cathepsin D (CATD)*	P07339	1	7	8	0,313	412	44,5
51	*Acid ceramidase (ASAH1)*	Q13510	1	4	4	0,309	395	44,6
52	*Galectin-3-binding protein (LG3BP)*	Q08380	1	7	8	0,307	585	65,3
53	*Collagen alpha-1(VI) chain (CO6A1)*	P12109	1	1	1	0,262	1028	108,5
54	*Thrombospondin-1 (TSP1)*	P07996	1	11	11	0,258	1170	129,3
55	*Cathepsin L1 (CATL1)*	P07711	2	9	11	0,228	333	37,5
56	*Laminin subunit alpha-4 (LAMA4)*	Q16363	1	6	9	0,221	1823	202,4
57	*Growth-regulated alpha protein (GROA)*	P09341	19	5	6	0,221	107	11,3
58	*Laminin subunit beta-1 (LAMB1)*	P07942	3	26	29	0,213	1786	197,9

59	*Immunoglobulin superfamily member 8 (IGSF8)*	Q969P0	1	8	8	0,198	613	65
60	*Beta-2-microglobulin (B2MG)*	P61769	1	2	2	0,197	119	13,7
61	*Protein jagged-1 (JAG1)*	P78504	1	3	3	0,193	1218	133,7
62	*Collagen alpha-2(IV) chain (CO4A2)*	P08572	1	13	13	0,173	1712	167,4
63	*Growth/differentiation factor 15 (GDF15)*	Q99988	1	13	14	0,166	308	34,1
64	*DnaJ homolog subfamily B member 11 (DJB11)*	Q9UBS4	1	2	2	0,156	358	40,5
65	*Nucleobindin-1 (NUCB1)*	Q02818	14	26	30	0,155	461	53,8
66	*Calnexin (CALX)*	P27824	1	3	4	0,153	592	67,5
67	*Alpha-2-macroglobulin (A2MG)*	P01023	1	2	4	0,152	1474	163,2
68	*Kunitz-type protease inhibitor 1 (SPIT1)*	O43278	1	1	1	0,15	529	58,4
69	*Receptor-type tyrosine-protein phosphatase S (PTPRS)*	Q13332	1	10	11	0,144	1948	216,9
70	*Protein disulfide-isomerase A4 (PDIA4)*	P13667	5	23	24	0,141	645	72,9
71	*Disintegrin and metalloproteinase domain-containing protein 10 (ADA10)*	O14672	1	9	9	0,134	748	84,1
72	*Metalloproteinase inhibitor 3 (TIMP-3)*	P35625	1	7	7	0,125	211	24,1
73	*Protein disulfide-isomerase A3 (PDIA3)*	P30101	1	21	22	0,11	505	56,7
74	*Melanocyte protein PMEL (PMEL)*	P40967	1	7	8	0,093	661	70,2
75	*Nucleobindin-2 (NUCB2)*	P80303	1	5	7	0,091	420	50,2
76	*Golgi apparatus protein 1 (GSLG1)*	Q92896	1	12	12	0,091	1179	134,5
77	*Multiple inositol polyphosphate phosphatase 1 (MINP1)*	Q9UNW1	1	1	1	0,089	487	55
78	*78 kDa glucose-regulated protein (GRP78)*	P11021	3	31	36	0,073	654	72,3
79	*Protein CYR61 (CYR61)*	O00622	1	9	11	0,071	381	42
80	*Trans-Golgi network integral membrane protein 2 (TGON2)*	O43493	1	6	7	0,069	480	51,1
81	*45 kDa calcium-binding protein (CAB45)*	Q9BRK5	1	9	11	0,067	362	41,8
82	*Cathepsin B (CATB)*	P07858	1	9	9	0,06	339	37,8
83	*Chondroitin sulfate proteoglycan 4 (CSPG4)*	Q6UVK1	1	21	23	0,055	2322	250,4
84	*Collagen triple helix repeat-containing protein 1 (CTHR1)*	Q96CG8	1	4	5	0,053	243	26,2
85	*Midkine (MK)*	P21741	1	3	4	0,052	143	15,6
86	*Procollagen-lysine,2-oxoglutarate 5-dioxygenase 3 (PLOD3)*	O60568	1	9	13	0,048	738	84,7
87	*Calreticulin (CALR)*	P27797	1	6	8	0,04	417	48,1
88	*Chitinase domain-containing protein 1 (CHID1)*	Q9BWS9	1	2	3	0,035	393	44,9
89	*Neural cell adhesion molecule L1 (L1CAM)*	P32004	2	8	8	0,031	1257	139,9
90	*Calumenin (CALU)*	O43852	1	10	10	0,024	315	37,1
91	*Polypeptide N-acetylgalactosaminyltransferase 2 (GALT2)*	Q10471	1	15	15	0,023	571	64,7
92	*Cell surface glycoprotein MUC18 (MUC18)*	P43121	2	16	16	0,02	646	71,6
93	*Glucosidase 2 subunit beta (GLU2B)*	P14314	1	11	11	0,011	528	59,4

Table 6.3. List of classically secreted isotope labelled proteins with signal peptide sequence showing alteration after gastrin treatment characterised from G361 secretome.

Proteomic data was validated with western blot. Prosaposin, which is a precursor for saposins A-D mostly recognised for the catabolism of glycosphingolipids (Carvelli et al. 2015) was added to the list as a gastrin-responsive benchmark since cellular secretion was equally increased in both gastrin-treated melanoma cell lines. Densitometry analysis of protein bands revealed 1.70-fold increase of MMP-2 in Skmel-2 and 0.58 and 0.74-fold change of TIMP-3 and TIMP-1 respectively in G361 gastrin treated melanoma cells. MMP-2 secretion in G316 and TIMP-3 inhibition in Skmel-2 cells was not influenced by gastrin (For full densitometry data see Table 6.4 and Fig. 6.2A).

ELISA analysis of conditioned media supported the previous observation that MMP-2 concentration was higher in gastrin treated Skmel-2 melanoma cells (student t-test; $p = 0.029$) while TIMP-3 secretion significantly decreased in G361 cells (student t-test; $p = 0.015$). Similar to western data, TIMP-3 concentration remained unchanged in Skmel-2 cells however there was a slight decrease in MMP-2 in the media of G361 cells after gastrin treatment (student t-test; $p = 0.009$) (Fig. 6.2B). Table 6.5 shows comparison of results obtained with different methods.

	Skmel-2	G361
Prosaposin	1.27	1.27
MMP2	1.70	0.92
TIMP3	-	0.58
TIMP1	1.05	0.74

Table 6.4. Densitometry data of western blot reveal upregulation of MMP-2 protein in Skmel-2 melanoma cells and downregulation of TIMP-3 in G361 cancer cells after gastrin stimulation. Responses to gastrin are expressed relative to untreated cells.

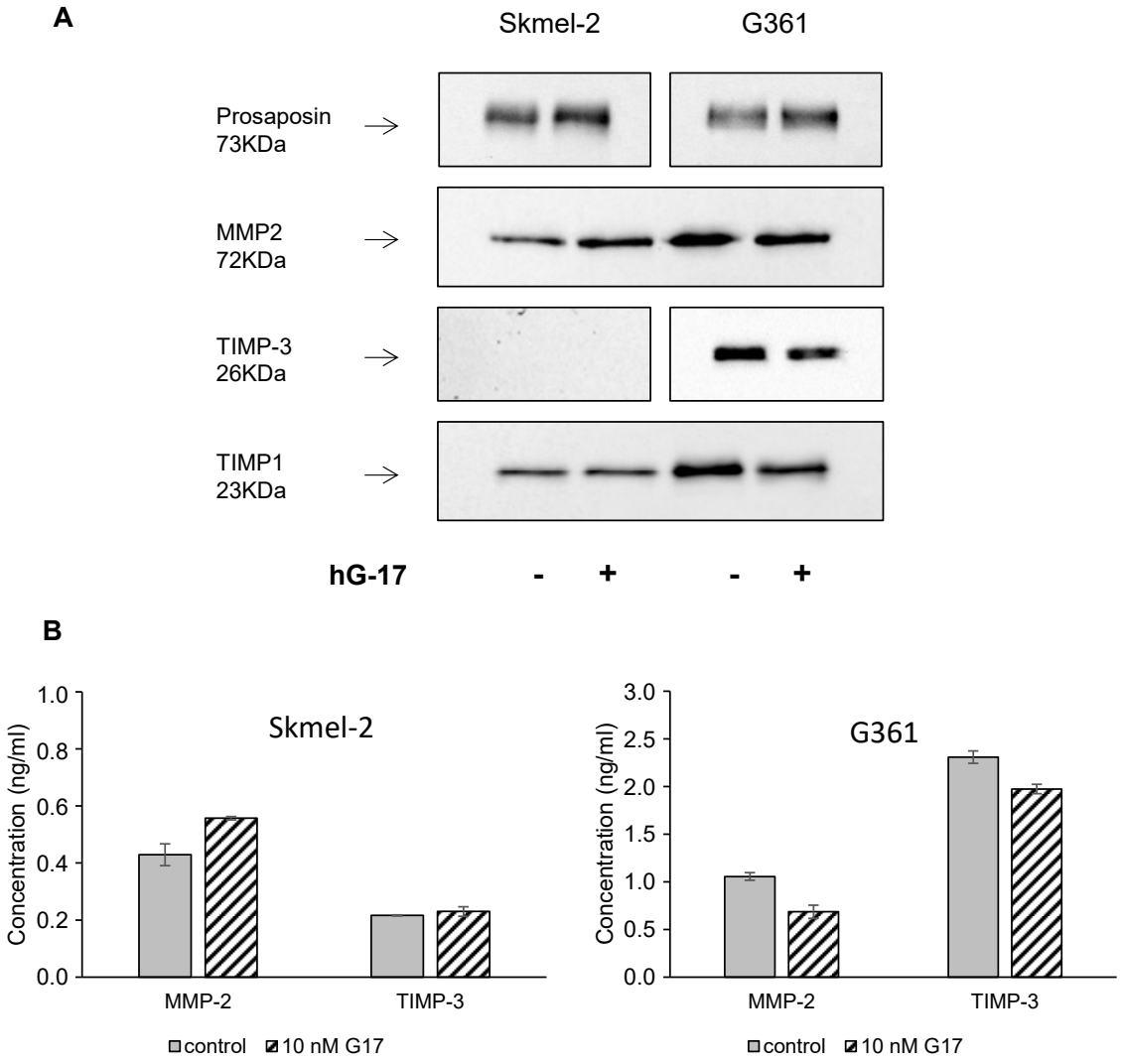

Figure 6.2. Gastrin upregulates MMP-2 and downregulates expression of TIMP-3 in melanoma. (A) Validation of proteomic data with western blot confirmed similar changes of MMP-2 and TIMP1,3 secretion following gastrin administration. Prosaposin was used as a gastrin responsive benchmark. (B) ELISA of conditioned media from hG17 stimulated melanoma cells consolidated data from western blots

	MMP-2		**TIMP-3**	
	Skmel-2	*G361*	*Skmel-2*	*G361*
SIDLS	1.50	0.90	-	0.13
WESTERN BLOT	1.70	0.92	-	0.58
ELISA	1.30	0.65	1.06	0.86

Table 6.5. Comparison of different techniques used to detect and measure changes of selected proteins after gastrin stimulation. Data of given responses are expressed relative to untreated cells.

6.3.2 Functional analysis and associated pathways of gastrin regulated proteins

Classically secreted proteins identified with SignalP v. 4.1 were uploaded to Panther v 10.0 database (Mi et al. 2013) which extrapolates proteomic data using phylogenetic trees in order to give information on protein function. It is a widely used platform to assign functions to genes in any species. The overall data generation process consists of family clustering using the reference proteome set maintained by UniProt, followed by phylogenetic tree building creating masked sequence alignments using MAFFT and GIGA programs (Katoh et al. 2002, Thomas 2010) and finally annotation of tree nodes. The gene attributes annotated in Panther for enriched proteins after gastrin treatment are protein class and biological function. In both melanoma cell lines overrepresentation analysis revealed adhesion (cell-cell adhesion, cell-matrix adhesion) as the main biological function of classically secreted proteins upregulated by gastrin. In terms of protein class, gastrin regulated proteins were characterised as metalloprotease inhibitors in case of G361 and complementary to that as proteases in Skmel-2 cells (Fig. 6.3A). Interestingly in the latter type of melanoma “receptor and extracellular matrix linker protein” were the highest represented protein classes which mostly accounts for the overexpression of CD166, also known as activated leukocyte cell adhesion molecule (ALCAM). CD166 is a transmembrane glycoprotein member of the immunoglobulin superfamily and is known to be associated with melanoma progression and metastasis formation (Donizy et al. 2015). ALCAM is reported to play role in the conversion of pro-MMP-2 into an active form through an

intermediate ternary complex MT1-MMP/TIMP-2/pro–MMP-2 at the cell surface (Lunter et al. 2005). These data suggest that gastrin might cause cancer progression through affecting extracellular matrix degradation by inhibiting TIMP-3 expression or upregulating MMP-2 synthesis directly or indirectly through ALCAM. Our findings also provide a deeper understanding of the mechanism involved in the regulation of ALCAM expression on gene level, which is yet poorly described.

Results from pathway analysis were validated by adhesion assays. Gastrin treatment for 45 min significantly increased the number of adherent cells in both cells lines in a dose dependent way (control vs. 10nM G17; student t test; $p = 0.025$ and 0.019 in Skmel-2 and G316 respectively) (Fig. 6.3B).

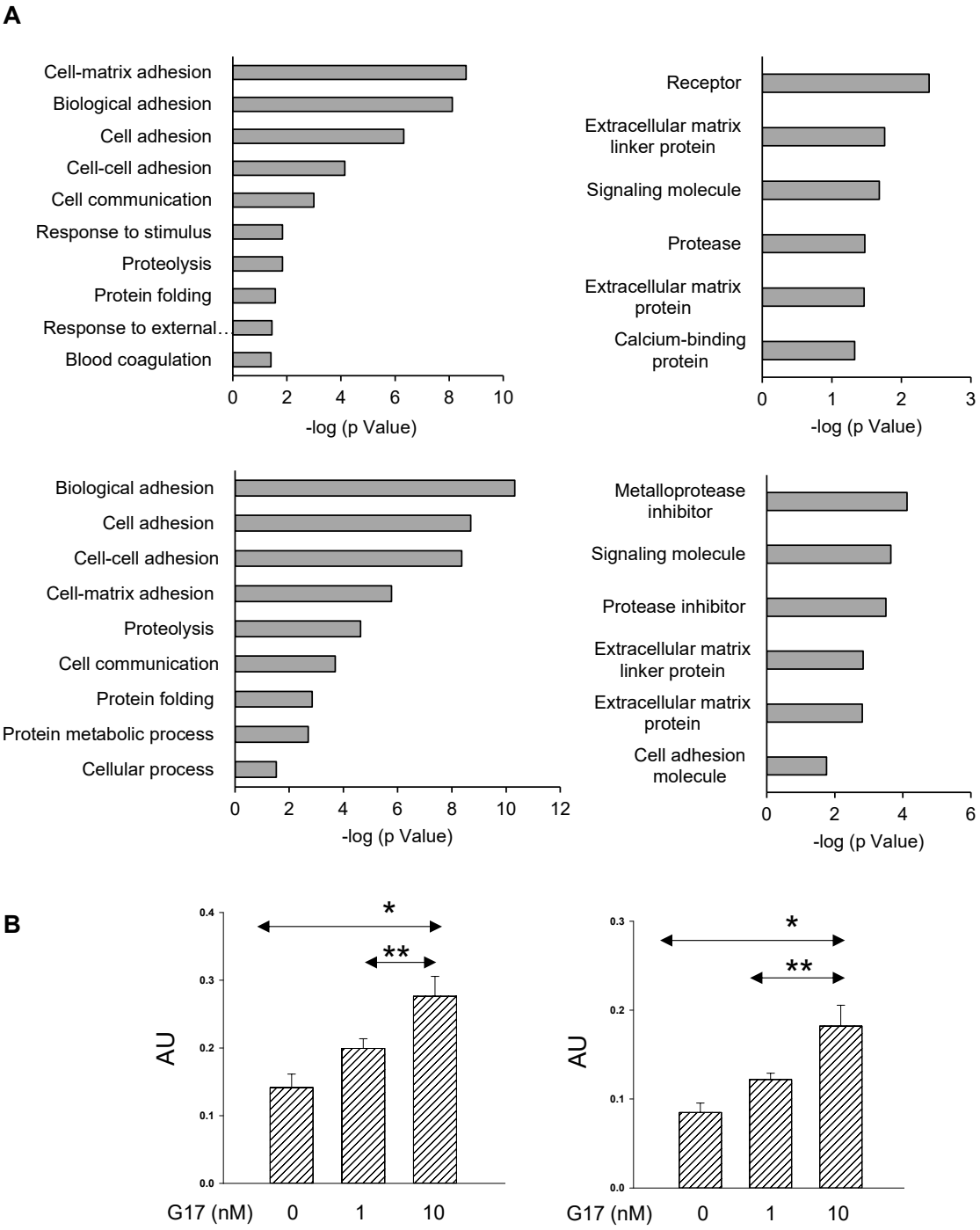

Figure 6.3. Functional analysis and associated pathways of gastrin regulated proteins. (A) Pathway analysis of melanoma secretome revealed cell adhesion as the main biological function of classically secreted proteins. Protease and metalloprotease inhibitor were identified as major protein classes in Skmel-2 and G361 respectively (upper panel Skmel-2, lower panel G361). (B) Adhesion assay confirms pathway data. Gastrin stimulation significantly increases cancer cell adhesion in both melanoma lines (left Skmel-2, right G361).

6.3.3 Chemotactic assays with MMP-2 siRNA transfected melanoma cultures reveal absence of migration and invasion after gastrin stimulation

To investigate the functional significance of proteomic data, we used siRNA to knock down MMP-2 expression in Skmel-2 melanoma cells. After successful transfection validated by western blot (densitometry analysis after silencing was 0.48 expressed relative to controls) melanoma monolayers on Boyden inserts and Matrigel coated bio-membranes were treated with gastrin for 24 h (Fig. 6.4A). The stimulatory effect of gastrin on cell migration was significantly impaired in the absence of MMP-2 (control treated *vs*. MMP-2 knock down: one-way ANOVA; $p < 0.05$) (Figure 6.4B). Nonetheless even with significantly reduced MMP-2 production gastrin still managed to stimulate migration compared to untreated controls (control *vs* knock down; one-way ANOVA; $p < 0.05$). This effect is most likely mediated through a number of paracrine signalling cascades similar to what has already been described with epithelial cells or gastric myofibroblasts (namely IGF system, IL-8 or prostaglandins) (Noble et al. 2003, Hemers et al. 2005, Varga et al. 2017). The invading capability of melanoma cells was more severely impaired by reduced MMP-2, but the stimulatory effect of gastrin was still present compared to controls (gastrin treated *vs* MMP-2 knock down; One-Way ANOVA; $p < 0.05$, MMP-2 knock down control vs. treated; One-Way ANOVA; $p < 0.05$) (Fig. 6.4C).

In G361 melanoma cells, where secretome analysis revealed reduced TIMP-3 secretion as a result of gastrin treatment substitution of this metalloproteinase inhibitor successfully reduced the number of migrating cells compared to controls (TIMP-3 + G17 vs. G17; One-Way ANOVA; $p < 0.05$) (Fig. 6.4D). This inhibitory effect was more robust when melanoma cells had to digest themselves through a collagen matrix with invasion almost reduced to basal levels (TIMP-3 + G17 vs G17; One-Way ANOVA; $p < 0.05$) (Fig. 6.4E).

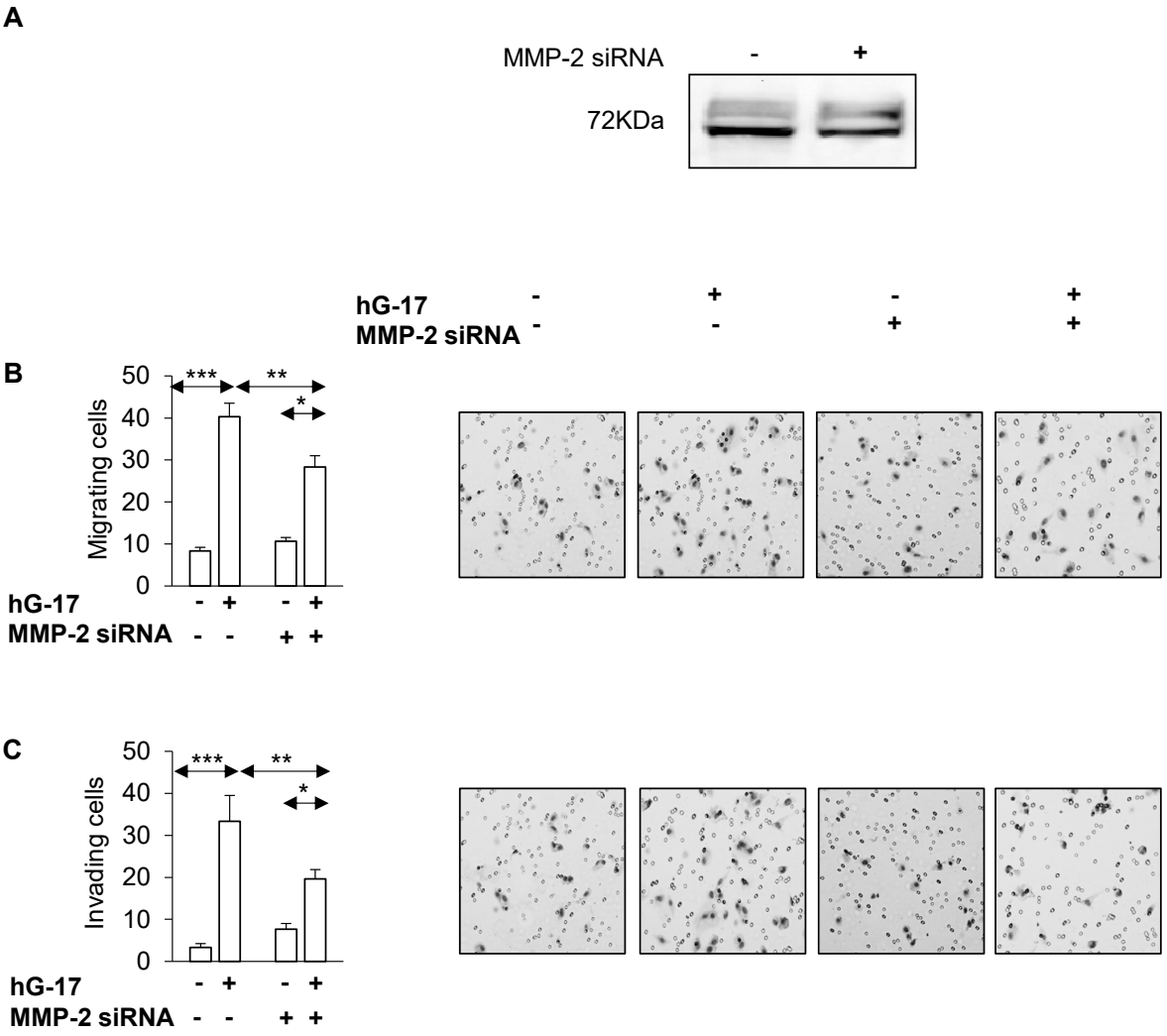

Figure 6.4. Chemotactic assays with MMP-2 siRNA transfected melanoma cultures reveal absence of migration and invasion after gastrin stimulation. (A) Western blot validated successful transfection of MMP-2 siRNA. (B) Gastrin stimulated melanoma migration was severely impaired after MMP-2 silencing. (C) Similar results were achieved with Matrigel coated membranes used to investigate cancer cell invasion.

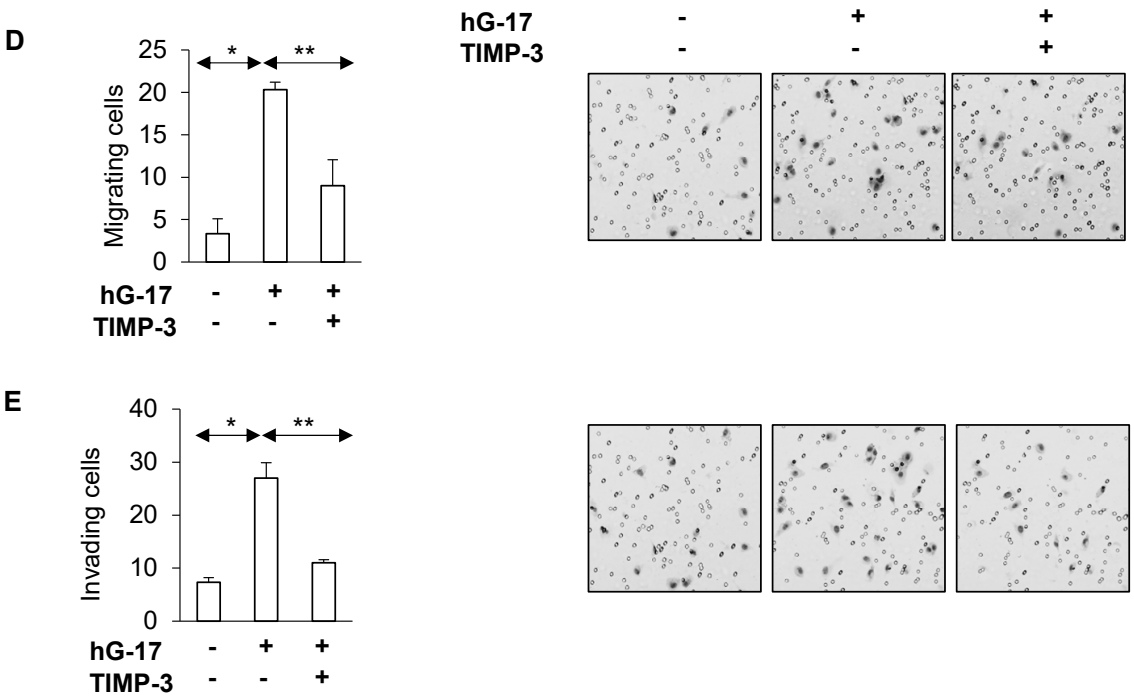

Figure 6.4. (D) TMIP-3 supplementation in media of G361 melanoma cells reduced the effect of gastrin on cancer cell migration. (E) A stronger inhibition was observable when chemotactic trigger was sustained in a collagen rich environment mimicking ECM, thus lack of functioning proteases severely impaired cancer cell movement.

6.3.4 Detection of MMP-2 and TIMP-3 in serum samples of melanoma and basal cell carcinoma patients

Serum collected from the same group of patients used for gastrin RIA analysis was also measured for MMP-2 and TIMP-3 concentrations with ELISA. It is well known that metalloproteases play an important role in the progression of several malignancies and also facilitate lymph node involvement. They are mainly involved in ECM degradation, but are also responsible for regulating a variety of chemokines (i.e. TNF, EGF, VEGF, FGF) (Fang et al. 2000, Hua et al. 2011). Measuring serum concentration might therefore provide a possible diagnostic tool which has already been proven successful in the case of oral squamous cell carcinoma, laryngeal SCC, Wilson's disease or breast cancer to name a few (Somiari et al. 2006, Cheng et al. 2015, Lotfi et al. 2015, Lotfi et al. 2015). Investigating MMP-2 serum concentrations in skin cancer showed no difference between patients with basal cell cancer or melanoma (227 ± 8 vs. 240 ± 17 in MM and BCC respectively) (Fig. 6.5A). There was also no correlation with tumour thickness and overall disease progression (230 ± 11 vs. 226 ± 12 in Stage I and II respectively). MMP-2 concentrations were in the range between 200-250 ng/ml which is the reported range for control, healthy individuals. Similar observations were made with TIMP-3. There was no difference between the two patient cohorts (14 ± 1 vs. 17 ± 4 in MM and BCC respectively) (Fig. 6.5A). Advanced melanoma stage did not influence serum TIMP-3 concentration (15 ± 2 vs. 14 ± 2 in Stage I and II respectively). For breakdown into different subcategories based on gastrin profile, *H.pylori* status, and ASI consumption see supplement (Figure S5-8).

In spite of these findings, the potential use of MMP-2 and TIMP-3 as biomarkers should, however, not be rejected immediately. A number of studies provide evidence, that increased local expression of MMP-2 identified by immunohistochemistry, gelatin zymography or RT-PCR can be associated with advanced melanoma stage, decreased survival and formation of distant metastasis (Vaisanen et al. 2008, Candrea et al. 2014, Kamyab-Hesari et al. 2014). This is not only true for different melanoma types, but was also confirmed for non-melanoma skin cancers, most commonly represented by basal cell cancer (Candrea et al. 2014, de Oliveira Poswar et al. 2015). We performed immunohistochemistry for MMP-2 and TIMP-3 on randomly selected histology samples from melanoma and basal cell cancer patients. Both in the case of MM and BCCs there was a distinct positive staining mainly localised to the tumour stroma (Fig. 6.5B). Although there are studies which report TIMP-3 expression to be decreased with melanoma progression, we were not able to detect TIMP-3 either in MM or in BCC (Das et al. 2016). (For antibody validation with prostate cancer samples see supplement Figure S11).

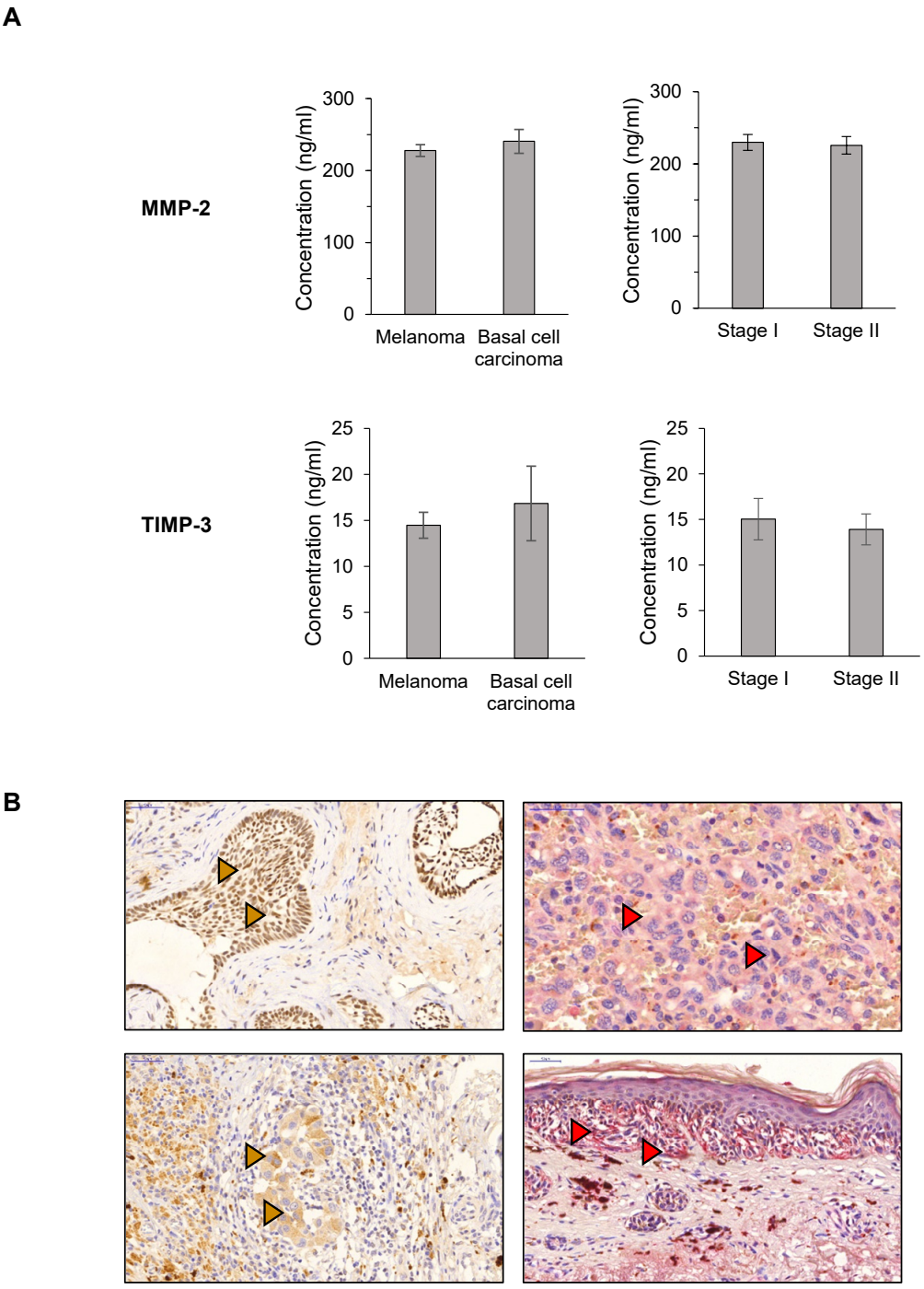

Figure 6.5. Detection of MMP-2 and TIMP-3 in serum samples of melanoma and basal cell carcinoma patients. (A) Serum MMP-2 (upper panel) and TIMP-3 (lower panel) measured in MM and BSC patients reveal no correlation between melanoma progressing and circulating metalloproteinase or complementary inhibitor concentrations. (B) Low and high power immunohistochemistry images of basal cell cancer (upper panel) and melanoma (lower panel) samples stained for MMP-2. Right side double labelled for MMP-2 (red) and TIMP-3 (brown) also. Arrows indicate positive cells (scale bar 50 μm).

6.4 Discussion

Previous experimental data suggested that gastrin is capable of influencing melanoma cell migration and invasion through CCK2R (see chapter 5). To have a better understanding of the possible protein mediators and mechanisms involved, conditioned media were collected for proteomic analysis to identify changes in the secretome relevant to gastrin.

Proteomic studies usually apply methods for secretome profiling where classically secreted proteins are defined by short signal peptide sequences located at the N-terminus using computational tools i.e. SignalP, SecretomeP or Phobius (Petersen et al. 2011). One disadvantage of single time point labelling is that beside actual secretory protein hits results are often "contaminated" with intracellular proteins due to cellular death and or membrane leakage (Brown et al. 2012). Hammond et al. reported a technique based on the faster turnover of secretory proteins when defining labelling periods (Hammond et al. 2018). This method utilises the kinetic differences in turnover between proteins that are destined for secretion as opposed to those which are sequestrated intracellularly and by this approach we were able to identify around hundred (65 and 93 in Skmel-2 and G361 respectively) classically secreted target proteins, which were up or downregulated in response to gastrin.

Protein hits were uploaded to Panther to assign biological functions. Protein ANalysis THrough Evolutionary Relationships (PANTHER) v. 11 is a comprehensive database containing protein-coding gene families from 104

sequenced genomes, which allows users to assign biological function and protein classes to an otherwise uncharacterised proteomic data set (Mi et al. 2013, Mi et al. 2017). One major weakness of this software - and other similar ones - is, that it uses a pre-set database of protein functions (including Gene Ontology and biological pathways) based on those listed genes structured into phylogenetic “trees” when predicting functions of uncharacterized genes. This therefore prohibits identification of novel functions for investigated proteins when relying solely on algorithm-based inferences, which should be noted when interpreting these results.

Proteomic analysis revealed increased secretion of metalloproteinases after gastrin stimulation of melanoma cultures. Data for MMP-2 and TIMP-3 was validated by Western blot and ELISA. Proteases play an important role in ECM remodelling (Hua et al. 2011). Through digestion of ECM components cancer cells can more easily migrate and invade vascular structures. From an oncological aspect MMPs are mainly involved in allowing local tumour expansion and formation of distant metastases. Novel roles of metal-dependent proteinases in regulating immunity (lymphocyte maturation, clonal expansion) and inflammation through clipping and shedding of chemokines, cytokines and growth factors have recently been described (Hojilla et al. 2008, Murphy et al. 2008). Overall these findings highlight the importance of MMPs in tumorigenesis and confirm a more complex function than previously recognised.

MMPs consist of a family with more than 20 members, out of which MMP-2 expression was identified in the melanoma secretome. Interestingly in one of the two investigated melanoma cell lines TIMP-2 (1 and 3 to a lesser extent) secretion was reduced affecting the proteolytic axis of MMPs, ADAMs and TIMPs similarly. Nonetheless there were secretome proteins (i.e. glia derived nexin), which remained unchanged and were not influenced by gastrin in either melanoma cell line.

MMP-2 and -9 are broadly investigated in human cancer (Somiari et al. 2006, Hojilla et al. 2008, Cheng et al. 2015). Both gelatinases participate in the breakdown of basement membrane, which provides a morphological barrier that restricts cells to the epithelial layer, thus preventing invasion of deeper structures. (Somiari et al. 2006).

Studies with metastatic melanoma cell lines identified MMP-2 expression in two of the most aggressive forms (MV3, BLM) of the investigated eight melanoma lines (Hofmann et al. 1999). In xenograft models MMP-2 expression showed a close relation with tumour growth (Hofmann et al. 1999). Retrospective immunohistochemical analysis of human melanocytic lesions revealed the presence of active MMP-2 in a majority of samples and was found to be an independent prognostic factor alongside Ki67 or p53 (Vaisanen et al. 2008, Vaisanen et al. 2011, Candrea et al. 2014). Some authors provide evidence linking MMP-9 expression and lymph node metastasis (Candrea et al. 2014), while others report the absence of this subtype of zinc-dependent endopeptidase in invading melanomas (van den Oord et al. 1997). We found

no trace of MMP-9 expression in the secretome of Skmel-2 and G361 melanoma lines, however there was an increased expression of MMP-2 in response to gastrin. A clinical correlation study with melanoma patients confirmed the presence of active MMP-2 in biopsy samples of primary lesions. This raises the possibility that gastrin might provoke melanoma progression through regulating MMP-2 expression.

The role of TIMPs as tumour suppressors in different malignancies is well established (Lambert et al. 2004, Hilska et al. 2007). With the inhibition of metalloproteases they reduce ECM turnover and neoangiogenesis therefore influencing the systemic dissemination of cancer cells (Fassina et al. 2000, Lambert et al. 2004). A number of studies report decreased TIMP-3 expression in pigmented neoplastic skin lesions that acquire an invasive phenotype (Das et al. 2016). We were not able to detect and correlate TIMP-3 expression with different melanoma stages using immunohistochemistry of patient samples, however proteomic analysis of G361 melanoma secretome revealed a decrease in the amount of secreted TIMP-3 after gastrin stimulation.

There have been suggestions that epigenetic changes i.e. promoter hypermethylation might be responsible for TIMP-3 inhibition in different tumours, however this does not seem to be the case for melanomas (Bachman et al. 1999, Hu et al. 2006). Some authors have proposed posttranscriptional modification through miRNAs (Martin del Campo et al. 2015). Whichever way gastrin might influence TIMP-3 expression remains to be investigated further.

Transfection with siRNA to inhibit the expression of MMP-2 resulted in significantly reduced invasion and migration of melanoma cells. Gastrin however still managed to stimulate cancer cell migration and to a lesser extent invasion compared to controls. This might be due to the fact that the efficacy of transfection did not reach 100% and - as described previously in chapter 3 and 5 - gastrin might liberate growth factors (IL-8, IGF-1-2) simultaneously, which activate alternative paracrine pathways. This nonetheless raises the potential of possible targets for cancer therapy. The inhibition of MMPs have been widely studied over the last decade. There have been different strategies and approaches including the development of synthetic, antibody-based or transcription blocking inhibitors as well as stimulation of endogenous antagonists (Hua et al. 2011). Broad spectrum synthetic inhibitors (i.e. Batimastat, Marimastat), which contain a zinc-binding group (hydroxamate) initially showed interesting results in preclinical studies. Lymph node metastasis was reduced in an oral squamous cell carcinoma (Maekawa et al. 2002). Gastric tumours in mice model also showed signs of regression upon treatment with Marimastat (Kimata et al. 2002). Unfortunately, clinical trials failed to confirm superior efficacy compared to other chemotherapeutic agents in pancreatic, gastric or ovarian carcinoma (Steward et al. 2000). To reduce unnecessary side-effects of targeting the whole MMP spectrum selective MMP specific anticancer inhibitors were developed. Prinomastat, which is a non-peptide inhibitor of MMPs-2, -9 and MT1-MMP significantly reduced the growth of uveal melanoma in xenograft model (Ozerdem et al. 2002). A thiirane based MMP-2 inhibitor, ND-322, effectively reduced in vitro migration, invasion and growth of melanoma cells (Marusak et al. 2016). Despite the promising results

with these novel selective MMP inhibitors in preclinical studies, only little clinical evidence is available and further research is clearly needed before considering the administration of these agents either in monotherapy or in combination with chemotherapy in patients with advanced stage melanoma.

Manipulating endogenous MMP inhibitors might also provide an alternative way to regulate MMP expression and thereby reduce dissemination of tumour cells. Currently micro RNAs are gaining recognition as regulators of gene expression. miR-21 has been found to inhibit RECK and TIMP-3 expression in various tumours (Volinia et al. 2006). Targeting certain micro RNAs might increase TIMP-3 expression and inhibit MMPs. We had similar results upon TIMP-3 supplementation in melanoma cultures.

Having a better understanding of how gastrin increases melanoma dissemination through metalloproteinases provides a tool that can be used both in adjuvant and neoadjuvant therapy. Although most of the potential anticancer drugs are still under development, recognising that melanomas also belong to the group of tumours where MMP-2 plays a major role adds another dimension to their possible applications.

Serum measurement of MMP-2 concentration has been widely used as a diagnostic and prognostic biomarker in a number of different tumours and other pathologies (i.e. breast cancer, laryngeal squamous cell carcinoma, Wilson's disease, etc.) (Somiari et al. 2006, Cheng et al. 2015, Lotfi et al. 2015). In our melanoma patient cohort serum concentrations of MMP-2 showed no correlation with disease progression and were mostly in the

reference range. Similar observations were made with TIMP-3. Despite the fact that both can be rejected as a serum biomarker, histological studies (as previously detailed) in accordance with our data support the addition of MMP-2 to the panel of markers used for routine immunohistochemistry for the diagnosis of melanoma since strong positivity supports an aggressive behaviour and higher risk of metastasis formation.

In summary, proteomic analysis of gastrin-treated melanoma cell secretomes revealed that the stimulatory effect of the antral hormone resulted in dysregulation of the protease-inhibitor axis responsible for ECM degradation by upregulating MMP-2 and downregulating TIMP-3 expression.

6.5 Conclusions

1. Proteomic analysis of melanoma secretomes revealed upregulation of MMP-2 and downregulation of TIMP-3 after gastrin treatment.
2. Pathway analysis of protein hits confirmed adhesion as a biological function of gastrin-regulated, classically secreted proteins.
3. Inhibition of MMP-2 secretion with siRNA and substitution of TIMP-3 resulted in reduced invasion and migration of melanoma cancer cells.
4. Serum concentrations of MMP-2 and TIMP-3 in melanoma and basal cell cancer patients showed no correlation with disease progression.
5. Immunohistochemical studies of melanoma tissue samples revealed MMP-2 expression, however TIMP-3 remained undetectable.

Chapter 7

Final discussion

7.1 Overview

This research was centred towards investigating the role of CCK2 receptors expressed by gastrointestinal myofibroblasts and human melanoma cells. The main findings of the thesis include: a) CCK2Rs are exhibited by a proportion of myofibroblasts ranging from 1 to 6%; b) cancer associated myofibroblasts have a higher prevalence of CCK2R expression; c) increased cytosolic calcium confirmed a functional receptor, which is temporarily present on the cells surface in S phase of the cell cycle; d) CCK2Rs on myofibroblasts are likely to be involved in gastrin regulated migration and cell invasion rather than proliferation; immunostaining of human melanoma samples revealed CCK2 expression of melanoma cell and melanocytes to a lesser extent; e) elevated serum gastrin concentration strongly correlates with advanced melanoma stage; f) primary cultures of melanoma cells (Skmel-2, G361), dermal fibroblasts and TGF-β transformed myofibroblasts also exhibit CCK2R expression; g) gastrin does not affect melanoma cell proliferation, but increases invasion and migration *in vitro*; h) stromal cells (gastric CAMs, MSCs, dermal fibroblasts) stimulate cancer growth independently of gastrin in spheroid model; i) gastrin increases melanoma cell invasion in the presence of stromal cells in an organotypic model; j) proteomic analysis of the gastrin stimulated melanoma secretome revealed upregulation of MMP-2 and downregulation of TIMP-3; k) inhibition of MMP-2 and substitution of TIMP-3 reduced invasion and migration of melanoma cells *in vitro*; l) alterations in serum concertation of MMP-2 and TIMP-3 showed no relation with disease progression, however MMP-2 remained detectable in all melanoma samples.

7.1.1 CCK2R expression by myofibroblasts

CCK2Rs were first described almost 40 years ago initially isolated from the brain (Saito et al. 1980). The main sites of expression in the gut include ECL, parietal and smooth muscle cells (Dockray 2004). Wound healing rodent models revealed *de novo* CCK2R expression in the mucosa and submucosa of repairing cryoulcers in the stomach. Many of these cells were found to be myofibroblasts based on coexpression of vimentin and smooth muscle α-actin (Schmassmann et al. 2000, Ashurst et al. 2008). Systematic screening of the GI tract revealed CCK2Rs expression in 1-6% of myofibroblasts. Expression was related to the proliferative activity of cells, since myofibroblasts from the tumour stoma (CAMs) exhibited higher levels compared to tumour adjacent and normal tissue derived ones (NTMs) (Holmberg et al. 2012). EdU labelling provided direct evidence of a cell cycle, specifically S phase associated transient receptor expression.

CCK2Rs belong to the G-protein coupled seven-transmembrane domain receptor family (Dufresne et al. 2006). Calcium detection after gastrin stimulation revealed a functional receptor present on myofibroblast. GPCR agonists are known to have a mitogenic effect through the release of different growth factors and cytokines (i.e. IGF, EGF etc.) (Varro et al. 2002). The trophic and modulatory effect of gastrin on cell migration and invasion via multiple paracrine pathways and direct CCK2R activation is well described with gastric glandular epithelial cells (Noble et al. 2003, Kumar et al. 2015).

There is little evidence, however, available on the role of CCKRs expressed by myofibroblasts. Although gastrin did not significantly influence overall cell

proliferation it did indeed increase the number of mitotic cells (with spindle structures and fragmented nuclei) suggesting an acceleratory effect on the cell cycle similar to that observed with chemokine receptors CXCR3 and GPR19 (Romagnani et al. 2001, Kastner et al. 2012). Furthermore, gastrin was found to stimulate migration and invasion of gastric myofibroblasts through CCK2Rs in chemotactic assays. Interestingly gastrin also stimulated migration of myofibroblasts that did not express independently of CCK2R and increased transcript abundance of IGF-2. These data suggest that gastrin not only has a direct effect on myofibroblasts but it is also capable of liberating paracrine acting factors i.e. IGF-2 and others, which need to be further characterised. Overall it looks like CCK2Rs expressed by myofibroblasts are mainly involved in tissue organisation and remodelling conducted by complex epithelial-mesenchymal interactions.

It is well known that myofibroblasts contribute to epithelial restitution and tissue regeneration through paracrine acting growth factors (i.e. HGFs, KGFs and CXCL12) of which their receptors are expressed by epithelial cells (Powell et al. 1999, Smith et al. 2005). Contrary to that, myofibroblast activation through epithelial derived TGF- β has also been described where increased αSMA and MMP expression related to changes in contractibility and matrix restoration respectively were observed in wound healing (Powell et al. 1999, Pender et al. 2004). Another site where epithelial-mesenchymal interaction is important became the centre of attention when the concept of the tumour microenvironment was introduced and neoplasias were no longer considered as a group of malignantly transformed cells that acquired limitless replicative

capacity but rather lesions that influence and alter their microenvironment to achieve self-sufficiency and evade apoptosis (Hanahan et al. 2000). Research in this area indicates that myofibroblast activation and recruitment plays an important role in cancer progression. As to whether these CAMs originate from transdifferentiated fibroblasts, IGF I-II/EGF/PDGF induced proliferation or circulating mesenchymal stem cells is still under debate (Elenbaas et al. 2001, Bhowmick et al. 2004, Brittan et al. 2004).

The role of CCK2Rs in epithelial-mesenchymal interaction in the gut is still not yet fully understood, however as stated before it is likely to be involved in defining the position of myofibroblasts once they exit S-phase of the cells cycle thereby contributing to tissue remodelling both in regenerative processes and also by allowing the assembly of a tumour microenvironment. Taken together this provides a novel dimension to understanding how gastrin might control gastric mucosal architecture both in health and disease.

7.1.2 CCK2R expression by melanoma cells

There is growing interest in the role of CCK2Rs in tissue regeneration and wound healing. As discussed earlier (in section 7.1.1) myofibroblasts can now be also listed among the known targets and key players of gastrin regulated epithelial restitution (Varga et al. 2017). In addition to these, there is ongoing intense research investigating CCK2Rs in cancer and precancerous conditions. Most of this work has been focused on gastrointestinal tumours, where the receptor was found to be involved in determining the tumour microenvironment (Hanahan et al. 2011, Quail et al. 2013). Data from the Human Protein Atlas provided preliminary evidence of a possible CCK2R expression by human melanoma cells . Given our previous observation with gastric and dermal myofibroblasts we decided to further investigate this relation.

Immunostaining of melanoma samples showed heterogeneous but nonetheless consistent CCK2R expression. A limitation of this study was that melanoma specimens were not assessed for alternative splice variants of the CCK2R, which would be worth studying in the future (Hellmich et al. 2000, Körner et al. 2010). Nonetheless dermal myofibroblasts, fibroblasts, melanoma cells and melanocytes to a lesser extent exhibited CCK2R expression. The latter raises the possibility that outside the CNS, there is another neural-derived cell population which expresses the gastrin receptor.

When fasting serum gastrin concentrations of melanoma patients were correlated with tumour thickness, there was a clear tendency indicating higher gastrin concentrations in advanced melanoma stages. *H.pylori* infection (which is a known risk of gastric cancer development) and long term acid inhibitor consumption were identified as main causes of moderate hypergastrinaemia observed in the investigated cohort. The percentage of patients with chronic hypergastrinaemia due to the aforementioned reasons were in the same range as reported by the literature (Krashias et al. 2013, Helgadottir et al. 2014). These data highlight the fact that overutilization of acid secretion inhibitors and asymptomatic *H.pylori* carriers represent a patient group with increased risk for melanoma progression. To have a better understanding how gastrin might control melanoma behaviour we used primary melanoma cultures (SKmel-2 and G361).

In vitro studies confirmed a functional CCK2R expression. The effect of gastrin on cancer progression has been in focus of gastrin related research in the last decade. CCK2Rs are reported to be expressed in a number of malignant conditions (i.e. pancreatic adenocarcinoma, medullary thyroid cancer, astrocytomas, etc.) (Goetze et al. 2000, Koh et al. 2004, Roy et al. 2016) however there is lack of data with skin tumours. The effect of gastrin on cancer progression is mainly associated with proliferation, adhesion and apoptosis through stimulation of Ras/Raf/MEK/ERK, JNK and p38-MAPK signalling pathways (Dehez et al. 2001, Dufresne et al. 2006).

A key step in melanoma progression is systemic dissemination of melanoma cells through invading lymphovascular structures in the vertical growth phase. CCK2R activation was shown to result in internalisation of β-catenins allowing epithelial cell detachment in non-tumorigenic models (Bierkamp et al. 2002). The involvement of integrins (namely β_3 integrin subunit of the $\alpha_v\beta_3$ vitronectin receptor) have also been identified to play role in vertical growth of melanoma (Sturm et al. 2002), which raises the possibility that gastrin might influence expression of adhesion molecules indirectly.

Although most available data indicates that gastrin is a direct growth factor of the gastric mucosa increasing evidence suggests that it also stimulates proliferation of cells absent the receptor via liberation of paracrine acting cytokines (Dockray et al. 2001, Varro et al. 2002). Melanoma cells did not respond to gastrin stimulation either in monocultures or spheroid like tumour aggregates embedded in a ECM mimicking collagen gel. Therefore, it seems unlikely that gastrin drives the growth of melanomas directly.

Interestingly however, when co-cultured with stromal cells (dermal myofibroblasts and MSCs) rapid tumour expansion was visible. This observation furthermore highlights the importance of the cancer milieu and cross communication between epithelial and mesenchymal structures. Cancer associated fibroblasts, myofibroblasts and macrophages (CAFs, CAMs and TAMs respectively) have emerged as key players sustaining a pro-tumorigenic environment (Joyce et al. 2009, Biswas et al. 2010). The association between CAMs and lymph node involvement in gastric cancer has also been described

(see Chapter 3). Increased tumour mass in these cases suggest a paracrine activation from the tumour stroma through factors such as FGF, HB-EGF, TGF-b and IGFII although the mediators and pathways involved are far not yet fully characterised.

On the other hand, there was a clear stimulatory effect of gastrin on cell migration and invasion in chemotactic assays using Boyden chambers and *in vitro* organoids; the latter is a frequently applied model in melanoma research (Hill et al. 2015). Altogether these data suggest that gastrin stimulates invasion and migration of melanoma cells both directly and indirectly through CCK2R expressed by cancer and stromal cells with several putative paracrine factors involved.

To identify proteins involved in gastrin mediated rapid ECM degradation leading to increased metastasising capacity of melanoma cells proteomic analysis was performed on conditioned media to define the melanoma secretome.

Gastrin relevant protein hits revealed upregulation of matrix metalloproteinase 2 and downregulation of tissue inhibitor of metalloprotease 3 expression. With the help of bioinformatics algorithms (PANTHER) pathway analysis confirmed adhesion as main biological function of classically secreted proteins related to gastrin stimulation, which was further validated by adhesion assays. MMPs have been broadly investigated in cancer as key elements responsible for ECM remodelling thereby allowing local tumour expansion and intravasation of cancer cells (Hojilla et al. 2008, Hua et al. 2011). Furthermore,

overexpression of MMP-2 (which is an important gelatinases responsible for the degradation of basement membranes) was identified in several aggressive melanoma cell lines (Hofmann et al. 1999, Hofmann et al. 2000). Some authors report a relation between MMPs and disease specific survival while others showed correlation with lymph node metastasis suggesting a prognostic value (Vaisanen et al. 2011, Candrea et al. 2014). We found no association between serum MMP-2 concertation and melanoma progression, even though immunostaining revealed an extensive presence of active MMP-2 in nearly all biopsy samples. Although we would be inclined not to proposed MMP-2 as a serum biomarker, the local expression pattern without doubt adds useful information on prognosis and in particular the aggressiveness of a melanoma. Inhibition of TIMP-3 via epigenetic changes or posttranslational modifications is also reported in a number of malignant conditions including pigmented skin lesions however we did not detect changes of TIMP-3 on a tissue level (Hu et al. 2006, Martin del Campo et al. 2015, Das et al. 2016).

Knock down of MMP-2 expression with siRNA and substitution of TIMP-3 resulted in reduced invasion and migration of melanoma cells. Overall proteomic and functional data suggests that gastrin might influence melanoma progression through interfering in the protease / inhibitor axis stimulating ECM degradation and increasing dissemination of cancer cells.

In conclusion melanoma can be added to the group of tumours known to express the CCK2 receptor. Gastrin can now be proposed to promote melanoma progression and metastasis through liberation of proteases and

growth factors directly and indirectly through stromal cells. Patients with hypergastrinaemia due to different reasons should therefore be considered as a high risk group for melanoma progression.

7.2 Future prospects

Gastrin is known to regulate a number of genes, which are involved in proliferation (i.e. c-Fos, c-Jun, c-Myc, cyclins D1, D3 and E), cell invasion (i.e. PAI-3, MMPs) or apoptosis (i.e. COX-2) (Zhukova et al. 2001, Varro et al. 2002, Wroblewski et al. 2002, Colucci et al. 2005). Whether there are other target genes through which gastrin is capable of influencing melanoma progression remains to be investigated. Moreover, the picture is further complicated since surrounding stromal cells (including dermal fibroblasts, myofibroblasts) also express CCK2R allowing gastrin to exert a paracrine effect. Nonetheless understanding signalling pathways and regulatory mechanisms provides an opportunity for targeted intervention. The potential use of CCK2R antagonists as anti-secretory drugs or in the treatment of CCK2R expressing tumours are currently under investigation (Dockray 2004). As up to date there is no commercially available licenced CCK2R antagonist mainly due to issues regarding their oral bioavailability, potency and selectivity towards the CCK2 receptor. However, promising results are available with Netazapide and Z-360 in the treatment of NETs and pancreatic tumours respectively (Meyer et al. 2010, Fossmark et al. 2012). Other indications for clinical research of CCK2R antagonists include Barrett's oesophagus, gastrointestinal stromal tumours and gastric adenocarcinoma (Boyce et al. 2016). It is now worth considering the addition of malignant melanoma among the aforementioned instances. Similar considerations apply to MMP inhibitors. They have been widely studied in pancreatic, gastric and ovarian carcinomas (Steward et al. 2000, Kimata et al. 2002). There is encouraging data available

on selective MMP-2 and 9 inhibitors in reducing uveal melanoma growth, which is alongside with our observation on the role of metalloproteinases in the migration and invasion of melanoma cells (Ozerdem et al. 2002, Marusak et al. 2016). The possible use of MMP inhibitors as part of combination target therapy is therefore also worth considering.

Last but not least the potential use of CCK2 receptor targeting for diagnostic purposes (i.e. immunoscintigraphy) has been investigated in medullary thyroid cancer (Behr et al. 2002, Gotthardt et al. 2006). In transit and satellite metastases of cutaneous melanomas are fortunately in most of the cases visible with dermatoscope, however CCK2R binding of radio labelled ligands might be helpful in the deferential diagnosis of internal lesions suspect for metastasis.

The previously mentioned points only represent a fraction of potential research areas and clinical fields where recent work on CCK2R described in this thesis could be successfully applied. Finally in this context it is worth stressing that the patients involved in the present study are now under surveillance and data from long term follow up will hopefully allow a deeper insight in how gastrin influences melanoma progression.

References

"http://www.cbs.dtu.dk/services/SignalP/."

"http://www.pantherdb.org/."

"https://www.proteinatlas.org/ENSG00000110148-CCKBR/pathology."

(1992). "Diagnosis and treatment of early melanoma. NIH Consensus Development Conference. January 27-29, 1992." Consens Statement **10**(1): 1-25.

(2007). "The association of use of sunbeds with cutaneous malignant melanoma and other skin cancers: A systematic review." Int J Cancer **120**(5): 1116-1122.

Airola, K., T. Karonen, M. Vaalamo, K. Lehti, J. Lohi, A. L. Kariniemi, J. Keski-Oja and U. K. Saarialho-Kere (1999). "Expression of collagenases-1 and -3 and their inhibitors TIMP-1 and -3 correlates with the level of invasion in malignant melanomas." Br J Cancer **80**(5-6): 733-743.

Akkerman, N. and L. H. Defize (2017). "Dawn of the organoid era: 3D tissue and organ cultures revolutionize the study of development, disease, and regeneration." Bioessays **39**(4).

Ashcroft, F. J., A. Varro, R. Dimaline and G. J. Dockray (2004). "Control of expression of the lectin-like protein Reg-1 by gastrin: role of the Rho family GTPase RhoA and a C-rich promoter element." Biochem J **381**(Pt 2): 397-403.

Ashurst, H. L., A. Varro and R. Dimaline (2008). "Regulation of mammalian gastrin/CCK receptor (CCK2R) expression in vitro and in vivo." Exp.Physiol **93**(2): 223-236.

Axon, A. T. (1995). "Review article: is Helicobacter pylori transmitted by the gastro-oral route?" Aliment Pharmacol Ther **9**(6): 585-588.

Bachman, K. E., J. G. Herman, P. G. Corn, A. Merlo, J. F. Costello, W. K. Cavenee, S. B. Baylin and J. R. Graff (1999). "Methylation-associated silencing of the tissue inhibitor of metalloproteinase-3 gene suggest a suppressor role in kidney, brain, and other human cancers." Cancer Res **59**(4): 798-802.

Baker, M. (2015). "Reproducibility crisis: Blame it on the antibodies." Nature **521**(7552): 274-276.

Balabanova, S., C. Holmberg, I. Steele, B. Ebrahimi, L. Rainbow, T. Burdyga, C. McCaig, L. Tiszlavicz, N. Lertkowit, O. T. Giger, S. Oliver, I. Prior, R. Dimaline, D. Simpson, R. Beynon, P. Hegyi, T. C. Wang, G. J. Dockray and A. Varro (2014). "The neuroendocrine phenotype of gastric myofibroblasts and its loss with cancer progression." Carcinogenesis **35**(8): 1798-1806.

Balch, C. M., J. E. Gershenwald, S. J. Soong, J. F. Thompson, M. B. Atkins, D. R. Byrd, A. C. Buzaid, A. J. Cochran, D. G. Coit, S. Ding, A. M. Eggermont, K. T. Flaherty, P. A. Gimotty, J. M. Kirkwood, K. M. McMasters, M. C. Mihm, Jr., D. L. Morton, M. I. Ross, A. J. Sober and V. K. Sondak (2009). "Final version of 2009 AJCC melanoma staging and classification." J Clin Oncol **27**(36): 6199-6206.

Balch, C. M., T. M. Murad, S. J. Soong, A. L. Ingalls, P. C. Richards and W. A. Maddox (1979). "Tumor thickness as a guide to surgical management of clinical stage I melanoma patients." Cancer **43**(3): 883-888.

Balch, C. M., S. J. Soong, T. Smith, M. I. Ross, M. M. Urist, C. P. Karakousis, W. J. Temple, M. C. Mihm, R. L. Barnhill, W. R. Jewell, H. J. Wanebo and R. Desmond (2001). "Long-term results of a prospective surgical trial comparing 2 cm vs. 4 cm excision margins for 740 patients with 1-4 mm melanomas." Ann Surg Oncol **8**(2): 101-108.

Bashford, J. N., J. Norwood and S. R. Chapman (1998). "Why are patients prescribed proton pump inhibitors? Retrospective analysis of link between morbidity and prescribing in the General Practice Research Database." Bmj **317**(7156): 452-456.

Behr, T. M. and M. P. Behe (2002). "Cholecystokinin-B/Gastrin receptor-targeting peptides for staging and therapy of medullary thyroid cancer and other cholecystokinin-B receptor-expressing malignancies." Semin Nucl Med **32**(2): 97-109.

Berglund, L., E. Bjorling, P. Oksvold, L. Fagerberg, A. Asplund, C. A. Szigyarto, A. Persson, J. Ottosson, H. Wernerus, P. Nilsson, E. Lundberg, A. Sivertsson, S. Navani, K. Wester, C. Kampf, S. Hober, F. Ponten

and M. Uhlen (2008). "A genecentric Human Protein Atlas for expression profiles based on antibodies." Mol Cell Proteomics **7**(10): 2019-2027.

Bevona, C., W. Goggins, T. Quinn, J. Fullerton and H. Tsao (2003). "Cutaneous melanomas associated with nevi." Arch Dermatol **139**(12): 1620-1624; discussion 1624.

Bhowmick, N. A., E. G. Neilson and H. L. Moses (2004). "Stromal fibroblasts in cancer initiation and progression." Nature **432**(7015): 332-337.

Bichakjian, C. K., A. C. Halpern, T. M. Johnson, A. Foote Hood, J. M. Grichnik, S. M. Swetter, H. Tsao, V. H. Barbosa, T. Y. Chuang, M. Duvic, V. C. Ho, A. J. Sober, K. R. Beutner, R. Bhushan and W. Smith Begolka (2011). "Guidelines of care for the management of primary cutaneous melanoma. American Academy of Dermatology." J Am Acad Dermatol **65**(5): 1032-1047.

Bierkamp, C., A. Kowalski-Chauvel, S. Dehez, D. Fourmy, L. Pradayrol and C. Seva (2002). "Gastrin mediated cholecystokinin-2 receptor activation induces loss of cell adhesion and scattering in epithelial MDCK cells." Oncogene **21**(50): 7656-7670.

Biswas, S. K. and A. Mantovani (2010). "Macrophage plasticity and interaction with lymphocyte subsets: cancer as a paradigm." Nat Immunol **11**(10): 889-896.

Black, J. W., W. A. Duncan, C. J. Durant, C. R. Ganellin and E. M. Parsons (1972). "Definition and antagonism of histamine H 2 -receptors." Nature **236**(5347): 385-390.

Blair, E. L., J. R. Greenwell, E. R. Grund, J. D. Reed and D. J. Sanders (1975). "Gastrin response to meals of different composition in normal subjects." Gut **16**(10): 766-773.

Blanchard, T. G. and S. J. Czinn (1998). "Review article: Immunological determinants that may affect the Helicobacter pylori cancer risk." Aliment Pharmacol Ther **12 Suppl 1**: 83-90.

Bleehen, N. M., E. S. Newlands, S. M. Lee, N. Thatcher, P. Selby, A. H. Calvert, G. J. Rustin, M. Brampton and M. F. Stevens (1995). "Cancer Research Campaign phase II trial of temozolomide in metastatic melanoma." J Clin Oncol **13**(4): 910-913.

Blumberg, B. S., B. J. Gerstley, D. A. Hungerford, W. T. London and A. I. Sutnick (1967). "A serum antigen (Australia antigen) in Down's syndrome, leukemia, and hepatitis." Ann Intern Med **66**(5): 924-931.

Boccaccio, C. and P. M. Comoglio (2006). "Invasive growth: a MET-driven genetic programme for cancer and stem cells." Nat Rev Cancer **6**(8): 637-645.

Bogenrieder, T. and M. Herlyn (2002). "Cell-surface proteolysis, growth factor activation and intercellular communication in the progression of melanoma." Crit Rev Oncol Hematol **44**(1): 1-15.

Bordi, C., T. D'Adda, C. Azzoni and G. Ferraro (1998). "Pathogenesis of ECL cell tumors in humans." Yale J Biol Med **71**(3-4): 273-284.

Bordi, C., T. D'Adda, C. Azzoni, F. P. Pilato and P. Caruana (1995). "Hypergastrinemia and gastric enterochromaffin-like cells." Am J Surg Pathol **19 Suppl 1**: S8-19.

Boyce, M., K. A. Lloyd and D. M. Pritchard (2016). "Potential clinical indications for a CCK2 receptor antagonist." Curr Opin Pharmacol **31**: 68-75.

Boyce, M., A. R. Moore, L. Sagatun, B. N. Parsons, A. Varro, F. Campbell, R. Fossmark, H. L. Waldum and D. M. Pritchard (2016). "Netazepide, a gastrin/CCK2 receptor antagonist, can eradicate gastric neuroendocrine tumours in patients with autoimmune chronic atrophic gastritis." Br J Clin Pharmacol.

Brittan, M. and N. A. Wright (2004). "Stem cell in gastrointestinal structure and neoplastic development." Gut **53**(6): 899-910.

Brown, K. J., C. A. Formolo, H. Seol, R. L. Marathi, S. Duguez, E. An, D. Pillai, J. Nazarian, B. R. Rood and Y. Hathout (2012). "Advances in the proteomic investigation of the cell secretome." Expert Rev Proteomics **9**(3): 337-345.

Callahan, M. K., C. R. Flaherty and M. A. Postow (2016). "Checkpoint Blockade for the Treatment of Advanced Melanoma." Cancer Treat Res **167**: 231-250.

Campos, R. V., A. M. Buchan, R. M. Meloche, R. A. Pederson, Y. N. Kwok and D. H. Coy (1990). "Gastrin secretion from human antral G cells in culture." Gastroenterology **99**(1): 36-44.

Candrea, E., S. Senila, C. Tatomir and R. Cosgarea (2014). "Active and inactive forms of matrix metalloproteinases 2 and 9 in cutaneous melanoma." Int J Dermatol **53**(5): 575-580.

Carmeliet, P. and R. K. Jain (2000). "Angiogenesis in cancer and other diseases." Nature **407**(6801): 249-257.

Carvelli, L., Y. Libin and C. R. Morales (2015). "Prosaposin: a protein with differential sorting and multiple functions." Histol Histopathol **30**(6): 647-660.

Castellano, M., P. M. Pollock, M. K. Walters, L. E. Sparrow, L. M. Down, B. G. Gabrielli, P. G. Parsons and N. K. Hayward (1997). "CDKN2A/p16 is inactivated in most melanoma cell lines." Cancer Res **57**(21): 4868-4875.

Cave, D. R. (1996). "Transmission and epidemiology of Helicobacter pylori." Am J Med **100**(5a): 12S-17S; discussion 17S-18S.

Chambers, A. F., A. C. Groom and I. C. MacDonald (2002). "Dissemination and growth of cancer cells in metastatic sites." Nat Rev Cancer **2**(8): 563-572.

Chan, A. O., J. Z. Peng, S. K. Lam, K. C. Lai, M. F. Yuen, H. K. Cheung, Y. L. Kwong, A. Rashid, C. K. Chan and B. C. Wong (2006). "Eradication of Helicobacter pylori infection reverses E-cadherin promoter hypermethylation." Gut **55**(4): 463-468.

Chappell, W. H., L. S. Steelman, J. M. Long, R. C. Kempf, S. L. Abrams, R. A. Franklin, J. Basecke, F. Stivala, M. Donia, P. Fagone, G. Malaponte, M. C. Mazzarino, F. Nicoletti, M. Libra, D. Maksimovic-Ivanic, S. Mijatovic, G. Montalto, M. Cervello, P. Laidler, M. Milella, A. Tafuri, A. Bonati, C. Evangelisti, L. Cocco, A. M. Martelli and J. A. McCubrey (2011). "Ras/Raf/MEK/ERK and PI3K/PTEN/Akt/mTOR inhibitors: rationale and importance to inhibiting these pathways in human health." Oncotarget **2**(3): 135-164.

Charles, A. C., J. E. Merrill, E. R. Dirksen and M. J. Sanderson (1991). "Intercellular signaling in glial cells: calcium waves and oscillations in response to mechanical stimulation and glutamate." Neuron **6**(6): 983-992.

Cheng, N., H. Wang, J. Dong, S. Pan, X. Wang, Y. Han, Y. Han and R. Yang (2015). "Elevated serum brain natriuretic peptide and matrix metalloproteinases 2 and 9 in Wilson's disease." Metab Brain Dis **30**(4): 1087-1091.

Ciccotosto, G. D., A. McLeish, K. J. Hardy and A. Shulkes (1995). "Expression, processing, and secretion of gastrin in patients with colorectal carcinoma." Gastroenterology **109**(4): 1142-1153.

Clark, E. A., T. R. Golub, E. S. Lander and R. O. Hynes (2000). "Genomic analysis of metastasis reveals an essential role for RhoC." Nature **406**(6795): 532-535.

Clark, I. M., T. E. Swingler, C. L. Sampieri and D. R. Edwards (2008). "The regulation of matrix metalloproteinases and their inhibitors." Int J Biochem Cell Biol **40**(6-7): 1362-1378.

Clarke, P. A., J. H. Dickson, J. C. Harris, A. Grabowska and S. A. Watson (2006). "Gastrin enhances the angiogenic potential of endothelial cells via modulation of heparin-binding epidermal-like growth factor." Cancer Res **66**(7): 3504-3512.

Clevers, H. (2016). "Modeling Development and Disease with Organoids." Cell **165**(7): 1586-1597.

Coit, D. G., J. A. Thompson, M. R. Albertini, C. Barker, W. E. Carson, C. Contreras, G. A. Daniels, D. DiMaio, R. C. Fields, M. D. Fleming, M. Freeman, A. Galan, B. Gastman, V. Guild, D. Johnson, R. W. Joseph, J. R. Lange, S. Nath, A. J. Olszanski, P. Ott, A. P. Gupta, M. I. Ross, A. K. Salama, J. Skitzki, J. Sosman, S. M. Swetter, K. K. Tanabe, E. Wuthrick, N. R. McMillian and A. M. Engh (2019). "Cutaneous Melanoma, Version 2.2019, NCCN Clinical Practice Guidelines in Oncology." J Natl Compr Canc Netw **17**(4): 367-402.

Colucci, R., C. Blandizzi, M. Tanini, C. Vassalle, M. C. Breschi and M. Del Tacca (2005). "Gastrin promotes human colon cancer cell growth via CCK-2 receptor-mediated cyclooxygenase-2 induction and prostaglandin E2 production." Br J Pharmacol **144**(3): 338-348.

Correa, P. and M. B. Piazuelo (2012). "The gastric precancerous cascade." J Dig Dis **13**(1): 2-9.

Cox, J. and M. Mann (2008). "MaxQuant enables high peptide identification rates, individualized p.p.b.-range mass accuracies and proteome-wide protein quantification." Nat Biotechnol **26**(12): 1367-1372.

Crosby, T., R. Fish, B. Coles and M. D. Mason (2000). "Systemic treatments for metastatic cutaneous melanoma." Cochrane Database Syst Rev(2): Cd001215.

Czepan, M., Z. Rakonczay, Jr., A. Varro, I. Steele, R. Dimaline, N. Lertkowit, J. Lonovics, A. Schnur, G. Biczo, A. Geisz, G. Lazar, Z. Simonka, V. Venglovecz, T. Wittmann and P. Hegyi (2012). "NHE1 activity contributes to migration and is necessary for proliferation of human gastric myofibroblasts." Pflugers Arch **463**(3): 459-475.

Dacha, S., M. Razvi, J. Massaad, Q. Cai and M. Wehbi (2015). "Hypergastrinemia." Gastroenterol Rep (Oxf) **3**(3): 201-208.

Dang, D., J. R. Bamburg and D. M. Ramos (2006). "Alphavbeta3 integrin and cofilin modulate K1735 melanoma cell invasion." Exp Cell Res **312**(4): 468-477.

Das, A. M., M. Bolkestein, T. van der Klok, C. M. Oude Ophuis, C. E. Vermeulen, J. A. Rens, W. N. Dinjens, P. N. Atmodimedjo, C. Verhoef, S. Koljenovic, R. Smits, T. L. Ten Hagen and A. M. Eggermont (2016). "Tissue inhibitor of metalloproteinase-3 (TIMP3) expression decreases during melanoma progression and inhibits melanoma cell migration." Eur J Cancer **66**: 34-46.

Das, A. M., S. Koljenovic, C. M. Oude Ophuis, T. van der Klok, B. Galjart, A. L. Nigg, W. A. van Cappellen, V. Noordhoek Hegt, W. N. Dinjens, P. N. Atmodimedjo, C. E. Vermeulen, C. Verhoef, A. M. Eggermont and T. L. ten Hagen (2016). "Association of TIMP3 expression with vessel density, macrophage infiltration and prognosis in human malignant melanoma." Eur J Cancer **53**: 135-143.

Daulhac, L., A. Kowalski-Chauvel, L. Pradayrol, N. Vaysse and C. Seva (1997). "Ca2+ and protein kinase C-dependent mechanisms involved in gastrin-induced Shc/Grb2 complex formation and P44-mitogen-activated protein kinase activation." Biochem J **325 (Pt 2)**: 383-389.

Davar, D., A. A. Tarhini and J. M. Kirkwood (2012). "Adjuvant therapy for melanoma." Cancer J **18**(2): 192-202.

Davies, H., G. R. Bignell, C. Cox, P. Stephens, S. Edkins, S. Clegg, J. Teague, H. Woffendin, M. J. Garnett, W. Bottomley, N. Davis, E. Dicks, R. Ewing, Y. Floyd, K. Gray, S. Hall, R. Hawes, J. Hughes, V. Kosmidou, A. Menzies, C. Mould, A. Parker, C. Stevens, S. Watt, S. Hooper, R. Wilson, H. Jayatilake, B. A. Gusterson, C. Cooper, J. Shipley, D. Hargrave, K. Pritchard-Jones, N. Maitland, G. Chenevix-Trench, G. J. Riggins, D. D. Bigner, G. Palmieri, A. Cossu, A. Flanagan, A. Nicholson, J. W. Ho, S. Y. Leung, S. T. Yuen, B. L. Weber, H. F. Seigler, T. L. Darrow, H. Paterson, R. Marais, C. J. Marshall, R. Wooster, M. R. Stratton and P. A. Futreal (2002). "Mutations of the BRAF gene in human cancer." Nature **417**(6892): 949-954.

de Oliveira Poswar, F., C. A. de Carvalho Fraga, E. S. Gomes, L. C. Farias, L. W. Souza, S. H. Santos, R. S. Gomez, A. M. de-Paula and A. L. Guimaraes (2015). "Protein expression of MMP-2 and MT1-MMP in actinic keratosis, squamous cell carcinoma of the skin, and basal cell carcinoma." Int J Surg Pathol **23**(1): 20-25.

De Wever, O., P. Demetter, M. Mareel and M. Bracke (2008). "Stromal myofibroblasts are drivers of invasive cancer growth." Int.J.Cancer **123**(10): 2229-2238.

Dehez, S., C. Bierkamp, A. Kowalski-Chauvel, L. Daulhac, C. Escrieut, C. Susini, L. Pradayrol, D. Fourmy and C. Seva (2002). "c-Jun NH(2)-terminal kinase pathway in growth-promoting effect of the G protein-coupled receptor cholecystokinin B receptor: a protein kinase C/Src-dependent-mechanism." Cell Growth Differ **13**(8): 375-385.

Dehez, S., L. Daulhac, A. Kowalski-Chauvel, D. Fourmy, L. Pradayrol and C. Seva (2001). "Gastrin-induced DNA synthesis requires p38-MAPK activation via PKC/Ca(2+) and Src-dependent mechanisms." FEBS Lett **496**(1): 25-30.

Desmouliere, A., C. Guyot and G. Gabbiani (2004). "The stroma reaction myofibroblast: a key player in the control of tumor cell behavior." Int.J.Dev.Biol. **48**(5-6): 509-517.

Dessinioti, C., C. Antoniou, A. Katsambas and A. J. Stratigos (2011). "Melanocortin 1 receptor variants: functional role and pigmentary associations." Photochem Photobiol **87**(5): 978-987.

Devy, L., L. Huang, L. Naa, N. Yanamandra, H. Pieters, N. Frans, E. Chang, Q. Tao, M. Vanhove, A. Lejeune, R. van Gool, D. J. Sexton, G. Kuang, D. Rank, S. Hogan, C. Pazmany, Y. L. Ma, S. Schoonbroodt, A. E. Nixon, R. C. Ladner, R. Hoet, P. Henderikx, C. Tenhoor, S. A. Rabbani, M. L. Valentino, C. R. Wood and D. T. Dransfield (2009). "Selective inhibition of matrix metalloproteinase-14 blocks tumor growth, invasion, and angiogenesis." Cancer Res **69**(4): 1517-1526.

Diamandopoulos, G. T. (1996). "Cancer: an historical perspective." Anticancer Res **16**(4a): 1595-1602.

Dicken, B. J., D. L. Bigam, C. Cass, J. R. Mackey, A. A. Joy and S. M. Hamilton (2005). "Gastric adenocarcinoma: review and considerations for future directions." Ann Surg **241**(1): 27-39.

Dimaline, R. and J. Struthers (1996). "Expression and regulation of a vesicular monoamine transporter in rat stomach: a putative histamine transporter." J Physiol **490 (Pt 1)**: 249-256.

Ding, L., G. Getz, D. A. Wheeler, E. R. Mardis, M. D. McLellan, K. Cibulskis, C. Sougnez, H. Greulich, D. M. Muzny, M. B. Morgan, L. Fulton, R. S. Fulton, Q. Zhang, M. C. Wendl, M. S. Lawrence, D. E. Larson, K. Chen, D. J. Dooling, A. Sabo, A. C. Hawes, H. Shen, S. N. Jhangiani, L. R. Lewis, O. Hall, Y. Zhu, T. Mathew, Y. Ren, J. Yao, S. E. Scherer, K. Clerc, G. A. Metcalf, B. Ng, A. Milosavljevic, M. L. Gonzalez-Garay, J. R. Osborne, R. Meyer, X. Shi, Y. Tang, D. C. Koboldt, L. Lin, R. Abbott, T. L. Miner, C. Pohl, G. Fewell, C. Haipek, H. Schmidt, B. H. Dunford-Shore, A. Kraja, S. D. Crosby, C. S. Sawyer, T. Vickery, S. Sander, J. Robinson, W. Winckler, J. Baldwin, L. R. Chirieac, A. Dutt, T. Fennell, M. Hanna, B. E. Johnson, R. C. Onofrio, R. K. Thomas, G. Tonon, B. A. Weir, X. Zhao, L. Ziaugra, M. C. Zody, T. Giordano, M. B. Orringer, J. A. Roth, M. R. Spitz, Wistuba, II, B. Ozenberger, P. J. Good, A. C. Chang, D. G. Beer, M. A. Watson, M. Ladanyi, S. Broderick, A. Yoshizawa, W. D. Travis, W. Pao, M. A. Province, G. M. Weinstock, H. E. Varmus, S. B. Gabriel, E. S. Lander, R. A. Gibbs, M. Meyerson and R. K. Wilson (2008). "Somatic mutations affect key pathways in lung adenocarcinoma." Nature **455**(7216): 1069-1075.

Dixon, M. F., R. M. Genta, J. H. Yardley and P. Correa (1996). "Classification and grading of gastritis. The updated Sydney System. International Workshop on the Histopathology of Gastritis, Houston 1994." Am J Surg Pathol **20**(10): 1161-1181.

Dockray, G., R. Dimaline and A. Varro (2005). "Gastrin: old hormone, new functions." Pflugers Arch **449**(4): 344-355.

Dockray, G. J. (1999). "Topical review. Gastrin and gastric epithelial physiology." J Physiol **518 (Pt 2)**: 315-324.

Dockray, G. J. (2004). "Clinical endocrinology and metabolism. Gastrin." Best.Pract.Res.Clin.Endocrinol.Metab **18**(4): 555-568.

Dockray, G. J., C. Hamer, D. Evans, A. Varro and R. Dimaline (1991). "The secretory kinetics of the G cell in omeprazole-treated rats." Gastroenterology **100**(5 Pt 1): 1187-1194.

Dockray, G. J., A. Moore, A. Varro and D. M. Pritchard (2012). "Gastrin receptor pharmacology." Curr Gastroenterol Rep **14**(6): 453-459.

Dockray, G. J., A. Varro and R. Dimaline (1996). "Gastric endocrine cells: gene expression, processing, and targeting of active products." Physiol Rev **76**(3): 767-798.

Dockray, G. J., A. Varro, R. Dimaline and T. Wang (2001). "The gastrins: their production and biological activities." Annu Rev Physiol **63**: 119-139.

Dockray, G. J. and J. H. Walsh (1975). "Amino terminal gastrin fragment in serum of Zollinger-Ellison syndrome patients." Gastroenterology **68**(2): 222-230.

Dockray, G. J., J. H. Walsh and E. Passaro, Jr. (1975). "Relative abundance of big and little gastrins in the tumours and blood of patients with the Zollinger Ellison syndrome." Gut **16**(5): 353-358.

Donizy, P., M. Zietek, A. Halon, M. Leskiewicz, C. Kozyra and R. Matkowski (2015). "Prognostic significance of ALCAM (CD166/MEMD) expression in cutaneous melanoma patients." Diagn Pathol **10**: 86.

Dossett, L. A., R. R. Kudchadkar and J. S. Zager (2015). "BRAF and MEK inhibition in melanoma." Expert Opin Drug Saf **14**(4): 559-570.

Dubois, R. N., S. B. Abramson, L. Crofford, R. A. Gupta, L. S. Simon, L. B. Van De Putte and P. E. Lipsky (1998). "Cyclooxygenase in biology and disease." Faseb j **12**(12): 1063-1073.

Dufresne, M., C. Seva and D. Fourmy (2006). "Cholecystokinin and gastrin receptors." Physiol Rev **86**(3): 805-847.

Duncan, L. M. (2009). "The classification of cutaneous melanoma." Hematol Oncol Clin North Am **23**(3): 501-513, ix.

Dvorak, H. F. (1986). "Tumors: wounds that do not heal. Similarities between tumor stroma generation and wound healing." N Engl J Med **315**(26): 1650-1659.

Edkins, J. S. (1906). "The chemical mechanism of gastric secretion." J Physiol **34**(1-2): 133-144.

Elenbaas, B. and R. A. Weinberg (2001). "Heterotypic signaling between epithelial tumor cells and fibroblasts in carcinoma formation." Exp Cell Res **264**(1): 169-184.

Elwood, J. M. and J. Jopson (1997). "Melanoma and sun exposure: an overview of published studies." Int J Cancer **73**(2): 198-203.

Epstein, M. A., G. Henle, B. G. Achong and Y. M. Barr (1965). "MORPHOLOGICAL AND BIOLOGICAL STUDIES ON A VIRUS IN CULTURED LYMPHOBLASTS FROM BURKITT'S LYMPHOMA." J Exp Med **121**: 761-770.

Eusebi, L. H., R. M. Zagari and F. Bazzoli (2014). "Epidemiology of Helicobacter pylori infection." Helicobacter **19 Suppl 1**: 1-5.

Fang, J., Y. Shing, D. Wiederschain, L. Yan, C. Butterfield, G. Jackson, J. Harper, G. Tamvakopoulos and M. A. Moses (2000). "Matrix metalloproteinase-2 is required for the switch to the angiogenic phenotype in a tumor model." Proc Natl Acad Sci U S A **97**(8): 3884-3889.

Fassina, G., N. Ferrari, C. Brigati, R. Benelli, L. Santi, D. M. Noonan and A. Albini (2000). "Tissue inhibitors of metalloproteases: regulation and biological activities." Clin Exp Metastasis **18**(2): 111-120.

Fatehullah, A., S. H. Tan and N. Barker (2016). "Organoids as an in vitro model of human development and disease." Nat Cell Biol **18**(3): 246-254.

Fedorenko, I. V., G. T. Gibney and K. S. Smalley (2013). "NRAS mutant melanoma: biological behavior and future strategies for therapeutic management." Oncogene **32**(25): 3009-3018.

Ferlay, J., I. Soerjomataram, R. Dikshit, S. Eser, C. Mathers, M. Rebelo, D. M. Parkin, D. Forman and F. Bray (2015). "Cancer incidence and mortality worldwide: sources, methods and major patterns in GLOBOCAN 2012." Int J Cancer **136**(5): E359-386.

Ferrand, A., A. Kowalski-Chauvel, C. Bertrand, C. Escrieut, A. Mathieu, G. Portolan, L. Pradayrol, D. Fourmy, M. Dufresne and C. Seva (2005). "A novel mechanism for JAK2 activation by a G protein-coupled receptor, the CCK2R: implication of this signaling pathway in pancreatic tumor models." J Biol Chem **280**(11): 10710-10715.

Ferrand, A., A. Kowalski-Chauvel, C. Bertrand, L. Pradayrol, D. Fourmy, M. Dufresne and C. Seva (2004). "Involvement of JAK2 upstream of the PI 3-kinase in cell-cell adhesion regulation by gastrin." Exp Cell Res **301**(2): 128-138.

Ferrand, A. and T. C. Wang (2006). "Gastrin and cancer: a review." Cancer Lett **238**(1): 15-29.

Fink, T., P. Lund, L. Pilgaard, J. G. Rasmussen, M. Duroux and V. Zachar (2008). "Instability of standard PCR reference genes in adipose-derived stem cells during propagation, differentiation and hypoxic exposure." BMC Mol Biol **9**: 98.

Forsea, A. M., V. Del Marmol, A. Stratigos and A. C. Geller (2014). "Melanoma prognosis in Europe: far from equal." Br J Dermatol **171**(1): 179-182.

Fossmark, R., O. Sordal, C. S. Jianu, G. Qvigstad, I. S. Nordrum, M. Boyce and H. L. Waldum (2012). "Treatment of gastric carcinoids type 1 with the gastrin receptor antagonist netazepide (YF476) results in regression of tumours and normalisation of serum chromogranin A." Aliment Pharmacol Ther **36**(11-12): 1067-1075.

Freeman, G. J., A. J. Long, Y. Iwai, K. Bourque, T. Chernova, H. Nishimura, L. J. Fitz, N. Malenkovich, T. Okazaki, M. C. Byrne, H. F. Horton, L. Fouser, L. Carter, V. Ling, M. R. Bowman, B. M. Carreno, M. Collins, C. R. Wood and T. Honjo (2000). "Engagement of the PD-1 immunoinhibitory receptor by a novel B7 family member leads to negative regulation of lymphocyte activation." J Exp Med **192**(7): 1027-1034.

Fritsch, C., E. A. Swietlicki, O. Lefebvre, M. Kedinger, H. Iordanov, M. S. Levin and D. C. Rubin (2002). "Epimorphin expression in intestinal myofibroblasts induces epithelial morphogenesis." J Clin Invest **110**(11): 1629-1641.

Fukata, Y., M. Amano and K. Kaibuchi (2001). "Rho-Rho-kinase pathway in smooth muscle contraction and cytoskeletal reorganization of non-muscle cells." Trends Pharmacol Sci **22**(1): 32-39.

Gaggioli, C. and E. Sahai (2007). "Melanoma invasion – current knowledge and future directions." Pigment Cell Research **20**(3): 161-172.

Gandini, S., F. Sera, M. S. Cattaruzza, P. Pasquini, D. Abeni, P. Boyle and C. F. Melchi (2005). "Meta-analysis of risk factors for cutaneous melanoma: I. Common and atypical naevi." Eur J Cancer **41**(1): 28-44.

Gershenwald, J., R. Scolyer and K. Hess (2017). "Melanoma of the Skin. In: AJCC Cancer Staging Manual: Eighth Edition, Amin MB (Ed), American Joint Committee on Cancer.".

Gershenwald, J. E., M. I. Colome, J. E. Lee, P. F. Mansfield, C. Tseng, J. J. Lee, C. M. Balch and M. I. Ross (1998). "Patterns of recurrence following a negative sentinel lymph node biopsy in 243 patients with stage I or II melanoma." J Clin Oncol **16**(6): 2253-2260.

Gibril, F., M. Schumann, A. Pace and R. T. Jensen (2004). "Multiple endocrine neoplasia type 1 and Zollinger-Ellison syndrome: a prospective study of 107 cases and comparison with 1009 cases from the literature." Medicine (Baltimore) **83**(1): 43-83.

Gillies, R. J., N. Didier and M. Denton (1986). "Determination of cell number in monolayer cultures." Anal Biochem **159**(1): 109-113.

Goerge, T., A. Barg, E. M. Schnaeker, B. Poppelmann, V. Shpacovitch, A. Rattenholl, C. Maaser, T. A. Luger, M. Steinhoff and S. W. Schneider (2006). "Tumor-derived matrix metalloproteinase-1 targets endothelial proteinase-activated receptor 1 promoting endothelial cell activation." Cancer Res **66**(15): 7766-7774.

Goetze, J. P., S. Eiland, L. B. Svendsen, B. Vainer, J. Hannibal and J. F. Rehfeld (2013). "Characterization of gastrins and their receptor in solid human gastric adenocarcinomas." Scand J Gastroenterol **48**(6): 688-695.

Goetze, J. P., F. C. Nielsen, F. Burcharth and J. F. Rehfeld (2000). "Closing the gastrin loop in pancreatic carcinoma: coexpression of gastrin and its receptor in solid human pancreatic adenocarcinoma." Cancer **88**(11): 2487-2494.

Goldstein, A. M. and M. A. Tucker (2001). "Genetic epidemiology of cutaneous melanoma: a global perspective." Arch Dermatol **137**(11): 1493-1496.

Gotthardt, M., M. P. Behe, J. Grass, A. Bauhofer, A. Rinke, M. L. Schipper, M. Kalinowski, R. Arnold, W. J. Oyen and T. M. Behr (2006). "Added value of gastrin receptor scintigraphy in comparison to

somatostatin receptor scintigraphy in patients with carcinoids and other neuroendocrine tumours." Endocr Relat Cancer **13**(4): 1203-1211.

Greenberg, G. R., B. Chan, T. J. McDonald and J. Alleyne (1985). "The role of vagal integrity in gastrin releasing peptide stimulated gastroenteropancreatic hormone release and gastric acid secretion." Regul Pept **10**(2-3): 179-187.

Gregory, R. A. and H. J. Tracy (1964). "THE CONSTITUTION AND PROPERTIES OF TWO GASTRINS EXTRACTED FROM HOG ANTRAL MUCOSA." Gut **5**: 103-114.

Grotendorst, G. R., H. Rahmanie and M. R. Duncan (2004). "Combinatorial signaling pathways determine fibroblast proliferation and myofibroblast differentiation." Faseb j **18**(3): 469-479.

Guo, Y. S., J. Z. Cheng, G. F. Jin, J. S. Gutkind, M. R. Hellmich and C. M. Townsend, Jr. (2002). "Gastrin stimulates cyclooxygenase-2 expression in intestinal epithelial cells through multiple signaling pathways. Evidence for involvement of ERK5 kinase and transactivation of the epidermal growth factor receptor." J Biol Chem **277**(50): 48755-48763.

Haastrup, P. F., W. Thompson, J. Sondergaard and D. E. Jarbol (2018). "Side Effects of Long-Term Proton Pump Inhibitor Use: A Review." Basic Clin Pharmacol Toxicol **123**(2): 114-121.

Haigh, C. R., S. E. Attwood, D. G. Thompson, J. A. Jankowski, C. M. Kirton, D. M. Pritchard, A. Varro and R. Dimaline (2003). "Gastrin induces proliferation in Barrett's metaplasia through activation of the CCK2 receptor." Gastroenterology **124**(3): 615-625.

Haigh, C. R., S. E. Attwood, D. G. Thompson, J. A. Jankowski, C. M. Kirton, D. M. Pritchard, A. Varro and R. Dimaline (2003). "Gastrin induces proliferation in Barrett's metaplasia through activation of the CCK2 receptor." Gastroenterology **124**(3): 615-625.

Hakanson, R., J. Oscarson and F. Sundler (1986). "Gastrin and the trophic control of gastric mucosa." Scand J Gastroenterol Suppl **118**: 18-30.

Hammond, D. E., J. D. Kumar, L. Raymond, D. M. Simpson, R. J. Beynon, G. J. Dockray and A. Varro (2018). "Stable Isotope Dynamic Labeling of Secretomes (SIDLS) Identifies Authentic Secretory Proteins Released by Cancer and Stromal Cells." Molecular & Cellular Proteomics **17**(9): 1837-1849.

Hanahan, D. and R. A. Weinberg (2000). "The hallmarks of cancer." Cell **100**(1): 57-70.

Hanahan, D. and R. A. Weinberg (2011). "Hallmarks of cancer: the next generation." Cell **144**(5): 646-674.

Handolias, D., R. Salemi, W. Murray, A. Tan, W. Liu, A. Viros, A. Dobrovic, J. Kelly and G. A. McArthur (2010). "Mutations in KIT occur at low frequency in melanomas arising from anatomical sites associated with chronic and intermittent sun exposure." Pigment Cell Melanoma Res **23**(2): 210-215.

Harootunian, A. T., J. P. Kao, S. Paranjape and R. Y. Tsien (1991). "Generation of calcium oscillations in fibroblasts by positive feedback between calcium and IP3." Science **251**(4989): 75-78.

Hauschild, A., J. J. Grob, L. V. Demidov, T. Jouary, R. Gutzmer, M. Millward, P. Rutkowski, C. U. Blank, W. H. Miller, Jr., E. Kaempgen, S. Martin-Algarra, B. Karaszewska, C. Mauch, V. Chiarion-Sileni, A. M. Martin, S. Swann, P. Haney, B. Mirakhur, M. E. Guckert, V. Goodman and P. B. Chapman (2012). "Dabrafenib in BRAF-mutated metastatic melanoma: a multicentre, open-label, phase 3 randomised controlled trial." Lancet **380**(9839): 358-365.

Hayakawa, Y., W. Chang, G. Jin and T. C. Wang (2016). "Gastrin and upper GI cancers." Curr Opin Pharmacol **31**: 31-37.

Heidelbaugh, J. J., K. L. Goldberg and J. M. Inadomi (2010). "Magnitude and economic effect of overuse of antisecretory therapy in the ambulatory care setting." Am J Manag Care **16**(9): e228-234.

Heidelbaugh, J. J., A. H. Kim, R. Chang and P. C. Walker (2012). "Overutilization of proton-pump inhibitors: what the clinician needs to know." Therap Adv Gastroenterol **5**(4): 219-232.

Helgadottir, H., D. C. Metz, Y. X. Yang, A. D. Rhim and E. S. Bjornsson (2014). "The effects of long-term therapy with proton pump inhibitors on meal stimulated gastrin." Dig Liver Dis **46**(2): 125-130.

Hellmich, M. R., X. L. Rui, H. L. Hellmich, R. Y. Fleming, B. M. Evers and C. M. Townsend, Jr. (2000). "Human colorectal cancers express a constitutively active cholecystokinin-B/gastrin receptor that stimulates cell growth." J Biol Chem **275**(41): 32122-32128.

Hemers, E., C. Duval, C. McCaig, M. Handley, G. J. Dockray and A. Varro (2005). "Insulin-like growth factor binding protein-5 is a target of matrix metalloproteinase-7: implications for epithelial-mesenchymal signaling." Cancer Res **65**(16): 7363-7369.

Hess, A. R., E. A. Seftor, R. E. Seftor and M. J. Hendrix (2003). "Phosphoinositide 3-kinase regulates membrane Type 1-matrix metalloproteinase (MMP) and MMP-2 activity during melanoma cell vasculogenic mimicry." Cancer Res **63**(16): 4757-4762.

Hibino, S., M. Shibuya, J. A. Engbring, M. Mochizuki, M. Nomizu and H. K. Kleinman (2004). "Identification of an active site on the laminin alpha5 chain globular domain that binds to CD44 and inhibits malignancy." Cancer Res **64**(14): 4810-4816.

Hill, D. R., N. J. Campbell, T. M. Shaw and G. N. Woodruff (1987). "Autoradiographic localization and biochemical characterization of peripheral type CCK receptors in rat CNS using highly selective nonpeptide CCK antagonists." J Neurosci **7**(9): 2967-2976.

Hill, D. S., N. D. Robinson, M. P. Caley, M. Chen, E. A. O'Toole, J. L. Armstrong, S. Przyborski and P. E. Lovat (2015). "A Novel Fully Humanized 3D Skin Equivalent to Model Early Melanoma Invasion." Mol Cancer Ther **14**(11): 2665-2673.

Hilska, M., P. J. Roberts, Y. U. Collan, V. J. Laine, J. Kossi, P. Hirsimaki, O. Rahkonen and M. Laato (2007). "Prognostic significance of matrix metalloproteinases-1, -2, -7 and -13 and tissue inhibitors of metalloproteinases-1, -2, -3 and -4 in colorectal cancer." Int J Cancer **121**(4): 714-723.

Hocker, M. (2004). "Molecular mechanisms of gastrin-dependent gene regulation." Ann N Y Acad Sci **1014**: 97-109.

Hodi, F. S., S. J. O'Day, D. F. McDermott, R. W. Weber, J. A. Sosman, J. B. Haanen, R. Gonzalez, C. Robert, D. Schadendorf, J. C. Hassel, W. Akerley, A. J. van den Eertwegh, J. Lutzky, P. Lorigan, J. M. Vaubel, G. P. Linette, D. Hogg, C. H. Ottensmeier, C. Lebbe, C. Peschel, I. Quirt, J. I. Clark, J. D. Wolchok, J. S. Weber, J. Tian, M. J. Yellin, G. M. Nichol, A. Hoos and W. J. Urba (2010). "Improved survival with ipilimumab in patients with metastatic melanoma." N Engl J Med **363**(8): 711-723.

Hodis, E., I. R. Watson, G. V. Kryukov, S. T. Arold, M. Imielinski, J. P. Theurillat, E. Nickerson, D. Auclair, L. Li, C. Place, D. Dicara, A. H. Ramos, M. S. Lawrence, K. Cibulskis, A. Sivachenko, D. Voet, G. Saksena, N. Stransky, R. C. Onofrio, W. Winckler, K. Ardlie, N. Wagle, J. Wargo, K. Chong, D. L. Morton, K. Stemke-Hale, G. Chen, M. Noble, M. Meyerson, J. E. Ladbury, M. A. Davies, J. E. Gershenwald, S. N. Wagner, D. S. Hoon, D. Schadendorf, E. S. Lander, S. B. Gabriel, G. Getz, L. A. Garraway and L. Chin (2012). "A landscape of driver mutations in melanoma." Cell **150**(2): 251-263.

Hofmann, U. B., J. R. Westphal, G. N. Van Muijen and D. J. Ruiter (2000). "Matrix metalloproteinases in human melanoma." J Invest Dermatol **115**(3): 337-344.

Hofmann, U. B., J. R. Westphal, E. T. Waas, A. J. Zendman, I. M. Cornelissen, D. J. Ruiter and G. N. van Muijen (1999). "Matrix metalloproteinases in human melanoma cell lines and xenografts: increased expression of activated matrix metalloproteinase-2 (MMP-2) correlates with melanoma progression." Br J Cancer **81**(5): 774-782.

Hofmann, U. B., J. R. Westphal, A. J. Zendman, J. C. Becker, D. J. Ruiter and G. N. van Muijen (2000). "Expression and activation of matrix metalloproteinase-2 (MMP-2) and its co-localization with membrane-type 1 matrix metalloproteinase (MT1-MMP) correlate with melanoma progression." J Pathol **191**(3): 245-256.

Hojilla, C. V., G. A. Wood and R. Khokha (2008). "Inflammation and breast cancer: metalloproteinases as common effectors of inflammation and extracellular matrix breakdown in breast cancer." Breast Cancer Res **10**(2): 205.

Hollande, F., A. Choquet, E. M. Blanc, D. J. Lee, J. P. Bali and G. S. Baldwin (2001). "Involvement of phosphatidylinositol 3-kinase and mitogen-activated protein kinases in glycine-extended gastrin-induced dissociation and migration of gastric epithelial cells." J Biol Chem **276**(44): 40402-40410.

Holmberg, C., M. Quante, I. Steele, J. Kumar, S. Balabanova, C. Duval, M. Czepan, Z. Rakonczayjr, L. Tiszlavicz, I. Nemeth, G. Lazar, Z. Simonka, R. Jenkins, P. Hegyi, T. Wang, G. Dockray and A. Varro (2012). "Release of TGFbetaig-h3 by gastric myofibroblasts slows tumor growth and is decreased with cancer progression." Carcinogenesis **33**: 1553-1562.

Homolya, L., Z. Hollo, U. A. Germann, I. Pastan, M. M. Gottesman and B. Sarkadi (1993). "Fluorescent cellular indicators are extruded by the multidrug resistance protein." J Biol Chem **268**(29): 21493-21496.

Horn, S., A. Figl, P. S. Rachakonda, C. Fischer, A. Sucker, A. Gast, S. Kadel, I. Moll, E. Nagore, K. Hemminki, D. Schadendorf and R. Kumar (2013). "TERT promoter mutations in familial and sporadic melanoma." Science **339**(6122): 959-961.

Hosaka, K., Y. Yang, T. Seki, C. Fischer, O. Dubey, E. Fredlund, J. Hartman, P. Religa, H. Morikawa, Y. Ishii, M. Sasahara, O. Larsson, G. Cossu, R. Cao, S. Lim and Y. Cao (2016). "Pericyte-fibroblast transition promotes tumor growth and metastasis." Proc Natl Acad Sci U S A **113**(38): E5618-5627.

Hsu, M. Y., D. T. Shih, F. E. Meier, P. Van Belle, J. Y. Hsu, D. E. Elder, C. A. Buck and M. Herlyn (1998). "Adenoviral gene transfer of beta3 integrin subunit induces conversion from radial to vertical growth phase in primary human melanoma." Am J Pathol **153**(5): 1435-1442.

Hu, L. T., P. A. Foxall, R. Russell and H. L. Mobley (1992). "Purification of recombinant Helicobacter pylori urease apoenzyme encoded by ureA and ureB." Infect Immun **60**(7): 2657-2666.

Hu, S., D. Liu, R. P. Tufano, K. A. Carson, E. Rosenbaum, Y. Cohen, E. H. Holt, K. Kiseljak-Vassiliades, K. J. Rhoden, S. Tolaney, S. Condouris, G. Tallini, W. H. Westra, C. B. Umbricht, M. A. Zeiger, J. A. Califano, V. Vasko and M. Xing (2006). "Association of aberrant methylation of tumor suppressor genes with tumor aggressiveness and BRAF mutation in papillary thyroid cancer." Int J Cancer **119**(10): 2322-2329.

Hua, H., M. Li, T. Luo, Y. Yin and Y. Jiang (2011). "Matrix metalloproteinases in tumorigenesis: an evolving paradigm." Cell Mol Life Sci **68**(23): 3853-3868.

Huang, F. W., E. Hodis, M. J. Xu, G. V. Kryukov, L. Chin and L. A. Garraway (2013). "Highly recurrent TERT promoter mutations in human melanoma." Science **339**(6122): 957-959.

Hurlimann, S., S. Dur, P. Schwab, L. Varga, L. Mazzucchelli, R. Brand and F. Halter (1998). "Effects of Helicobacter pylori on gastritis, pentagastrin-stimulated gastric acid secretion, and meal-stimulated plasma gastrin release in the absence of peptic ulcer disease." Am J Gastroenterol **93**(8): 1277-1285.

Iida, J., K. L. Wilhelmson, M. A. Price, C. M. Wilson, D. Pei, L. T. Furcht and J. B. McCarthy (2004). "Membrane type-1 matrix metalloproteinase promotes human melanoma invasion and growth." J Invest Dermatol **122**(1): 167-176.

Ingraffea, A. (2013). "Melanoma." Facial Plast Surg Clin North Am **21**(1): 33-42.

Ito, R., K. Sato, T. Helmer, G. Jay and K. Agarwal (1984). "Structural analysis of the gene encoding human gastrin: the large intron contains an Alu sequence." Proc Natl Acad Sci U S A **81**(15): 4662-4666.

Jacobson, B. C., T. G. Ferris, T. L. Shea, E. M. Mahlis, T. H. Lee and T. C. Wang (2003). "Who is using chronic acid suppression therapy and why?" Am J Gastroenterol **98**(1): 51-58.

Jakob, J. A., R. L. Bassett, Jr., C. S. Ng, J. L. Curry, R. W. Joseph, G. C. Alvarado, M. L. Rohlfs, J. Richard, J. E. Gershenwald, K. B. Kim, A. J. Lazar, P. Hwu and M. A. Davies (2012). "NRAS mutation status is an independent prognostic factor in metastatic melanoma." Cancer **118**(16): 4014-4023.

Jalili, A., C. Wagner, M. Pashenkov, G. Pathria, K. D. Mertz, H. R. Widlund, M. Lupien, J. P. Brunet, T. R. Golub, G. Stingl, D. E. Fisher, S. Ramaswamy and S. N. Wagner (2012). "Dual suppression of the cyclin-dependent kinase inhibitors CDKN2C and CDKN1A in human melanoma." J Natl Cancer Inst **104**(21): 1673-1679.

Javier, R. T. and J. S. Butel (2008). "The history of tumor virology." Cancer Res **68**(19): 7693-7706.

Jemal, A., S. S. Devesa, P. Hartge and M. A. Tucker (2001). "Recent trends in cutaneous melanoma incidence among whites in the United States." J Natl Cancer Inst **93**(9): 678-683.

Jensen, R. T. (2002). "Involvement of cholecystokinin/gastrin-related peptides and their receptors in clinical gastrointestinal disorders." Pharmacol Toxicol **91**(6): 333-350.

Jiao, Y., X. Feng, Y. Zhan, R. Wang, S. Zheng, W. Liu and X. Zeng (2012). "Matrix metalloproteinase-2 promotes alphavbeta3 integrin-mediated adhesion and migration of human melanoma cells by cleaving fibronectin." PLoS One **7**(7): e41591.

Jin, G., V. Ramanathan, M. Quante, G. H. Baik, X. Yang, S. S. Wang, S. Tu, S. A. Gordon, D. M. Pritchard, A. Varro, A. Shulkes and T. C. Wang (2009). "Inactivating cholecystokinin-2 receptor inhibits progastrin-dependent colonic crypt fission, proliferation, and colorectal cancer in mice." J Clin Invest **119**(9): 2691-2701.

Johnson, L. R. and M. I. Grossman (1971). "Intestinal hormones as inhibitors of gastric secretion." Gastroenterology **60**(1): 120-144.

Joyce, J. A. and J. W. Pollard (2009). "Microenvironmental regulation of metastasis." Nat Rev Cancer **9**(4): 239-252.

Kalluri, R. and M. Zeisberg (2006). "Fibroblasts in cancer." Nat Rev Cancer **6**(5): 392-401.

Kaloudi, A., B. A. Nock, E. P. Krenning, T. Maina and M. De Jong (2015). "Radiolabeled gastrin/CCK analogs in tumor diagnosis: towards higher stability and improved tumor targeting." Q J Nucl Med Mol Imaging **59**(3): 287-302.

Kamada, T., K. Haruma, K. Komoto, M. Mihara, K. Sumii and G. Kajiyama (1999). "Comparison of meal-stimulated serum gastrin response in Helicobacter pylori-positive duodenal ulcer and asymptomatic volunteers with and without H. pylori infection." Helicobacter **4**(3): 170-177.

Kamyab-Hesari, K., N. Mohtasham, N. Aghazadeh, M. Biglarian, B. Memar and H. Kadeh (2014). "The expression of MMP-2 and Ki-67 in head and neck melanoma, and their correlation with clinic-pathologic indices." J Cancer Res Ther **10**(3): 696-700.

Kanitakis, J. (2002). "Anatomy, histology and immunohistochemistry of normal human skin." Eur J Dermatol **12**(4): 390-399; quiz 400-391.

Kao, J. P. (1994). "Practical aspects of measuring [Ca2+] with fluorescent indicators." Methods Cell Biol **40**: 155-181.

Karagas, M. R., H. H. Nelson, M. S. Zens, M. Linet, T. A. Stukel, S. Spencer, K. M. Applebaum, L. Mott and K. Mabuchi (2007). "Squamous cell and basal cell carcinoma of the skin in relation to radiation therapy and potential modification of risk by sun exposure." Epidemiology **18**(6): 776-784.

Kardinal, C. G. and J. W. Yarbro (1979). "A conceptual history of cancer." Semin Oncol **6**(4): 396-408.

Karnes, W. E., Jr., G. V. Ohning, B. Sytnik, S. W. Kim and J. H. Walsh (1991). "Elevation of meal-stimulated gastrin release in subjects with Helicobacter pylori infection: reversal by low intragastric pH." Rev Infect Dis **13 Suppl 8**: S665-670.

Kastner, S., T. Voss, S. Keuerleber, C. Glockel, M. Freissmuth and W. Sommergruber (2012). "Expression of G protein-coupled receptor 19 in human lung cancer cells is triggered by entry into S-phase and supports G(2)-M cell-cycle progression." Mol Cancer Res **10**(10): 1343-1358.

Kato, S., K. Ozawa, T. Koike, H. Sekine, S. Ohara, T. Minoura and K. Iinuma (2004). "Effect of Helicobacter pylori infection on gastric acid secretion and meal-stimulated serum gastrin in children." Helicobacter **9**(2): 100-105.

Katoh, K., K. Misawa, K. Kuma and T. Miyata (2002). "MAFFT: a novel method for rapid multiple sequence alignment based on fast Fourier transform." Nucleic Acids Res **30**(14): 3059-3066.

Kemeny, L. V., Z. Kurgyis, T. Buknicz, G. Groma, A. Jakab, K. Zanker, T. Dittmar, L. Kemeny and I. B. Nemeth (2016). "Melanoma Cells Can Adopt the Phenotype of Stromal Fibroblasts and Macrophages by Spontaneous Cell Fusion in Vitro." Int J Mol Sci **17**(6).

Keung, E. Z. and J. E. Gershenwald (2018). "The eighth edition American Joint Committee on Cancer (AJCC) melanoma staging system: implications for melanoma treatment and care." **18**(8): 775-784.

Kimata, M., Y. Otani, T. Kubota, N. Igarashi, T. Yokoyama, N. Wada, N. Yoshimizu, M. Fujii, K. Kameyama, Y. Okada, K. Kumai and M. Kitajima (2002). "Matrix metalloproteinase inhibitor, marimastat, decreases peritoneal spread of gastric carcinoma in nude mice." Jpn J Cancer Res **93**(7): 834-841.

Kleeberg, U. R., S. Suciu, E. B. Brocker, D. J. Ruiter, C. Chartier, D. Lienard, J. Marsden, D. Schadendorf and A. M. Eggermont (2004). "Final results of the EORTC 18871/DKG 80-1 randomised phase III trial. rIFN-alpha2b versus rIFN-gamma versus ISCADOR M versus observation after surgery in melanoma patients with either high-risk primary (thickness >3 mm) or regional lymph node metastasis." Eur J Cancer **40**(3): 390-402.

Koh, T. J., G. J. Dockray, A. Varro, R. J. Cahill, C. A. Dangler, J. G. Fox and T. C. Wang (1999). "Overexpression of glycine-extended gastrin in transgenic mice results in increased colonic proliferation." J Clin Invest **103**(8): 1119-1126.

Koh, T. J., J. K. Field, A. Varro, T. Liloglou, P. Fielding, G. Cui, J. Houghton, G. J. Dockray and T. C. Wang (2004). "Glycine-extended gastrin promotes the growth of lung cancer." Cancer Res **64**(1): 196-201.

Koh, T. J., J. R. Goldenring, S. Ito, H. Mashimo, A. S. Kopin, A. Varro, G. J. Dockray and T. C. Wang (1997). "Gastrin deficiency results in altered gastric differentiation and decreased colonic proliferation in mice." Gastroenterology **113**(3): 1015-1025.

Kovac, S., A. Shulkes and G. S. Baldwin (2008). "Peptide processing and biology in human disease." Curr Opin Endocrinol Diabetes Obes **16**(1): 79-85.

Kowalski-Chauvel, A., S. Najib, C. Bertrand, L. Martinez, A. Ferrand and C. Seva (2010). Cell surface F1ATPase binds the Gastrin precursor, G-gly, and mediates its proliferative effects on colorectal cancer cells and vascular endothelial cells.

Kozera, B. and M. Rapacz (2013). "Reference genes in real-time PCR." J Appl Genet **54**(4): 391-406.

Körner, M., B. Waser, J. C. Reubi and L. J. Miller (2010). "CCK(2) receptor splice variant with intron 4 retention in human gastrointestinal and lung tumours." J Cell Mol Med **14**(4): 933-943.

Krashias, G., S. Bashiardes, A. Potamitou, G. S. Potamitis and C. Christodoulou (2013). "Prevalence of Helicobacter pylori cagA and vacA genes in Cypriot patients." J Infect Dev Ctries **7**(9): 642-650.

Kristensen, L. P., L. Chen, M. O. Nielsen, D. W. Qanie, I. Kratchmarova, M. Kassem and J. S. Andersen (2012). "Temporal profiling and pulsed SILAC labeling identify novel secreted proteins during ex vivo osteoblast differentiation of human stromal stem cells." Mol Cell Proteomics **11**(10): 989-1007.

Kueng, W., E. Silber and U. Eppenberger (1989). "Quantification of cells cultured on 96-well plates." Anal Biochem **182**(1): 16-19.

Kumar, J. D., C. Holmberg, S. Kandola, I. Steele, P. Hegyi, L. Tiszlavicz, R. Jenkins, R. J. Beynon, D. Peeney, O. T. Giger, A. Alqahtani, T. C. Wang, T. T. Charvat, M. Penfold, G. J. Dockray and A. Varro (2014). "Increased expression of chemerin in squamous esophageal cancer myofibroblasts and role in recruitment of mesenchymal stromal cells." PLoS One **9**(7): e104877.

Kumar, J. D., S. Kandola, L. Tiszlavicz, Z. Reisz, G. J. Dockray and A. Varro (2016). "The role of chemerin and ChemR23 in stimulating the invasion of squamous oesophageal cancer cells." Br J Cancer **114**(10): 1152-1159.

Kumar, J. D., I. Steele, A. R. Moore, S. V. Murugesan, Z. Rakonczay, V. Venglovecz, D. M. Pritchard, R. Dimaline, L. Tiszlavicz, A. Varro and G. J. Dockray (2015). "Gastrin stimulates MMP-1 expression in gastric epithelial cells: putative role in gastric epithelial cell migration." Am J Physiol Gastrointest Liver Physiol **309**(2): G78-86.

Kun, Z., G. Hanqing, T. Hailing, Y. Yuan, Z. Jun, Z. Lingxia, H. Kun and Z. Xin (2017). "Gastrin Enhances Autophagy and Promotes Gastric Carcinoma Proliferation via Inducing AMPKalpha." Oncol Res **25**(8): 1399-1407.

Kurisu, S., S. Suetsugu, D. Yamazaki, H. Yamaguchi and T. Takenawa (2005). "Rac-WAVE2 signaling is involved in the invasive and metastatic phenotypes of murine melanoma cells." Oncogene **24**(8): 1309-1319.

Kurschat, P., C. Wickenhauser, W. Groth, T. Krieg and C. Mauch (2002). "Identification of activated matrix metalloproteinase-2 (MMP-2) as the main gelatinolytic enzyme in malignant melanoma by in situ zymography." J Pathol **197**(2): 179-187.

Lambert, E., E. Dasse, B. Haye and E. Petitfrere (2004). "TIMPs as multifacial proteins." Crit Rev Oncol Hematol **49**(3): 187-198.

Lamberts, R., G. Brunner and E. Solcia (2001). "Effects of very long (up to 10 years) proton pump blockade on human gastric mucosa." Digestion **64**(4): 205-213.

Lancaster, M. A. and J. A. Knoblich (2014). "Organogenesis in a dish: modeling development and disease using organoid technologies." Science **345**(6194): 1247125.

Lasithiotakis, K., U. Leiter, S. Kruger-Krasagakis, A. Tosca and C. Garbe (2006). "Comparative analysis of incidence and clinical features of cutaneous malignant melanoma in Crete (Greece) and southern Germany (central Baden-Wurttemberg)." Br J Dermatol **154**(6): 1123-1127.

Lederle, W., B. Hartenstein, A. Meides, H. Kunzelmann, Z. Werb, P. Angel and M. M. Mueller (2010). "MMP13 as a stromal mediator in controlling persistent angiogenesis in skin carcinoma." Carcinogenesis **31**(7): 1175-1184.

Lee, F., C. Iliescu, F. Yu and H. Yu (2018). "Constrained spheroids/organoids in perfusion culture." Methods Cell Biol **146**: 43-65.

Lei, S., A. Dubeykovskiy, A. Chakladar, L. Wojtukiewicz and T. C. Wang (2004). "The murine gastrin promoter is synergistically activated by transforming growth factor-beta/Smad and Wnt signaling pathways." J Biol Chem **279**(41): 42492-42502.

Leonardi, G. C., L. Falzone, R. Salemi, A. Zanghi, D. A. Spandidos, J. A. McCubrey, S. Candido and M. Libra (2018). "Cutaneous melanoma: From pathogenesis to therapy (Review)." Int J Oncol **52**(4): 1071-1080.

Levine, E. M., Y. Becker, C. W. Boone and H. Eagle (1965). "CONTACT INHIBITION, MACROMOLECULAR SYNTHESIS, AND POLYRIBOSOMES IN CULTURED HUMAN DIPLOID FIBROBLASTS." Proc Natl Acad Sci U S A **53**: 350-356.

Lewin, K. J., F. Dowling, J. P. Wright and K. B. Taylor (1976). "Gastric morphology and serum gastrin levels in pernicious anaemia." Gut **17**(7): 551-560.

Li, D., J. Ding and X. Z. Wang (2008). "[Effect of gastrin on tyrosine phosphorylation of focal adhesion kinase in human gastric cancer cell line SGC7901]." Ai Zheng **27**(1): 41-45.

Lin, J. Y. and D. E. Fisher (2007). "Melanocyte biology and skin pigmentation." Nature **445**(7130): 843-850.

Liu, H., C. Semino-Mora and A. Dubois (2012). "Mechanism of H. pylori intracellular entry: an in vitro study." Front Cell Infect Microbiol **2**: 13.

Logan, R. P. (1996). "Adherence of Helicobacter pylori." Aliment Pharmacol Ther **10 Suppl 1**: 3-15.

Lotfi, A., G. Mohammadi, L. Saniee, M. Mousaviagdas, H. Chavoshi and A. Tavassoli (2015). "Serum Level of Matrix Metalloproteinase-2 and -9 in Patients with Laryngeal Squamous Cell Carcinoma and Clinical Significance." Asian Pac J Cancer Prev **16**(15): 6749-6751.

Lotfi, A., G. Mohammadi, A. Tavassoli, M. Mousaviagdas, H. Chavoshi and L. Saniee (2015). "Serum levels of MMP9 and MMP2 in patients with oral squamous cell carcinoma." Asian Pac J Cancer Prev **16**(4): 1327-1330.

Lundell, L., M. Vieth, F. Gibson, P. Nagy and P. J. Kahrilas (2015). "Systematic review: the effects of long-term proton pump inhibitor use on serum gastrin levels and gastric histology." Aliment Pharmacol Ther **42**(6): 649-663.

Lunter, P. C., J. W. van Kilsdonk, H. van Beek, I. M. Cornelissen, M. Bergers, P. H. Willems, G. N. van Muijen and G. W. Swart (2005). "Activated leukocyte cell adhesion molecule (ALCAM/CD166/MEMD), a novel actor in invasive growth, controls matrix metalloproteinase activity." Cancer Res **65**(19): 8801-8808.

MacKie, R. M. (1990). "Clinical recognition of early invasive malignant melanoma." Bmj **301**(6759): 1005-1006.

MacKie, R. M., A. Hauschild and A. M. Eggermont (2009). "Epidemiology of invasive cutaneous melanoma." Ann Oncol **20 Suppl 6**: vi1-7.

Maehata, Y., S. Nakamura, K. Fujisawa, M. Esaki, T. Moriyama, K. Asano, Y. Fuyuno, K. Yamaguchi, I. Egashira, H. Kim, M. Kanda, M. Hirahashi and T. Matsumoto (2012). "Long-term effect of Helicobacter pylori eradication on the development of metachronous gastric cancer after endoscopic resection of early gastric cancer." Gastrointest Endosc **75**(1): 39-46.

Maekawa, K., H. Sato, M. Furukawa and T. Yoshizaki (2002). "Inhibition of cervical lymph node metastasis by marimastat (BB-2516) in an orthotopic oral squamous cell carcinoma implantation model." Clin Exp Metastasis **19**(6): 513-518.

Maertens, O., B. Johnson, P. Hollstein, D. T. Frederick, Z. A. Cooper, L. Messiaen, R. T. Bronson, M. McMahon, S. Granter, K. Flaherty, J. A. Wargo, R. Marais and K. Cichowski (2013). "Elucidating distinct roles for NF1 in melanomagenesis." Cancer Discov **3**(3): 338-349.

Magnan, R., B. Masri, C. Escrieut, M. Foucaud, P. Cordelier and D. Fourmy (2011). "Regulation of membrane cholecystokinin-2 receptor by agonists enables classification of partial agonists as biased agonists." J Biol Chem **286**(8): 6707-6719.

Mao, J. D., P. Wu, J. X. Huang, J. Wu and G. Yang (2014). "Role of ERK-MAPK signaling pathway in pentagastrin-regulated growth of large intestinal carcinoma." World J Gastroenterol **20**(35): 12542-12550.

Markovic, S. N., L. A. Erickson, R. D. Rao, R. H. Weenig, B. A. Pockaj, A. Bardia, C. M. Vachon, S. E. Schild, R. R. McWilliams, J. L. Hand, S. D. Laman, L. A. Kottschade, W. J. Maples, M. R. Pittelkow, J. S. Pulido, J. D. Cameron and E. T. Creagan (2007). "Malignant melanoma in the 21st century, part 1: epidemiology, risk factors, screening, prevention, and diagnosis." Mayo Clin Proc **82**(3): 364-380.

Martin del Campo, S. E., N. Latchana, K. M. Levine, V. P. Grignol, E. T. Fairchild, A. C. Jaime-Ramirez, T. V. Dao, V. I. Karpa, M. Carson, A. Ganju, A. N. Chan and W. E. Carson, 3rd (2015). "MiR-21 enhances melanoma invasiveness via inhibition of tissue inhibitor of metalloproteinases 3 expression: in vivo effects of MiR-21 inhibitor." PLoS One **10**(1): e0115919.

Marusak, C., I. Bayles, J. Ma, M. Gooyit, M. Gao, M. Chang and B. Bedogni (2016). "The thiirane-based selective MT1-MMP/MMP2 inhibitor ND-322 reduces melanoma tumor growth and delays metastatic dissemination." Pharmacol Res **113**(Pt A): 515-520.

Mathieu, A., P. Clerc, G. Portolan, C. Bierkamp, H. Lulka, L. Pradayrol, C. Seva, D. Fourmy and M. Dufresne (2005). "Transgenic expression of CCK2 receptors sensitizes murine pancreatic acinar cells to carcinogen-induced preneoplastic lesions formation." Int J Cancer **115**(1): 46-54.

Mathieu, V., T. Mijatovic, M. van Damme and R. Kiss (2005). "Gastrin exerts pleiotropic effects on human melanoma cell biology." Neoplasia **7**(10): 930-943.

Mathot, L. and J. Stenninger (2012). "Behavior of seeds and soil in the mechanism of metastasis: a deeper understanding." Cancer Sci **103**(4): 626-631.

Maton, P. (1994). Gut Peptides: Biochemistry and Physiology. New York, Raven Press.

McArthur, G. A., P. B. Chapman, C. Robert, J. Larkin, J. B. Haanen, R. Dummer, A. Ribas, D. Hogg, O. Hamid, P. A. Ascierto, C. Garbe, A. Testori, M. Maio, P. Lorigan, C. Lebbe, T. Jouary, D. Schadendorf, S. J. O'Day, J. M. Kirkwood, A. M. Eggermont, B. Dreno, J. A. Sosman, K. T. Flaherty, M. Yin, I. Caro, S. Cheng, K. Trunzer and A. Hauschild (2014). "Safety and efficacy of vemurafenib in BRAF(V600E) and BRAF(V600K) mutation-positive melanoma (BRIM-3): extended follow-up of a phase 3, randomised, open-label study." Lancet Oncol **15**(3): 323-332.

McCaig, C., C. Duval, E. Hemers, I. Steele, D. M. Pritchard, S. Przemeck, R. Dimaline, S. Ahmed, K. Bodger, D. D. Kerrigan, T. C. Wang, G. J. Dockray and A. Varro (2006). "The role of matrix metalloproteinase-7 in redefining the gastric microenvironment in response to Helicobacter pylori." Gastroenterology **130**(6): 1754-1763.

McCracken, K. W., E. M. Cata, C. M. Crawford, K. L. Sinagoga, M. Schumacher, B. E. Rockich, Y. H. Tsai, C. N. Mayhew, J. R. Spence, Y. Zavros and J. M. Wells (2014). "Modelling human development and disease in pluripotent stem-cell-derived gastric organoids." Nature **516**(7531): 400-404.

McGillicuddy, L. T., J. A. Fromm, P. E. Hollstein, S. Kubek, R. Beroukhim, T. De Raedt, B. W. Johnson, S. M. Williams, P. Nghiemphu, L. M. Liau, T. F. Cloughesy, P. S. Mischel, A. Parret, J. Seiler, G. Moldenhauer, K. Scheffzek, A. O. Stemmer-Rachamimov, C. L. Sawyers, C. Brennan, L. Messiaen, I. K. Mellinghoff and K. Cichowski (2009). "Proteasomal and genetic inactivation of the NF1 tumor suppressor in gliomagenesis." Cancer Cell **16**(1): 44-54.

McGuigan, J. E. and W. L. Trudeau (1970). "Serum gastrin concentrations in pernicious anemia." N Engl J Med **282**(7): 358-361.

Merchant, J. L., B. Demediuk and S. J. Brand (1991). "A GC-rich element confers epidermal growth factor responsiveness to transcription from the gastrin promoter." Mol Cell Biol **11**(5): 2686-2696.

Meyer, T., M. E. Caplin, D. H. Palmer, J. W. Valle, M. Larvin, J. S. Waters, F. Coxon, I. Borbath, M. Peeters, E. Nagano and H. Kato (2010). "A phase Ib/IIa trial to evaluate the CCK2 receptor antagonist Z-360 in combination with gemcitabine in patients with advanced pancreatic cancer." Eur J Cancer **46**(3): 526-533.

Mi, H., X. Huang, A. Muruganujan, H. Tang, C. Mills, D. Kang and P. D. Thomas (2017). "PANTHER version 11: expanded annotation data from Gene Ontology and Reactome pathways, and data analysis tool enhancements." Nucleic Acids Res **45**(D1): D183-d189.

Mi, H., A. Muruganujan and P. D. Thomas (2013). "PANTHER in 2013: modeling the evolution of gene function, and other gene attributes, in the context of phylogenetic trees." Nucleic Acids Res **41**(Database issue): D377-386.

Midgley, A. C., M. Rogers, M. B. Hallett, A. Clayton, T. Bowen, A. O. Phillips and R. Steadman (2013). "Transforming growth factor-beta1 (TGF-beta1)-stimulated fibroblast to myofibroblast differentiation is mediated by hyaluronan (HA)-facilitated epidermal growth factor receptor (EGFR) and CD44 co-localization in lipid rafts." J Biol Chem **288**(21): 14824-14838.

Miyazaki, Y., Y. Shinomura, S. Tsutsui, S. Zushi, Y. Higashimoto, S. Kanayama, S. Higashiyama, N. Taniguchi and Y. Matsuzawa (1999). "Gastrin induces heparin-binding epidermal growth factor-like growth factor in rat gastric epithelial cells transfected with gastrin receptor." Gastroenterology **116**(1): 78-89.

Moore, T. C., L. I. Jepeal, M. O. Boylan, S. K. Singh, N. Boyd, D. G. Beer, A. J. Chang and M. M. Wolfe (2004). "Gastrin stimulates receptor-mediated proliferation of human esophageal adenocarcinoma cells." Regul Pept **120**(1-3): 195-203.

Morgan, A. J. and R. Jacob (1994). "Ionomycin enhances Ca2+ influx by stimulating store-regulated cation entry and not by a direct action at the plasma membrane." Biochem J **300 (Pt 3)**: 665-672.

Moro, N., C. Mauch and P. Zigrino (2014). "Metalloproteinases in melanoma." Eur J Cell Biol **93**(1-2): 23-29.

Morris, A. and G. Nicholson (1987). "Ingestion of Campylobacter pyloridis causes gastritis and raised fasting gastric pH." Am J Gastroenterol **82**(3): 192-199.

Mort, R. L., I. J. Jackson and E. E. Patton (2015). "The melanocyte lineage in development and disease." Development **142**(4): 620-632.

Morton, D. L., J. F. Thompson, A. J. Cochran, N. Mozzillo, R. Elashoff, R. Essner, O. E. Nieweg, D. F. Roses, H. J. Hoekstra, C. P. Karakousis, D. S. Reintgen, B. J. Coventry, E. C. Glass and H. J. Wang (2006). "Sentinel-node biopsy or nodal observation in melanoma." N Engl J Med **355**(13): 1307-1317.

Morton, D. L., J. F. Thompson, R. Essner, R. Elashoff, S. L. Stern, O. E. Nieweg, D. F. Roses, C. P. Karakousis, N. Mozzillo, D. Reintgen, H. J. Wang, E. C. Glass and A. J. Cochran (1999). "Validation of the accuracy of intraoperative lymphatic mapping and sentinel lymphadenectomy for early-stage melanoma: a multicenter trial. Multicenter Selective Lymphadenectomy Trial Group." Ann Surg **230**(4): 453-463; discussion 463-455.

Morton, D. L., D. R. Wen, J. H. Wong, J. S. Economou, L. A. Cagle, F. K. Storm, L. J. Foshag and A. J. Cochran (1992). "Technical details of intraoperative lymphatic mapping for early stage melanoma." Arch Surg **127**(4): 392-399.

Muller, M. S., L. F. Obel, H. S. Waagepetersen, A. Schousboe and L. K. Bak (2013). "Complex actions of ionomycin in cultured cerebellar astrocytes affecting both calcium-induced calcium release and store-operated calcium entry." Neurochem Res **38**(6): 1260-1265.

Murphy, G., A. Murthy and R. Khokha (2008). "Clipping, shedding and RIPping keep immunity on cue." Trends Immunol **29**(2): 75-82.

Nahhas, A. F., C. A. Scarbrough and S. Trotter (2017). "A Review of the Global Guidelines on Surgical Margins for Nonmelanoma Skin Cancers." J Clin Aesthet Dermatol **10**(4): 37-46.

Najib, S., A. Kowalski-Chauvel, C. Do, S. Roche, E. Cohen-Jonathan-Moyal and C. Seva (2015). "Progastrin a new pro-angiogenic factor in colorectal cancer." Oncogene **34**(24): 3120-3130.

Neila, J. and H. P. Soyer (2011). "Key points in dermoscopy for diagnosis of melanomas, including difficult to diagnose melanomas, on the trunk and extremities." J Dermatol **38**(1): 3-9.

Nemeth, J., B. Taylor, S. Pauwels, A. Varro and G. J. Dockray (1993). "Identification of progastrin derived peptides in colorectal carcinoma extracts." Gut **34**(1): 90-95.

Nishimura, S., K. Bilguvar, K. Ishigame, N. Sestan, M. Gunel and A. Louvi (2015). "Functional synergy between cholecystokinin receptors CCKAR and CCKBR in mammalian brain development." PLoS One **10**(4): e0124295.

Noble, P. J., G. Wilde, M. R. White, S. R. Pennington, G. J. Dockray and A. Varro (2003). "Stimulation of gastrin-CCKB receptor promotes migration of gastric AGS cells via multiple paracrine pathways." Am J Physiol Gastrointest Liver Physiol **284**(1): G75-84.

Nowell, P. C. (1976). "The clonal evolution of tumor cell populations." Science **194**(4260): 23-28.

Nystrom, M. L., G. J. Thomas, M. Stone, I. C. Mackenzie, I. R. Hart and J. F. Marshall (2005). "Development of a quantitative method to analyse tumour cell invasion in organotypic culture." J Pathol **205**(4): 468-475.

Ohlund, D., E. Elyada and D. Tuveson (2014). "Fibroblast heterogeneity in the cancer wound." J Exp Med **211**(8): 1503-1523.

Olsen, G. (1964). "REMOVAL OF FASCIA--CAUSE OF MORE FREQUENT METASTASES OF MALIGNANT MELANOMAS OF THE SKIN TO REGIONAL LYMPH NODES?" Cancer **17**: 1159-1164.

Ostrowski, M., N. B. Carmo, S. Krumeich, I. Fanget, G. Raposo, A. Savina, C. F. Moita, K. Schauer, A. N. Hume, R. P. Freitas, B. Goud, P. Benaroch, N. Hacohen, M. Fukuda, C. Desnos, M. C. Seabra, F. Darchen, S. Amigorena, L. F. Moita and C. Thery (2010). "Rab27a and Rab27b control different steps of the exosome secretion pathway." Nat Cell Biol **12**(1): 19-30; sup pp 11-13.

Ottewell, P. D., A. J. Watson, T. C. Wang, A. Varro, G. J. Dockray and D. M. Pritchard (2003). "Progastrin stimulates murine colonic epithelial mitosis after DNA damage." Gastroenterology **124**(5): 1348-1357.

Ozerdem, U., B. Mach-Hofacre, N. Varki, R. Folberg, A. J. Mueller, R. Ochabski, T. Pham, K. Appelt and W. R. Freeman (2002). "The effect of prinomastat (AG3340), a synthetic inhibitor of matrix metalloproteinases, on uveal melanoma rabbit model." Curr Eye Res **24**(2): 86-91.

Paek, S., A. Sober and H. Tsao (2008). "Cutaneous melanoma. In: Fitzpatrick's Dermatology in General Medicine, 7th, Wolff K, Goldsmith LA, Katz SI, Gilchrest BA, Paller AS, Leffell DJ (Eds), McGraw Hill Medical." **Vol I, p.1134.**

Paget, S. (1989). "The distribution of secondary growths in cancer of the breast. 1889." Cancer Metastasis Rev **8**(2): 98-101.

Patel, O., K. M. Marshall, G. Bramante, G. S. Baldwin and A. Shulkes (2010). "The C-terminal flanking peptide (CTFP) of progastrin inhibits apoptosis via a PI3-kinase-dependent pathway." Regul Pept **165**(2-3): 224-231.

Peinado, H., M. Aleckovic, S. Lavotshkin, I. Matei, B. Costa-Silva, G. Moreno-Bueno, M. Hergueta-Redondo, C. Williams, G. Garcia-Santos, C. Ghajar, A. Nitadori-Hoshino, C. Hoffman, K. Badal, B. A. Garcia, M. K. Callahan, J. Yuan, V. R. Martins, J. Skog, R. N. Kaplan, M. S. Brady, J. D. Wolchok, P. B. Chapman, Y. Kang, J. Bromberg and D. Lyden (2012). "Melanoma exosomes educate bone marrow progenitor cells toward a pro-metastatic phenotype through MET." Nat Med **18**(6): 883-891.

Pender, S. L. and T. T. MacDonald (2004). "Matrix metalloproteinases and the gut - new roles for old enzymes." Curr Opin Pharmacol **4**(6): 546-550.

Pennington, S. R., B. J. Foster, S. R. Hawley, R. E. Jenkins, O. Zolle, M. R. White, C. J. McNamee, P. Sheterline and A. W. Simpson (2007). "Cell shape-dependent Control of Ca2+ influx and cell cycle progression in Swiss 3T3 fibroblasts." J Biol Chem **282**(44): 32112-32120.

Petersen, T. N., S. Brunak, G. von Heijne and H. Nielsen (2011). "SignalP 4.0: discriminating signal peptides from transmembrane regions." Nat Methods **8**(10): 785-786.

Polk, D. B. and R. M. Peek, Jr. (2010). "Helicobacter pylori: gastric cancer and beyond." Nat Rev Cancer **10**(6): 403-414.

Popielski, L. (1919). "beta-imidazo aethyl amine and the organ extracts. Second Part: The influence of acids on the stomach juice secretion stimulatinf effect of organ extracts." Pflugers Archiv Fur Die Gesamte Physiologie Des Menschen Und Der Tiere **177**: 237-259.

Powell, D. W., P. A. Adegboyega, J. F. Di Mari and R. C. Mifflin (2005). "Epithelial cells and their neighbors I. Role of intestinal myofibroblasts in development, repair, and cancer." Am.J.Physiol Gastrointest.Liver Physiol **289**(1): G2-G7.

Powell, D. W., R. C. Mifflin, J. D. Valentich, S. E. Crowe, J. I. Saada and A. B. West (1999). "Myofibroblasts. I. Paracrine cells important in health and disease." Am J Physiol **277**(1 Pt 1): C1-9.

Powell, D. W., R. C. Mifflin, J. D. Valentich, S. E. Crowe, J. I. Saada and A. B. West (1999). "Myofibroblasts. I. Paracrine cells important in health and disease." Am.J.Physiol **277**(1 Pt 1): C1-C9.

Powell, D. W., R. C. Mifflin, J. D. Valentich, S. E. Crowe, J. I. Saada and A. B. West (1999). "Myofibroblasts. II. Intestinal subepithelial myofibroblasts." Am J Physiol **277**(2 Pt 1): C183-201.

Pradeep, A., C. Sharma, P. Sathyanarayana, C. Albanese, J. V. Fleming, T. C. Wang, M. M. Wolfe, K. M. Baker, R. G. Pestell and B. Rana (2004). "Gastrin-mediated activation of cyclin D1 transcription involves beta-catenin and CREB pathways in gastric cancer cells." Oncogene **23**(20): 3689-3699.

Pratt, J. M., D. M. Simpson, M. K. Doherty, J. Rivers, S. J. Gaskell and R. J. Beynon (2006). "Multiplexed absolute quantification for proteomics using concatenated signature peptides encoded by QconCAT genes." Nat Protoc **1**(2): 1029-1043.

Prenzel, N., E. Zwick, H. Daub, M. Leserer, R. Abraham, C. Wallasch and A. Ullrich (1999). "EGF receptor transactivation by G-protein-coupled receptors requires metalloproteinase cleavage of proHB-EGF." Nature **402**(6764): 884-888.

Qian, B. Z. and J. W. Pollard (2010). "Macrophage diversity enhances tumor progression and metastasis." Cell **141**(1): 39-51.

Quail, D. F. and J. A. Joyce (2013). "Microenvironmental regulation of tumor progression and metastasis." Nat Med **19**(11): 1423-1437.

Quante, M., S. P. Tu, H. Tomita, T. Gonda, S. S. Wang, S. Takashi, G. H. Baik, W. Shibata, B. Diprete, K. S. Betz, R. Friedman, A. Varro, B. Tycko and T. C. Wang (2011). "Bone marrow-derived myofibroblasts contribute to the mesenchymal stem cell niche and promote tumor growth." Cancer Cell **19**(2): 257-272.

Read, J., K. A. Wadt and N. K. Hayward (2016). "Melanoma genetics." J Med Genet **53**(1): 1-14.

Rehfeld, J. F. and L. Hilsted (1992). "Gastrin and cancer." Adv Clin Chem **29**: 239-262.

Rehfeld, J. F. and W. W. van Solinge (1994). "The tumor biology of gastrin and cholecystokinin." Adv Cancer Res **63**: 295-347.

Reubi, J. C., J. C. Schaer and B. Waser (1997). "Cholecystokinin(CCK)-A and CCK-B/gastrin receptors in human tumors." Cancer Res **57**(7): 1377-1386.

Reubi, J. C. and B. Waser (1996). "Unexpected high incidence of cholecystokinin-B/gastrin receptors in human medullary thyroid carcinomas." Int J Cancer **67**(5): 644-647.

Reubi, J. C. and B. Waser (2003). "Concomitant expression of several peptide receptors in neuroendocrine tumours: molecular basis for in vivo multireceptor tumour targeting." Eur J Nucl Med Mol Imaging **30**(5): 781-793.

Reubi, J. C., B. Waser, M. Gugger, H. Friess, J. Kleeff, H. Kayed, M. W. Buchler and J. A. Laissue (2003). "Distribution of CCK1 and CCK2 receptors in normal and diseased human pancreatic tissue." Gastroenterology **125**(1): 98-106.

Ribatti, D. (2009). "Endogenous inhibitors of angiogenesis: a historical review." Leuk Res **33**(5): 638-644.

Ribatti, D., G. Mangialardi and A. Vacca (2006). "Stephen Paget and the 'seed and soil' theory of metastatic dissemination." Clin Exp Med **6**(4): 145-149.

Ridley, A. J. (2006). "Rho GTPases and actin dynamics in membrane protrusions and vesicle trafficking." Trends Cell Biol **16**(10): 522-529.

Rigel, D. S. and R. J. Friedman (1993). "The rationale of the ABCDs of early melanoma." J Am Acad Dermatol **29**(6): 1060-1061.

Robert, C., A. Ribas, J. D. Wolchok, F. S. Hodi, O. Hamid, R. Kefford, J. S. Weber, A. M. Joshua, W. J. Hwu, T. C. Gangadhar, A. Patnaik, R. Dronca, H. Zarour, R. W. Joseph, P. Boasberg, B. Chmielowski, C. Mateus, M. A. Postow, K. Gergich, J. Elassaiss-Schaap, X. N. Li, R. Iannone, S. W. Ebbinghaus, S. P. Kang and A. Daud (2014). "Anti-programmed-death-receptor-1 treatment with pembrolizumab in ipilimumab-refractory advanced melanoma: a randomised dose-comparison cohort of a phase 1 trial." Lancet **384**(9948): 1109-1117.

Robinson, J. K. and R. Turrisi (2006). "Skills training to learn discrimination of ABCDE criteria by those at risk of developing melanoma." Arch Dermatol **142**(4): 447-452.

Romagnani, P., F. Annunziato, L. Lasagni, E. Lazzeri, C. Beltrame, M. Francalanci, M. Uguccioni, G. Galli, L. Cosmi, L. Maurenzig, M. Baggiolini, E. Maggi, S. Romagnani and M. Serio (2001). "Cell cycle–dependent expression of CXC chemokine receptor 3 by endothelial cells mediates angiostatic activity." J Clin Invest **107**(1): 53-63.

Rotte, A., M. Martinka and G. Li (2012). "MMP2 expression is a prognostic marker for primary melanoma patients." Cell Oncol (Dordr) **35**(3): 207-216.

Rous, P. (1911). "A SARCOMA OF THE FOWL TRANSMISSIBLE BY AN AGENT SEPARABLE FROM THE TUMOR CELLS." J Exp Med **13**(4): 397-411.

Roy, J., K. S. Putt, D. Coppola, M. E. Leon, F. K. Khalil, B. A. Centeno, N. Clark, V. E. Stark, D. L. Morse and P. S. Low (2016). "Assessment of cholecystokinin 2 receptor (CCK2R) in neoplastic tissue." Oncotarget **7**(12): 14605-14615.

Ryberg, A., K. Borch and H. J. Monstein (2011). "Expression of multiple forms of 3'-end variant CCK2 receptor mRNAs in human pancreatic adenocarcinomas." BMC Res Notes **4**: 131.

Saito, A., H. Sankaran, I. D. Goldfine and J. A. Williams (1980). "Cholecystokinin receptors in the brain: characterization and distribution." Science **208**(4448): 1155-1156.

Sano, T., D. G. Coit, H. H. Kim, F. Roviello, P. Kassab, C. Wittekind, Y. Yamamoto and Y. Ohashi (2017). "Proposal of a new stage grouping of gastric cancer for TNM classification: International Gastric Cancer Association staging project." Gastric Cancer **20**(2): 217-225.

Sarkar, S., C. Kantara and P. Singh (2012). "Clathrin mediates endocytosis of progastrin and activates MAPKs: role of cell surface annexin A2." Am J Physiol Gastrointest Liver Physiol **302**(7): G712-722.

Sato, T., R. G. Vries, H. J. Snippert, M. van de Wetering, N. Barker, D. E. Stange, J. H. van Es, A. Abo, P. Kujala, P. J. Peters and H. Clevers (2009). "Single Lgr5 stem cells build crypt-villus structures in vitro without a mesenchymal niche." Nature **459**(7244): 262-265.

Schmassmann, A. and J. C. Reubi (2000). "Cholecystokinin-B/gastrin receptors enhance wound healing in the rat gastric mucosa." J.Clin.Invest **106**(8): 1021-1029.

Schmitz, F., J. M. Otte, H. U. Stechele, B. Reimann, T. Banasiewicz, U. R. Folsch, W. E. Schmidt and K. H. Herzig (2001). "CCK-B/gastrin receptors in human colorectal cancer." Eur J Clin Invest **31**(9): 812-820.

Schubert, M. L. (2016). "Gastric acid secretion." Curr Opin Gastroenterol **32**(6): 452-460.

Schubert, M. L. (2017). "Physiologic, pathophysiologic, and pharmacologic regulation of gastric acid secretion." Curr Opin Gastroenterol **33**(6): 430-438.

Schwarz, S., G. Morelli, B. Kusecek, A. Manica, F. Balloux, R. J. Owen, D. Y. Graham, S. van der Merwe, M. Achtman and S. Suerbaum (2008). "Horizontal versus familial transmission of Helicobacter pylori." PLoS Pathog **4**(10): e1000180.

Semenza, G. L. (2013). "Cancer-stromal cell interactions mediated by hypoxia-inducible factors promote angiogenesis, lymphangiogenesis, and metastasis." Oncogene **32**(35): 4057-4063.

Shain, A. H. and B. C. Bastian (2016). "From melanocytes to melanomas." Nat Rev Cancer **16**(6): 345-358.

Shawe-Taylor, M., J. D. Kumar, W. Holden, S. Dodd, A. Varga, O. Giger, A. Varro and G. J. Dockray (2017). "Glucagon-like petide-2 acts on colon cancer myofibroblasts to stimulate proliferation, migration and invasion of both myofibroblasts and cancer cells via the IGF pathway." Peptides **91**: 49-57.

Shuppan, K. (1993). "The General Rules for the Gastric Cancer Study in Surgery and Pathology, 12th, Japanese Research Society for Gastric Cancer (Ed), Kanahara Shuppan, Tokyo."

Silvente-Poirot, S. and S. A. Wank (1996). "A segment of five amino acids in the second extracellular loop of the cholecystokinin-B receptor is essential for selectivity of the peptide agonist gastrin." J Biol Chem **271**(25): 14698-14706.

Sim, F. H., W. F. Taylor, D. J. Pritchard and E. H. Soule (1986). "Lymphadenectomy in the management of stage I malignant melanoma: a prospective randomized study." Mayo Clin Proc **61**(9): 697-705.

Simpson, A. W. M. (2013). Fluorescent Measurement of [Ca2+]: Basic Practical Considerations. Calcium Signaling Protocols. D. G. Lambert and R. D. Rainbow, Springer Business Media. **937:** 3 -.

Singh, P., S. Sarkar, C. Kantara and C. Maxwell (2012). "Progastrin Peptides Increase the Risk of Developing Colonic Tumors: Impact on Colonic Stem Cells." Curr Colorectal Cancer Rep **8**(4): 277-289.

Sipponen, P., P. Ranta, T. Helske, I. Kaariainen, T. Maki, A. Linnala, O. Suovaniemi, A. Alanko and M. Harkonen (2002). "Serum levels of amidated gastrin-17 and pepsinogen I in atrophic gastritis: an observational case-control study." Scand J Gastroenterol **37**(7): 785-791.

Slingluff, C. L., Jr., K. R. Stidham, W. M. Ricci, W. E. Stanley and H. F. Seigler (1994). "Surgical management of regional lymph nodes in patients with melanoma. Experience with 4682 patients." Ann Surg **219**(2): 120-130.

Smalley, K. S., P. Brafford, N. K. Haass, J. M. Brandner, E. Brown and M. Herlyn (2005). "Up-regulated expression of zonula occludens protein-1 in human melanoma associates with N-cadherin and contributes to invasion and adhesion." Am J Pathol **166**(5): 1541-1554.

Smith, J. M., P. A. Johanesen, M. K. Wendt, D. G. Binion and M. B. Dwinell (2005). "CXCL12 activation of CXCR4 regulates mucosal host defense through stimulation of epithelial cell migration and promotion of intestinal barrier integrity." Am J Physiol Gastrointest Liver Physiol **288**(2): G316-326.

Smith, J. P., J. F. Harms, G. L. Matters, C. O. McGovern, F. M. Ruggiero, J. Liao, K. K. Fino, E. E. Ortega, E. L. Gilius and J. A. Phillips, 3rd (2012). "A single nucleotide polymorphism of the cholecystokinin-B receptor predicts risk for pancreatic cancer." Cancer Biol Ther **13**(3): 164-174.

Smola, H., G. Thiekotter and N. E. Fusenig (1993). "Mutual induction of growth factor gene expression by epidermal-dermal cell interaction." J Cell Biol **122**(2): 417-429.

Smolka, A. J. and S. Backert (2012). "How Helicobacter pylori infection controls gastric acid secretion." J Gastroenterol **47**(6): 609-618.

Somiari, S. B., R. I. Somiari, C. M. Heckman, C. H. Olsen, R. M. Jordan, S. J. Russell and C. D. Shriver (2006). "Circulating MMP2 and MMP9 in breast cancer -- potential role in classification of patients into low risk, high risk, benign disease and breast cancer categories." Int J Cancer **119**(6): 1403-1411.

Soura, E., P. J. Eliades, K. Shannon, A. J. Stratigos and H. Tsao (2016). "Hereditary melanoma: Update on syndromes and management: Genetics of familial atypical multiple mole melanoma syndrome." J Am Acad Dermatol **74**(3): 395-407; quiz 408-310.

Speeckaert, R., N. van Geel, K. V. Vermaelen, J. Lambert, M. Van Gele, M. M. Speeckaert and L. Brochez (2011). "Immune reactions in benign and malignant melanocytic lesions: lessons for immunotherapy." Pigment Cell Melanoma Res **24**(2): 334-344.

Stanbridge, E. J. (1990). "Human tumor suppressor genes." Annu Rev Genet **24**: 615-657.

Stepan, V. M., M. Tatewaki, M. Matsushima, C. J. Dickinson, J. del Valle and A. Todisco (1999). "Gastrin induces c-fos gene transcription via multiple signaling pathways." Am J Physiol **276**(2): G415-424.

Stern, R. S. (2001). "The risk of melanoma in association with long-term exposure to PUVA." J Am Acad Dermatol **44**(5): 755-761.

Steward, W. P. and A. L. Thomas (2000). "Marimastat: the clinical development of a matrix metalloproteinase inhibitor." Expert Opin Investig Drugs **9**(12): 2913-2922.

Sturm, R. A., K. Satyamoorthy, F. Meier, B. B. Gardiner, D. J. Smit, B. Vaidya and M. Herlyn (2002). "Osteonectin/SPARC induction by ectopic beta(3) integrin in human radial growth phase primary melanoma cells." Cancer Res **62**(1): 226-232.

Swetter, S. M., H. Tsao, C. K. Bichakjian, C. Curiel-Lewandrowski, D. E. Elder, J. E. Gershenwald, V. Guild, J. M. Grant-Kels, A. C. Halpern, T. M. Johnson, A. J. Sober, J. A. Thompson, O. J. Wisco, S. Wyatt, S. Hu and T. Lamina (2019). "Guidelines of care for the management of primary cutaneous melanoma." J Am Acad Dermatol **80**(1): 208-250.

Thomas, P. D. (2010). "GIGA: a simple, efficient algorithm for gene tree inference in the genomic age." BMC Bioinformatics **11**: 312.

Thompson, C. B. and J. P. Allison (1997). "The emerging role of CTLA-4 as an immune attenuator." Immunity **7**(4): 445-450.

Tlsty, T. D. and L. M. Coussens (2006). "Tumor stroma and regulation of cancer development." Annu Rev Pathol **1**: 119-150.

Tucker, M. A., A. Halpern, E. A. Holly, P. Hartge, D. E. Elder, R. W. Sagebiel, D. t. Guerry and W. H. Clark, Jr. (1997). "Clinically recognized dysplastic nevi. A central risk factor for cutaneous melanoma." Jama **277**(18): 1439-1444.

Uemura, N., S. Okamoto, S. Yamamoto, N. Matsumura, S. Yamaguchi, H. Mashiba, N. Sasaki and K. Taniyama (2000). "Changes in Helicobacter pylori-induced gastritis in the antrum and corpus during long-term acid-suppressive treatment in Japan." Aliment Pharmacol Ther **14**(10): 1345-1352.

Vaananen, H., M. Vauhkonen, T. Helske, I. Kaariainen, M. Rasmussen, H. Tunturi-Hihnala, J. Koskenpato, M. Sotka, M. Turunen, R. Sandstrom, M. Ristikankare, A. Jussila and P. Sipponen (2003). "Non-endoscopic diagnosis of atrophic gastritis with a blood test. Correlation between gastric histology and serum levels of gastrin-17 and pepsinogen I: a multicentre study." Eur J Gastroenterol Hepatol **15**(8): 885-891.

Vaisanen, A., P. Kuvaja, M. Kallioinen and T. Turpeenniemi-Hujanen (2011). "A prognostic index in skin melanoma through the combination of matrix metalloproteinase-2, Ki67, and p53." Hum Pathol **42**(8): 1103-1111.

Vaisanen, A. H., M. Kallioinen and T. Turpeenniemi-Hujanen (2008). "Comparison of the prognostic value of matrix metalloproteinases 2 and 9 in cutaneous melanoma." Hum Pathol **39**(3): 377-385.

van den Oord, J. J., L. Paemen, G. Opdenakker and C. de Wolf-Peeters (1997). "Expression of gelatinase B and the extracellular matrix metalloproteinase inducer EMMPRIN in benign and malignant pigment cell lesions of the skin." Am J Pathol **151**(3): 665-670.

Van Elsland, D. and J. Neefjes (2018). "Bacterial infections and cancer." EMBO reports **19**(11): e46632.

Varga, A., J. Kumar, A. W. Simpson, S. Dodd, P. Hegyi, G. J. Dockray and A. Varro (2017). "Cell cycle dependent expression of the CCK2 receptor by gastrointestinal myofibroblasts: putative role in determining cell migration." **5**(19).

Varro, A. and J. E. Ardill (2003). "Gastrin: an analytical review." Ann Clin Biochem **40**(Pt 5): 472-480.

Varro, A., G. J. Dockray, G. W. Bate, C. Vaillant, A. Higham, E. Armitage and D. G. Thompson (1997). "Gastrin biosynthesis in the antrum of patients with pernicious anemia." Gastroenterology **112**(3): 733-741.

Varro, A., E. Hemers, D. Archer, A. Pagliocca, C. Haigh, S. Ahmed, R. Dimaline and G. J. Dockray (2002). "Identification of plasminogen activator inhibitor-2 as a gastrin-regulated gene: Role of Rho GTPase and menin." Gastroenterology **123**(1): 271-280.

Varro, A., J. Henry, C. Vaillant and G. J. Dockray (1994). "Discrimination between temperature- and brefeldin A-sensitive steps in the sulfation, phosphorylation, and cleavage of progastrin and its derivatives." J Biol Chem **269**(32): 20764-20770.

Varro, A., S. Kenny, E. Hemers, C. McCaig, S. Przemeck, T. C. Wang, K. Bodger and D. M. Pritchard (2007). "Increased gastric expression of MMP-7 in hypergastrinemia and significance for epithelial-mesenchymal signaling." Am J Physiol Gastrointest Liver Physiol **292**(4): G1133-1140.

Varro, A., P. J. Noble, D. M. Pritchard, S. Kennedy, C. A. Hart, R. Dimaline and G. J. Dockray (2004). "Helicobacter pylori induces plasminogen activator inhibitor 2 (PAI-2) in gastric epithelial cells through NF-kB and RhoA: implications for invasion and apoptosis." Cancer Res. **64**: 1695-1702.

Varro, A., P. J. Noble, L. E. Wroblewski, L. Bishop and G. J. Dockray (2002). "Gastrin-cholecystokinin(B) receptor expression in AGS cells is associated with direct inhibition and indirect stimulation of cell proliferation via paracrine activation of the epidermal growth factor receptor." Gut **50**(6): 827-833.

Veronesi, U., N. Cascinelli, J. Adamus, C. Balch, D. Bandiera, A. Barchuk, R. Bufalino, P. Craig, J. De Marsillac, J. C. Durand and et al. (1988). "Thin stage I primary cutaneous malignant melanoma. Comparison of excision with margins of 1 or 3 cm." N Engl J Med **318**(18): 1159-1162.

Vihinen, P., I. Koskivuo, K. Syrjanen, T. Tervahartiala, T. Sorsa and S. Pyrhonen (2008). "Serum matrix metalloproteinase-8 is associated with ulceration and vascular invasion of malignant melanoma." Melanoma Res **18**(4): 268-273.

Vogelstein, B. and K. W. Kinzler (1993). "The multistep nature of cancer." Trends Genet **9**(4): 138-141.

Volinia, S., G. A. Calin, C. G. Liu, S. Ambs, A. Cimmino, F. Petrocca, R. Visone, M. Iorio, C. Roldo, M. Ferracin, R. L. Prueitt, N. Yanaihara, G. Lanza, A. Scarpa, A. Vecchione, M. Negrini, C. C. Harris and C. M. Croce (2006). "A microRNA expression signature of human solid tumors defines cancer gene targets." Proc Natl Acad Sci U S A **103**(7): 2257-2261.

Waghorne, C., M. Thomas, A. Lagarde, R. S. Kerbel and M. L. Breitman (1988). "Genetic evidence for progressive selection and overgrowth of primary tumors by metastatic cell subpopulations." Cancer Res **48**(21): 6109-6114.

Wagle, N., C. Emery, M. F. Berger, M. J. Davis, A. Sawyer, P. Pochanard, S. M. Kehoe, C. M. Johannessen, L. E. Macconaill, W. C. Hahn, M. Meyerson and L. A. Garraway (2011). "Dissecting therapeutic resistance to RAF inhibition in melanoma by tumor genomic profiling." J Clin Oncol **29**(22): 3085-3096.

Walsh, J. H. (1975). "Clinical significance of gastrin radioimmunoassay." Semin Nucl Med **5**(3): 247-254.

Walsh, J. H., C. T. Richardson and J. S. Fordtran (1975). "pH dependence of acid secretion and gastrin release in normal and ulcer subjects." J Clin Invest **55**(3): 462-468.

Wan, P. T., M. J. Garnett, S. M. Roe, S. Lee, D. Niculescu-Duvaz, V. M. Good, C. M. Jones, C. J. Marshall, C. J. Springer, D. Barford and R. Marais (2004). "Mechanism of activation of the RAF-ERK signaling pathway by oncogenic mutations of B-RAF." Cell **116**(6): 855-867.

Wang, T. C., C. A. Dangler, D. Chen, J. R. Goldenring, T. Koh, R. Raychowdhury, R. J. Coffey, S. Ito, A. Varro, G. J. Dockray and J. G. Fox (2000). "Synergistic interaction between hypergastrinemia and Helicobacter infection in a mouse model of gastric cancer." Gastroenterology **118**(1): 36-47.

Wang, T. C. and G. J. Dockray (1999). "Lessons from genetically engineered animal models. I. Physiological studies with gastrin in transgenic mice." Am J Physiol **277**(1): G6-11.

Wang, X., F. Teng, L. Kong and J. Yu (2016). "PD-L1 expression in human cancers and its association with clinical outcomes." Onco Targets Ther **9**: 5023-5039.

Warren, J. R. and B. Marshall (1983). "Unidentified curved bacilli on gastric epithelium in active chronic gastritis." Lancet **1**(8336): 1273-1275.

Watari, J., N. Chen, P. S. Amenta, H. Fukui, T. Oshima, T. Tomita, H. Miwa, K. J. Lim and K. M. Das (2014). "Helicobacter pylori associated chronic gastritis, clinical syndromes, precancerous lesions, and pathogenesis of gastric cancer development." World J Gastroenterol **20**(18): 5461-5473.

Watari, J., K. K. Das, P. S. Amenta, H. Tanabe, A. Tanaka, X. Geng, J. J. Lin, Y. Kohgo and K. M. Das (2008). "Effect of eradication of Helicobacter pylori on the histology and cellular phenotype of gastric intestinal metaplasia." Clin Gastroenterol Hepatol **6**(4): 409-417.

Watson, F., R. S. Kiernan, D. G. Deavall, A. Varro and R. Dimaline (2001). "Transcriptional activation of the rat vesicular monoamine transporter 2 promoter in gastric epithelial cells: regulation by gastrin." J Biol Chem **276**(10): 7661-7671.

Watson, S. A., A. M. Grabowska, M. El-Zaatari and A. Takhar (2006). "Gastrin - active participant or bystander in gastric carcinogenesis?" Nat Rev Cancer **6**(12): 936-946.

Weigert, N., Y. Y. Li, R. R. Schick, D. H. Coy, M. Classen and V. Schusdziarra (1997). "Role of vagal fibers and bombesin/gastrin-releasing peptide-neurons in distention-induced gastrin release in rats." Regul Pept **69**(1): 33-40.

Wells, S. A., Jr., S. B. Baylin, W. M. Linehan, R. E. Farrell, E. B. Cox and C. W. Cooper (1978). "Provocative agents and the diagnosis of medullary carcinoma of the thyroid gland." Ann Surg **188**(2): 139-141.

Willard, M. D., M. E. Lajiness, I. H. Wulur, B. Feng, M. L. Swearingen, M. T. Uhlik, K. W. Kinzler, V. E. Velculescu, T. Sjoblom, S. D. Markowitz, S. M. Powell, B. Vogelstein and T. D. Barber (2012). "Somatic mutations in CCK2R alter receptor activity that promote oncogenic phenotypes." Mol Cancer Res **10**(6): 739-749.

Williams, P. F., C. M. Olsen, N. K. Hayward and D. C. Whiteman (2011). "Melanocortin 1 receptor and risk of cutaneous melanoma: a meta-analysis and estimates of population burden." Int J Cancer **129**(7): 1730-1740.

Wilson, M. A. and L. M. Schuchter (2016). "Chemotherapy for Melanoma." Cancer Treat Res **167**: 209-229.

Wolfe, M. M., G. M. Short and J. E. McGuigan (1987). "Beta-adrenergic stimulation of gastrin release mediated by gastrin-releasing peptide in rat antral mucosa." Regul Pept **17**(3): 133-142.

Woussen-Colle, M. C., G. Willems and G. D. Graef (1977). "Relationship of the gastrin response to the amount of food ingested in normal subjects." Digestion **15**(4): 322-328.

Wroblewski, L. E., P. J. Noble, A. Pagliocca, D. M. Pritchard, C. A. Hart, F. Campbell, A. R. Dodson, G. J. Dockray and A. Varro (2003). "Stimulation of MMP-7 (matrilysin) by Helicobacter pylori in human gastric epithelial cells: role in epithelial cell migration." J.Cell Sci. **116**: 3017-3026.

Wroblewski, L. E., D. M. Pritchard, S. Carter and A. Varro (2002). "Gastrin-stimulated gastric epithelial cell invasion: the role and mechanism of increased matrix metalloproteinase 9 expression." Biochem J **365**(Pt 3): 873-879.

Wu, H., V. Goel and F. G. Haluska (2003). "PTEN signaling pathways in melanoma." Oncogene **22**(20): 3113-3122.

Xie, L. and F. L. Meyskens, Jr. (2013). "The pan-Aurora kinase inhibitor, PHA-739358, induces apoptosis and inhibits migration in melanoma cell lines." Melanoma Res **23**(2): 102-113.

Zeisberg, E. M., S. Potenta, L. Xie, M. Zeisberg and R. Kalluri (2007). "Discovery of endothelial to mesenchymal transition as a source for carcinoma-associated fibroblasts." Cancer Res **67**(21): 10123-10128.

Zhukova, E., J. Sinnett-Smith, H. Wong, T. Chiu and E. Rozengurt (2001). "CCK(B)/gastrin receptor mediates synergistic stimulation of DNA synthesis and cyclin D1, D3, and E expression in Swiss 3T3 cells." J Cell Physiol **189**(3): 291-305.

zur Hausen, H. (1996). "Papillomavirus infections--a major cause of human cancers." Biochim Biophys Acta **1288**(2): F55-78.

Supplements

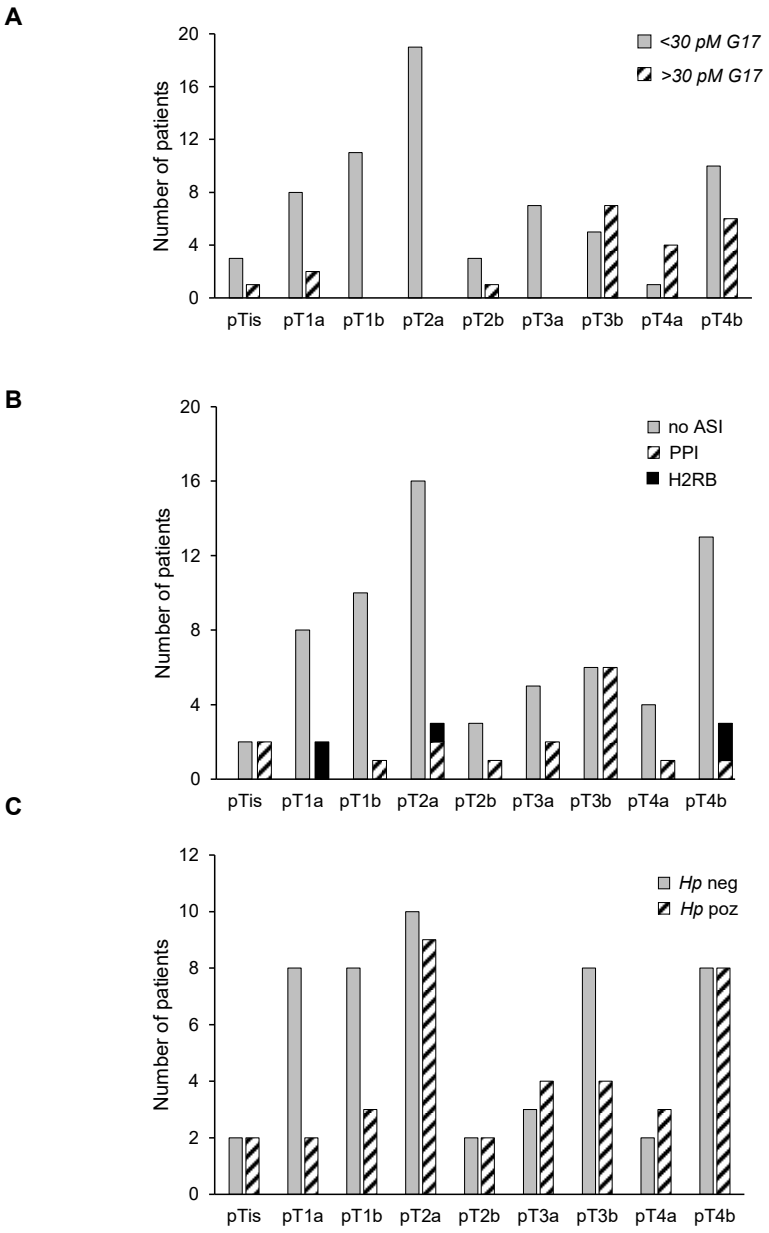

Figure S1. Distribution of melanoma patients among different pT (pTis-pT4b) stages based on serum gastrin concentrations (A), ASI consumption (B) and *Hp* status (C).

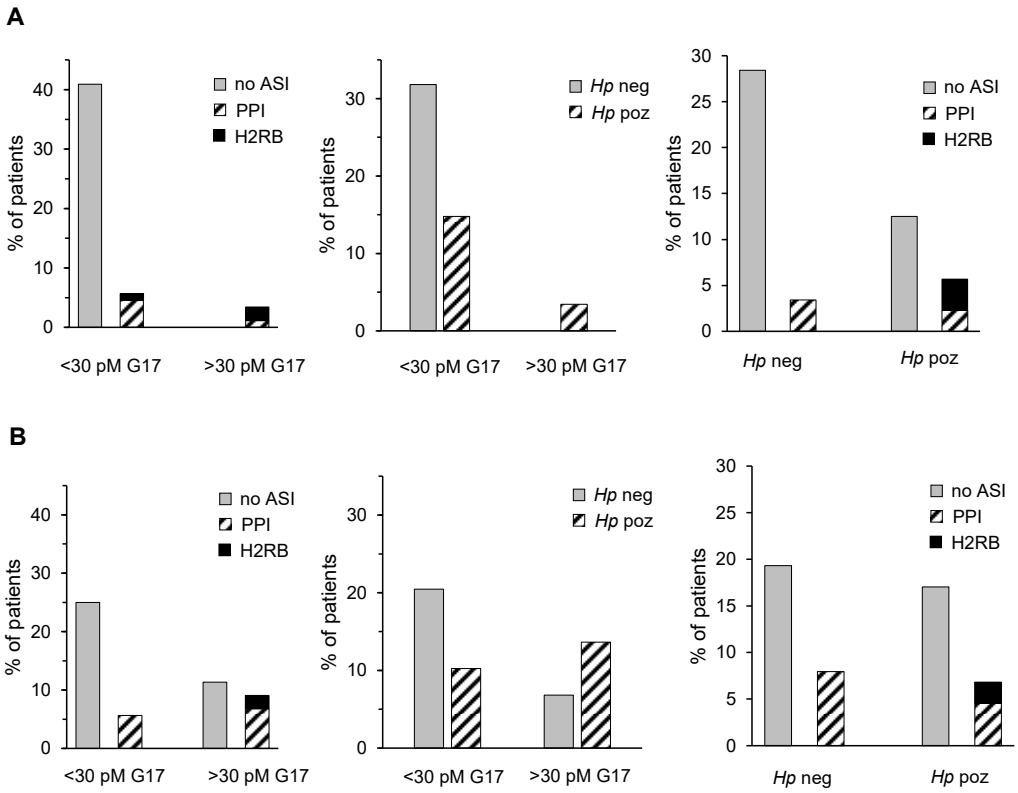

Figure S2. Distribution of melanoma patients in cross-sections of measured parameters (i.e. *Hp* vs. ASI; hG17 vs ASI, hG17 vs *Hp*) in Stage I (A) and Stage II (B) groups. (Y-axis shows percentage of patients).

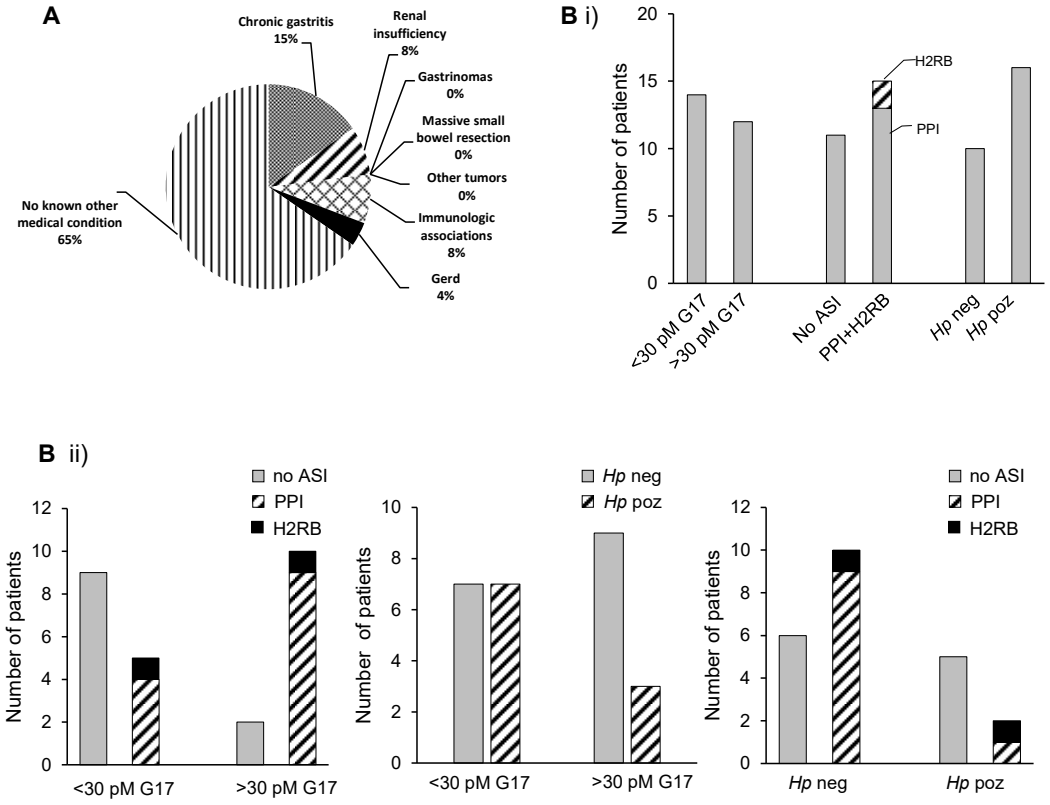

Figure S3. (A) Percentage of basal cell cancer patients (BCC) with known additional medical conditions that can be related to hypergastrinaemia. (B) Distribution of BCC patients based on serum gastrin concentration, ASI consumption and *Hp* status in total group (i) and in cross-sections of investigated parameters (i.e. *Hp* vs. ASI; hG17 vs ASI, hG17 vs *Hp*) (ii).

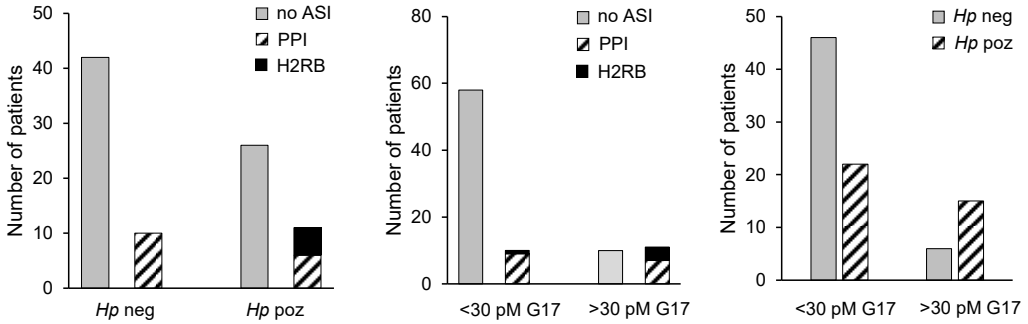

Figure S4. Distribution of melanoma patients in cross-sections of investigated parameters (i.e. *Hp* vs. ASI; hG17 vs ASI, hG17 vs *Hp*) (Y-axis shows number of patients). Patients on ASI had significantly higher serum gastrin concentrations, than dose absent of acid inhibitors (Fisher exact test p <0.0011). Same was true for patients with *H.pylori* infection (Fisher exact test p <0.002).

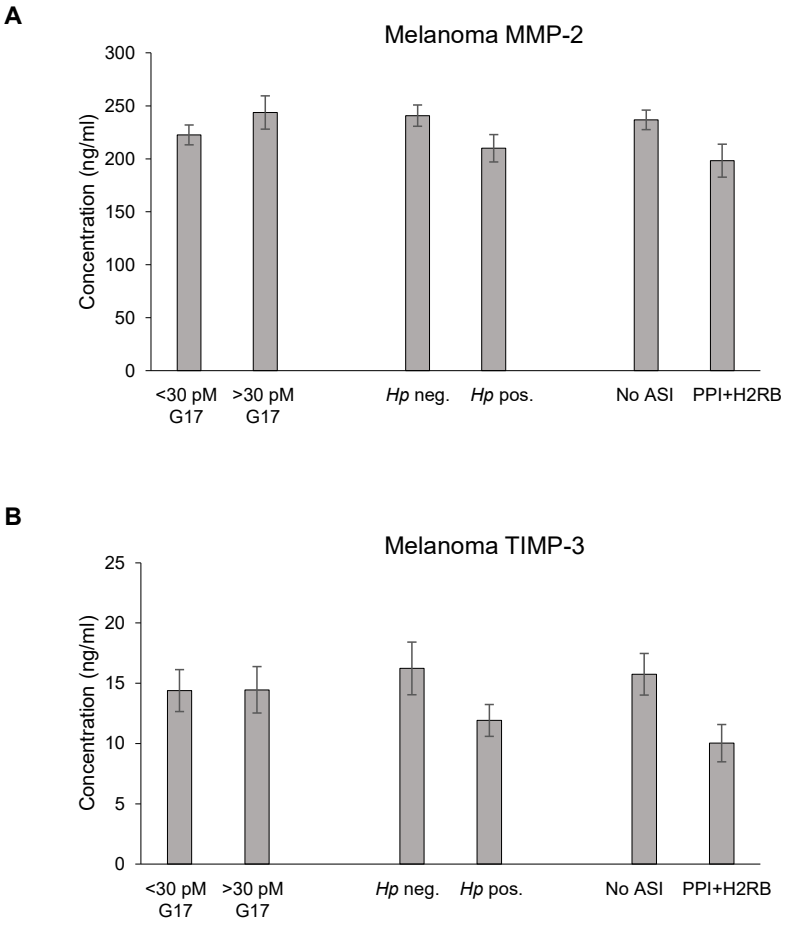

Figure S5. (A) Serum MMP-2 concentration of melanoma patients in specific subgroups defined based on circulating gastrin concertation, HP infection and ASI consumption. (B) Serum TIMP-3 concentration of melanoma patients in the aforementioned groups.

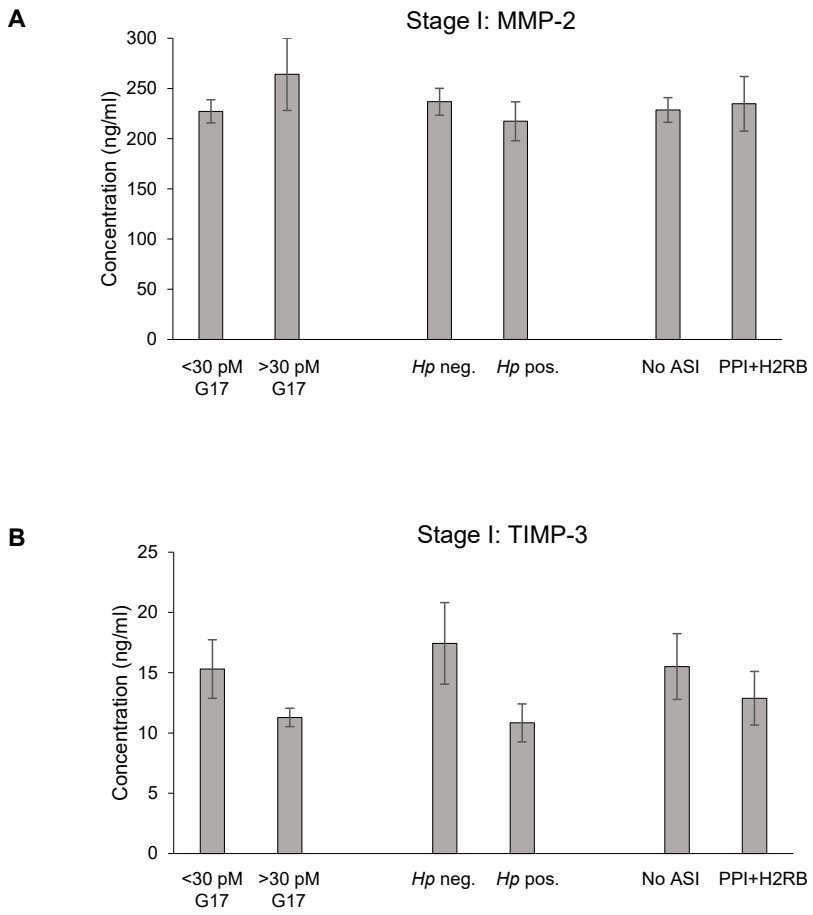

Figure S6. Serum MMP-2 (A) and TIMP-3 (B) concentrations in Stage I (<pT2a) melanoma patients within specific subgroups.

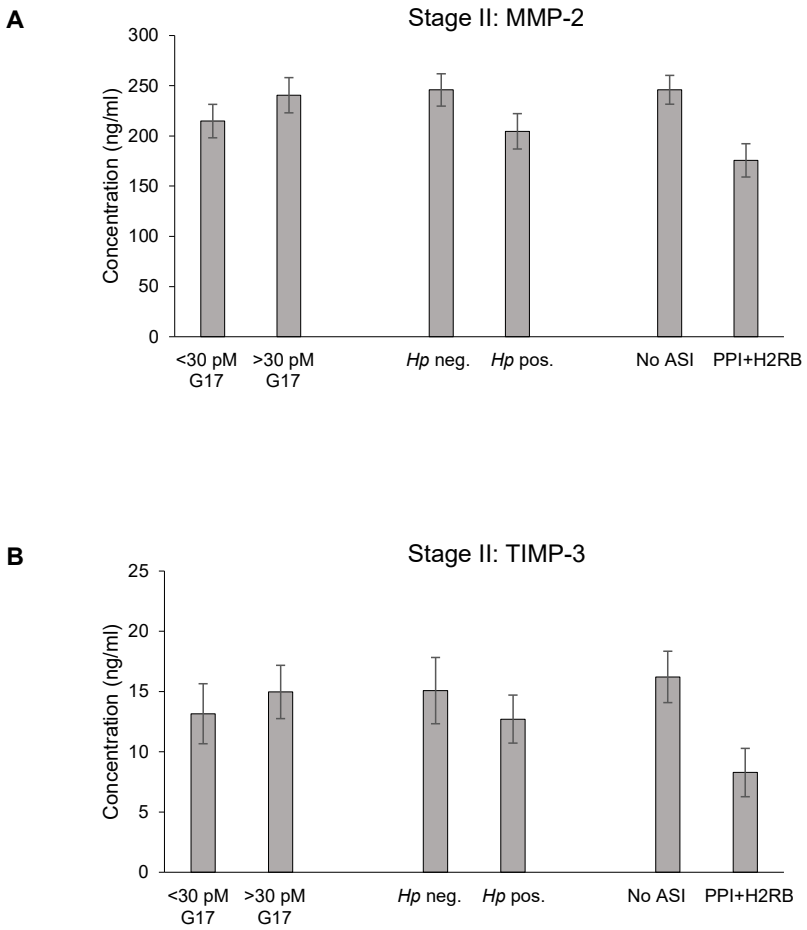

Figure S7. Serum MMP-2 (A) and TIMP-3 (B) concentrations in Stage II (>pT2b) melanoma patients within specific subgroups.

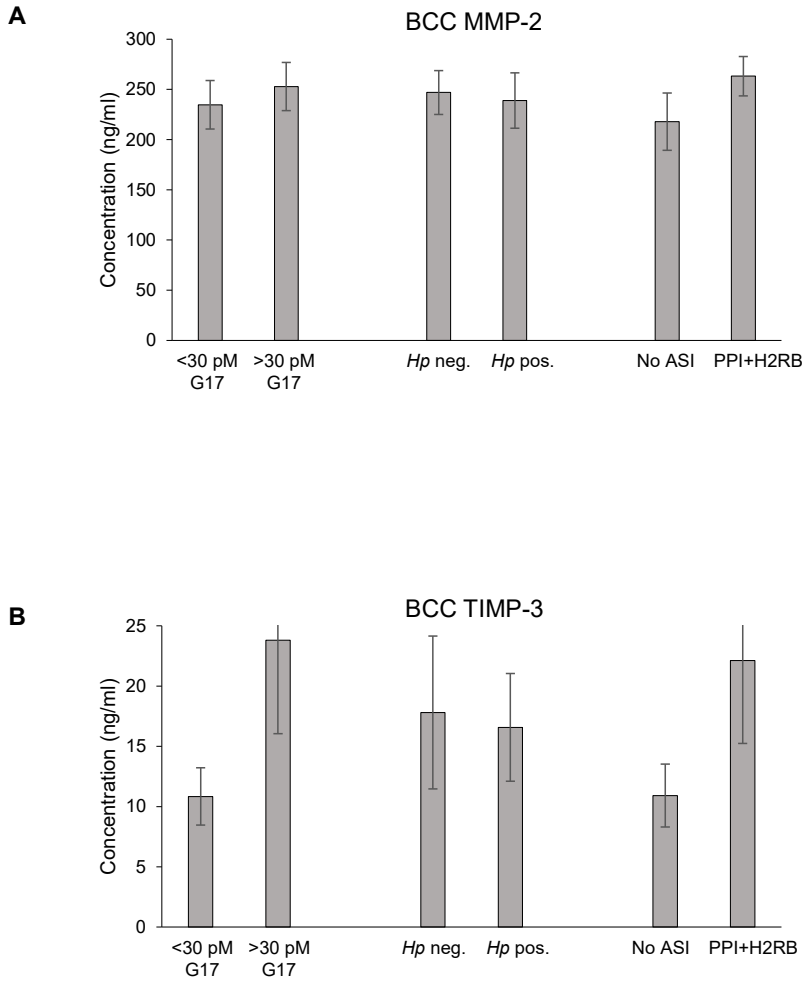

Figure S8. (A) Serum MMP-2 concentration of basal cell cancer patients (BCC) in specific subgroups defined based on circulating gastrin concertation, HP infection and ASI consumption. (B) Serum TIMP-3 concentration of BCC patients in the aforementioned groups

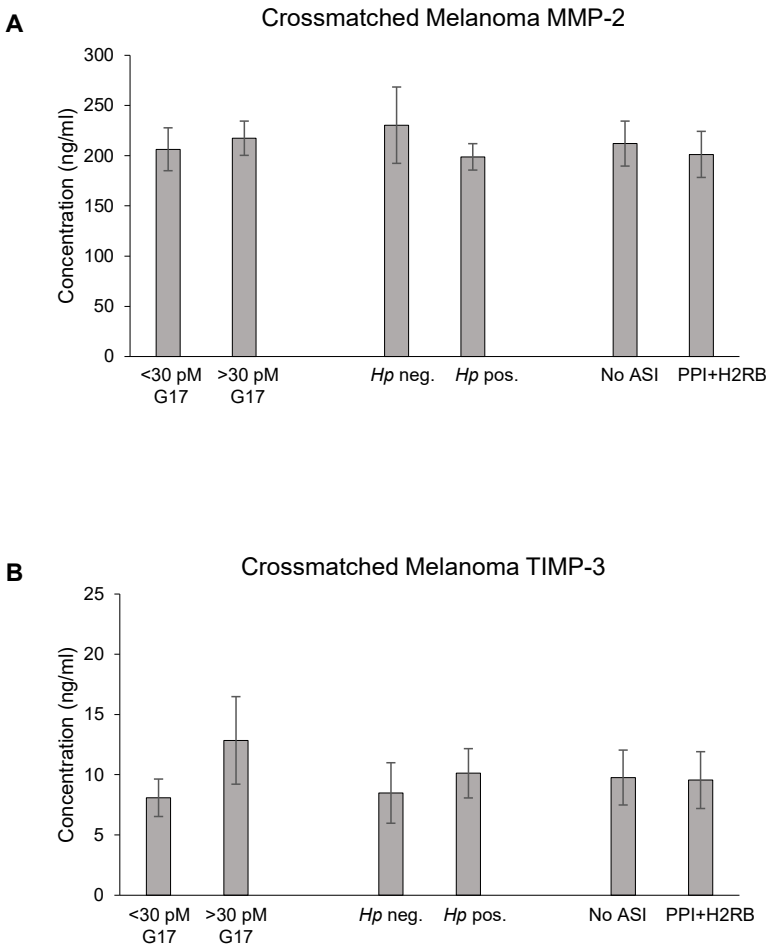

Figure S9. (A) Serum MMP-2 concentration in specific subgroups of melanoma patients age and sex matched to the BCC control cohort. Groups are divided based on circulating gastrin concertation, HP infection and ASI consumption. (B) Serum TIMP-3 concentration of aforementioned matched melanoma groups.

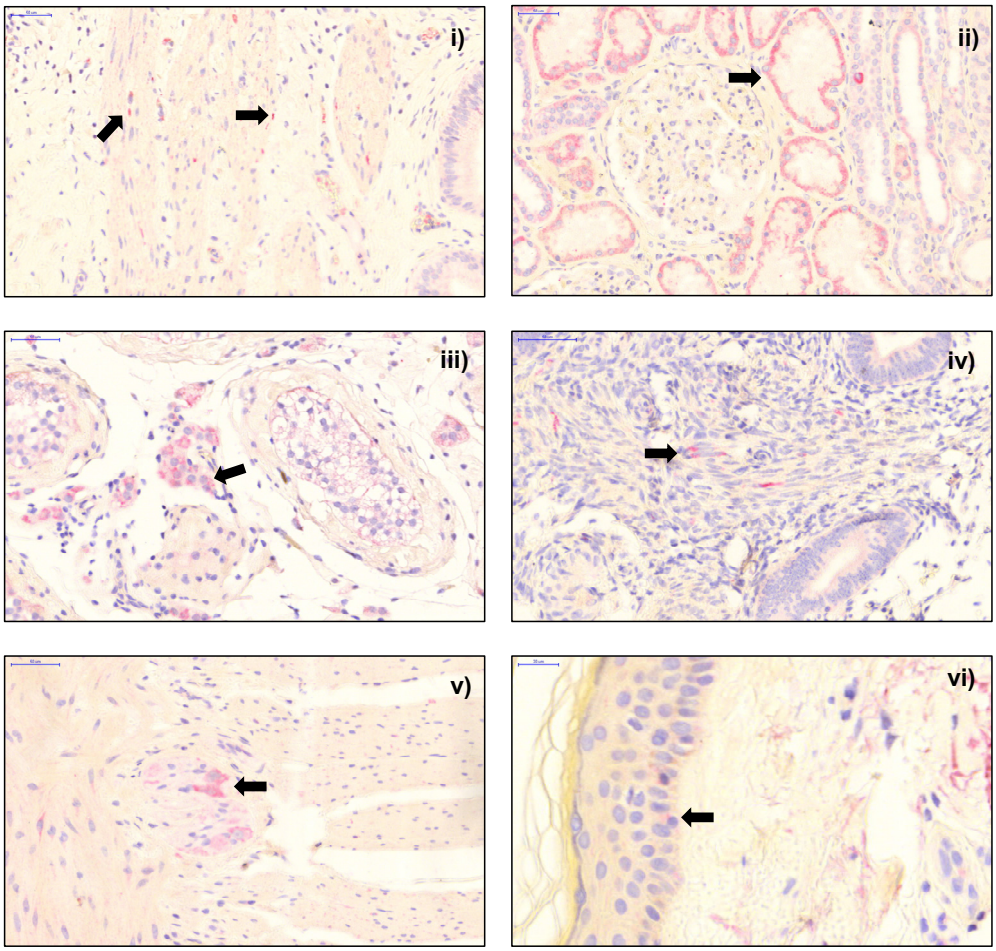

Figure S10. CCK2R tissue microarray.
Immunostaining revealed receptor expression by (i) interstitial cells of Cajal in gall bladder, (ii) proximal tubule cells of nephrons in kidney, (iii) testosterone producing Leydig cells in testes, (iv) myofibroblasts within the uterine wall, (v) enteric neurons of Meissner's plexus of the submucosa and (vi) skin melanocytes. Arrows indicate CCK2 positive cells. Scale bar 50 µm.

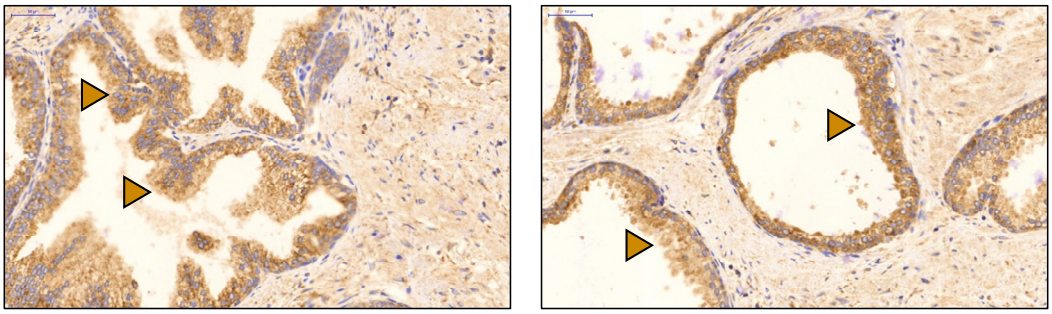

Figure S11. Immunostained samples of prostate tumour for TIMP-3 antibody validation. Brown discolouring indicates positive cells (marked with arrows). Scale bar 50 µm.

Table S1. Complete list of protein hits from secretome analysis of gastrin treated Skmel-2 melanoma cultures.

No.:	*0*	*Accession*	*Proteins*	*Unique Pep.*	*Pep.*	*Heavy/Light*	*AAs*	*MW [kDa]*
1	Thymidylate kinase OS=Homo sapiens GN=DTYMK PE=1 SV=4 - [KTHY_HUMAN]	P23919	1	1	1	**6,905**	212	23,8
2	Proteasome subunit beta type-7 OS=Homo sapiens GN=PSMB7 PE=1 SV=1 - [PSB7_HUMAN]	Q99436	1	3	3	**5,212**	277	29,9
3	Chloride intracellular channel protein 1 OS=Homo sapiens GN=CLIC1 PE=1 SV=4 - [CLIC1_HUMAN]	O00299	1	1	1	**3,649**	241	26,9
4	Proteasome subunit alpha type-3 OS=Homo sapiens GN=PSMA3 PE=1 SV=2 - [PSA3_HUMAN]	P25788	1	3	4	**2,255**	255	28,4
5	CD166 antigen OS=Homo sapiens GN=ALCAM PE=1 SV=2 - [CD166_HUMAN]	Q13740	1	1	1	**2,193**	583	65,1
6	U2 small nuclear ribonucleoprotein B'' OS=Homo sapiens GN=SNRPB2 PE=1 SV=1 - [RU2B_HUMAN]	P08579	2	2	3	**2,097**	225	25,5
7	Prosaposin OS=Homo sapiens GN=PSAP PE=1 SV=2 - [SAP_HUMAN]	P07602	1	4	4	**1,907**	524	58,1
8	Myosin-9 OS=Homo sapiens GN=MYH9 PE=1 SV=4 - [MYH9_HUMAN]	P35579	9	34	40	**1,639**	1960	226,4
9	Hepatoma-derived growth factor-related protein 3 OS=Homo sapiens GN=HDGFRP3 PE=1 SV=1 - [HDGR3_HUMAN]	Q9Y3E1	2	1	2	**1,543**	203	22,6
10	72 kDa type IV collagenase OS=Homo sapiens GN=MMP2 PE=1 SV=2 - [MMP2_HUMAN]	P08253	1	7	7	**1,495**	660	73,8
11	Septin-11 OS=Homo sapiens GN=SEPT11 PE=1 SV=3 - [SEP11_HUMAN]	Q9NVA2	5	9	10	**1,361**	429	49,4
12	Cysteine and glycine-rich protein 2 OS=Homo sapiens GN=CSRP2 PE=1 SV=3 - [CSRP2_HUMAN]	Q16527	1	2	2	**1,331**	193	20,9
13	Heterogeneous nuclear ribonucleoprotein Q OS=Homo sapiens GN=SYNCRIP PE=1 SV=2 - [HNRPQ_HUMAN]	O60506	1	5	9	**1,208**	623	69,6
14	Arf-GAP domain and FG repeat-containing protein 1 OS=Homo sapiens GN=AGFG1 PE=1 SV=2 - [AGFG1_HUMAN]	P52594	1	3	3	**1,013**	562	58,2
15	Glia-derived nexin OS=Homo sapiens GN=SERPINE2 PE=1 SV=1 - [GDN_HUMAN]	P07093	1	10	11	**0,941**	398	44
16	Sushi repeat-containing protein SRPX OS=Homo sapiens GN=SRPX PE=1 SV=1 - [SRPX_HUMAN]	P78539	1	8	9	**0,939**	464	51,5
17	Calsyntenin-1 OS=Homo sapiens GN=CLSTN1 PE=1 SV=1 - [CSTN1_HUMAN]	O94985	2	15	16	**0,939**	981	109,7
18	Fatty acid synthase OS=Homo sapiens GN=FASN PE=1 SV=3 - [FAS_HUMAN]	P49327	1	10	11	**0,868**	2511	273,3
19	Dystroglycan OS=Homo sapiens GN=DAG1 PE=1 SV=2 - [DAG1_HUMAN]	Q14118	1	9	9	**0,863**	895	97,4
20	Fibronectin OS=Homo sapiens GN=FN1 PE=1 SV=4 - [FINC_HUMAN]	P02751	1	59	63	**0,863**	2386	262,5
21	Splicing factor, proline- and glutamine-rich OS=Homo sapiens GN=SFPQ PE=1 SV=2 - [SFPQ_HUMAN]	P23246	1	16	20	**0,833**	707	76,1
22	26S protease regulatory subunit 10B OS=Homo sapiens GN=PSMC6 PE=1 SV=1 - [PRS10_HUMAN]	P62333	1	1	1	**0,814**	389	44,1
23	Neurosecretory protein VGF OS=Homo sapiens GN=VGF PE=1 SV=2 - [VGF_HUMAN]	O15240	1	14	15	**0,795**	615	67,2
24	Cystatin-C OS=Homo sapiens GN=CST3 PE=1 SV=1 - [CYTC_HUMAN]	P01034	2	4	5	**0,782**	146	15,8
25	60S ribosomal protein L38 OS=Homo sapiens GN=RPL38 PE=1 SV=2 - [RL38_HUMAN]	P63173	6	4	6	**0,779**	70	8,2
26	Interleukin enhancer-binding factor 3 OS=Homo sapiens GN=ILF3 PE=1 SV=3 - [ILF3_HUMAN]	Q12906	2	5	8	**0,778**	894	95,3
27	Protein NOV homolog OS=Homo sapiens GN=NOV PE=1 SV=1 - [NOV_HUMAN]	P48745	1	10	13	**0,777**	357	39,1
28	Basement membrane-specific heparan sulfate proteoglycan core protein OS=Homo sapiens GN=HSPG2 PE=1 SV=4 - [PGBM_HUMAN]	P98160	1	44	45	**0,715**	4391	468,5
29	Metalloproteinase inhibitor 2 OS=Homo sapiens GN=TIMP2 PE=1 SV=2 - [TIMP2_HUMAN]	P16035	1	10	12	**0,705**	220	24,4
30	Insulin-like growth factor-binding protein 7 OS=Homo sapiens GN=IGFBP7 PE=1 SV=1 - [IBP7_HUMAN]	Q16270	2	14	15	**0,676**	282	29,1
31	Insulin-like growth factor-binding protein 2 OS=Homo sapiens GN=IGFBP2 PE=1 SV=2 - [IBP2_HUMAN]	P18065	1	9	10	**0,674**	325	34,8
32	T-complex protein 1 subunit delta OS=Homo sapiens GN=CCT4 PE=1 SV=4 - [TCPD_HUMAN]	P50991	1	4	6	**0,673**	539	57,9
33	Cadherin-2 OS=Homo sapiens GN=CDH2 PE=1 SV=4 - [CADH2_HUMAN]	P19022	1	2	2	**0,655**	906	99,7
34	SPARC OS=Homo sapiens GN=SPARC PE=1 SV=1 - [SPRC_HUMAN]	P09486	1	3	4	**0,648**	303	34,6
35	Tumor necrosis factor-inducible gene 6 protein OS=Homo sapiens GN=TNFAIP6 PE=1 SV=2 - [TSG6_HUMAN]	P98066	1	2	2	**0,628**	277	31,2

36	Sulfhydryl oxidase 1 OS=Homo sapiens GN=QSOX1 PE=1 SV=3 - [QSOX1_HUMAN]	O00391	1	7	7	**0,626**	747	82,5
37	Protein arginine N-methyltransferase 1 OS=Homo sapiens GN=PRMT1 PE=1 SV=2 - [ANM1_HUMAN]	Q99873	1	2	2	**0,618**	361	41,5
38	Actin-related protein 2/3 complex subunit 4 OS=Homo sapiens GN=ARPC4 PE=1 SV=3 - [ARPC4_HUMAN]	P59998	1	4	5	**0,615**	168	19,7
39	Thrombospondin-1 OS=Homo sapiens GN=THBS1 PE=1 SV=2 - [TSP1_HUMAN]	P07996	1	22	23	**0,613**	1170	129,3
40	Tissue-type plasminogen activator OS=Homo sapiens GN=PLAT PE=1 SV=1 - [TPA_HUMAN]	P00750	1	7	8	**0,612**	562	62,9
41	Melanoma-derived growth regulatory protein OS=Homo sapiens GN=MIA PE=1 SV=1 - [MIA_HUMAN]	Q16674	1	3	3	**0,594**	131	14,5
42	Nidogen-1 OS=Homo sapiens GN=NID1 PE=1 SV=3 - [NID1_HUMAN]	P14543	2	13	14	**0,559**	1247	136,3
43	Complement factor I OS=Homo sapiens GN=CFI PE=1 SV=2 - [CFAI_HUMAN]	P05156	1	1	1	**0,555**	583	65,7
44	Lactadherin OS=Homo sapiens GN=MFGE8 PE=1 SV=2 - [MFGM_HUMAN]	Q08431	1	1	1	**0,549**	387	43,1
45	Caprin-1 OS=Homo sapiens GN=CAPRIN1 PE=1 SV=2 - [CAPR1_HUMAN]	Q14444	1	5	5	**0,532**	709	78,3
46	Neuroblastoma suppressor of tumorigenicity 1 OS=Homo sapiens GN=NBL1 PE=1 SV=2 - [NBL1_HUMAN]	P41271	1	1	1	**0,527**	181	19,4
47	Carbohydrate sulfotransferase 11 OS=Homo sapiens GN=CHST11 PE=1 SV=1 - [CHSTB_HUMAN]	Q9NPF2	1	3	3	**0,514**	352	41,5
48	Insulin-like growth factor-binding protein 3 OS=Homo sapiens GN=IGFBP3 PE=1 SV=2 - [IBP3_HUMAN]	P17936	1	4	4	**0,501**	291	31,7
49	Follistatin-related protein 1 OS=Homo sapiens GN=FSTL1 PE=1 SV=1 - [FSTL1_HUMAN]	Q12841	1	4	6	**0,496**	308	35
50	Activated RNA polymerase II transcriptional coactivator p15 OS=Homo sapiens GN=SUB1 PE=1 SV=3 - [TCP4_HUMAN]	P53999	1	6	6	**0,473**	127	14,4
51	40S ribosomal protein S25 OS=Homo sapiens GN=RPS25 PE=1 SV=1 - [RS25_HUMAN]	P62851	1	2	2	**0,467**	125	13,7
52	Tenascin OS=Homo sapiens GN=TNC PE=1 SV=3 - [TENA_HUMAN]	P24821	2	51	57	**0,462**	2201	240,7
53	Lysyl oxidase homolog 2 OS=Homo sapiens GN=LOXL2 PE=1 SV=1 - [LOXL2_HUMAN]	Q9Y4K0	1	7	7	**0,461**	774	86,7
54	Granulocyte-macrophage colony-stimulating factor receptor subunit alpha OS=Homo sapiens GN=CSF2RA PE=1 SV=1 - [CSF2R_HUMAN]	P15509	1	2	2	**0,454**	400	46,2
55	Disintegrin and metalloproteinase domain-containing protein 9 OS=Homo sapiens GN=ADAM9 PE=1 SV=1 - [ADAM9_HUMAN]	Q13443	1	3	3	**0,452**	819	90,5
56	Vinculin OS=Homo sapiens GN=VCL PE=1 SV=4 - [VINC_HUMAN]	P18206	1	4	5	**0,443**	1134	123,7
57	DBIRD complex subunit ZNF326 OS=Homo sapiens GN=ZNF326 PE=1 SV=2 - [ZN326_HUMAN]	Q5BKZ1	1	1	1	**0,437**	582	65,6
58	Lysine--tRNA ligase OS=Homo sapiens GN=KARS PE=1 SV=3 - [SYK_HUMAN]	Q15046	1	10	11	**0,382**	597	68
59	Tumor necrosis factor receptor superfamily member 12A OS=Homo sapiens GN=TNFRSF12A PE=1 SV=1 - [TNR12_HUMAN]	Q9NP84	1	1	1	**0,381**	129	13,9
60	Peptidyl-glycine alpha-amidating monooxygenase OS=Homo sapiens GN=PAM PE=1 SV=2 - [AMD_HUMAN]	P19021	1	3	3	**0,376**	973	108,3
61	Galectin-3-binding protein OS=Homo sapiens GN=LGALS3BP PE=1 SV=1 - [LG3BP_HUMAN]	Q08380	1	9	10	**0,366**	585	65,3
62	Laminin subunit alpha-4 OS=Homo sapiens GN=LAMA4 PE=1 SV=4 - [LAMA4_HUMAN]	Q16363	1	21	25	**0,361**	1823	202,4
63	Protein disulfide-isomerase A4 OS=Homo sapiens GN=PDIA4 PE=1 SV=2 - [PDIA4_HUMAN]	P13667	5	14	16	**0,337**	645	72,9
64	Collagen alpha-1(XII) chain OS=Homo sapiens GN=COL12A1 PE=1 SV=2 - [COCA1_HUMAN]	Q99715	1	34	34	**0,324**	3063	332,9
65	Matrilin-2 OS=Homo sapiens GN=MATN2 PE=1 SV=4 - [MATN2_HUMAN]	O00339	1	10	14	**0,318**	956	106,8
66	Extracellular matrix protein 1 OS=Homo sapiens GN=ECM1 PE=1 SV=2 - [ECM1_HUMAN]	Q16610	1	7	7	**0,273**	540	60,6
67	Cathepsin L1 OS=Homo sapiens GN=CTSL PE=1 SV=2 - [CATL1_HUMAN]	P07711	1	3	3	**0,271**	333	37,5
68	Apolipoprotein D OS=Homo sapiens GN=APOD PE=1 SV=1 - [APOD_HUMAN]	P05090	1	3	3	**0,245**	189	21,3
69	Serine protease 23 OS=Homo sapiens GN=PRSS23 PE=1 SV=1 - [PRS23_HUMAN]	O95084	1	2	3	**0,221**	383	43
70	Peptidyl-prolyl cis-trans isomerase FKBP1A OS=Homo sapiens GN=FKBP1A PE=1 SV=2 - [FKB1A_HUMAN]	P62942	1	3	3	**0,219**	108	11,9
71	Beta-2-microglobulin OS=Homo sapiens GN=B2M PE=1 SV=1 - [B2MG_HUMAN]	P61769	1	2	3	**0,218**	119	13,7
72	Fatty acid-binding protein, epidermal OS=Homo sapiens GN=FABP5 PE=1 SV=3 - [FABP5_HUMAN]	Q01469	2	6	8	**0,213**	135	15,2
73	Laminin subunit gamma-1 OS=Homo sapiens GN=LAMC1 PE=1 SV=3 - [LAMC1_HUMAN]	P11047	1	30	34	**0,198**	1609	177,5

74	UBX domain-containing protein 1 OS=Homo sapiens GN=UBXN1 PE=1 SV=2 - [UBXN1_HUMAN]	Q04323	1	4	6	**0,195**	297	33,3
75	Coatomer subunit alpha OS=Homo sapiens GN=COPA PE=1 SV=2 - [COPA_HUMAN]	P53621	1	6	6	**0,195**	1224	138,3
76	Matrix metalloproteinase-14 OS=Homo sapiens GN=MMP14 PE=1 SV=3 - [MMP14_HUMAN]	P50281	1	1	1	**0,191**	582	65,9
77	Protein disulfide-isomerase A3 OS=Homo sapiens GN=PDIA3 PE=1 SV=4 - [PDIA3_HUMAN]	P30101	1	20	20	**0,19**	505	56,7
78	Protein disulfide-isomerase OS=Homo sapiens GN=P4HB PE=1 SV=3 - [PDIA1_HUMAN]	P07237	1	6	7	**0,175**	508	57,1
79	Disintegrin and metalloproteinase domain-containing protein 10 OS=Homo sapiens GN=ADAM10 PE=1 SV=1 - [ADA10_HUMAN]	O14672	1	4	4	**0,173**	748	84,1
80	Serine/threonine-protein kinase PAK 2 OS=Homo sapiens GN=PAK2 PE=1 SV=3 - [PAK2_HUMAN]	Q13177	3	8	8	**0,154**	524	58
81	Laminin subunit beta-1 OS=Homo sapiens GN=LAMB1 PE=1 SV=2 - [LAMB1_HUMAN]	P07942	1	19	19	**0,15**	1786	197,9
82	Cathepsin D OS=Homo sapiens GN=CTSD PE=1 SV=1 - [CATD_HUMAN]	P07339	1	2	2	**0,15**	412	44,5
83	Hsc70-interacting protein OS=Homo sapiens GN=ST13 PE=1 SV=2 - [F10A1_HUMAN]	P50502	3	7	8	**0,145**	369	41,3
84	Vascular endothelial growth factor receptor 1 OS=Homo sapiens GN=FLT1 PE=1 SV=2 - [VGFR1_HUMAN]	P17948	1	5	5	**0,142**	1338	150,7
85	Spectrin alpha chain, non-erythrocytic 1 OS=Homo sapiens GN=SPTAN1 PE=1 SV=3 - [SPTN1_HUMAN]	Q13813	1	15	17	**0,141**	2472	284,4
86	Utrophin OS=Homo sapiens GN=UTRN PE=1 SV=2 - [UTRO_HUMAN]	P46939	1	1	4	**0,139**	3433	394,2
87	Lactoylglutathione lyase OS=Homo sapiens GN=GLO1 PE=1 SV=4 - [LGUL_HUMAN]	Q04760	1	1	1	**0,135**	184	20,8
88	Splicing factor 3B subunit 4 OS=Homo sapiens GN=SF3B4 PE=1 SV=1 - [SF3B4_HUMAN]	Q15427	1	1	1	**0,13**	424	44,4
89	Ezrin OS=Homo sapiens GN=EZR PE=1 SV=4 - [EZRI_HUMAN]	P15311	5	18	28	**0,118**	586	69,4
90	Trans-Golgi network integral membrane protein 2 OS=Homo sapiens GN=TGOLN2 PE=1 SV=2 - [TGON2_HUMAN]	O43493	1	5	5	**0,115**	480	51,1
91	LDLR chaperone MESD OS=Homo sapiens GN=MESDC2 PE=1 SV=2 - [MESD_HUMAN]	Q14696	1	4	5	**0,112**	234	26,1
92	Connective tissue growth factor OS=Homo sapiens GN=CTGF PE=1 SV=2 - [CTGF_HUMAN]	P29279	1	26	26	**0,112**	349	38,1
93	Rab GDP dissociation inhibitor beta OS=Homo sapiens GN=GDI2 PE=1 SV=2 - [GDIB_HUMAN]	P50395	2	5	9	**0,104**	445	50,6
94	Transcription elongation factor A protein 1 OS=Homo sapiens GN=TCEA1 PE=1 SV=2 - [TCEA1_HUMAN]	P23193	2	4	4	**0,098**	301	33,9
95	Adenylyl cyclase-associated protein 1 OS=Homo sapiens GN=CAP1 PE=1 SV=5 - [CAP1_HUMAN]	Q01518	2	17	19	**0,093**	475	51,9
96	Heterogeneous nuclear ribonucleoprotein K OS=Homo sapiens GN=HNRNPK PE=1 SV=1 - [HNRPK_HUMAN]	P61978	1	18	19	**0,091**	463	50,9
97	Multiple inositol polyphosphate phosphatase 1 OS=Homo sapiens GN=MINPP1 PE=1 SV=1 - [MINP1_HUMAN]	Q9UNW1	1	1	1	**0,084**	487	55
98	Collagen triple helix repeat-containing protein 1 OS=Homo sapiens GN=CTHRC1 PE=1 SV=1 - [CTHR1_HUMAN]	Q96CG8	1	5	6	**0,079**	243	26,2
99	Caldesmon OS=Homo sapiens GN=CALD1 PE=1 SV=3 - [CALD1_HUMAN]	Q05682	1	14	16	**0,071**	793	93,2
100	Stathmin OS=Homo sapiens GN=STMN1 PE=1 SV=3 - [STMN1_HUMAN]	P16949	3	12	14	**0,064**	149	17,3
101	Filamin-A OS=Homo sapiens GN=FLNA PE=1 SV=4 - [FLNA_HUMAN]	P21333	2	73	81	**0,06**	2647	280,6
102	Chromobox protein homolog 3 OS=Homo sapiens GN=CBX3 PE=1 SV=4 - [CBX3_HUMAN]	Q13185	1	7	9	**0,06**	183	20,8
103	Small nuclear ribonucleoprotein-associated proteins B and B' OS=Homo sapiens GN=SNRPB PE=1 SV=2 - [RSMB_HUMAN]	P14678	2	5	6	**0,056**	240	24,6
104	TATA-binding protein-associated factor 2N OS=Homo sapiens GN=TAF15 PE=1 SV=1 - [RBP56_HUMAN]	Q92804	1	3	7	**0,056**	592	61,8
105	Nucleobindin-1 OS=Homo sapiens GN=NUCB1 PE=1 SV=4 - [NUCB1_HUMAN]	Q02818	2	12	15	**0,054**	461	53,8
106	Granulins OS=Homo sapiens GN=GRN PE=1 SV=2 - [GRN_HUMAN]	P28799	1	5	8	**0,054**	593	63,5
107	Calumenin OS=Homo sapiens GN=CALU PE=1 SV=2 - [CALU_HUMAN]	O43852	1	4	4	**0,053**	315	37,1
108	Radixin OS=Homo sapiens GN=RDX PE=1 SV=1 - [RADI_HUMAN]	P35241	4	8	20	**0,053**	583	68,5
109	Eukaryotic translation initiation factor 1 OS=Homo sapiens GN=EIF1 PE=1 SV=1 - [EIF1_HUMAN]	P41567	2	5	6	**0,052**	113	12,7
110	Growth-regulated alpha protein OS=Homo sapiens GN=CXCL1 PE=1 SV=1 - [GROA_HUMAN]	P09341	17	3	6	**0,044**	107	11,3
111	Zinc finger protein 766 OS=Homo sapiens GN=ZNF766 PE=2 SV=1 - [ZN766_HUMAN]	Q5HY98	1	1	2	**0,04**	468	54,5
112	Transforming protein RhoA OS=Homo sapiens GN=RHOA PE=1 SV=1 - [RHOA_HUMAN]	P61586	3	6	6	**0,038**	193	21,8
113	45 kDa calcium-binding protein OS=Homo sapiens GN=SDF4 PE=1 SV=1 - [CAB45_HUMAN]	Q9BRK5	1	10	10	**0,037**	362	41,8

114	Elongation factor 1-alpha 1 OS=Homo sapiens GN=EEF1A1 PE=1 SV=1 - [EF1A1_HUMAN]	P68104	2	5	14	**0,036**	462	50,1
115	Peroxiredoxin-1 OS=Homo sapiens GN=PRDX1 PE=1 SV=1 - [PRDX1_HUMAN]	Q06830	2	10	13	**0,036**	199	22,1
116	Cytochrome c oxidase subunit 5B, mitochondrial OS=Homo sapiens GN=COX5B PE=1 SV=2 - [COX5B_HUMAN]	P10606	1	5	5	**0,033**	129	13,7
117	Calreticulin OS=Homo sapiens GN=CALR PE=1 SV=1 - [CALR_HUMAN]	P27797	1	1	1	**0,029**	417	48,1
118	Cell surface glycoprotein MUC18 OS=Homo sapiens GN=MCAM PE=1 SV=2 - [MUC18_HUMAN]	P43121	5	12	13	**0,029**	646	71,6
119	E3 ubiquitin-protein ligase CBL-B OS=Homo sapiens GN=CBLB PE=1 SV=2 - [CBLB_HUMAN]	Q13191	1	1	2	**0,028**	982	109,4
120	40S ribosomal protein S21 OS=Homo sapiens GN=RPS21 PE=1 SV=1 - [RS21_HUMAN]	P63220	1	4	4	**0,027**	83	9,1
121	Protein-L-isoaspartate(D-aspartate) O-methyltransferase OS=Homo sapiens GN=PCMT1 PE=1 SV=4 - [PIMT_HUMAN]	P22061	1	5	5	**0,027**	227	24,6
122	Heat shock protein HSP 90-beta OS=Homo sapiens GN=HSP90AB1 PE=1 SV=4 - [HS90B_HUMAN]	P08238	6	9	17	**0,026**	724	83,2
123	Zinc finger C3H1 domain-containing protein OS=Homo sapiens GN=ZFC3H1 PE=1 SV=3 - [ZC3H1_HUMAN]	O60293	1	1	1	**0,023**	1989	226,2
124	Actin, cytoplasmic 1 OS=Homo sapiens GN=ACTB PE=1 SV=1 - [ACTB_HUMAN]	P60709	12	10	23	**0,021**	375	41,7
125	Pyruvate kinase PKM OS=Homo sapiens GN=PKM PE=1 SV=4 - [KPYM_HUMAN]	P14618	2	42	44	**0,019**	531	57,9
126	Elongation factor 2 OS=Homo sapiens GN=EEF2 PE=1 SV=4 - [EF2_HUMAN]	P13639	1	21	25	**0,019**	858	95,3
127	Src substrate cortactin OS=Homo sapiens GN=CTTN PE=1 SV=2 - [SRC8_HUMAN]	Q14247	1	25	28	**0,018**	550	61,5
128	Glucosidase 2 subunit beta OS=Homo sapiens GN=PRKCSH PE=1 SV=2 - [GLU2B_HUMAN]	P14314	1	12	13	**0,014**	528	59,4
129	Ubiquitin-40S ribosomal protein S27a OS=Homo sapiens GN=RPS27A PE=1 SV=2 - [RS27A_HUMAN]	P62979	4	6	8	**0,013**	156	18
130	KH domain-containing, RNA-binding, signal transduction-associated protein 1 OS=Homo sapiens GN=KHDRBS1 PE=1 SV=1 - [KHDR1_HUMAN]	Q07666	6	5	8	**0,013**	443	48,2
131	Interleukin-8 OS=Homo sapiens GN=CXCL8 PE=1 SV=1 - [IL8_HUMAN]	P10145	1	4	5	**0,012**	99	11,1
132	Vimentin OS=Homo sapiens GN=VIM PE=1 SV=4 - [VIME_HUMAN]	P08670	7	44	48	**0,012**	466	53,6
133	Nucleolin OS=Homo sapiens GN=NCL PE=1 SV=3 - [NUCL_HUMAN]	P19338	3	28	31	**0,011**	710	76,6
134	60 kDa heat shock protein, mitochondrial OS=Homo sapiens GN=HSPD1 PE=1 SV=2 - [CH60_HUMAN]	P10809	1	11	12	**0,01**	573	61

Table S2. Complete list of protein hits from secretome analysis of gastrin treated G361 melanoma cultures.

No.:	*Description*	*Accession*	*Proteins*	*Unique Pep.*	*Pep.*	Heavy/Light	*AAs*	*MW [kDa]*
1	Heterogeneous nuclear ribonucleoprotein Q OS=Homo sapiens GN=SYNCRIP PE=1 SV=2 - [HNRPQ_HUMAN]	O60506	10	5	11	**2,851**	623	69,6
2	Hepatoma-derived growth factor-related protein 3 OS=Homo sapiens GN=HDGFRP3 PE=1 SV=1 - [HDGR3_HUMAN]	Q9Y3E1	1	2	3	**2,401**	203	22,6
3	Prosaposin OS=Homo sapiens GN=PSAP PE=1 SV=2 - [SAP_HUMAN]	P07602	1	7	8	**1,785**	524	58,1
4	Arf-GAP domain and FG repeat-containing protein 1 OS=Homo sapiens GN=AGFG1 PE=1 SV=2 - [AGFG1_HUMAN]	P52594	1	3	3	**1,601**	562	58,2
5	AP-2 complex subunit beta OS=Homo sapiens GN=AP2B1 PE=1 SV=1 - [AP2B1_HUMAN]	P63010	1	3	3	**1,47**	937	104,5
6	26S protease regulatory subunit 10B OS=Homo sapiens GN=PSMC6 PE=1 SV=1 - [PRS10_HUMAN]	P62333	6	2	4	**1,353**	389	44,1
7	Coiled-coil-helix-coiled-coil-helix domain-containing protein 2 OS=Homo sapiens GN=CHCHD2 PE=1 SV=1 - [CHCH2_HUMAN]	Q9Y6H1	2	2	2	**0,964**	151	15,5
8	Neurosecretory protein VGF OS=Homo sapiens GN=VGF PE=1 SV=2 - [VGF_HUMAN]	O15240	1	34	34	**0,933**	615	67,2
9	Glia-derived nexin OS=Homo sapiens GN=SERPINE2 PE=1 SV=1 - [GDN_HUMAN]	P07093	1	4	4	**0,917**	398	44
10	72 kDa type IV collagenase OS=Homo sapiens GN=MMP2 PE=1 SV=2 - [MMP2_HUMAN]	P08253	1	17	17	**0,9**	660	73,8
11	Metalloproteinase inhibitor 1 OS=Homo sapiens GN=TIMP1 PE=1 SV=1 - [TIMP1_HUMAN]	P01033	1	5	5	**0,87**	207	23,2
12	Lamin-B1 OS=Homo sapiens GN=LMNB1 PE=1 SV=2 - [LMNB1_HUMAN]	P20700	1	24	33	**0,87**	586	66,4
13	Granulins OS=Homo sapiens GN=GRN PE=1 SV=2 - [GRN_HUMAN]	P28799	1	15	16	**0,839**	593	63,5
14	Myotrophin OS=Homo sapiens GN=MTPN PE=1 SV=2 - [MTPN_HUMAN]	P58546	1	2	2	**0,815**	118	12,9
15	Dystroglycan OS=Homo sapiens GN=DAG1 PE=1 SV=2 - [DAG1_HUMAN]	Q14118	1	12	12	**0,811**	895	97,4
16	Sushi repeat-containing protein SRPX OS=Homo sapiens GN=SRPX PE=1 SV=1 - [SRPX_HUMAN]	P78539	1	9	9	**0,791**	464	51,5
17	Calsyntenin-1 OS=Homo sapiens GN=CLSTN1 PE=1 SV=1 - [CSTN1_HUMAN]	O94985	2	17	18	**0,771**	981	109,7
18	Actin-related protein 2/3 complex subunit 4 OS=Homo sapiens GN=ARPC4 PE=1 SV=3 - [ARPC4_HUMAN]	P59998	1	4	4	**0,763**	168	19,7
19	Insulin-like growth factor-binding protein 2 OS=Homo sapiens GN=IGFBP2 PE=1 SV=2 - [IBP2_HUMAN]	P18065	1	15	16	**0,761**	325	34,8
20	Stanniocalcin-1 OS=Homo sapiens GN=STC1 PE=1 SV=1 - [STC1_HUMAN]	P52823	1	2	2	**0,734**	247	27,6
21	Metalloproteinase inhibitor 2 OS=Homo sapiens GN=TIMP2 PE=1 SV=2 - [TIMP2_HUMAN]	P16035	1	14	16	**0,7**	220	24,4
22	Insulin-like growth factor-binding protein 3 OS=Homo sapiens GN=IGFBP3 PE=1 SV=2 - [IBP3_HUMAN]	P17936	20	13	13	**0,695**	291	31,7
23	Fibronectin OS=Homo sapiens GN=FN1 PE=1 SV=4 - [FINC_HUMAN]	P02751	3	78	78	**0,683**	2386	262,5
24	Cadherin-2 OS=Homo sapiens GN=CDH2 PE=1 SV=4 - [CADH2_HUMAN]	P19022	1	1	1	**0,675**	906	99,7
25	Sulfhydryl oxidase 1 OS=Homo sapiens GN=QSOX1 PE=1 SV=3 - [QSOX1_HUMAN]	O00391	1	5	5	**0,661**	747	82,5
26	ADM OS=Homo sapiens GN=ADM PE=1 SV=1 - [ADML_HUMAN]	P35318	1	5	6	**0,647**	185	20,4
27	Cathepsin L2 OS=Homo sapiens GN=CTSV PE=1 SV=2 - [CATL2_HUMAN]	O60911	2	1	3	**0,638**	334	37,3
28	Vinculin OS=Homo sapiens GN=VCL PE=1 SV=4 - [VINC_HUMAN]	P18206	1	6	6	**0,63**	1134	123,7
29	T-complex protein 1 subunit eta OS=Homo sapiens GN=CCT7 PE=1 SV=2 - [TCPH_HUMAN]	Q99832	17	10	12	**0,629**	543	59,3
30	Cadherin-1 OS=Homo sapiens GN=CDH1 PE=1 SV=3 - [CADH1_HUMAN]	P12830	1	1	1	**0,628**	882	97,4
31	Protein NOV homolog OS=Homo sapiens GN=NOV PE=1 SV=1 - [NOV_HUMAN]	P48745	1	12	13	**0,619**	357	39,1
32	Cystatin-C OS=Homo sapiens GN=CST3 PE=1 SV=1 - [CYTC_HUMAN]	P01034	2	6	6	**0,608**	146	15,8
33	Melanoma-derived growth regulatory protein OS=Homo sapiens GN=MIA PE=1 SV=1 - [MIA_HUMAN]	Q16674	1	5	5	**0,606**	131	14,5
34	Testican-1 OS=Homo sapiens GN=SPOCK1 PE=1 SV=1 - [TICN1_HUMAN]	Q08629	2	8	9	**0,599**	439	49,1
35	Follistatin-related protein 5 OS=Homo sapiens GN=FSTL5 PE=2 SV=2 - [FSTL5_HUMAN]	Q8N475	2	3	3	**0,585**	847	95,7

36	SPARC OS=Homo sapiens GN=SPARC PE=1 SV=1 - [SPRC_HUMAN]	P09486	1	5	6	**0,572**	303	34,6
37	Malate dehydrogenase, mitochondrial OS=Homo sapiens GN=MDH2 PE=1 SV=3 - [MDHM_HUMAN]	P40926	1	19	20	**0,561**	338	35,5
38	Cell migration-inducing and hyaluronan-binding protein OS=Homo sapiens GN=CEMIP PE=1 SV=2 - [CEMIP_HUMAN]	Q8WUJ3	1	7	9	**0,553**	1361	152,9
39	Tubulin beta-6 chain OS=Homo sapiens GN=TUBB6 PE=1 SV=1 - [TBB6_HUMAN]	Q9BUF5	1	3	8	**0,546**	446	49,8
40	Tenascin OS=Homo sapiens GN=TNC PE=1 SV=3 - [TENA_HUMAN]	P24821	2	24	27	**0,544**	2201	240,7
41	ATP synthase subunit epsilon, mitochondrial OS=Homo sapiens GN=ATP5E PE=1 SV=2 - [ATP5E_HUMAN]	P56381	2	1	1	**0,539**	51	5,8
42	Amyloid beta A4 protein OS=Homo sapiens GN=APP PE=1 SV=3 - [A4_HUMAN]	P05067	2	11	12	**0,534**	770	86,9
43	Insulin-like growth factor-binding protein 7 OS=Homo sapiens GN=IGFBP7 PE=1 SV=1 - [IBP7_HUMAN]	Q16270	1	12	12	**0,532**	282	29,1
44	Peptidyl-glycine alpha-amidating monooxygenase OS=Homo sapiens GN=PAM PE=1 SV=2 - [AMD_HUMAN]	P19021	1	10	11	**0,528**	973	108,3
45	Tissue-type plasminogen activator OS=Homo sapiens GN=PLAT PE=1 SV=1 - [TPA_HUMAN]	P00750	1	10	11	**0,514**	562	62,9
46	Inter-alpha-trypsin inhibitor heavy chain H5 OS=Homo sapiens GN=ITIH5 PE=2 SV=2 - [ITIH5_HUMAN]	Q86UX2	1	9	10	**0,502**	942	104,5
47	Neuroblastoma suppressor of tumorigenicity 1 OS=Homo sapiens GN=NBL1 PE=1 SV=2 - [NBL1_HUMAN]	P41271	1	3	3	**0,499**	181	19,4
48	Coatomer subunit delta OS=Homo sapiens GN=ARCN1 PE=1 SV=1 - [COPD_HUMAN]	P48444	1	6	7	**0,498**	511	57,2
49	Collagen alpha-3(V) chain OS=Homo sapiens GN=COL5A3 PE=1 SV=3 - [CO5A3_HUMAN]	P25940	1	2	3	**0,489**	1745	172
50	Laminin subunit alpha-1 OS=Homo sapiens GN=LAMA1 PE=1 SV=2 - [LAMA1_HUMAN]	P25391	2	48	51	**0,487**	3075	336,9
51	Hemicentin-1 OS=Homo sapiens GN=HMCN1 PE=1 SV=2 - [HMCN1_HUMAN]	Q96RW7	1	20	22	**0,479**	5635	613
52	Amyloid-like protein 2 OS=Homo sapiens GN=APLP2 PE=1 SV=2 - [APLP2_HUMAN]	Q06481	1	2	3	**0,477**	763	86,9
53	Follistatin-related protein 1 OS=Homo sapiens GN=FSTL1 PE=1 SV=1 - [FSTL1_HUMAN]	Q12841	1	8	9	**0,468**	308	35
54	Serine protease 23 OS=Homo sapiens GN=PRSS23 PE=1 SV=1 - [PRS23_HUMAN]	O95084	1	3	4	**0,467**	383	43
55	Phosphatidylethanolamine-binding protein 1 OS=Homo sapiens GN=PEBP1 PE=1 SV=3 - [PEBP1_HUMAN]	P30086	1	8	9	**0,454**	187	21
56	Plectin OS=Homo sapiens GN=PLEC PE=1 SV=3 - [PLEC_HUMAN]	Q15149	2	59	66	**0,45**	4684	531,5
57	EMILIN-2 OS=Homo sapiens GN=EMILIN2 PE=1 SV=3 - [EMIL2_HUMAN]	Q9BXX0	1	6	8	**0,445**	1053	115,6
58	Transmembrane glycoprotein NMB OS=Homo sapiens GN=GPNMB PE=1 SV=2 - [GPNMB_HUMAN]	Q14956	1	3	4	**0,426**	572	63,9
59	Serine protease HTRA1 OS=Homo sapiens GN=HTRA1 PE=1 SV=1 - [HTRA1_HUMAN]	Q92743	1	12	13	**0,425**	480	51,3
60	Basement membrane-specific heparan sulfate proteoglycan core protein OS=Homo sapiens GN=HSPG2 PE=1 SV=4 - [PGBM_HUMAN]	P98160	1	47	48	**0,412**	4391	468,5
61	Small nuclear ribonucleoprotein-associated proteins B and B' OS=Homo sapiens GN=SNRPB PE=1 SV=2 - [RSMB_HUMAN]	P14678	2	5	5	**0,411**	240	24,6
62	Tartrate-resistant acid phosphatase type 5 OS=Homo sapiens GN=ACP5 PE=1 SV=3 - [PPA5_HUMAN]	P13686	1	2	2	**0,391**	325	36,6
63	Apolipoprotein D OS=Homo sapiens GN=APOD PE=1 SV=1 - [APOD_HUMAN]	P05090	1	4	5	**0,39**	189	21,3
64	40S ribosomal protein S3a OS=Homo sapiens GN=RPS3A PE=1 SV=2 - [RS3A_HUMAN]	P61247	1	14	16	**0,383**	264	29,9
65	Transcription elongation factor B polypeptide 2 OS=Homo sapiens GN=TCEB2 PE=1 SV=1 - [ELOB_HUMAN]	Q15370	1	4	4	**0,382**	118	13,1
66	Lactadherin OS=Homo sapiens GN=MFGE8 PE=1 SV=2 - [MFGM_HUMAN]	Q08431	1	1	1	**0,37**	387	43,1
67	Uncharacterized protein C9orf78 OS=Homo sapiens GN=C9orf78 PE=1 SV=1 - [CI078_HUMAN]	Q9NZ63	1	2	2	**0,368**	289	33,7
68	NEDD8 OS=Homo sapiens GN=NEDD8 PE=1 SV=1 - [NEDD8_HUMAN]	Q15843	2	3	3	**0,357**	81	9,1
69	Vitamin K-dependent protein S OS=Homo sapiens GN=PROS1 PE=1 SV=1 - [PROS_HUMAN]	P07225	1	5	5	**0,353**	676	75,1
70	Extracellular matrix protein 1 OS=Homo sapiens GN=ECM1 PE=1 SV=2 - [ECM1_HUMAN]	Q16610	1	16	16	**0,351**	540	60,6
71	60S ribosomal protein L5 OS=Homo sapiens GN=RPL5 PE=1 SV=3 - [RL5_HUMAN]	P46777	1	12	14	**0,349**	297	34,3
72	Laminin subunit gamma-1 OS=Homo sapiens GN=LAMC1 PE=1 SV=3 - [LAMC1_HUMAN]	P11047	1	43	46	**0,343**	1609	177,5
73	Angiopoietin-related protein 2 OS=Homo sapiens GN=ANGPTL2 PE=2 SV=1 - [ANGL2_HUMAN]	Q9UKU9	2	5	5	**0,341**	493	57,1
74	Matrix metalloproteinase-14 OS=Homo sapiens GN=MMP14 PE=1 SV=3 - [MMP14_HUMAN]	P50281	1	6	6	**0,341**	582	65,9
75	Activated RNA polymerase II transcriptional coactivator p15 OS=Homo sapiens GN=SUB1 PE=1 SV=3 - [TCP4_HUMAN]	P53999	2	8	8	**0,336**	127	14,4

76	Splicing factor 3A subunit 2 OS=Homo sapiens GN=SF3A2 PE=1 SV=2 - [SF3A2_HUMAN]	Q15428	1	4	4	**0,318**	464	49,2
77	Cathepsin D OS=Homo sapiens GN=CTSD PE=1 SV=1 - [CATD_HUMAN]	P07339	1	7	8	**0,313**	412	44,5
78	Acid ceramidase OS=Homo sapiens GN=ASAH1 PE=1 SV=5 - [ASAH1_HUMAN]	Q13510	1	4	4	**0,309**	395	44,6
79	Galectin-3-binding protein OS=Homo sapiens GN=LGALS3BP PE=1 SV=1 - [LG3BP_HUMAN]	Q08380	1	7	8	**0,307**	585	65,3
80	Ubiquitin-conjugating enzyme E2 L3 OS=Homo sapiens GN=UBE2L3 PE=1 SV=1 - [UB2L3_HUMAN]	P68036	2	4	6	**0,304**	154	17,9
81	ATP synthase subunit alpha, mitochondrial OS=Homo sapiens GN=ATP5A1 PE=1 SV=1 - [ATPA_HUMAN]	P25705	1	13	13	**0,297**	553	59,7
82	Carbohydrate sulfotransferase 11 OS=Homo sapiens GN=CHST11 PE=1 SV=1 - [CHSTB_HUMAN]	Q9NPF2	1	3	3	**0,293**	352	41,5
83	Transitional endoplasmic reticulum ATPase OS=Homo sapiens GN=VCP PE=1 SV=4 - [TERA_HUMAN]	P55072	1	8	10	**0,276**	806	89,3
84	Phosphoglycerate kinase 1 OS=Homo sapiens GN=PGK1 PE=1 SV=3 - [PGK1_HUMAN]	P00558	3	17	19	**0,267**	417	44,6
85	Collagen alpha-1(VI) chain OS=Homo sapiens GN=COL6A1 PE=1 SV=3 - [CO6A1_HUMAN]	P12109	1	1	1	**0,262**	1028	108,5
86	60S ribosomal protein L38 OS=Homo sapiens GN=RPL38 PE=1 SV=2 - [RL38_HUMAN]	P63173	6	4	5	**0,259**	70	8,2
87	Thrombospondin-1 OS=Homo sapiens GN=THBS1 PE=1 SV=2 - [TSP1_HUMAN]	P07996	1	11	11	**0,258**	1170	129,3
88	Actin-related protein 2 OS=Homo sapiens GN=ACTR2 PE=1 SV=1 - [ARP2_HUMAN]	P61160	1	6	7	**0,258**	394	44,7
89	Coronin-1B OS=Homo sapiens GN=CORO1B PE=1 SV=1 - [COR1B_HUMAN]	Q9BR76	2	8	8	**0,239**	489	54,2
90	Cathepsin L1 OS=Homo sapiens GN=CTSL PE=1 SV=2 - [CATL1_HUMAN]	P07711	2	9	11	**0,228**	333	37,5
91	Fatty acid-binding protein, epidermal OS=Homo sapiens GN=FABP5 PE=1 SV=3 - [FABP5_HUMAN]	Q01469	2	6	6	**0,226**	135	15,2
92	Ribosome-binding protein 1 OS=Homo sapiens GN=RRBP1 PE=1 SV=4 - [RRBP1_HUMAN]	Q9P2E9	1	15	16	**0,222**	1410	152,4
93	Laminin subunit alpha-4 OS=Homo sapiens GN=LAMA4 PE=1 SV=4 - [LAMA4_HUMAN]	Q16363	1	6	9	**0,221**	1823	202,4
94	Growth-regulated alpha protein OS=Homo sapiens GN=CXCL1 PE=1 SV=1 - [GROA_HUMAN]	P09341	19	5	6	**0,221**	107	11,3
95	Laminin subunit beta-1 OS=Homo sapiens GN=LAMB1 PE=1 SV=2 - [LAMB1_HUMAN]	P07942	3	26	29	**0,213**	1786	197,9
96	Plastin-3 OS=Homo sapiens GN=PLS3 PE=1 SV=4 - [PLST_HUMAN]	P13797	2	3	3	**0,209**	630	70,8
97	Sialidase-1 OS=Homo sapiens GN=NEU1 PE=1 SV=1 - [NEUR1_HUMAN]	Q99519	1	5	5	**0,207**	415	45,4
98	Elongation factor 2 OS=Homo sapiens GN=EEF2 PE=1 SV=4 - [EF2_HUMAN]	P13639	1	23	26	**0,207**	858	95,3
99	Triosephosphate isomerase OS=Homo sapiens GN=TPI1 PE=1 SV=3 - [TPIS_HUMAN]	P60174	1	6	6	**0,203**	286	30,8
100	Immunoglobulin superfamily member 8 OS=Homo sapiens GN=IGSF8 PE=1 SV=1 - [IGSF8_HUMAN]	Q969P0	1	8	8	**0,198**	613	65
101	Beta-2-microglobulin OS=Homo sapiens GN=B2M PE=1 SV=1 - [B2MG_HUMAN]	P61769	1	2	2	**0,197**	119	13,7
102	Protein jagged-1 OS=Homo sapiens GN=JAG1 PE=1 SV=3 - [JAG1_HUMAN]	P78504	1	3	3	**0,193**	1218	133,7
103	60S ribosomal protein L27 OS=Homo sapiens GN=RPL27 PE=1 SV=2 - [RL27_HUMAN]	P61353	1	5	5	**0,19**	136	15,8
104	Collagen alpha-2(IV) chain OS=Homo sapiens GN=COL4A2 PE=1 SV=4 - [CO4A2_HUMAN]	P08572	1	13	13	**0,173**	1712	167,4
105	UMP-CMP kinase OS=Homo sapiens GN=CMPK1 PE=1 SV=3 - [KCY_HUMAN]	P30085	1	4	5	**0,172**	196	22,2
106	Growth/differentiation factor 15 OS=Homo sapiens GN=GDF15 PE=2 SV=3 - [GDF15_HUMAN]	Q99988	1	13	14	**0,166**	308	34,1
107	40S ribosomal protein S25 OS=Homo sapiens GN=RPS25 PE=1 SV=1 - [RS25_HUMAN]	P62851	1	4	4	**0,161**	125	13,7
108	rRNA 2'-O-methyltransferase fibrillarin OS=Homo sapiens GN=FBL PE=1 SV=2 - [FBRL_HUMAN]	P22087	1	8	8	**0,16**	321	33,8
109	Glucosylceramidase OS=Homo sapiens GN=GBA PE=1 SV=3 - [GLCM_HUMAN]	P04062	1	3	3	**0,158**	536	59,7
110	DnaJ homolog subfamily B member 11 OS=Homo sapiens GN=DNAJB11 PE=1 SV=1 - [DJB11_HUMAN]	Q9UBS4	1	2	2	**0,156**	358	40,5
111	Nucleobindin-1 OS=Homo sapiens GN=NUCB1 PE=1 SV=4 - [NUCB1_HUMAN]	Q02818	14	26	30	**0,155**	461	53,8
112	Calnexin OS=Homo sapiens GN=CANX PE=1 SV=2 - [CALX_HUMAN]	P27824	1	3	4	**0,153**	592	67,5
113	Alpha-2-macroglobulin OS=Homo sapiens GN=A2M PE=1 SV=3 - [A2MG_HUMAN]	P01023	1	2	4	**0,152**	1474	163,2
114	Kunitz-type protease inhibitor 1 OS=Homo sapiens GN=SPINT1 PE=1 SV=2 - [SPIT1_HUMAN]	O43278	1	1	1	**0,15**	529	58,4
115	Cysteine and glycine-rich protein 1 OS=Homo sapiens GN=CSRP1 PE=1 SV=3 - [CSRP1_HUMAN]	P21291	1	8	8	**0,15**	193	20,6
116	Receptor-type tyrosine-protein phosphatase S OS=Homo sapiens GN=PTPRS PE=1 SV=3 - [PTPRS_HUMAN]	Q13332	1	10	11	**0,144**	1948	216,9
117	Protein disulfide-isomerase A4 OS=Homo sapiens GN=PDIA4 PE=1 SV=2 - [PDIA4_HUMAN]	P13667	5	23	24	**0,141**	645	72,9

118	Signal recognition particle 9 kDa protein OS=Homo sapiens GN=SRP9 PE=1 SV=2 - [SRP09_HUMAN]	P49458	1	4	4	**0,137**	86	10,1
119	H/ACA ribonucleoprotein complex subunit 2 OS=Homo sapiens GN=NHP2 PE=1 SV=1 - [NHP2_HUMAN]	Q9NX24	1	1	1	**0,136**	153	17,2
120	Disintegrin and metalloproteinase domain-containing protein 10 OS=Homo sapiens GN=ADAM10 PE=1 SV=1 - [ADA10_HUMAN]	O14672	1	9	9	**0,134**	748	84,1
121	Metalloproteinase inhibitor 3 OS=Homo sapiens GN=TIMP3 PE=1 SV=2 - [TIMP3_HUMAN]	P35625	1	7	7	**0,125**	211	24,1
122	Protein disulfide-isomerase A3 OS=Homo sapiens GN=PDIA3 PE=1 SV=4 - [PDIA3_HUMAN]	P30101	1	21	22	**0,11**	505	56,7
123	Histone H3.1 OS=Homo sapiens GN=HIST1H3A PE=1 SV=2 - [H31_HUMAN]	P68431	4	1	10	**0,107**	136	15,4
124	Coronin-1C OS=Homo sapiens GN=CORO1C PE=1 SV=1 - [COR1C_HUMAN]	Q9ULV4	1	16	17	**0,104**	474	53,2
125	Serine/arginine-rich splicing factor 3 OS=Homo sapiens GN=SRSF3 PE=1 SV=1 - [SRSF3_HUMAN]	P84103	1	6	9	**0,103**	164	19,3
126	Shugoshin-like 2 OS=Homo sapiens GN=SGOL2 PE=1 SV=2 - [SGOL2_HUMAN]	Q562F6	1	1	1	**0,094**	1265	144,6
127	Melanocyte protein PMEL OS=Homo sapiens GN=PMEL PE=1 SV=2 - [PMEL_HUMAN]	P40967	1	7	8	**0,093**	661	70,2
128	Nuclear autoantigenic sperm protein OS=Homo sapiens GN=NASP PE=1 SV=2 - [NASP_HUMAN]	P49321	1	7	8	**0,093**	788	85,2
129	Heterogeneous nuclear ribonucleoprotein H OS=Homo sapiens GN=HNRNPH1 PE=1 SV=4 - [HNRH1_HUMAN]	P31943	1	8	17	**0,093**	449	49,2
130	Histone H4 OS=Homo sapiens GN=HIST1H4A PE=1 SV=2 - [H4_HUMAN]	P62805	1	9	9	**0,093**	103	11,4
131	Nucleobindin-2 OS=Homo sapiens GN=NUCB2 PE=1 SV=2 - [NUCB2_HUMAN]	P80303	1	5	7	**0,091**	420	50,2
132	Golgi apparatus protein 1 OS=Homo sapiens GN=GLG1 PE=1 SV=2 - [GSLG1_HUMAN]	Q92896	1	12	12	**0,091**	1179	134,5
133	Prohibitin OS=Homo sapiens GN=PHB PE=1 SV=1 - [PHB_HUMAN]	P35232	2	6	6	**0,091**	272	29,8
134	Multiple inositol polyphosphate phosphatase 1 OS=Homo sapiens GN=MINPP1 PE=1 SV=1 - [MINP1_HUMAN]	Q9UNW1	1	1	1	**0,089**	487	55
135	Tubulin alpha-1B chain OS=Homo sapiens GN=TUBA1B PE=1 SV=1 - [TBA1B_HUMAN]	P68363	4	2	11	**0,089**	451	50,1
136	Profilin-1 OS=Homo sapiens GN=PFN1 PE=1 SV=2 - [PROF1_HUMAN]	P07737	1	8	8	**0,088**	140	15
137	Histone H3.2 OS=Homo sapiens GN=HIST2H3A PE=1 SV=3 - [H32_HUMAN]	Q71DI3	4	1	10	**0,085**	136	15,4
138	Src substrate cortactin OS=Homo sapiens GN=CTTN PE=1 SV=2 - [SRC8_HUMAN]	Q14247	1	20	23	**0,083**	550	61,5
139	Heterogeneous nuclear ribonucleoprotein K OS=Homo sapiens GN=HNRNPK PE=1 SV=1 - [HNRPK_HUMAN]	P61978	6	19	20	**0,083**	463	50,9
140	78 kDa glucose-regulated protein OS=Homo sapiens GN=HSPA5 PE=1 SV=2 - [GRP78_HUMAN]	P11021	3	31	36	**0,073**	654	72,3
141	DnaJ homolog subfamily C member 7 OS=Homo sapiens GN=DNAJC7 PE=1 SV=2 - [DNJC7_HUMAN]	Q99615	1	3	3	**0,073**	494	56,4
142	Actin, cytoplasmic 1 OS=Homo sapiens GN=ACTB PE=1 SV=1 - [ACTB_HUMAN]	P60709	11	10	24	**0,073**	375	41,7
143	Protein CYR61 OS=Homo sapiens GN=CYR61 PE=1 SV=1 - [CYR61_HUMAN]	O00622	1	9	11	**0,071**	381	42
144	Trans-Golgi network integral membrane protein 2 OS=Homo sapiens GN=TGOLN2 PE=1 SV=2 - [TGON2_HUMAN]	O43493	1	6	7	**0,069**	480	51,1
145	45 kDa calcium-binding protein OS=Homo sapiens GN=SDF4 PE=1 SV=1 - [CAB45_HUMAN]	Q9BRK5	1	9	11	**0,067**	362	41,8
146	Squamous cell carcinoma antigen recognized by T-cells 3 OS=Homo sapiens GN=SART3 PE=1 SV=1 - [SART3_HUMAN]	Q15020	1	2	2	**0,067**	963	109,9
147	Chromobox protein homolog 3 OS=Homo sapiens GN=CBX3 PE=1 SV=4 - [CBX3_HUMAN]	Q13185	1	6	9	**0,065**	183	20,8
148	Pyruvate kinase PKM OS=Homo sapiens GN=PKM PE=1 SV=4 - [KPYM_HUMAN]	P14618	3	42	42	**0,064**	531	57,9
149	Cathepsin B OS=Homo sapiens GN=CTSB PE=1 SV=3 - [CATB_HUMAN]	P07858	1	9	9	**0,06**	339	37,8
150	Splicing factor 3B subunit 4 OS=Homo sapiens GN=SF3B4 PE=1 SV=1 - [SF3B4_HUMAN]	Q15427	1	2	2	**0,06**	424	44,4
151	Heterogeneous nuclear ribonucleoprotein M OS=Homo sapiens GN=HNRNPM PE=1 SV=3 - [HNRPM_HUMAN]	P52272	1	19	19	**0,057**	730	77,5
152	Chondroitin sulfate proteoglycan 4 OS=Homo sapiens GN=CSPG4 PE=1 SV=2 - [CSPG4_HUMAN]	Q6UVK1	1	21	23	**0,055**	2322	250,4
153	RNA-binding protein FUS OS=Homo sapiens GN=FUS PE=1 SV=1 - [FUS_HUMAN]	P35637	1	6	10	**0,055**	526	53,4
154	40S ribosomal protein S3 OS=Homo sapiens GN=RPS3 PE=1 SV=2 - [RS3_HUMAN]	P23396	1	10	10	**0,054**	243	26,7
155	Collagen triple helix repeat-containing protein 1 OS=Homo sapiens GN=CTHRC1 PE=1 SV=1 - [CTHR1_HUMAN]	Q96CG8	1	4	5	**0,053**	243	26,2
156	Midkine OS=Homo sapiens GN=MDK PE=1 SV=1 - [MK_HUMAN]	P21741	1	3	4	**0,052**	143	15,6
157	Ribosomal L1 domain-containing protein 1 OS=Homo sapiens GN=RSL1D1 PE=1 SV=3 - [RL1D1_HUMAN]	O76021	1	12	13	**0,052**	490	54,9
158	Flap endonuclease 1 OS=Homo sapiens GN=FEN1 PE=1 SV=1 - [FEN1_HUMAN]	P39748	1	4	5	**0,05**	380	42,6

159	Staphylococcal nuclease domain-containing protein 1 OS=Homo sapiens GN=SND1 PE=1 SV=1 - [SND1_HUMAN]	Q7KZF4	2	29	31	**0,049**	910	101,9
160	Procollagen-lysine,2-oxoglutarate 5-dioxygenase 3 OS=Homo sapiens GN=PLOD3 PE=1 SV=1 - [PLOD3_HUMAN]	O60568	1	9	13	**0,048**	738	84,7
161	Calreticulin OS=Homo sapiens GN=CALR PE=1 SV=1 - [CALR_HUMAN]	P27797	1	6	8	**0,04**	417	48,1
162	TATA-binding protein-associated factor 2N OS=Homo sapiens GN=TAF15 PE=1 SV=1 - [RBP56_HUMAN]	Q92804	1	3	7	**0,04**	592	61,8
163	Chitinase domain-containing protein 1 OS=Homo sapiens GN=CHID1 PE=1 SV=1 - [CHID1_HUMAN]	Q9BWS9	1	2	3	**0,035**	393	44,9
164	Myosin-9 OS=Homo sapiens GN=MYH9 PE=1 SV=4 - [MYH9_HUMAN]	P35579	8	58	66	**0,033**	1960	226,4
165	Neural cell adhesion molecule L1 OS=Homo sapiens GN=L1CAM PE=1 SV=2 - [L1CAM_HUMAN]	P32004	2	8	8	**0,031**	1257	139,9
166	Elongation factor 1-alpha 1 OS=Homo sapiens GN=EEF1A1 PE=1 SV=1 - [EF1A1_HUMAN]	P68104	3	16	17	**0,031**	462	50,1
167	GTP-binding nuclear protein Ran OS=Homo sapiens GN=RAN PE=1 SV=3 - [RAN_HUMAN]	P62826	1	4	5	**0,031**	216	24,4
168	Zinc finger protein 766 OS=Homo sapiens GN=ZNF766 PE=2 SV=1 - [ZN766_HUMAN]	Q5HY98	1	1	2	**0,029**	468	54,5
169	tRNA-splicing ligase RtcB homolog OS=Homo sapiens GN=RTCB PE=1 SV=1 - [RTCB_HUMAN]	Q9Y3I0	1	8	10	**0,029**	505	55,2
170	Galectin-1 OS=Homo sapiens GN=LGALS1 PE=1 SV=2 - [LEG1_HUMAN]	P09382	1	7	7	**0,026**	135	14,7
171	Stress-induced-phosphoprotein 1 OS=Homo sapiens GN=STIP1 PE=1 SV=1 - [STIP1_HUMAN]	P31948	1	27	30	**0,025**	543	62,6
172	Calumenin OS=Homo sapiens GN=CALU PE=1 SV=2 - [CALU_HUMAN]	O43852	1	10	10	**0,024**	315	37,1
173	Polypeptide N-acetylgalactosaminyltransferase 2 OS=Homo sapiens GN=GALNT2 PE=1 SV=1 - [GALT2_HUMAN]	Q10471	1	15	15	**0,023**	571	64,7
174	Ubiquitin-40S ribosomal protein S27a OS=Homo sapiens GN=RPS27A PE=1 SV=2 - [RS27A_HUMAN]	P62979	4	10	10	**0,023**	156	18
175	ATP synthase subunit d, mitochondrial OS=Homo sapiens GN=ATP5H PE=1 SV=3 - [ATP5H_HUMAN]	O75947	1	1	2	**0,022**	161	18,5
176	Cell surface glycoprotein MUC18 OS=Homo sapiens GN=MCAM PE=1 SV=2 - [MUC18_HUMAN]	P43121	2	16	16	**0,02**	646	71,6
177	Peptidyl-prolyl cis-trans isomerase A OS=Homo sapiens GN=PPIA PE=1 SV=2 - [PPIA_HUMAN]	P62937	10	13	14	**0,02**	165	18
178	60S ribosomal protein L9 OS=Homo sapiens GN=RPL9 PE=1 SV=1 - [RL9_HUMAN]	P32969	1	4	4	**0,018**	192	21,8
179	Hepatoma-derived growth factor OS=Homo sapiens GN=HDGF PE=1 SV=1 - [HDGF_HUMAN]	P51858	1	8	11	**0,017**	240	26,8
180	Eukaryotic translation initiation factor 1 OS=Homo sapiens GN=EIF1 PE=1 SV=1 - [EIF1_HUMAN]	P41567	2	4	4	**0,015**	113	12,7
181	Stathmin OS=Homo sapiens GN=STMN1 PE=1 SV=3 - [STMN1_HUMAN]	P16949	3	11	14	**0,015**	149	17,3
182	Transforming protein RhoA OS=Homo sapiens GN=RHOA PE=1 SV=1 - [RHOA_HUMAN]	P61586	3	6	7	**0,014**	193	21,8
183	Alpha-enolase OS=Homo sapiens GN=ENO1 PE=1 SV=2 - [ENOA_HUMAN]	P06733	3	24	24	**0,013**	434	47,1
184	Moesin OS=Homo sapiens GN=MSN PE=1 SV=3 - [MOES_HUMAN]	P26038	2	24	38	**0,013**	577	67,8
185	Nucleolin OS=Homo sapiens GN=NCL PE=1 SV=3 - [NUCL_HUMAN]	P19338	4	30	32	**0,012**	710	76,6
186	Glucosidase 2 subunit beta OS=Homo sapiens GN=PRKCSH PE=1 SV=2 - [GLU2B_HUMAN]	P14314	1	11	11	**0,011**	528	59,4
187	UV excision repair protein RAD23 homolog B OS=Homo sapiens GN=RAD23B PE=1 SV=1 - [RD23B_HUMAN]	P54727	2	7	7	**0,011**	409	43,1